Third Benchmark Workshop

on

NUMERICAL ANALYSIS OF DAMS

Paris, France
September 29–30, 1994

Organized by
the **ICOLD**
"ad-hoc" Committee on Computational Aspects
of Dam Analysis and Design

Under the auspices of the
French Committee on Large Dams
in cooperation with

and

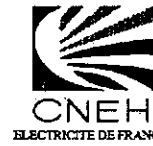

Volume IV

Third Benchmark Workshop on
NUMERICAL ANALYSIS OF DAMS
Gennevilliers, France, September 29-30, 1994

THEME B2

Dynamic analysis of an embankment dam under a strong earthquake

PRESENTATION

&

REFERENCE INFORMATION AND DATA

CONTENTS

1. INTRODUCTION

This theme is proposed along the same lines as the previous Benchmark Workshop. The present instructions consist of :

- the data of the second Benchmark Workshop,
- specific instructions for the 3rd Benchmark Workshop.

The enclosed floppy disk contains :

- data for the F.E. mesh,
- earthquakes upstream/downstream horizontal acceleration time-histories,
- material properties (curves from the laboratory tests).

Any method that gives an evaluation of the requested results or of some of them may be used :

- simplified methods,
- linear equivalent method,
- uncoupled non linear method,
- fully coupled non linear method.

The paper should not exceed 14 pages including Figures and Tables. The text should report :

- the methodology of the analysis,
- the selected computation method,
- the main assumptions of the numerical model adopted,
- the software used,
- the computation time for the dynamic analysis and the hardware used.

2. MATERIAL PROPERTIES

All the information available on the materials properties of materials are presented in the file "data of the 2nd B-W" § 2 and appendices A1 to A3.

Material property zones

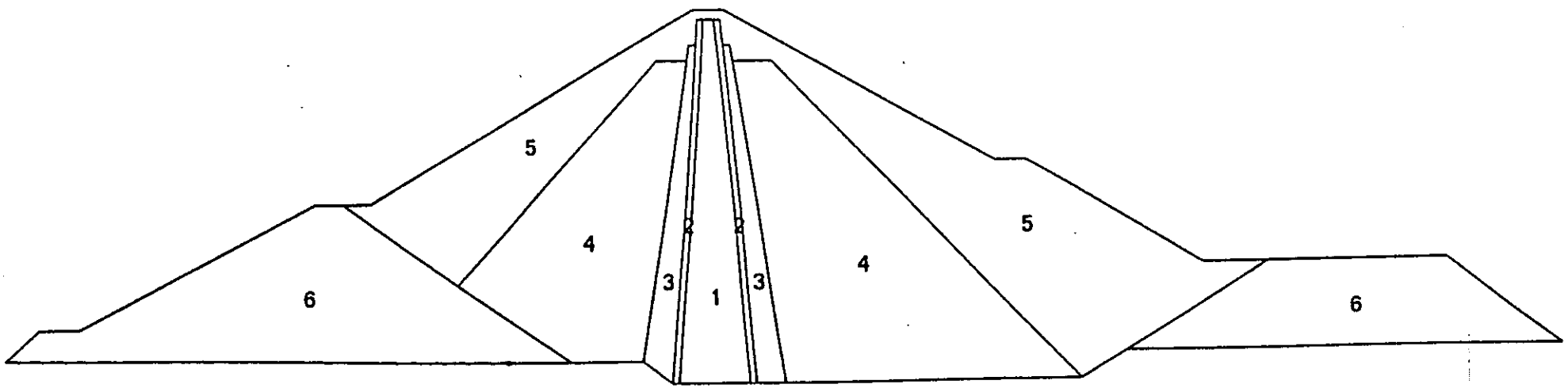

Fig. 1

2.3. Filter

El Infiernillo filters are composed of "Pinzandaran" sand, on which little information is available.

Triaxial tests are given in Appendix 2. A special apparatus was used for testing cylindrical specimens 113 cm in diameter and 250 cm high. Confining pressures were limited to 1 kg/cm^2, and tests were performed under dry conditions.

File FILTER.DAT on the diskette gives the data corresponding to Fig. A2.1, A2.2 and A2.4.

Dam Material		
Zone	**Name**	**Description**
1	Impervious Core	Plastic clayey soils, average liquid limit 49%, average optimum water content 19.3%
2	Filters	Sand from alluvial deposits, washed and screened, max. size 1/4 inch sieve, D10 average 0.22 mm
3	Transition Zone	Muck from underground excavations, silicified conglomerate, maximum size 150 mm, D10 average 2 mm
4	Inner Shoulder	Compacted rockfill, Dioritic rock or silicified conglomerate, maximum size 45 cm
5	Outer Shoulder	Dumped rockfill: same material as 4 above
6	Cofferdams (integrated)	Dumped rockfill, same material as 4 above

Table 1 : Basic Description of Materials

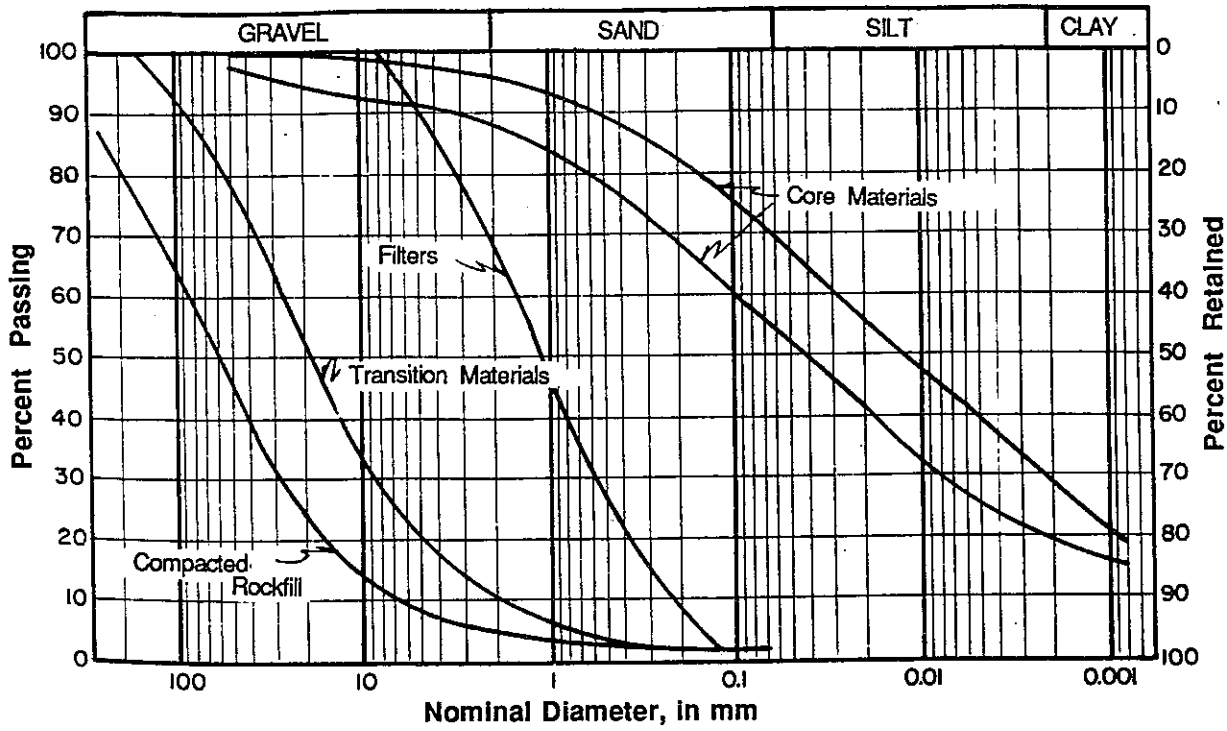

GRANULOMETRY OF THE DAM'S MATERIALS (From Ref. (2))

Fig. 2

Properties	Core	Filters	Transitions	Rockfill	
Grain density	2.75	2.76	2.75	2.71	
Dry density	1.59	1.87	2.02	Dumped	Compacted
				1.76	1.85
Permeability (cm/s)	2.10^{-8}	8.10^{-3}	7.10^{-2}	-	

Table 2

2.4. Transition Material

No further information is available on this material. The participant may either estimate parameters on the basis of known results on similar materials, or adapt parameters from the filter or rockfill materials.

2.5. Rockfill

Different types of rockfill were used on the site, particularly dumped and compacted rockfill for the dam shoulders and large size rockfill on the upstream slope of the dam above el. 110. The large size rockfill will be assimilated to "dumped rockfill".

Two series of tests were carried out on loose and dense samples at mean densities closely corresponding to those of the dumped and compacted rockfill respectively. The materials tested were a mix of the different quarries products actually used on the site, with no blocks larger than 200 mm in diameter (see Appendix 3).

As for the filter tests, special triaxial apparatus were used for studying cylindrical specimens of 113 cm in diameter and 250 cm in height. The results and description of these tests can be found in Appendix 3. No detailed information is available on the consolidation phase.

File ROCKFILL.DAT on the diskette gives the data corresponding to Fig. A3.2 to A3.7.

2.6. Rock Foundation

The foundation is composed of sound rock consisting of silicified conglomerate with basaltic dykes. It will be considered rigid and impermeable in all the study.

2.7. Other Material Static Properties

Material properties other than those given above, which may be required for various material models or analytic methods, must be established by the participant on the basis of known results for similar materials. The assumptions and references should be clearly stated, so as to enable the given data to be compared in this and future workshops.

NOTES

APPENDIX 1

Laboratory Tests with Samples Obtained from the Core Material During Construction

Impervious Core Materials

Obtention of Samples

During construction, the personnel of the Laboratory at the site obtained chunk samples with sides approximately 25 cm long. These samples were transported by plane from El Infiernillo to Mexico City, protected by means of wax and surrounded with saw dust in wooden boxes. Sampling was performed a few days after compaction at various elevations in the dam between elevations 112 and 170, approximately. Samples were sent to Mexico City on a weekly basis during the period May-November 1963 with a total of 26 samples sent from El Infiernillo. Except for sample No. 23, which corresponds to material "laminated" by the effect of compaction, samples were processed according to the program which is described.

Tests

With the purpose of identifying materials sampled, the following characteristics were determined :

a) Initial water content, void ratio and degree of saturation (by duplicate sampling)

b) Liquid and plastic limits

c) Specific gravity (by duplicate sampling)

d) Unconfined compression (by duplicate sampling)

The shear strength was determined for two conditions of consolidation and drainage :

a) Unconsolidated, undrained tests (UU tests)

b) Consolidated, undrained tests (CU tests).

The specimens were tested under confining pressures of 1, 3 and 10 kg/cm^2. Samples 3.6 cm in diameter and 8 cm high were trimmed, and water contents and void ratios were determined systematically. Specimens were not saturated prior to testing. In order to detect the compressibility of the materials, one-dimensional consolidation tests were carried out by duplicate sampling, in floating rings 8 cm in diameter and 2.5 cm high. The specimens were kept in a humid atmosphere during the tests. The load increment ratio was 1 and the duration of each increment equal to 24 hours, approximately. Besides, specimens trimmed from samples 2 and 19 were subjected to long-term consolidation tests, allowing equilibrium to be reached

TABLE 1

EL INFIERNILLO DAM - MATERIALS FROM THE IMPERVIOUS CORE CLASSIFICATION TESTS

Sample	Elev.	ω_l	ω_p	I_ω	F_ω	ω_i	e_i	S_s	S_u	S_r
	m	%	--	--	--	%	--	--	Kg/cm^2	%
1	112.47	56.6	22.8	33.8	11.6	24.0	0.69	2.68	2.05	7.5
						22.5	0.65	2.69	2.16	6.0
2	115.95	59.3	23.1	36.2	11.6	23.1	0.65	2.71	0.94	2.7
						21.3	0.66	2.71	2.06	5.3
3	120.12	44.6	19.6	25.0	6.5	19.5	0.60	2.69	3.38	3.9
						20.8	0.54	2.67	1.05	3.4
4	122.47	57.8	22.4	35.4	12.9	21.1	0.62	2.72	1.84	12.3
						19.7	0.58	2.72	2.08	12.8
5	123.50	48.0	20.2	27.8	12.4	20.1	0.59	2.68	2.63	8.3
						20.4	0.56	2.69	2.88	8.7
6	127.53	44.5	21.3	23.2	6.4	15.6	0.48	2.71	2.69	6.8
						17.8	0.51	2.72	2.31	7.9
7	128.49	46.9	20.8	26.1	10.8	18.5	0.53	2.70	2.34	8.5
						20.1	0.60	2.70	1.58	5.2
8	129.33	47.1	21.4	25.7	10.9	21.0	0.59	2.70	1.67	12.7
						21.3	0.59	2.70	1.28	9.9
9	130.88	45.4	21.5	23.9	9.5	30.3	0.57	2.68	1.38	10.7
						19.6	0.56	2.71	1.35	8.2
10	131.87	45.2	19.9	25.3	11.3	21.3	0.62	2.71	1.20	13.3
						21.3	0.61	2.71	1.06	9.7
11	135.33	44.3	19.7	24.6	10.9	17.5	0.50	2.71	1.88	5.1
						17.6	0.49	2.71	2.52	5.6
12	138.00	45.6	19.3	26.3	9.8	17.6	0.51	2.70	3.03	
						17.6	0.53	2.71	2.97	4.4
13	141.77	44.8	18.9	24.9	13.6	19.9	0.63	2.70	1.63	5.3
						20.1	0.58	2.70	1.92	2.7
14	141.85	42.8	20.8	22.0	13.0	16.7	0.49	2.71	2.72	8.7
						16.4	0.47	2.71	2.93	3.8
15	149.83	44.6	22.0	22.6	9.7	18.3	0.48	2.71	1.27	11.2
						17.8	0.51	2.71	1.86	11.0
16	147.22	40.7	20.5	20.2	13.3	19.9	0.55	2.71	1.27	6.4
						18.6	0.56	2.71	1.61	7.9
17	149.93	43.3	21.7	21.6	10.9	18.6	0.55	2.71	1.67	5.4
						17.6	0.48	2.71	1.79	4.1
18	151.19	44.7	20.3	24.4	14.6	20.0	0.52	2.70	2.02	13.1
						18.8	0.53	2.70	2.32	10.4
19	149.83	50.1	20.2	29.9	12.8	19.7	0.57	2.71	1.69	9.4
						19.4	0.52	2.71	1.92	11.4
20	154.83	43.2	20.4	22.8	14.5	18.8	0.54	2.71	2.04	10.7
						18.8	0.56	2.71	0.79	3.2
21	155.33	50.2	20.2	30.0	8.8	20.1	0.56	2.71	1.37	3.9
						20.7	0.56	2.71	0.86	12.2
22			No Result							
23	164.39	40.8	19.1	21.7	9.7	18.6	0.52	2.70	0.76	5.2
						18.4	0.46	2.72	1.53	12.8
24	166.22	44.2	19.1	25.1	14.4	17.3	0.49	2.72	1.35	6.6
						17.2	0.51	2.72	1.94	12.3
25	165.01	43.4	20.0	23.4	14.1	18.9	0.52	2.71	1.12	6.4
									1.56	7.8
26	169.17					18.0	0.50	2.71	1.92	9.6
Mean Value		46.6	20.6	26.0	11.4	19.3	0.55	2.71	1.84	
Standard Deviation		4.7	1.6	3.6	2.3	2.1	.07	0.01	0.78	

EL INFIERNILLO DAM - MATERIALS FROM THE IMPERVIOUS CORE
INITIAL WATER CONTENT HISTOGRAMS

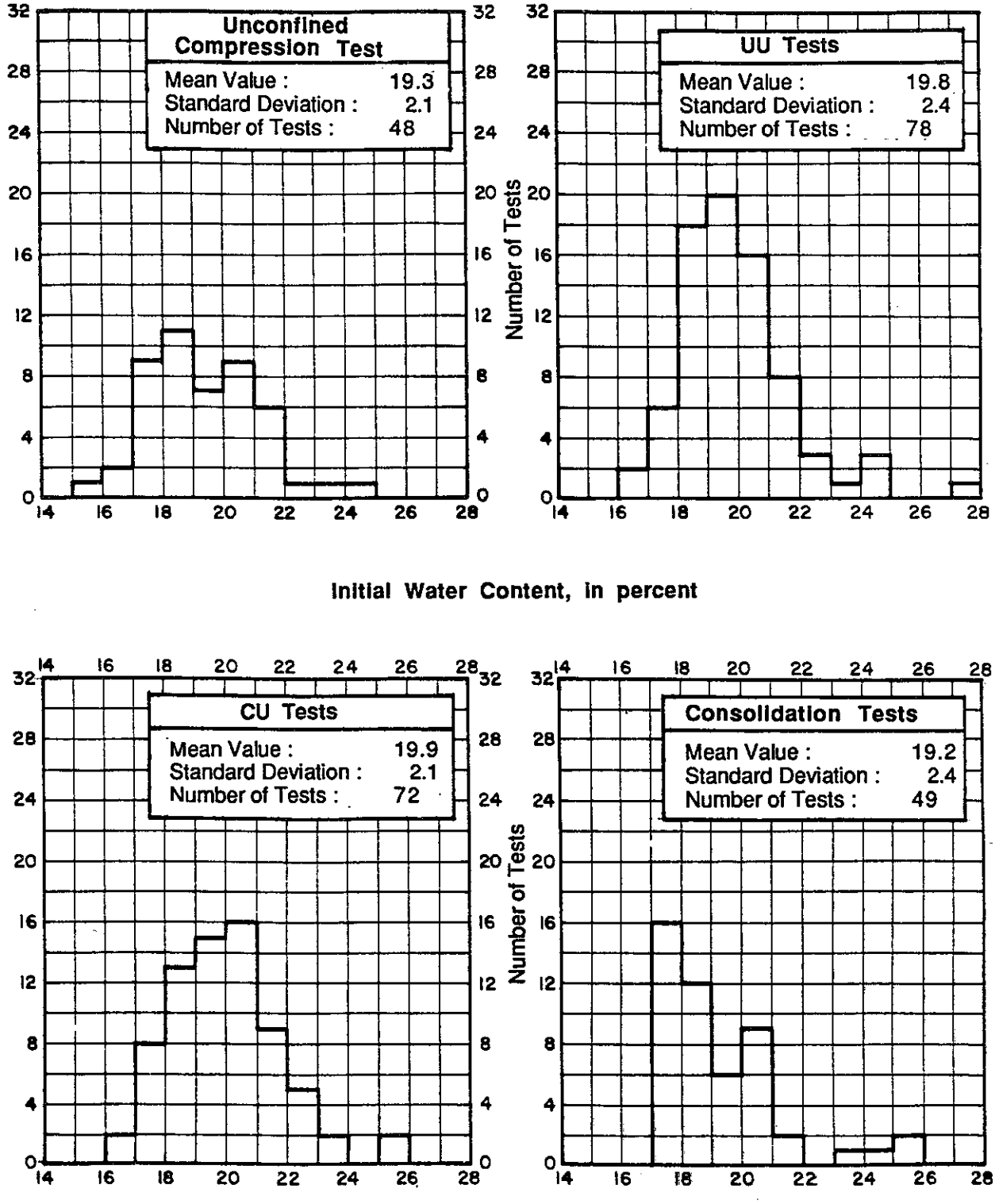

Fig. A1.2

TABLE 2

EL INFIERNILLO DAM - MATERIALS FROM THE IMPERVIOUS CORE
UU TRIAXIAL TESTS

Sample	Elev.	ω_i	e_i	σ_3	$\sigma_1-\sigma_3$	ω_i	e_i	σ_3	$\sigma_1-\sigma_3$	ω_i	e_i	σ_3	$\sigma_1-\sigma_3$
	m		--	Kg/cm²	Kg/cm²	%	--	Kg/cm²	Kg/cm²	%	--	Kg/cm²	Kg/cm²
1	112.47	24.8	0.71	1.00	2.04	24.9	0.69	2.99	2.36	22.2	0.63	10.1	3.36
2	115.95	23.1	0.66	1.02	2.01	27.3	0.76	3.04	1.89	24.8	0.70	10.1	2.44
3	120.12	20.4	0.57	1.00	2.89	21.6	0.60	3.02	2.86	18.7	0.58	10.1	4.90
4	122.47	20.1	0.58	1.01	2.22	21.0	0.59	3.03	2.10	22.0	0.63	10.1	2.49
5	123.50	19.5	0.54	1.01	2.21	19.8	0.59	3.00	3.19	20.9	0.61	10.1	2.17
6	127.53	18.7	0.58	1.07	2.36	19.0	0.57	3.03	2.95	21.4	0.62	10.1	2.94
7	128.49	19.4	0.56	1.17	2.30	20.0	0.59	3.00	2.66	19.3	0.57	10.0	3.07
8	129.33	21.0	0.59	1.02	1.24	21.3	0.59	3.01	1.76	20.8	0.54	10.1	1.73
9	130.88	21.0	0.65	1.09	1.65	20.7	0.59	3.09	1.68	20.6	0.62	10.0	1.95
10	131.87	20.7	0.58	1.01	1.35	22.4	0.54	3.04	0.91	21.2	0.58	10.1	1.55
11	135.33	19.1	0.48	1.00	1.61	18.3	0.47	3.02	1.84	18.1	0.52	10.1	3.05
12	138.00	18.9	0.56	1.00	2.73	18.2	0.55	3.00	3.73	17.8	0.51	10.1	3.99
13	141.77	19.4	0.57	1.01	2.20	19.1	0.57	3.02	2.40	20.1	0.58	10.0	2.53
14	141.85	16.6	0.51	1.00	3.13	17.8	0.55	3.00	3.00	17.6	0.54	10.0	3.58
15	149.83	20.5	0.56	1.05	1.56	20.3	0.56	3.00	1.64	20.0	0.55	10.0	1.78
16	147.22	19.5	0.58	1.03	1.89	20.2	0.61	3.00	2.05	18.2	0.57	10.0	3.47
17	149.93	19.5	0.49	1.04	2.14	19.6	0.53	3.00	2.22	18.9	0.56	10.0	3.10
18	151.19	19.1	0.54	1.11	3.08	18.5	0.54	3.00	3.18	18.8	0.55	10.0	3.21
19	149.83	18.8	0.54	1.08	2.35	20.1	0.55	3.09	2.07	19.6	0.61	10.0	2.06
20	154.83	18.1	0.51	1.04	2.04	18.8	0.56	3.00	2.80	18.8	0.55	10.0	2.36
21	155.33	18.2	0.47	1.04	2.11	20.0	0.59	3.00	2.26	20.5	0.60	10.0	2.32
22						No Result							
23	164.39	19.0	0.54	1.00	1.98	19.2	0.49	3.00	1.80	19.0	0.51	10.0	2.09
24	166.22	17.0	0.46	1.07	3.15	16.8	0.47	3.00	3.28	17.9	0.48	10.0	2.41
25	165.01	19.2	0.55	1.03	1.99	18.9	0.50	3.07	2.09	19.8	0.58	10.0	2.03
26	169.17	18.4	0.51	0.98	1.98	18.5	0.52	3.00	2.40	17.4	0.48	10.0	5.74
Mean Value		19.6	0.55	1.03	2.17	20.1	0.57	3.02	2.36	19.6	0.57	10.04	2.81
Standard Deviation		1.7	0.01	0.11	0.50	2.20	0.06	0.11	0.65	3.1	0.06	.05	0.98

TABLE 3

EL INFIERNILLO DAM - MATERIALS FROM THE IMPERVIOUS CORE CU TRIAXIAL TESTS

Sample	Elev. m	ω_i %	e_i --	σ_3 Kg/cm²	$\sigma-\sigma_3$ Kg/cm²	ω_f %	ω_i %	e_i --	σ_3 Kg/cm²	$\sigma-\sigma_3$ Kg/cm²	ω_f %	ω_i %	e_i --	σ_3 Kg/cm²	$\sigma-\sigma_3$ Kg/cm²	ω_f %
1	112.47	22.3	0.61	1.00	2.41	23.9	22.7	0.65	3.00	3.98	23.5	23.6	0.68	10.0	6.56	21.8
2	115.95	23.9	0.69	1.02	2.69	22.7	22.9	0.69	2.95	3.39	23.4	22.3	0.63	10.1	7.40	20.5
3	120.12	19.7	0.54	1.02	2.81	20.7	18.6	0.57	3.00	4.03	20.0	22.3	0.63	10.1	8.15	20.9
4	122.47	21.2	0.59	1.00	2.04	22.1	20.9	0.59	3.00	3.70	21.3	18.9	0.56	10.0	9.62	17.4
5	123.50	18.5	0.58	0.95	2.76	19.3	19.7	0.59	3.00	3.11	19.6	20.2	0.55	10.1	8.61	17.3
6	127.53	19.7	0.60	0.95	2.71	20.3	17.9	0.58	3.00	4.24	17.5	18.5	0.61	10.0	8.36	16.2
7	128.49	19.8	0.62	1.09	2.34	20.7	25.2	0.77	3.00	2.22	24.8					
8	129.33	21.1	0.59	1.03	2.45	21.7	21.6	0.62	3.00	3.37	20.0	20.5	0.58	10.0	8.80	18.4
9	130.88	21.2	0.59	1.09	1.79	20.6	21.1	0.63	3.00	3.22	20.2	21.6	0.59	10.0	8.07	18.2
10	131.87	20.5	0.59	0.98	1.91	20.1	19.4	0.54	3.00	4.06	19.3	21.2	0.60	10.0	7.79	17.0
11	135.33	17.9	0.47	1.02	2.16	18.1	18.1	0.50	3.10	3.83	17.6	18.3	0.52	10.0	9.11	15.4
12	138.00	17.9	0.43	1.00	2.91	17.9	19.2	0.54	3.10	3.96	18.6	17.7	0.58	10.0	8.16	16.3
13	141.77	25.9	0.62	1.10	1.91	26.3	20.2	0.55	3.00	3.09	21.1	20.1	0.56	10.0	8.00	17.3
14	141.85	17.6	0.51	1.02	3.22	18.1	18.6	0.49	3.01	4.49	17.5	17.7	0.46	10.0	9.33	15.5
15	149.83	20.4	0.57	1.02	1.89	20.0	20.2	0.51	3.00	3.73	18.4	20.7	0.56	10.0	7.86	17.7
16	147.22	16.0	0.57	1.02	2.28	16.0	19.4	0.56	3.00	4.36	18.6	20.0	0.60	10.0	8.31	16.9
17	149.93	20.1	0.57	1.06	2.75	20.2	20.0	0.54	3.00	3.67	21.3	20.9	0.60	10.0	7.44	18.1
18	151.19	18.9	0.54	1.09	3.00	19.6	21.0	0.53	3.03	3.41	19.5	20.3	0.57	10.0	7.66	17.7
19	149.83	18.0	0.61	1.02	2.45	19.1	20.2	0.53	3.00	3.29	19.1	19.4	0.52	10.0	8.24	16.5
20	154.83	19.1	0.54	1.04	2.82	19.1	18.8	0.53	3.06	3.72	17.4	19.0	0.54	10.0	10.25	16.2
21	155.33	20.3	0.55	1.06	2.41	20.6	21.6	0.60	3.00	3.11	20.9	19.8	0.54	10.0	8.80	17.0
22							No Result									
23	164.39	19.0	0.54	1.03	2.86	18.5	19.0	0.51	3.00	4.74	17.1	18.9	0.51	10.0	10.37	15.8
24	166.22	18.5	0.52	1.01	2.91	18.2	17.7	0.49	3.00	5.30	16.9	19.0	0.52	10.0	9.91	16.2
25	165.01						18.8	0.50	3.00	3.99	17.5	19.3	0.53	10.0	8.72	18.6
26	169.17						17.5	0.51	3.00	4.56	17.2	16.9	0.51	10.0	9.53	15.4
Mean Value		19.9	0.57	1.03	2.48	20.1	20.0	0.56	3.01	3.77	19.5	19.8	0.56	10.01	8.59	17.4
Standard Deviation		2.1	0.05	0.04	0.50	2.8	1.8	0.10	0.03	0.70	2.1	2.4	0.09	0.03	0.26	1.6

EL INFIERNILLO DAM - MATERIALS FROM THE IMPERVIOUS CORE
OEDOMETER CONSOLIDATION TESTS

Void Ratio vs. Normal Pressure
Coefficient of Compressibility vs. Normal Pressure

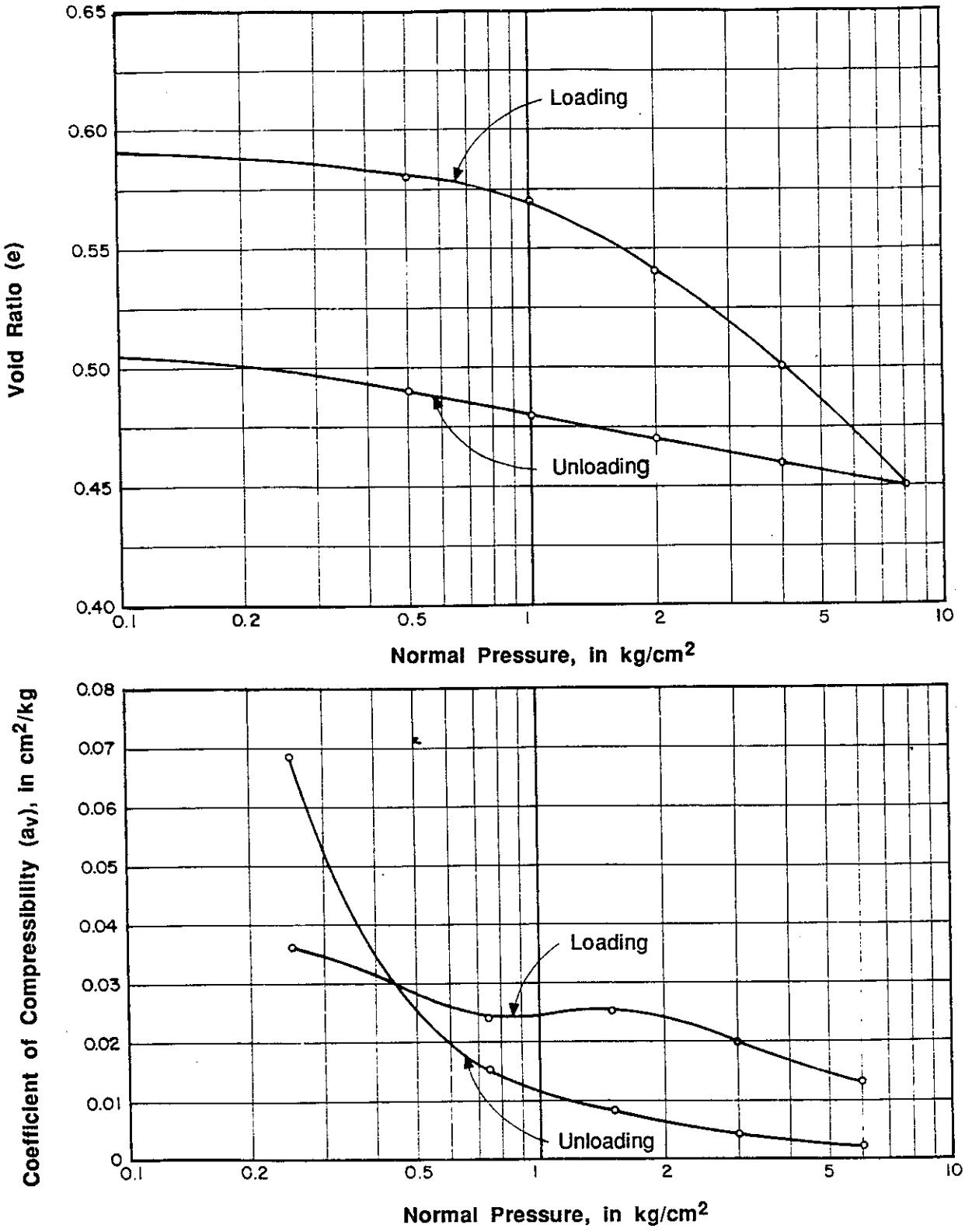

Fig. A1.5

EL INFIERNILLO DAM - MATERIALS FROM THE IMPERVIOUS CORE
OEDOMETER CONSOLIDATION TESTS

Strain vs. Time

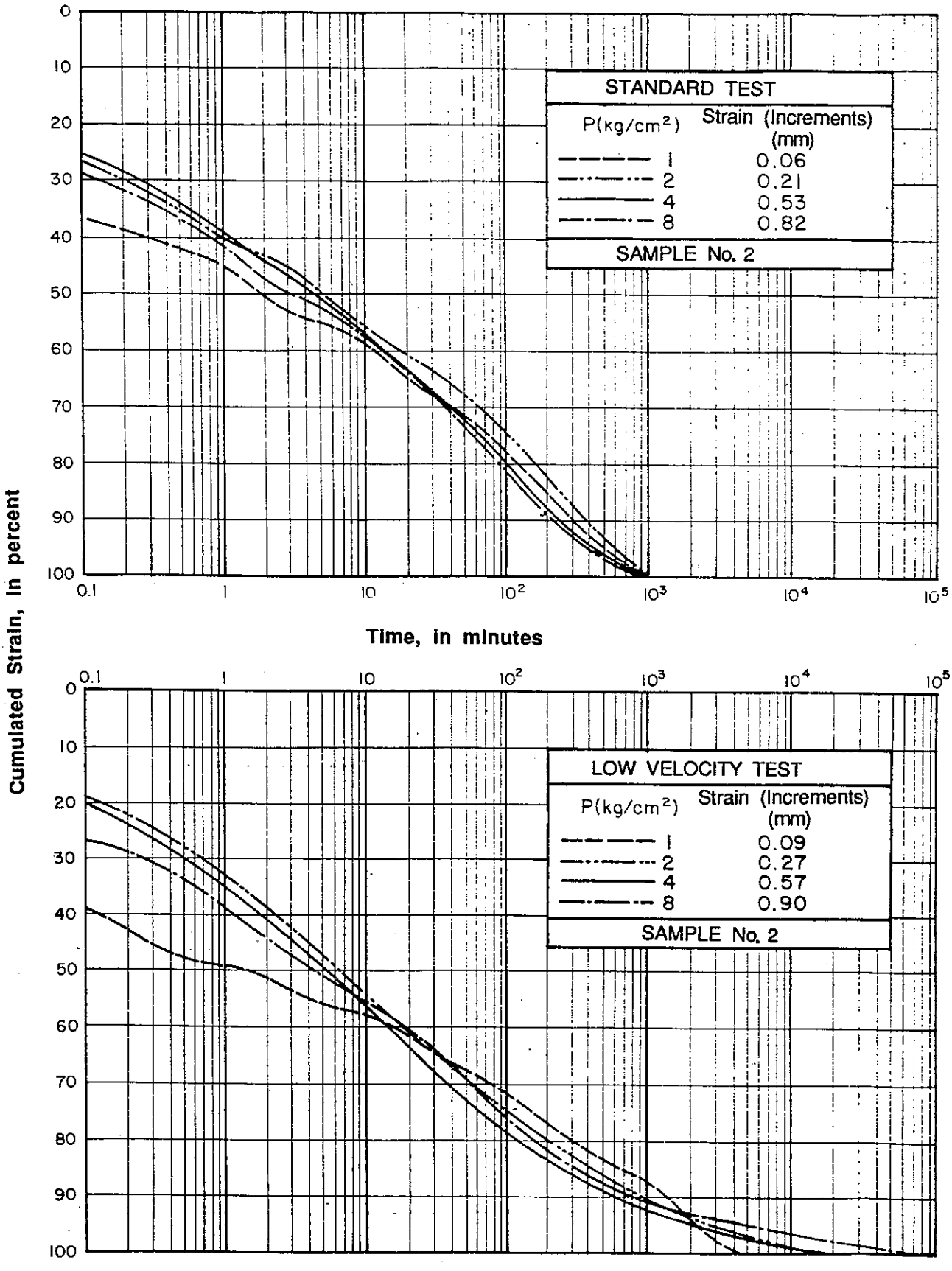

Fig. A1.6

TABLE 4

EL INFIERNILLO DAM - MATERIALS FROM THE IMPERVIOUS CORE OEDOMETER CONSOLIDATION TESTS

Sample	Elev. m	ω_i %	e_i --	a_v (loading) 0.25	0.75	1.5	3	6	a_v (unloading) 0.25	0.75	1.5	3	6
1	112.47	25.4	0.76	0.028	0.024	0.029	0.024	0.018	0.070	0.013	0.008	0.005	0.004
		24.6	0.76	0.030	0.038	0.030	0.030	0.020	0.100	0.024	0.008	0.005	0.004
2	115.95	21.2	0.64	0.023	0.021	0.024	0.019	0.014	0.068	0.014	0.007	0.004	0.002
		20.6	0.63	0.020	0.010	0.011	0.015	0.013	0.094	0.020	0.008	0.006	0.002
3	120.12	17.5	0.53	0.021	0.006	0.012	0.010	0.008	0.050	0.012	0.006	0.003	0.001
		17.5	0.53	0.025	0.008	0.013	0.015	0.010	0.068	0.014	0.008	0.003	0.001
4	122.47	25.2	0.76	0.030	0.033	0.046	0.027	0.017	0.107	0.020	0.011	0.005	0.002
		23.4	0.69	0.030	0.027	0.032	0.023	0.015	0.089	0.016	0.010	0.004	0.002
5	123.50	20.6	0.60	0.044	0.022	0.028	0.020	0.012	0.072	0.016	0.009	0.003	0.002
		19.1	0.58	0.032	0.016	0.020	0.017	0.011	0.074	0.017	0.009	0.004	0.002
6	127.53	17.8	0.56	0.037	0.027	0.029	0.013	0.012	0.064	0.016	0.009	0.003	0.001
		18.7	0.58	0.039	0.024	0.026	0.020	0.012	0.067	0.015	0.009	0.004	0.001
7	128.49	19.6	0.61	0.022	0.022	0.022	0.020	0.014	0.051	0.014	0.008	0.004	0.002
		18.5	0.59	0.022	0.020	0.023	0.019	0.012	0.039	0.014	0.009	0.004	0.002
8	129.33	21.1	0.63	0.032	0.033	0.031	0.023	0.014	0.078	0.017	0.010	0.004	0.002
		20.4	0.62	0.030	0.035	0.030	0.021	0.013	0.083	0.016	0.009	0.004	0.002
9	130.88	20.0	0.59	0.039	0.029	0.030	0.022	0.013	0.073	0.014	0.003	0.007	0.002
		20.2	0.60	0.041	0.033	0.032	0.022	0.013	0.078	0.014	0.009	0.004	0.002
10	131.87	20.0	0.61	0.039	0.036	0.031	0.020	0.014	0.081	0.013	0.009	0.004	0.002
		20.3	0.61	0.044	0.043	0.036	0.025	0.015	0.087	0.014	0.009	0.004	0.002
11	135.33	18.9	0.57	0.030	0.025	0.027	0.019	0.012	0.043	0.026	0.007	0.004	0.001
		17.9	0.53	0.032	0.023	0.023	0.016	0.010	0.049	0.027	0.008	0.004	0.001
12	138.00	18.5	0.57	0.028	0.015	0.017	0.015	0.012	0.060	0.016	0.008	0.003	0.002
		17.9	0.55	0.028	0.018	0.021	0.016	0.011	0.069	0.014	0.008	0.004	0.002
13	141.77	20.2	0.61	0.043	0.032	0.032	0.025	0.017	0.079	0.016	0.009	0.005	0.001
		20.0	0.62	0.029	0.025	0.029	0.022	0.014	0.109	0.014	0.008	0.004	0.002
14	141.85	17.7	0.56	0.026	0.018	0.018	0.015	0.011	0.063	0.017	0.006	0.004	0.001
		17.8	0.55	0.026	0.018	0.021	0.015	0.010	0.058	0.015	0.007	0.004	0.001
15	145.14	19.6	0.60	0.047	0.036	0.030	0.020	0.012	0.065	0.017	0.008	0.003	0.001
		19.0	0.58	0.039	0.035	0.028	0.018	0.012	0.079	0.013	0.007	0.003	0.001
16	147.22	18.4	0.58	0.046	0.020	0.021	0.043	0.012	0.069	0.015	0.009	0.004	0.002
		18.0	0.54	0.028	0.022	0.018	0.033	0.011	0.045	0.011	0.007	0.003	0.001
17	149.93	18.6	0.56	0.049	0.014	0.018	0.015	0.011	0.054	0.015	0.010	0.003	0.001
18	151.19	17.9	0.60	0.051	0.019	0.020	0.020	0.016	0.096	0.012	0.008	0.003	0.001
		17.8	0.59	0.032	0.016	0.018	0.016	0.013	0.066	0.010	0.009	0.004	0.002
19	149.83	17.9	0.59	0.037	0.018	0.024	0.020	0.013	0.082	0.014	0.007	0.004	0.002
		18.1	0.59	0.028	0.021	0.024	0.021	0.015	0.060	0.014	0.009	0.004	0.001
20	154.83	19.4	0.65	0.032	0.043	0.037	0.024	0.013	0.061	0.014	0.008	0.003	0.002
		19.5	0.63	0.049	0.028	0.029	0.020	0.013	0.057	0.015	0.008	0.004	0.001
21	155.33	18.2	0.57	0.044	0.028	0.027	0.018	0.011	0.056	0.018	0.005	0.003	0.001
		17.8	0.56	0.039	0.026	0.025	0.019	0.012	0.058	0.014	0.009	0.003	0.002
22				No Result									
23	164.39	17.6	0.53	0.039	0.023	0.021	0.015	0.011	0.049	0.012	0.006	0.003	0.001
		18.0	0.55	0.052	0.026	0.025	0.017	0.011	0.054	0.012	0.008	0.003	0.002
24	166.22	17.8	0.55	0.023	0.014	0.018	0.016	0.012	0.064	0.014	0.006	0.004	0.001
		17.7	0.54	0.032	0.016	0.018	0.014	0.009	0.057	0.016	0.007	0.004	0.001
25	165.01	18.1	0.63	0.044	0.029	0.038	0.024	0.015	0.066	0.012	0.010	0.004	0.002
		18.2	0.59	0.032	0.026	0.026	0.019	0.012	0.061	0.014	0.009	0.004	0.002
26	169.17	17.3	0.56	0.047	0.023	0.023	0.015	0.010	0.047	0.014	0.008	0.004	0.002
		17.6	0.58	0.046	0.022	0.022	0.017	0.011	0.056	0.015	0.009	0.004	0.002
Mean Value		19.2	0.60	0.036	0.024	0.025	0.020	0.013	0.068	0.015	0.008	0.004	0.002
Standard Deviation		2.4	0.06	0.011	0.009	0.007	0.006	0.002	0.016	0.004	0.002	0.001	0.001

APPENDIX 2

Laboratory Tests with Samples from the Sand Used for the Filters

Filter Materials

Introduction

Two series of tests were performed : in one series the material was placed in the loosest possible state ; in the other, compaction was used in order to achieve a better arrangement of the particles. For the first series, the material was dropped from a 50 liter bucket and distributed in layers ; to obtain the second condition, the sample was placed in layers 25 cm thick and compacted with blows by a hand tamper. The materials were tested in dry state and under two or three confining pressures in the range 0.3-0.7 kg/cm^2.

Due to various problems relative to the operation of the equipment and the performance of the tests, the information presented may be incomplete in several respects or may even contain dubious data.

Tests

After applying the confining pressure and checking that the specimen had reached an equilibrium condition, the axial load was applied in at least ten increments, before failure. Readings of three axial strain meters and five circumferential strain meters were made approximately five minutes after the application of each load increment. When a state of failure was reached, it was specified that the pressure in the jacks be measured at equally spaced intervals of axial deformation, as pumping proceeded at uniform speed. When the necessary care was taken in the preparation of the specimen and in centering the cap with respect to the load application devices, performance of the tests presented no special problem.

Results

Axial and circumferential deformations were divided by the length and the initial perimeter of the specimen, respectively, in order to obtain corresponding strains ϵ_a and ϵ_r. From readings made in the Bourdon gauges and with the aid of calibration curves, axial loads were computed ; the quotient between this and the corrected area provided values of the deviator stress $(\sigma_1 - \sigma_3)$. It must be noted that the above-mentioned areas of the specimen were computed on the basis of the average perimeter measured in each increment. Information obtained in this manner for Pinzandaran sand is presented in Fig. A2.1 and A2.2. Curves from Fig. A2.1 were obtained from the denser sample, showing variations of the deviator stress $(\sigma_1 - \sigma_3)$ and the radial strain ϵ_r in terms of the axial strain ϵ_a ; in addition, changes of unit

volume ϵ_v are included ; these were computed using values of ϵ_a and ϵ_r through the known formula $\epsilon_v = 2\,\epsilon_r + \epsilon_a$.

Graphs of Fig. A2.2 present data of all tests performed (loose and dense samples), but drawn on logarithmic paper.

This type of presentation has been favored because it was noticed that the relationships between $(\sigma_1 - \sigma_3)$, ϵ_r and ϵ_a can best be appreciated in this manner. The group of graphs has an adjoining table in which the values of the initial void ratio, confining pressure, maximum principal stress at failure, and two parameters which define the shape of curves shown, are tabulated. Fig. A2.3 includes a photograph of a specimen of the sand after failure and corresponding Mohr envelopes.

Graphs of Fig. A2.4 present results of confined compression tests performed with loose and dense samples.

Appendix 2

FILTER MATERIALS

List of the Figures

EL INFIERNILLO DAM - MATERIALS FROM THE FILTERS
PINZANDARAN SAND

Triaxial Test

Denser Sample

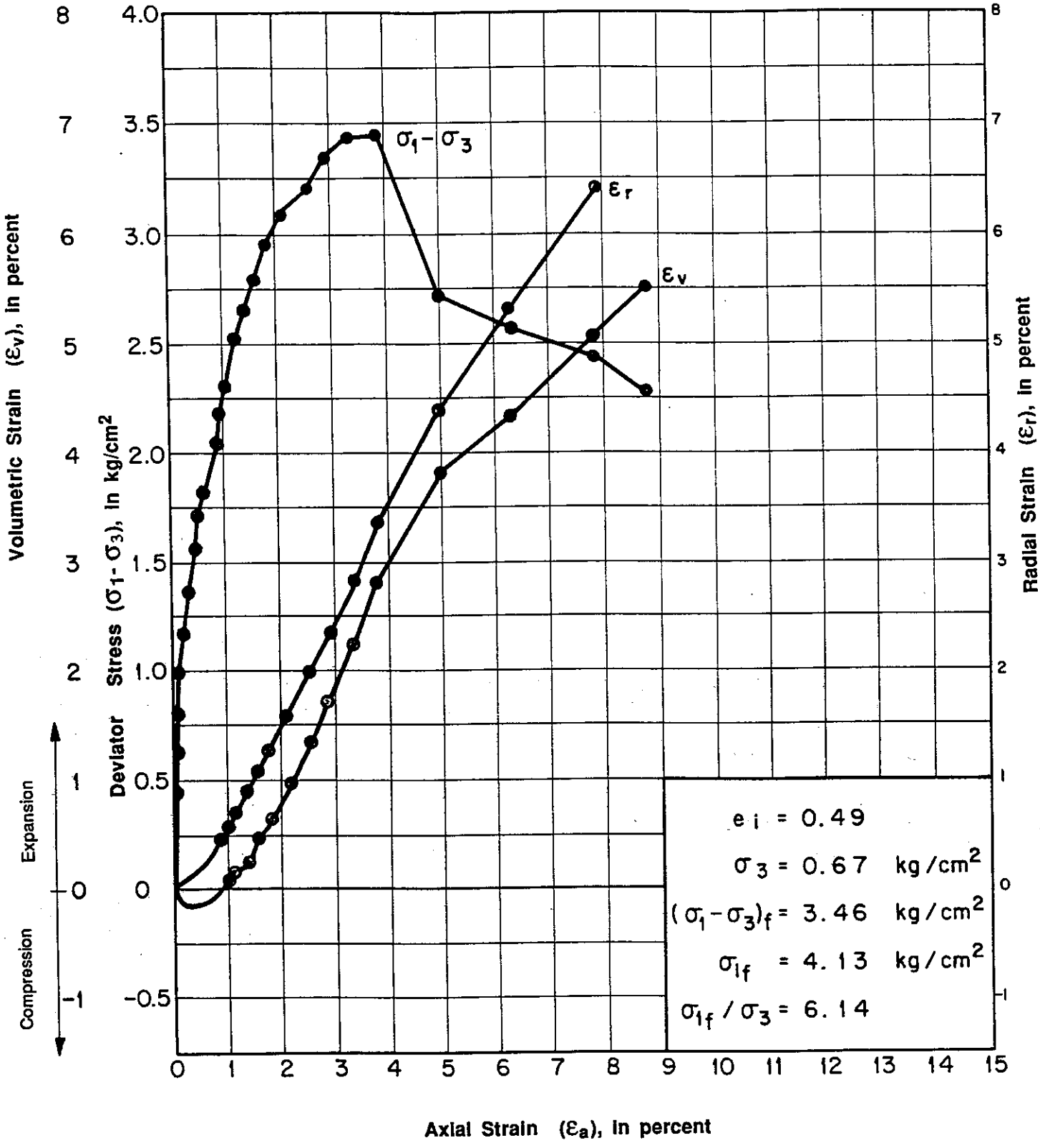

Samples 113 cm in Diameter, Dry State
Confining Pressures Less Than 1 kg/cm²

Fig. A2.1

EL INFIERNILLO DAM - MATERIALS FROM THE FILTERS
PINZANDARAN SAND

Triaxial Tests

Samples 113 cm In Diameter, Dry State
Confining Pressures Less Than 1 kg/cm²

Fig. A2.2

EL INFIERNILLO DAM - MATERIALS FROM THE FILTERS
PINZANDARAN SAND

Triaxial Tests

Samples 113 cm in Diameter, Dry State
Confining Pressures Less Than 1 kg/cm^2

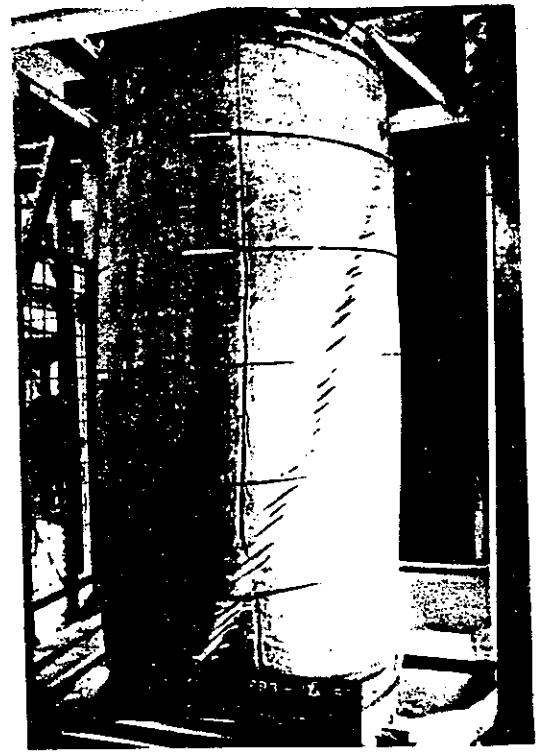

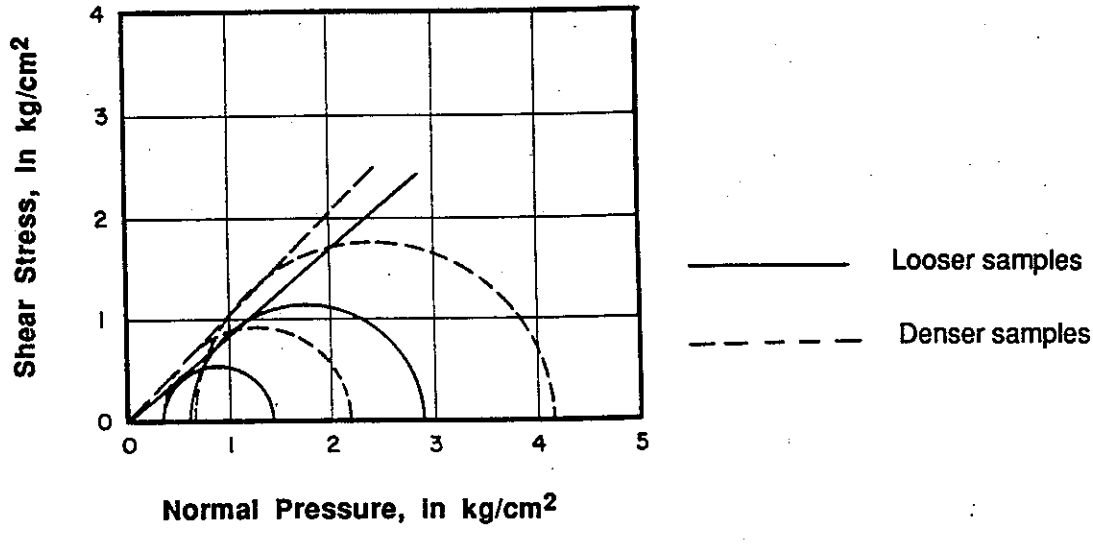

MOHR ENVELOPES

Fig. A2.3

EL INFIERNILLO DAM - MATERIALS FROM THE FILTERS
PINZANDARAN SAND

Confined Compression Test

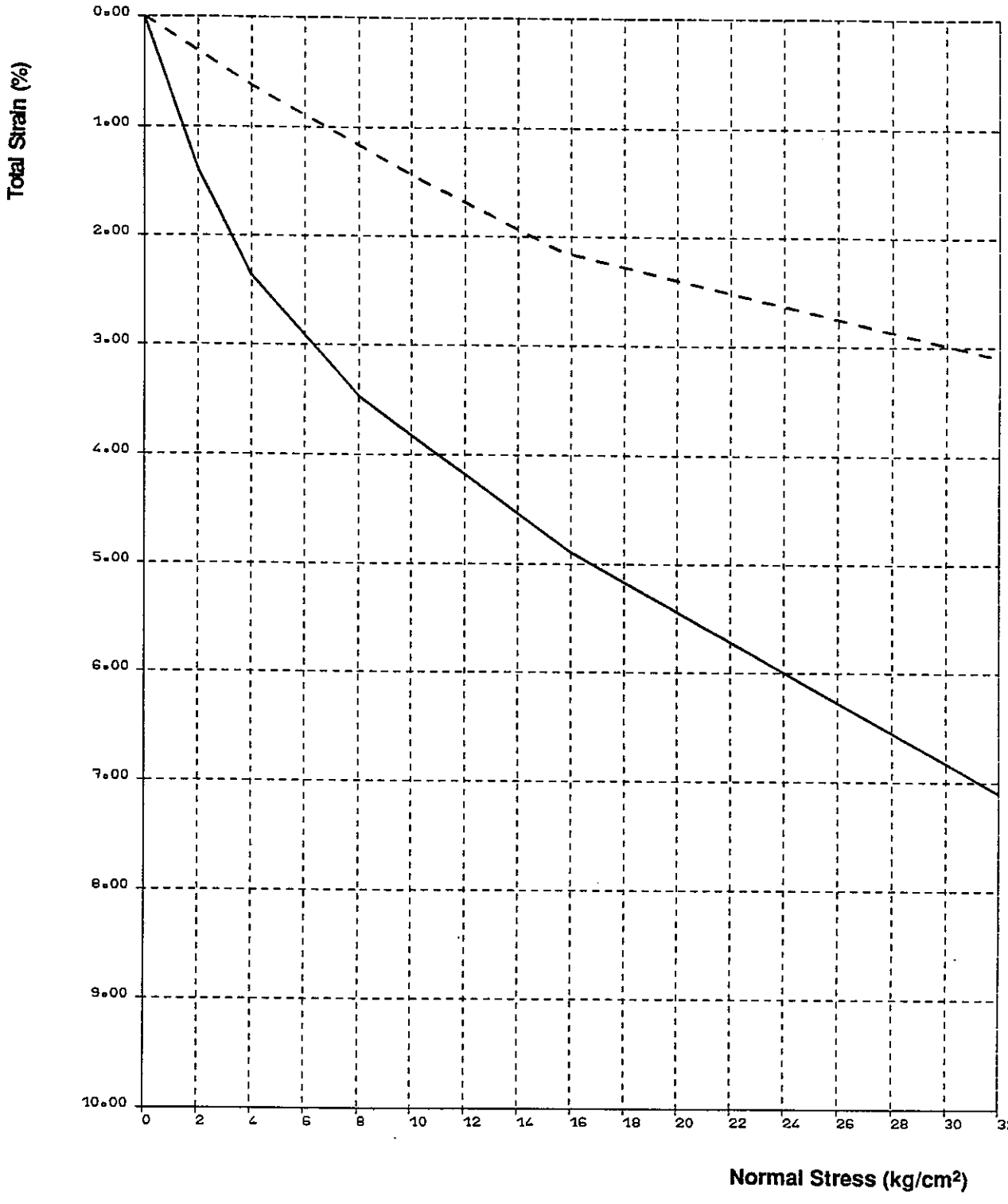

Fig. A2.4

NOTES

APPENDIX 3

Laboratory Tests with Samples Obtained from the Rockfill Shoulders During Construction

Rockfill Shoulders Materials

Introduction

The material tested was obtained from field density tests on samples excavated both in the compacted and dumped rockfill zones of the dam, with the purpose of determining dry unit weights during construction. In some layers, the material placed was a sound diorite, the product of excavation by blasting one of the quarries and in others it was a silicified conglomerate from other quarries excavated closer to the dam. Both rockfill materials are formed by angular fragments but the granulometric composition presents appreciable discrepancies. Notwithstanding that materials for the specimens were carefully mixed at the laboratory, curves of Fig. A3.1 show that specimens tested had gradations differing appreciably from one to another.

Testing Procedure

The rockfill samples described above were tested under confining pressures of 2, 5, 10, 17 and 25 kg/cm^2, approximately.

It was intended to prepare the specimens with two densities, one corresponding to the loosest state and one to the densest, by using different specifications for the placing of layers ; these operations were carried out by hand and the required time for building up each specimen was approximately twelve hours.

Axial loads were applied to the specimens following the stress control procedure. Each increment was applied after reaching apparent equilibrium under the effect of the preceding one ; the resulting duration of each load increment varied between 20 minutes and one hour.

Results

Data obtained in the tests have been summarized in Tables 1 and 2. The laws of variation of deviator stresses ($\sigma_1 - \sigma_3$), radial strains (ϵ_r) and volumetric strains (ϵ_v) in terms of axial strains (ϵ_a) recorded in each test, are shown in Fig. A3.2 to A3.7

It must be emphasized that the radial strain ϵ_r is measured with circumferential extensometers, and that ϵ_v is deduced from ϵ_r and ϵ_a by the formula $\epsilon_v = \epsilon_a + 2.\epsilon_r$. However, later tests on different materials have shown that the volumetric strain ϵ'_v obtained from the measurement of water volumes flowing out the sample could be noticeably different from ϵ_v. As a matter of comparison, Fig. A3.9 at the end of this

appendix gives an appreciation of this difference. ϵ'_v can be considered here as more realistic than ϵ_v.

Observations relative to difficulties affecting the tests are included, because they can be useful in the interpretation of results. In Fig. A3.8, Mohr circles have been drawn for the failure condition and the tangent to each circle passing through the origin of coordinates is indicated. For reasons of clarity, the corresponding envelopes have not been drawn.

Comments and conclusions

As was noted at the beginning, the construction of the specimens was affected by several defects ; the average volumetric weight varied between 1.7 and 1.9 ton/m^3, which corresponds to void ratios of 0.62 and 0.40, respectively (Tables 1 and 2). It must be noted that the volumetric weight of rockfills at El Infiernillo was 1.85 ton/m^3, on the average.

Grain size distribution determinations at the end of testing was not systematically determined. The principal stress ratio at failure undergoes an appreciable decrease when the confining pressure is raised from 1 to 25 kg/cm^2 ; for instance, in the first testing series (Table 1), it varies between 6 and 4, which corresponds to a reduction in the friction angle ϕ from 45 to 37°, approximately. It must be pointed out that materials tested were a mixture of sound fragments of silicified conglomerate and diorite, classified by geologists among the best materials that nature offers as a source for rockfill.

Deviator stress vs strain curves shown in Fig. A3.2 to A3.7 are usual in triaxial compression tests. However, attention must be paid to the magnitude of the strain necessary to produce failure of the specimen as the confining pressure increases. For instance, for σ_3 = 25 kg/cm^2, the strain that can be imposed on the specimen in the retained apparatus is hardly sufficient.

The analysis of graphs plotted in Fig. A3.2 to A3.7, shows that radial strains are practically zero during the first load increments, this effect being more noticeable when confining pressures are high. Consequently, reductions in volume are greater in these latter cases and the tendency for dilatancy of the specimen is observed only in the vicinity of failure.

With respect to the shape of the specimens after testing, it is interesting to note that no failure planes but only slight bulging has been observed for confining pressures of 10, 17 and 25 kg/cm^2. Failure planes do occur when σ_3 is less than 5 kg/cm^2.

Appendix 3

ROCKFILL SHOULDERS MATERIAL

List of the Figures and Tables

EL INFIERNILLO DAM - MATERIALS FROM THE ROCKFILL SHOULDERS
INITIAL GRANULOMETRIES

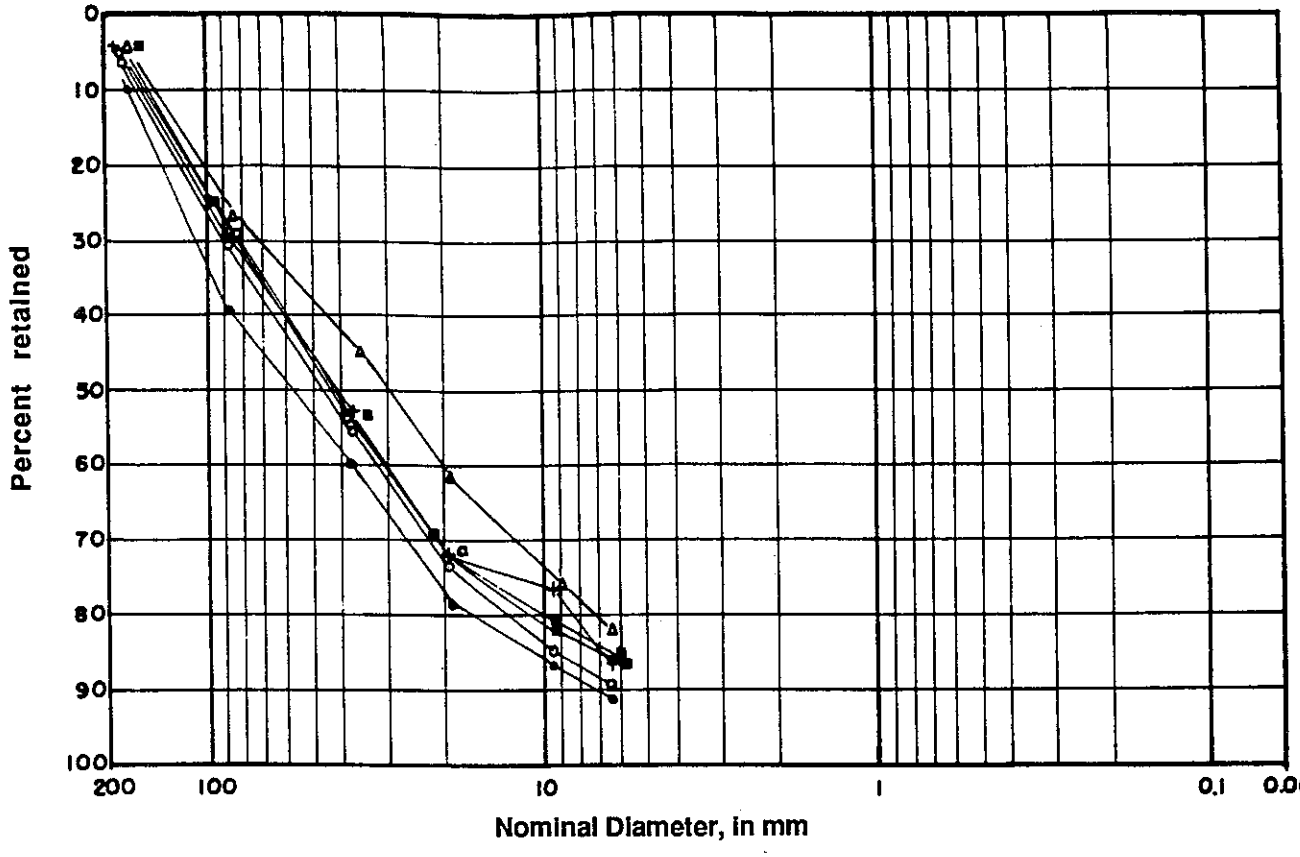

Percent Retained

Sieves	Tests					
	● 19	Δ 14	○ 21	+ 22	□ 23	■ 24
6" - 8"	8.7	4.4	6.5	4.4	5.2	4.8
3" - 4"	29.8	21.8	24.0	25.5	23.8	23.3
1 1/2"	21.1	18.7	24.8	23.3	24.4	25.0
3/4"	17.9	17.0	17.9	18.5	18.3	19.0
3/8"	8.9	14.0	11.6	4.4	8.8	9.3
1/4"	4.6	6.6	4.6	10.4	4.7	4.5
1/4"	9.0	17.5	10.6	13.5	14.8	14.1
D_{10} (mm)	77.00	* 2.80	5.95	* 5.20	* 2.70	* 3.60
C_u	12.4	* 15.8	11.1	* 11.6	* 22.2	* 16.4

* Estimated Values

Fig. A3.1

EL INFIERNILLO DAM - MATERIALS FROM THE ROCKFILL SHOULDERS

Triaxial Tests

Samples 113 cm in Diameter, Dry State
Confining Pressures from 0.5 to 25 kg/cm^2

Test No.	42	16	19	12	18	14
Date	May 18,64	Mar 18,64	Mar 24,64	Feb 20,64	Mar.22,64	Mar.10,64
Unit Weight of Rockfill Material (γ mat) in t/m^3	1.65	1.71	1.72	-	1.76	1.84
Unit Weight of Sand (γ sand) in t/m^3	1.47	1.84	1.84	1.74	1.74	1.75
Unit Weight Mean Value (γ mean) in t/m^3	1.62	1.73	1.74	1.75	1.76	1.83
Rockfill Void Ratio (e_R)	0.62	0.55	0.55	0.62	0.51	0.45
σ_3 in kg/cm^2	0.67	1.88	4.88	9.98	16.88	24.89
Max. Deviator Stress ($\sigma_1 - \sigma_3$) in kg/cm^2	3.47	9.40	18.60	34.70	53.70	75.50
σ_1 max in kg/cm^2	4.14	11.28	23.48	44.68	70.58	100.39
(σ_1 / σ_3) max	6.17	5.99	4.81	4.48	4.18	4.03
Friction Angle Φ at the Origin	46.1°	45.5°	41.0°	39.4°	37.8°	37.1°
Axial Strain at the Failure (ε_{1f}) in %	13.3	14.6	15.0	14.1	13.1	13.8
* Max. Volumetric Compression Strain (ε_V max) in %	- 0.9	- 1.6	- 4.6	- 7.4	- 7.2	- 7.9
* Volumetric Strain at the Failure (ε_{Vf}) in %	+ 8.6	+ 4.8	- 3.9	- 3.6	- 7.2	- 7.9

* - Compression
\+ Expansion

TABLE 1 : Looser Samples

EL INFIERNILLO DAM - MATERIALS FROM THE ROCKFILL SHOULDERS

Triaxial Tests

Samples 113 cm in Diameter, Dry State
Confining Pressures from 0.5 to 25 kg/cm^2

Test No.	42	16	19	12	18	
Date	Apr 1,64	Apr 3,64	Apr 8,64	Apr 10,64	Apr 14,64	
Unit Weight of Rockfill Material (γ mat) in t/m^3	1.77	1.78	1.90	1.90	1.82	
Unit Weight of Sand (γ sand) in t/m^3	1.79	1.70	1.70	1.78	1.94	
Unit Weight Mean Value (γ mean) in t/m^3	1.77	1.76	1.87	1.86	1.84	
Rockfill Void Ratio (e_R)	0.51	0.50	0.40	0.40	0.46	
σ_3 in kg/cm^2	1.88	4.88	9.98	16.88	24.89	
Max. Deviator Stress ($\sigma_1 - \sigma_3$) in kg/cm^2	9.44	20.04	34.52	53.24	72.36	
σ_1 max in kg/cm^2	11.32	24.92	44.50	70.10	97.25	
(σ_1 / σ_3) max	6.01	5.10	4.46	4.15	3.91	
Friction Angle Φ at the Origin	45.6°	42.2°	39.5°	37.6°	36.3°	
Axial Strain at the Failure (ε_{1f}) in %	12.8	16.6	14.7	14.7	13.8	
* Max. Volumetric Compression Strain (ε_V max) in %	- 2.3	- 5.6	- 4.4	- 5.6	- 5.4	
* Volumetric Strain at the Failure (ε_{Vf}) in %	+ 0.09	- 4.3	- 3.1	- 4.6	- 5.4	

* - Compression
\+ Expansion

TABLE 2 : Denser Samples

EL INFIERNILLO DAM - MATERIALS FROM THE ROCKFILL SHOULDERS

Triaxial Tests : Looser Samples

Samples 113 cm in Diameter, Dry State
Confining Pressures from 0.5 to 25 kg/cm^2

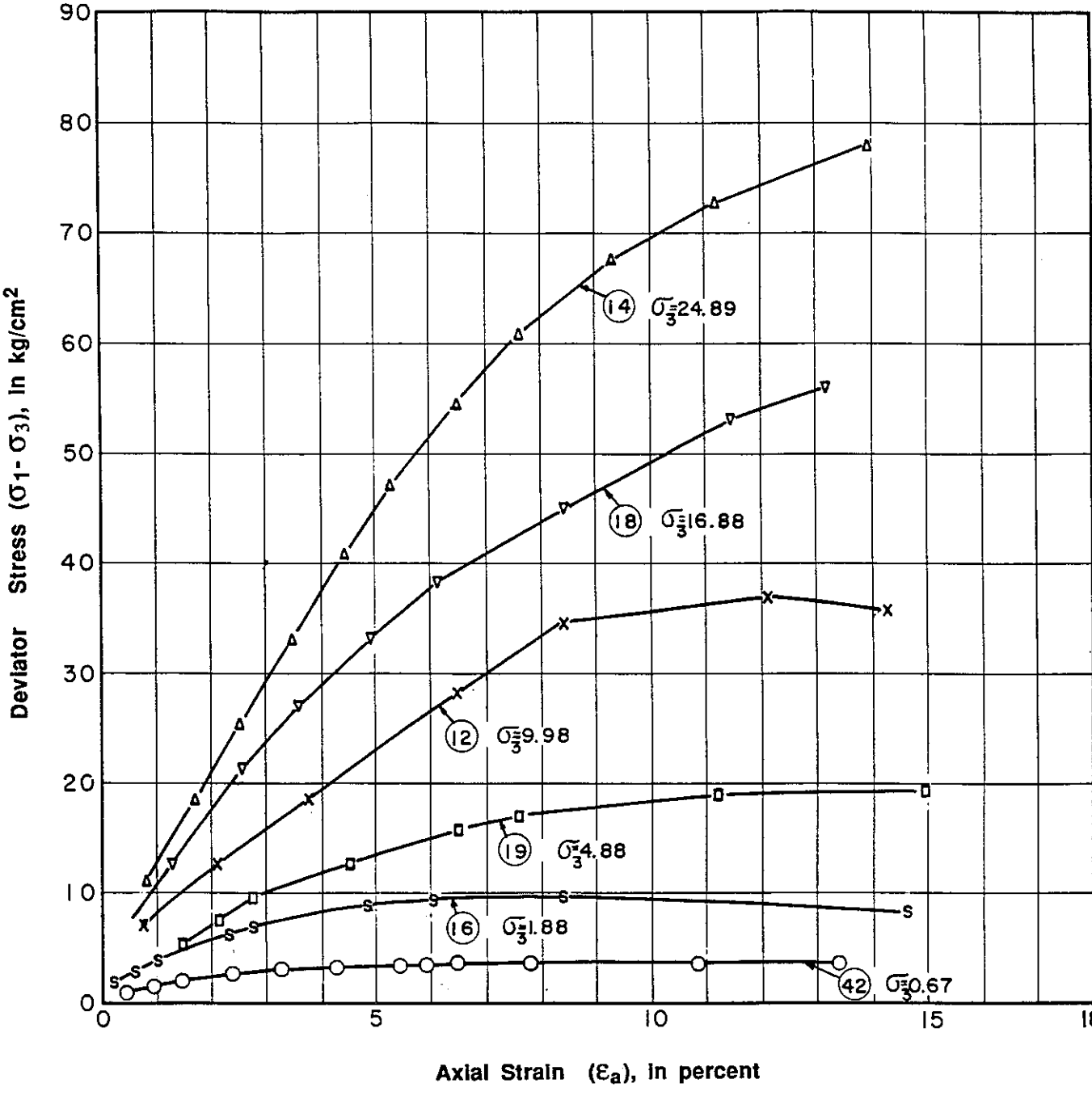

Fig. A3.2

EL INFIERNILLO DAM - MATERIALS FROM THE ROCKFILL SHOULDERS

Triaxial Tests : Looser Samples

Samples 113 cm in Diameter, Dry State
Confining Pressures from 0.5 to 25 kg/cm²

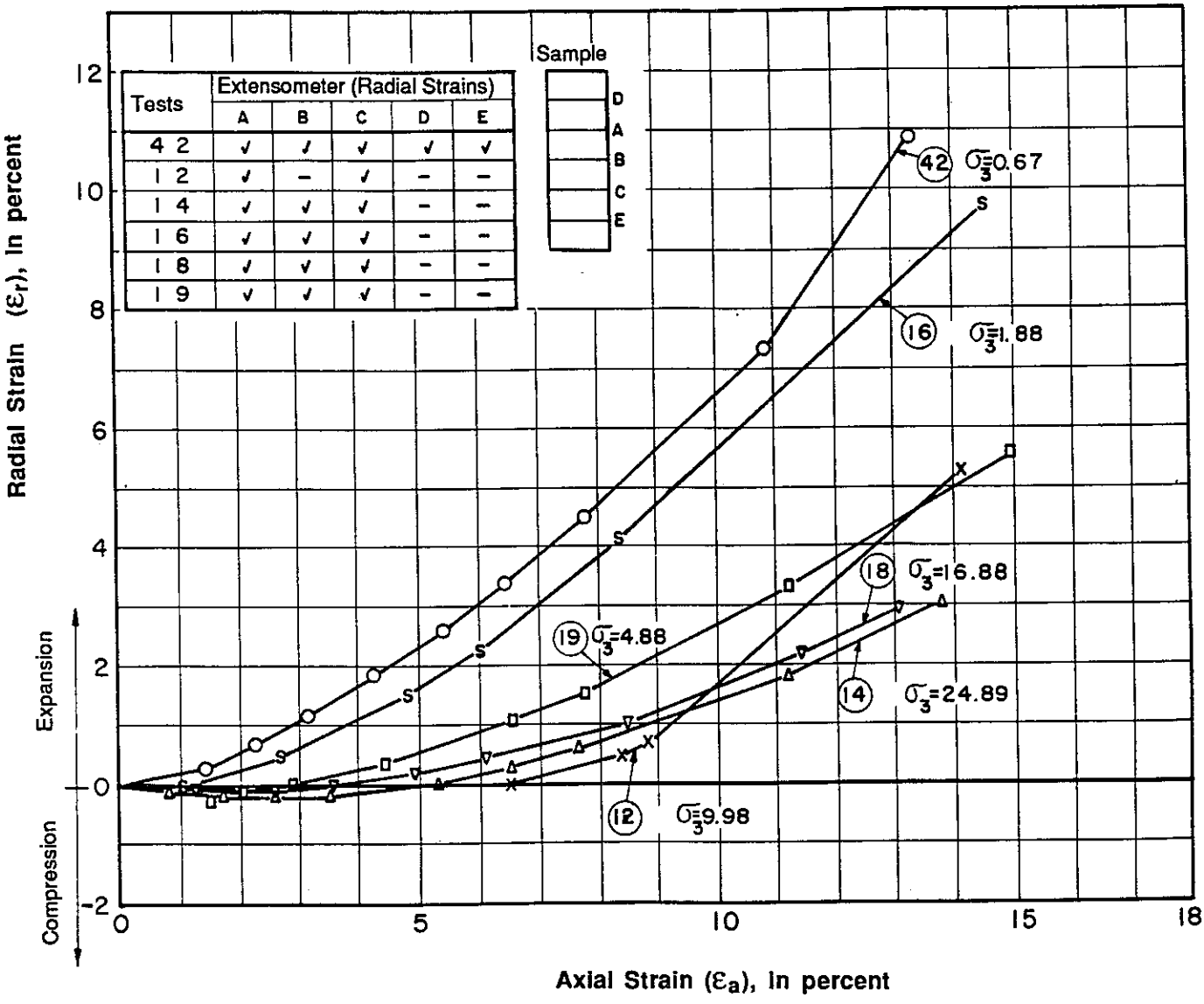

NB : The table shows the different circumferential extensometers which were used for each test. The resulting radial strain of the samples is the mean value of the different measurements made with these gauges.

Fig. A3.3

EL INFIERNILLO DAM - MATERIALS FROM THE ROCKFILL SHOULDERS

Triaxial Tests : Looser Samples

Samples 113 cm in Diameter, Dry State
Confining Pressures from 0.5 to 25 kg/cm²

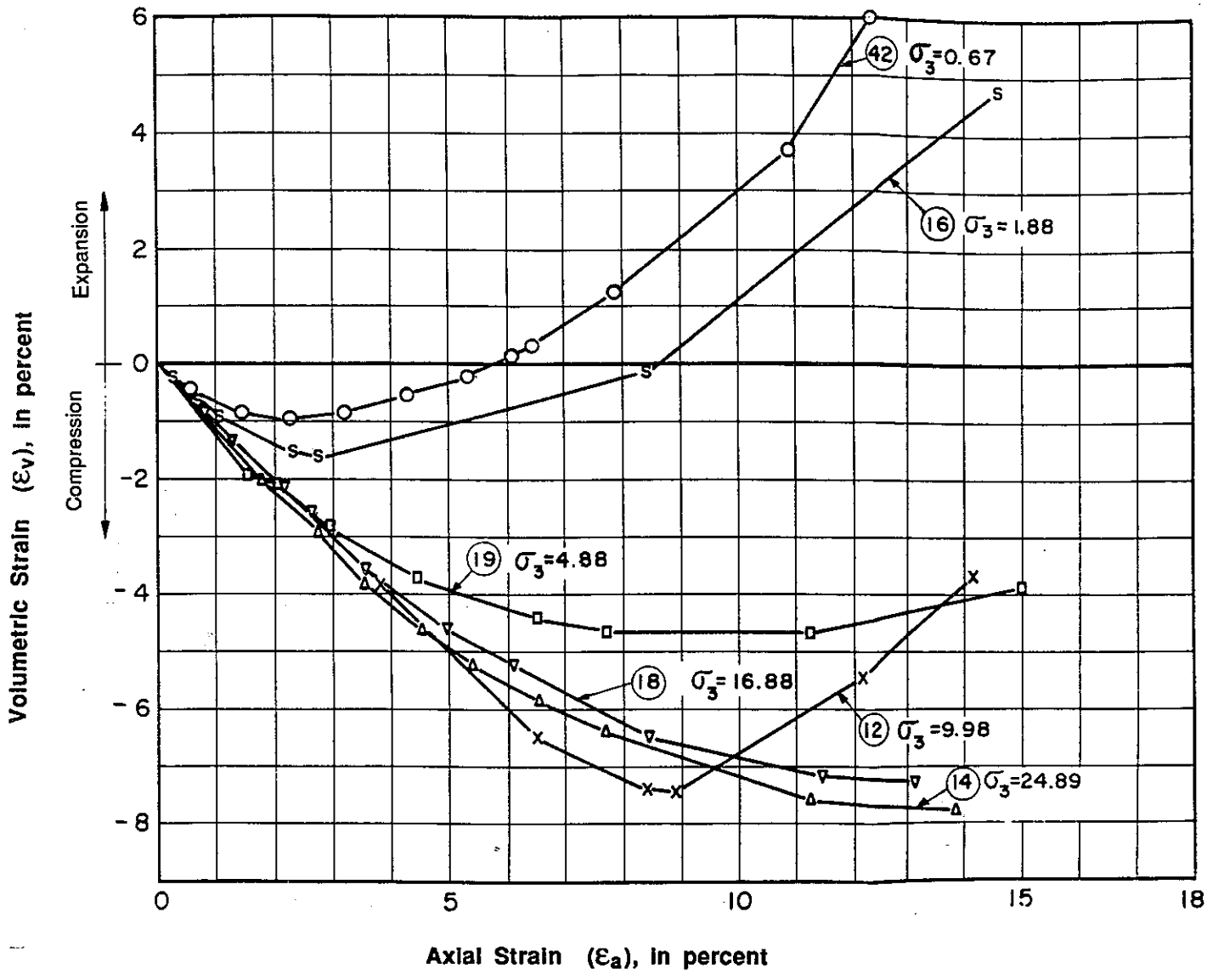

NB : The volumetric strain is calculated on the basis of measurements made with circumferential extensometers.

Fig. A3.4

EL INFIERNILLO DAM - MATERIALS FROM THE ROCKFILL SHOULDERS

Triaxial Tests : Denser Samples

Samples 113 cm in Diameter, Dry State
Confining Pressures from 0.5 to 25 kg/cm^2

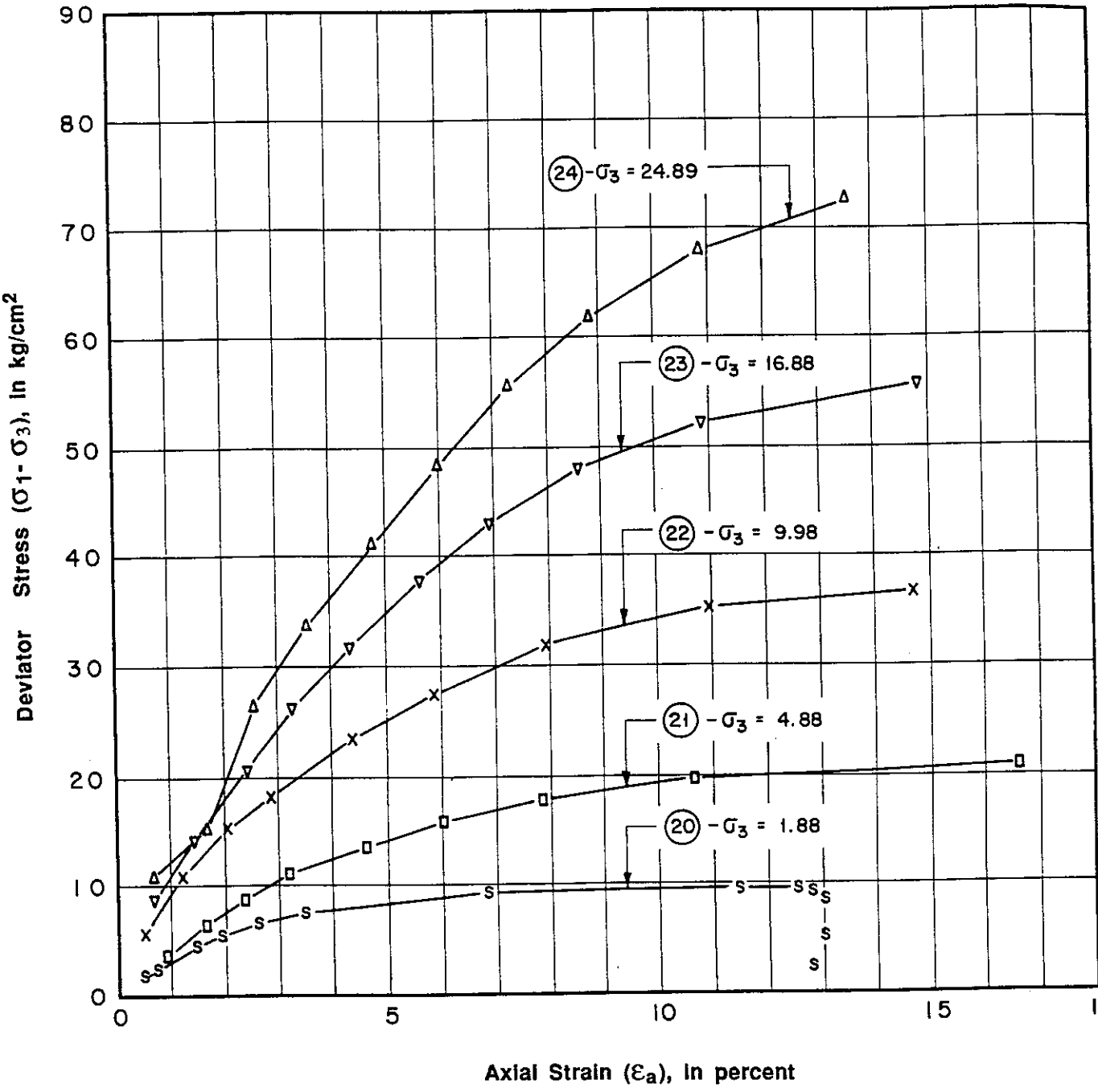

Fig. A3.5

EL INFIERNILLO DAM - MATERIALS FROM THE ROCKFILL SHOULDERS

Triaxial Tests : Denser Samples

Samples 113 cm in Diameter, Dry State
Confining Pressures from 0.5 to 25 kg/cm^2

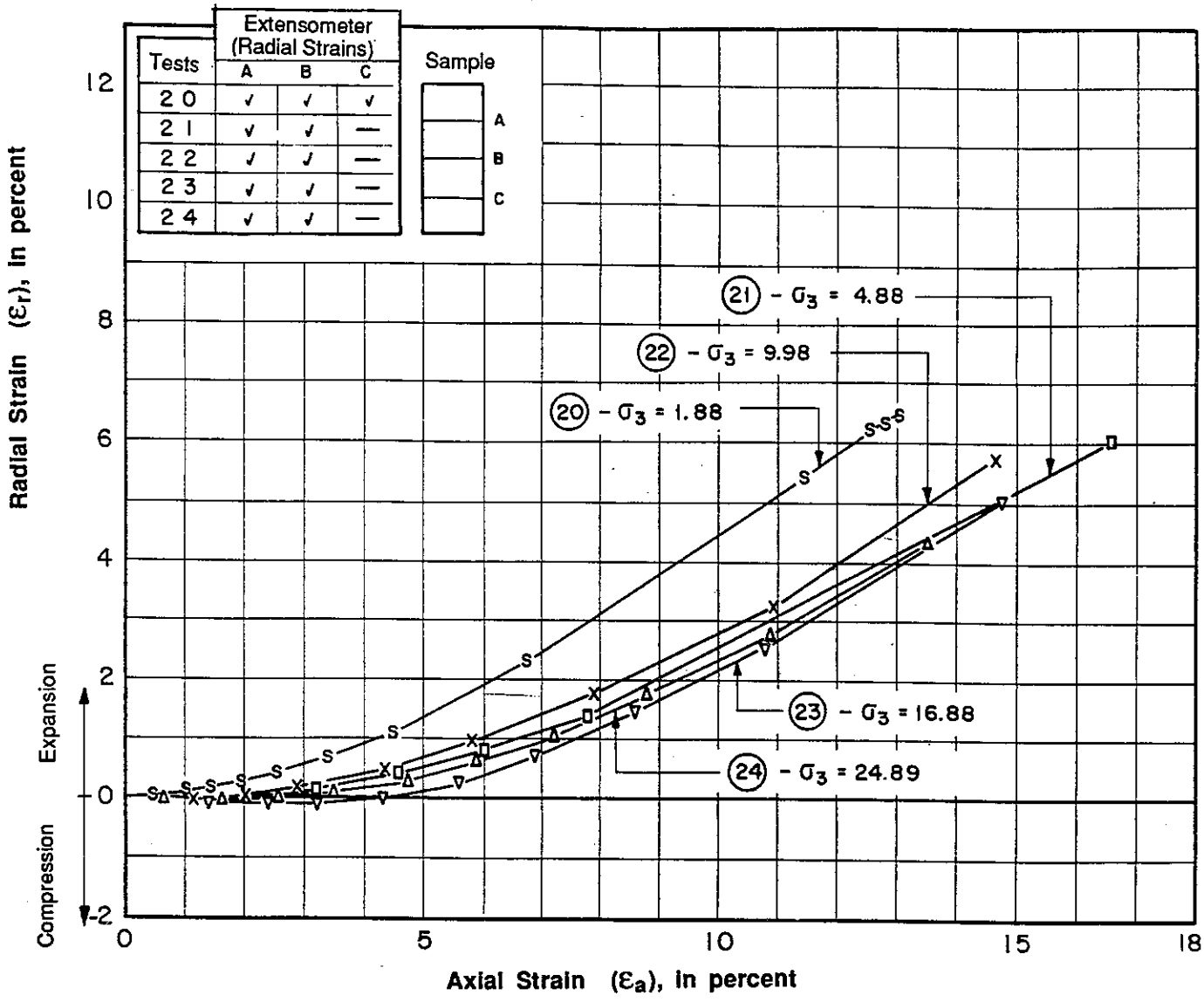

NB : The table shows the different circumferential extensometers which were used for each test. The resulting radial strain of the samples is the mean value of the different measurements made with these gauges.

Fig. A3.6

EL INFIERNILLO DAM - MATERIALS FROM THE ROCKFILL SHOULDERS

Triaxial Tests : Denser Samples

Samples 113 cm in Diameter, Dry State
Confining Pressures from 0.5 to 25 kg/cm^2

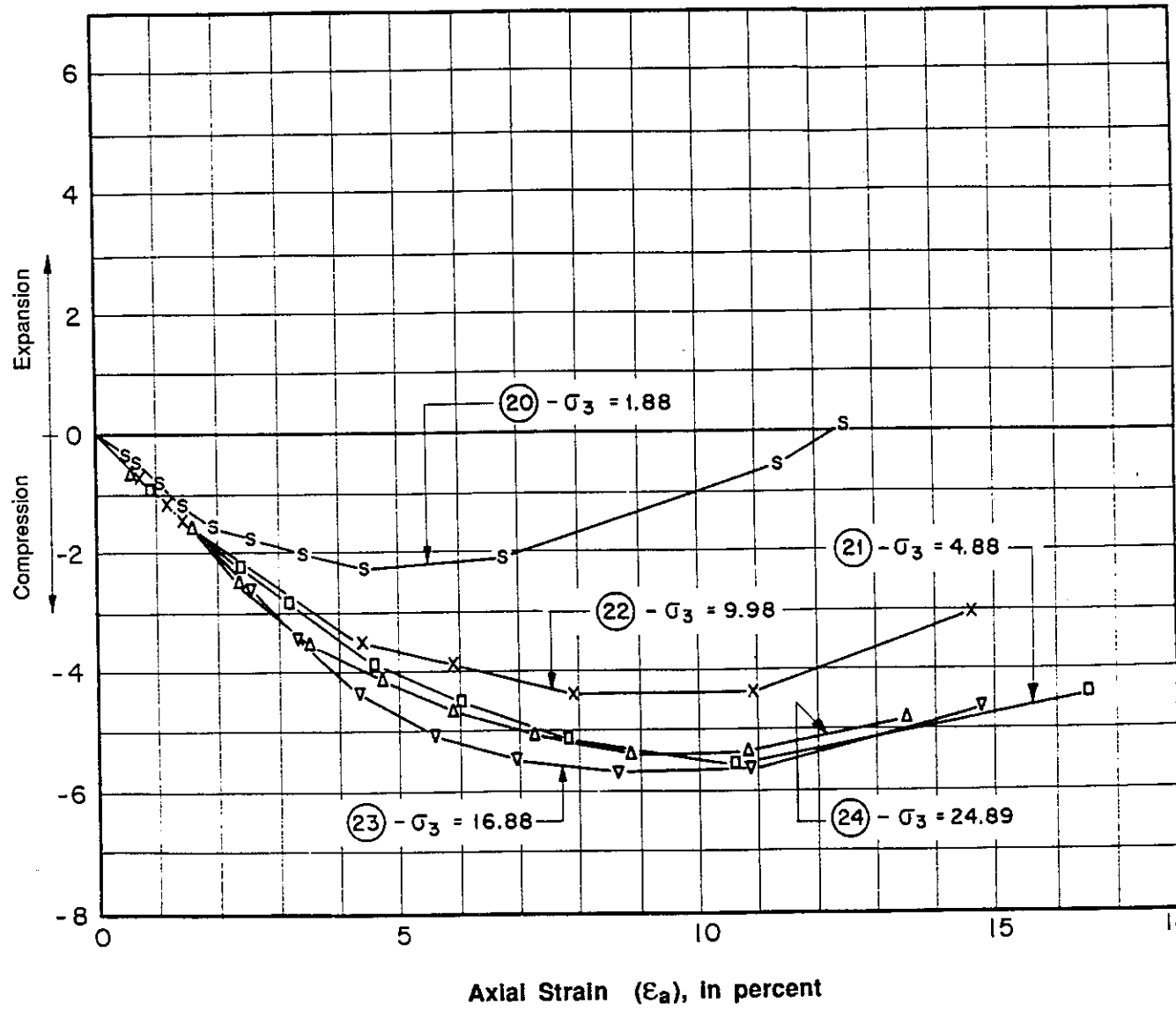

NB : The volumetric strain is calculated on the basis of measurements made with circumferential extensometers.

Fig. A3.7

EL INFIERNILLO DAM - MATERIALS FROM THE ROCKFILL SHOULDERS

Triaxial Tests

MOHR ENVELOPES

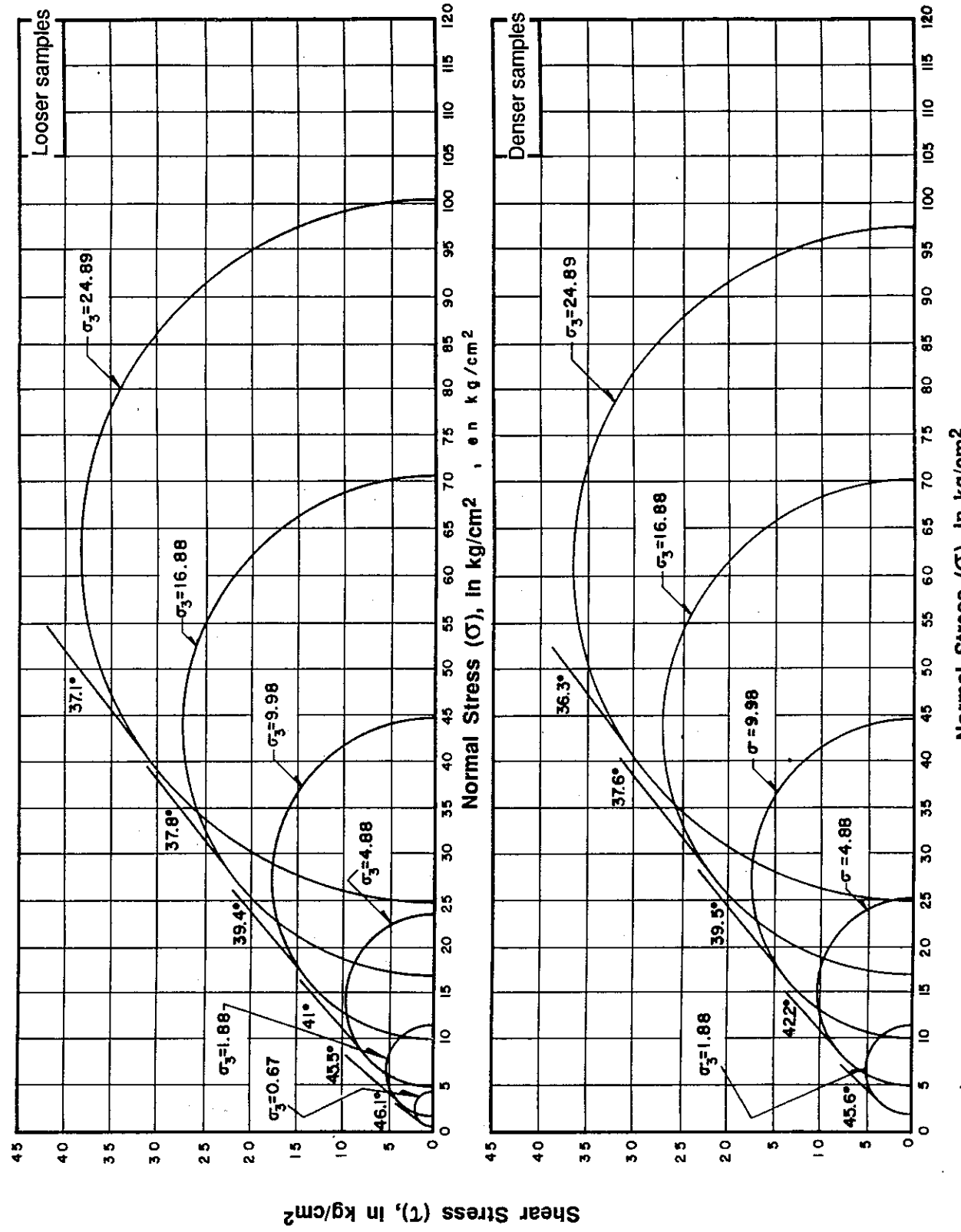

Fig. A3.8

EL INFIERNILLO DAM - LABORATORY ROCKFILL MATERIAL

Triaxial Tests
Effects of the Method Used for the Evaluation of Volumetric Changes

(Samples 113 cm in Diameter, Dry State
Confining Pressures from 0.5 to 25 kg/cm^2)

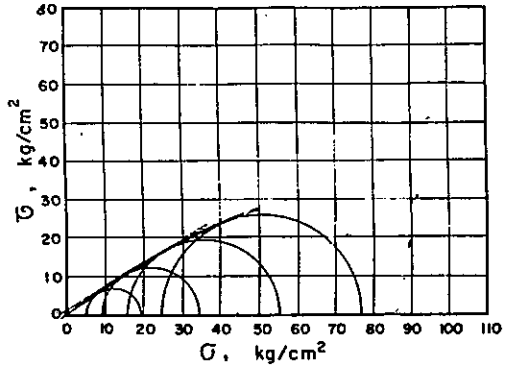

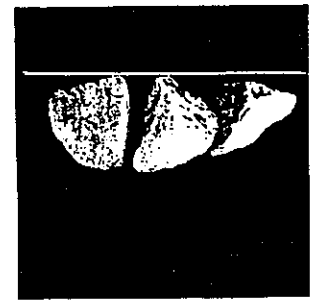

TYPICAL PARTICLES

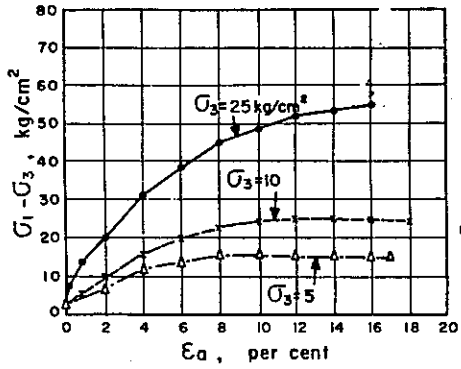

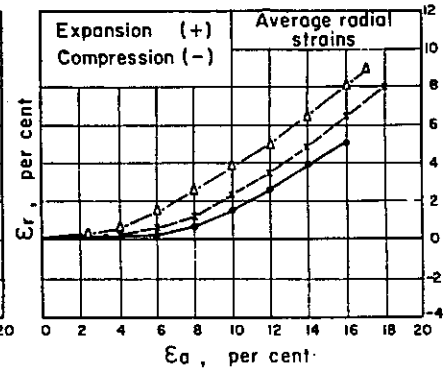

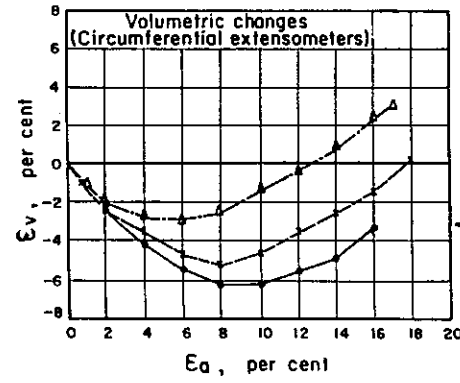

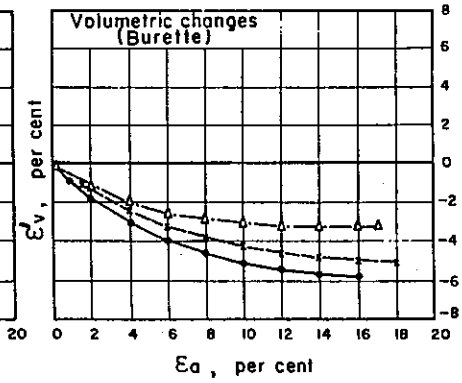

NB: The rockfill material of this figure is given for comparison only and shall not be considered as representative of the actual rockfill shoulders material .

Fig. A3.9

NOTES

NOTES

Third Benchmark Workshop on
NUMERICAL ANALYSIS OF DAMS
Gennevilliers, France, September 29-30, 1994

THEME B2

Dynamic analysis of an embankment dam under a strong earthquake

SYNTHESIS

&

COMPARISON OF RESULTS

Third Benchmark Workshop on Numerical Analysis of Dams
Gennevilliers (France) - September 29-30, 1994

Theme B2 :

DYNAMIC ANALYSIS OF AN EMBANKMENT DAM UNDER A STRONG EARTHQUAKE

SYNTHESIS

O.OZANAM*, G. LA BARBERA**

*Coyne et Bellier, Bureau d'Ingénieurs Conseils
9, Allée des Barbanniers - 92632 Gennevilliers CEDEX
** ISMES S.p.A.

The dynamic analysis of embankment dam is a difficult subject, because of the non-linear behaviour of dam materials, the water pore pressure effect in the core during earthquake and postseismic consolidation, and the evaluation of irrecoverable displacements during and after the seismic event. Two different approaches can be used:

- simplified methods based on linear equivalent analysis completed with different tried and proven empirical methods used to evaluate the excess pore pressure and irrecoverable movements;
- sophisticated numerical tools able to reproduce the cyclic non-linear behaviour of materials by using elastoplastic constitutive models, which take account of the hardening/softening and cyclic hysteresis, and the coupling between pore pressure and strains in the core under dynamic loading.

Table 1 presents the different methods used by the participants in theme B2. Two of the 4 proposed papers (CVG EDELCA [1] and the Civil Engineering Institute of Bucharest [2]) adopted the simplified approach by using FLUSH and other specific software and the other two (ISMES [3] and Coyne et Bellier [4]) applied the numerical elastoplastic approach by using static and dynamic hydraulic/ mechanical coupled finite-element software (OMEGA and GEFDYN). In this last case, only one program is used to compute the initial state used for the dynamic analysis, the excess pore pressure during the earthquake, and the irrecoverable displacement at its end. The simplified method needs to:

- compute the initial state with a particular finite-element program able to perform static analysis (FEADAM, MATLOC);
- compute the acceleration time history at each nodal point of the dam with FLUSH,
- compute the irrecoverable displacement with classical stability analysis and the Newmark method (CVG EDELCA) or by using the maximum shear strain (Civil Eng. Inst. of Bucharest),
- compute the excess pore pressure by using liquefaction curves (CVG EDELCA) or by coupled analysis on a column (Civil Eng. Inst. of Bucharest).

The two simplified approaches are also restricted to an accelerogram with the horizontal component only. The other two applied the two components (horizontal and vertical) of the accelerogram. In addition, ISMES also tested the influence of the vertical component by a computation with an input motion restricted to the horizontal component.

Table 1 : Recapitulative table of the different methods used for theme B2

software	company	mesh	constit. model	Initial conditions		Accelerogram	Fitting of parameters	Comput. of excess pore pressure	Comput. of irrecoverable displacements
				software	constit. model				
FLUSH	CVG EDELCA	standard	non-linear elasticity	FEADAM	Duncan, Byrne, Wong, Mabry	EQ2 horizontal 0 s to 120 s	with EQ1	liquefaction curve	Newmark Makdisi Seed
FLUSH DEFORM LASIII	Civil Eng. Inst. of Bucharest	less refined	non-linear elasticity	MATLOC	Duncan Chang	EQ2 horizontal 15 s to 55 s	with EQ1	LAS III coupled analysis on a column	DEFORM max. shear strain
GEFDYN	Coyne et Bellier	standard	Mohr Coulomb + Hujeux	GEFDYN	Mohr Coulomb + Hujeux	EQ2 horizontal & vertical 0 s to 120 s	with triaxial tests	coupled undrained analysis in core	computed by GEFDYN
OMEGA	ISMES ENEL	standard	Drücker Prager	OMEGA	Drücker Prager	EQ2 hor. only & EQ2 hor.&vert. 0 s to 120 s		coupled undrained analysis in core	computed by OMEGA

1. COMPARISON OF RESULTS

1.1 Cyclic trixial tests

In order to quantify the ability of the constitutive model chosen by the participants, and of their determined parameter set, to reproduce typical dynamic material behaviour, it was required to provide the results of undrained cyclic triaxial tests for the core material only at two different confining pressures.

No simulation of the cyclic triaxial tests was performed by the participants, who used the simplified method, because their tools are not adapted to dealing with that type of computation.

Therefore two simulations of these tests were performed by ISMES and Coyne et Bellier. Table 2 presents the main characteristics of the cyclic curves:

- maximum axial strain,
- final excess pore pressure,
- final ratio between the excess pore pressure and the confining stress.

Table 2 : Summarized results of cyclic triaxial tests

	maximum axial strain ε_{zz} (%)		final excess pore pressure u (MPa)		ratio u / σ_3 (%)	
σ_3 (MPa)	0.1	0.3	0.1	0.3	0.1	0.3
Coyne et Bellier	0.08	0.13	0.1	0.13	1.	43
ISMES	0.46	0.28	0.035	0.09	35	30

The constitutive model and the parameter set used by ISMES seem to generate larger irrecoverable strain and less excess pore pressure than those of Coyne et Bellier. This will be confirmed in the dynamic analyses under earthquakes EQ1 and EQ2 (see next section).

1.2 Typical time histories of displacement

The form of the time histories of horizontal and vertical displacements provided by the participants in their contributions and corresponding to the earthquake EQ2 will be compared in order to better understand how the final irrecoverable displacement values were obtained.

According to the method used by CVG EDELCA (Newmark method), no displacement time histories were given by the authors.

The other FLUSH user, Civil Eng. Institute of Bucharest, used a specific tool, named DEFORM, to compute the displacement. The curves obtained (Fig. 1a and 1b) show a linearly regular irrecoverable displacement and a very small reversible elastic oscillation, except for the vertical displacement at the crest, where large elastic oscillations occur.

ISMES, who studies the influence of the vertical base acceleration component, provides these curves in both cases. The form of these curves (Fig. 2a, 2b, 3a and 3b) is not significantly modified by the addition of a vertical acceleration component. Their main characteristic is that

they are relatively smoothed with small elastic oscillations. The effect of the main shocks of the input accelerogram is not clearly observable, except for the first one at 17 seconds. The irrecoverable displacement increases more or less regularly from 20 to 60 seconds.

The curves obtained by Coyne et Bellier (Fig. 4a and 4b) have completely different characteristics. The elastic oscillations are evident and their amplitude varies from a few centimetres to a little more than 10 centimetres. The second main point is that each main shock of the base accelerogram induces a rapid and significant increase of the irrecoverable displacement. Between two main shocks this increase is more regular and has a smaller rate.

The type of curves obtained by the Institute of Bucharest is entirely due to the method used by the authors and cannot be directly compared to the others.

The differences observed between the curves obtained by Coyne et Bellier and ISMES can be explained by 2 factors:

- numerical damping and selected value of the damping factor, which seems to be one of the most significant factors,
- hardening law of the numerical constitutive models.

1.3 Accelerations at 5 selected points

The most frequently presented result of dynamic analysis is the maximum horizontal acceleration to which the dam is subjected. Fig. 5 represents the maximum horizontal and vertical accelerations obtained at the 5 selected points by the 4 participants. The vertical maximum acceleration is not provided by CVG EDELCA, because it is assumed to be zero in its methodology.

The comparison of the two applications of FLUSH shows a relatively large discrepancy on the horizontal maximum acceleration: the values computed by CVG EDELCA are equal to 1.3 to 2.8 times the values computed by the Institute of Bucharest. This could be mainly explained by a different choice of the maximum shear moduli and of the shear modulus and damping curves.

The two computations performed by ISMES show a great influence of the vertical acceleration component on the horizontal maximum acceleration at the crest and on the vertical maximum acceleration (at least in the scope of the OMEGA model). The value of these accelerations is always larger if both components are applied than if the base acceleration has only a horizontal component.

The comparison of the two comparable applications performed by ISMES (X and Y input) and by Coyne et Bellier points out that the amplification factors are close except at the crest and downstream for the vertical acceleration. These factors are relatively uniform for Coyne et Bellier (from 1.3 to 2.4) and close to 2 in comparison with the wide variation obtained by ISMES (from 0.86 to 6.4).

But the amplitude of the maximum acceleration in some points is not sufficient to determine the safety of the dam.

1.4 Irrecoverable displacements at 5 selected points

As shown in Figure 6A, which represents the irrecoverable horizontal and vertical displacements obtained by the participants at the 5 selected points, the largest values have been computed by ISMES (event with X-input or X- and Y-input) and especially for the horizontal displacement of points UM (-180 cm) and DM (75 cm) and for the settlement at the crest (CC: 70 cm) and at the upstream point UM (103 cm). Coyne et Bellier also obtained a large value for the crest settlement (48 cm). At all points (except horizontal displacement at crest) the irrecoverable displacements obtained by Coyne et Bellier are smaller than those computed by ISMES. This is mainly due to the constitutive models and to the parameter sets adopted by each of them, as indicated previously in section 1.1.

In order to better analyze the amplitude of the other participants, the same graph at a finer scale is drawn in Figure 6b.

The method used by the Institute of Bucharest induces very small displacements (less than 5 cm). This remark is also noticeable for the first earthquake (EQ1), for which the computed settlements at the crest are around 3 times smaller than that actually measured.

The two values provided by CVG EDELCA (horizontal displacements at crest -CC- and downstream -DM) are much larger than those computed by the other FLUSH method used by the Institute of Bucharest, because the evaluation of displacement is made by completely different methods. In the case of CVG EDELCA, it depends mainly on the acceleration amplification. The values are relatively close to the ISMES results with X- and Y- input base acceleration.

In order to allow a kind of critical judgement on these widely varying results, the monitored data on the real dam during the 1985 earthquake will be presented. The measurements performed after the earthquake provide settlements and amplification factors of the same order as those measured after the 1979 earthquake (0.1g) : for example, the crest settlement varies from 10.5 to 11 cm. The main difficulty comes from the absence of several recordings of accelerograms during the 1985 earthquake and especially of the base acceleration on rock. Now the base accelerogram provided to the benchmark participants and used in the numerical computations is in fact the recorded horizontal (tranversal) acceleration at elevation 120. This means that the real maximum horizontal base acceleration in 1985 should be slightly larger than that in 1979 because of the slightly higher Richter magnitude (8.1 compared to 7.6) and of the hardening of dam materials due to previous earthquakes. This value was perhaps around 0.15g, i.e. half of the input accelerogram used in the computations. In any case it would certainely be considerably smaller than the adopted value (0.29g) and the duration would perhaps be shorter.

For the benchmark specifications it was chosen to use a strong input accelerogram in order to test the ability of the tools to deal with such analysis (where the dam state could be close to unstable) and in order to use an input different from the EQ1 input.

These remarks imply that:

- no comparison with measured data is possible,
- the computed settlements should be higher than the settlements actually measured,
- the irrecoverable crest settlement does not vary linearly with the maximum base acceleration and it should vary with an increasing rate.

Therefore the classic methods seem to underestimate the amplitude of settlements at the crest. However it is not possible with the available data to determined if the ISMES and Coyne et Bellier results are correct.

One of the main results of these sophisticated methods is that the deformation of the dam is concentrated on sliding surfaces, which generate sliding blocks. The graphic outputs drawn in Figures 7a (ISMES) and 7b (Coyne et Bellier) show that the elastoplastic finite element analysis is able to provide results in terms of potentially sliding surfaces, which is the main element (assumption) of the classic stability analyses. Thus these two types of methods, which are usually considered to be impossible to compare, present here a first common point and make it possible to imagine an homogeneous approach which can reconcile the two schools of thought. This could be considered to be important progress.

1.5 Pore pressure

The form of the time history curves is, as for displacement, largely dependent on the computation method :

- The Civil Engineering Institute of Bucharest (Fig.8) obtains an excess pore pressure which increases by steps, and the main steps are correlated to the main shocks of the input accelerogram;
- ISMES with both X-input (Fig.9a) or X- and Y-input accelerograms (Fig.9b) obtains an irrecoverable decrease of pore pressure with a large « elastic » oscillation and a high frequency;
- Coyne et Bellier (Fig.10) obtains a variable evolution of excess pore pressure during the seismic loading with an « elastic » oscillation smaller than that of ISMES. Globally the excess pore pressure remains positive.

As shown in Figures 11a (ISMES) and 11b (Coyne et Bellier), the space distribution of excess pore pressure in the core is absolutely not uniform and the comparison of computed values at only 2 points inside the core seems to be not sufficient to really compare the results. In Figure 11a the positive excess pore pressure is mainly concentrated at the upstream base part of the core, and, on the contrary, in Figure 11b the positive excess pore pressure is mainly located on the downstream face and in the upper part of the core.

However these values have been brought together in Figure 12. Only one positive excess pore pressure value has been provided by CVG EDELCA at the crest by using liquefaction curves.

The final (equal to the maximum) excess pore pressure computed by the Institute of Bucharest remains very small (5 kPa) compared to the values computed by ISMES and Coyne et Bellier (several hundred kPa). The final excess pore pressure is more or less positive in Coyne et Bellier's computation and negative in ISMES's computation. This is in agreement with the previous remark relative to the influence of the constitutive models and of the parameter sets (see section 1.1).

In conclusion to this section, it is not possible to decide what is correct because no sufficient in situ data is available to have an idea about the amplitude of the core consolidation after the earthquake and therefore about the excess pore pressure during the event.

1.6 Computation times

The computation times are given in table 3. The main remark is that the necessary computation time is significantly larger for the elastoplastic finite element approaches compared to the classic FLUSH method.

Table 3 : Computation times of each participants for EQ2 simulation only

Authors	Company	Code	Hardware	CPU time
P. I. Perazzo	CVG EDELCA	FLUSH	386 IBM with math coprocessor	3 h 23 '
A. Popovici et al.	Civil Eng. Instit. of Bucharest	FLUSH DEFORM LASIII	CORAL 8730	15' (*) 2' 3'
G. La Barbera et al.	ISMES S.p.A. ENEL	OMEGA	CONVEX	65 h
O.Ozanam et al.	Coyne et Bellier	GEFDYN	HP9000/715	23 h

(*) computed with coarser mesh and from 15s to 55s of EQ2

2. MAIN CONCLUSIONS

2.1 Linear equivalent method

This method has the advantages of :

- low computation costs (as shown in section 1.6)
- being used widely by engineers, who have in mind stability criteria based on their experience,
- providing an estimation of the amplification factor, frequently used in linear elastic finite element methods.

Its main disadvantages are that :

- the sliding lines should be assumed *a priori*, or a large set of sliding lines should be tested in order to find the line along which the irrecoverable displacement is the largest, i.e. the kinematics of the dam « damage » is assumed presumptively;
- it is limited to the horizontal component of the input accelerogram;
- the parameters of the non-linear elastic constitutive model are not easy to determine, in laboratory tests (cyclic shear tests or cyclic trixial tests) or by correlations;
- this method is not able to predict excess pore pressure in undrained materials.

2.2 Coupled elastoplastic method

This method has the advantages of :

- direct computing of the displacement at all dam points,
- direct computing of excess pore pressure in undrained material by taking the plastic volumetric strain into account,
- the possibility to obtain the potentially sliding line(s) as a computation result,

- the use of a single program and also of a single parameter set for static and dynamic analyses; this parameter set may be tested and progressively tuned during construction, impounding and, possibly, a first earthquake.

Its main disadvantages are that :

- computation costs are relatively high,
- such numerical tools are not easy to use and need specific training and (like classic methods) some experience in them.

As discussed in section 1.4, these numerical tools could be used to complement classic methods in order to:

- check if the a priori selected sliding lines are in agreement with those numerically computed;
- compute the effect of excess pore pressure in undrained materials, if necessary.

2.3 Subjects discussed during the round table

The definition of the input accelerogram with vertical and horizontal components, which are exactly identical, certainly gives a pessimistic approach which does not represent reality. For a future benchmark, it is recommended to generate two accelerograms, one for the vertical component and the other for the horizontal component, with the same frequency spectrum, such that the peaks are not exactly simultaneous.

The damping factors introduced in the computations have a substantial influence on the irrecoverable displacements. There are four types of damping :

- numerical damping, introduced in the equilibrium equation ($M\ddot{u}+\lambda \dot{u}+Ku=f(t)$), as a scalar λ multiplied by the time derivative of the displacement - this scalar, called damping factor, is constant during the earthquake -;
- damping introduced in the simplified method - this coefficient varies with the shear strain according to a given curve; it depends on the actual shear strain of each finite element of the mesh -;
- numerical damping induced by the Newmark scheme used to compute velocities and accelerations from the displacements - in that case, the damping factor is variable and depends on the eigenfrequencies of the dam -;
- mechanical damping generated by the hysteretic plastic behaviour of the material and modelized by a cyclic elastoplastic constitutive model.

This last damping is mechanically close to reality and does not require any parameters other than the elastoplastic parameters, which is certainly a better approach.

REFERENCES

[1] PERAZZO P.H.Ch. (1994) : Analyses of the El Infiernillo Dam based on the methodology adopted in recent dynamic analyses of embankment dams in Venezuela (software FLUSH) - 3rd Benchmark Workshop on Numerical Analysis of Dams -Theme B2 - Gennevilliers (France) - September 29-30, 1994.

[2] POPOVICI A., TOMA I., SARGHIUTA R. (1994) : Nonlinear seismic analysis of an embankment dam (software FLUSH+LASIII+DEFORM) - 3rd Benchmark Workshop on Numerical Analysis of Dams -Theme B2 - Gennevilliers (France) - September 29-30, 1994.

[3] LA BARBERA G., BANI A., MAZZA' (1994) : Dynamic analysis of an embankment dam under a strong earthquake (software OMEGA) - 3rd Benchmark Workshop on Numerical Analysis of Dams -Theme B2 - Gennevilliers (France) - September 29-30, 1994.

[4] OZANAM O., LACROIX F., TARDIEU B. (1994) : Dynamic analysis of an embankment dam under a strong earthquake - GEFDYN analysis - 3rd Benchmark Workshop on Numerical Analysis of Dams -Theme B2 - Gennevilliers (France) - September 29-30, 1994.

NOTES

Third Benchmark Workshop on Numerical Analysis of Dams
Gennevilliers (France) - September 29-30, 1994

Theme B2 :

DYNAMIC ANALYSIS OF AN EMBANKMENT DAM UNDER A STRONG EARTHQUAKE

SYNTHESIS

FIGURES

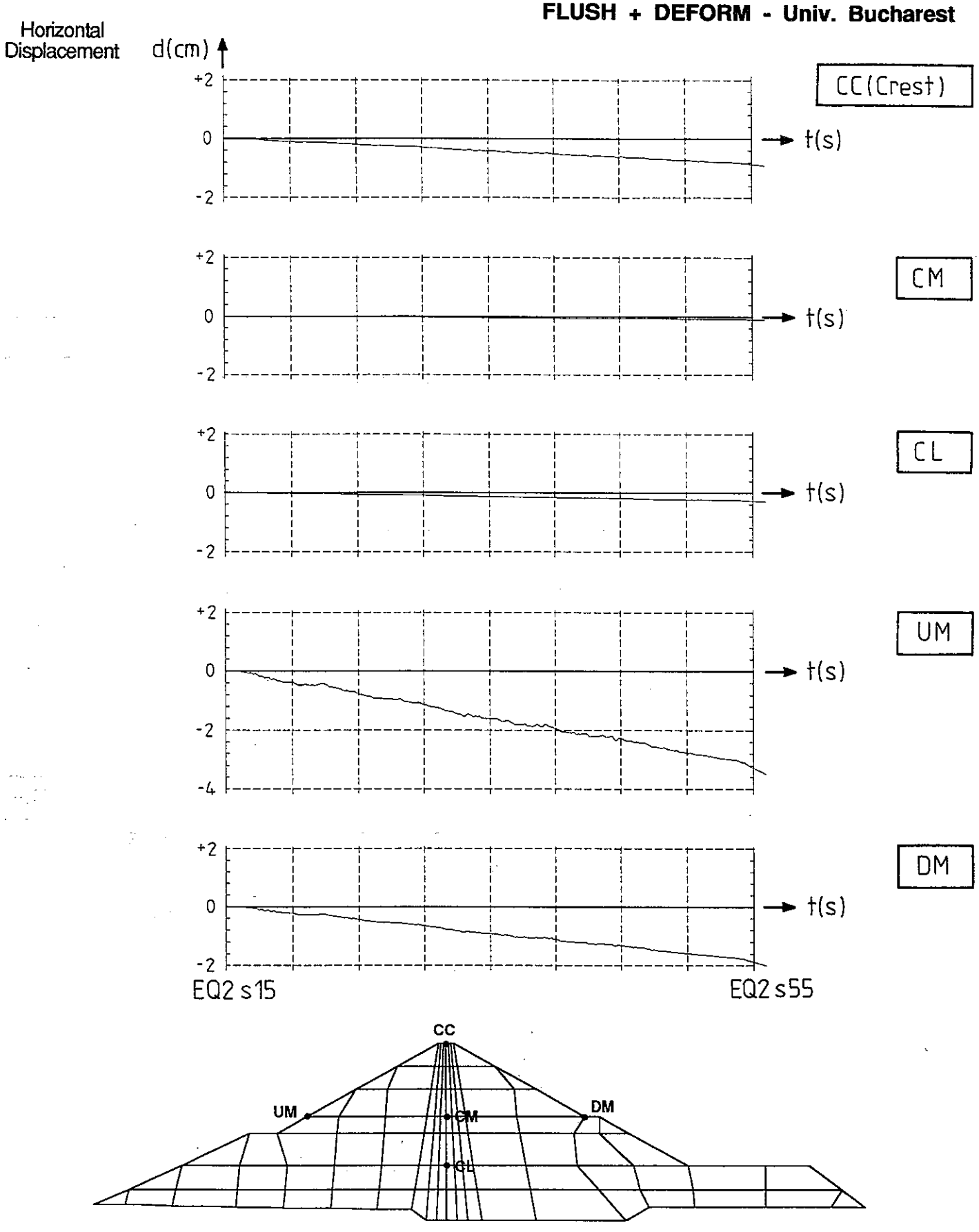

El Infiernillo dam - Horizontal displacement time history during EQ2 accelerogram applied horizontally.

Fig. 1a

3rd. ICOLD 1994 - DYNAMIC ANALYSIS OF AN EMBANKMENT DAM

EQ2 earthquake considering only horizontal component
VERTICAL DISPLACEMENTS VS TIME

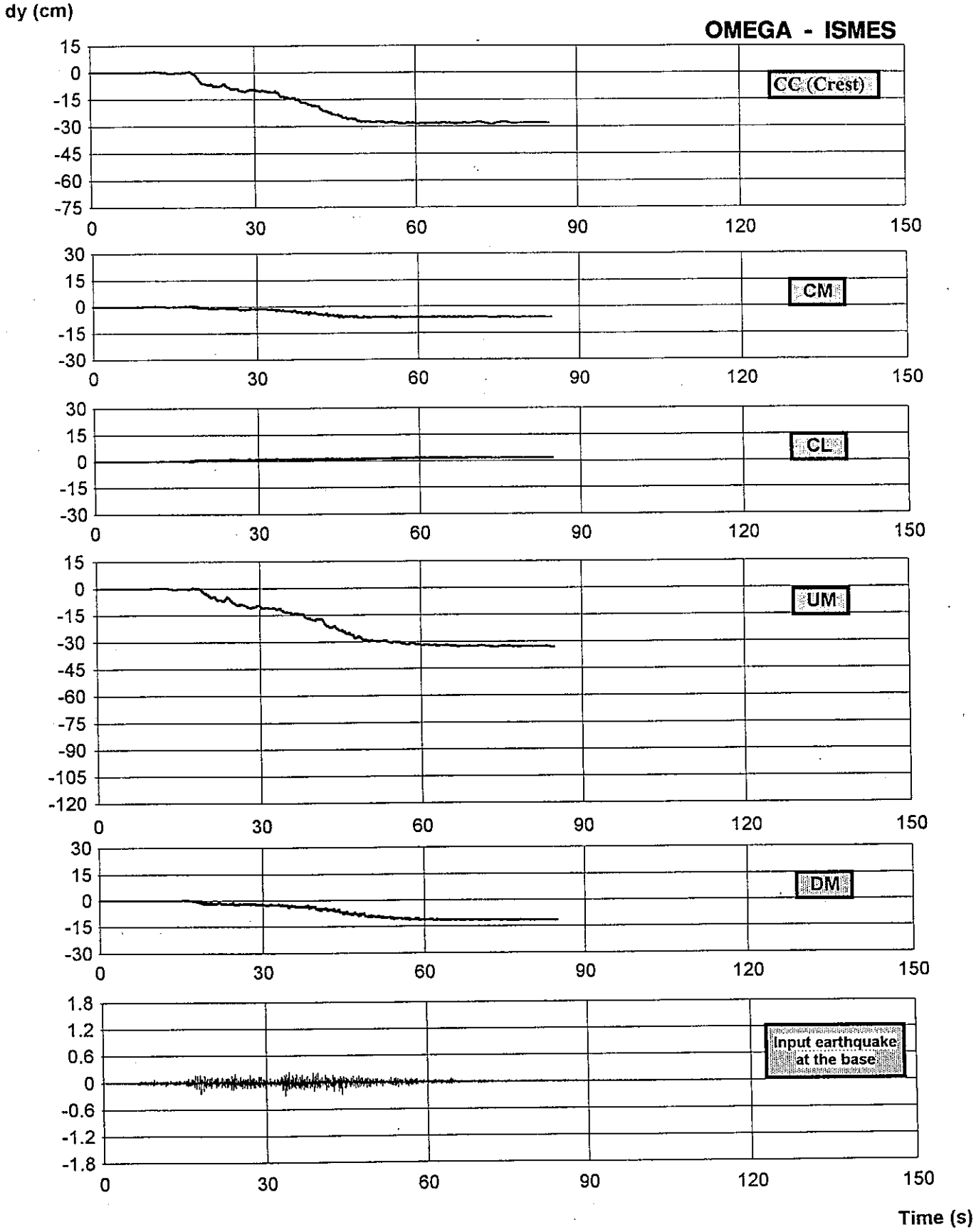

Fig. 2b

3rd. ICOLD 1994 - DYNAMIC ANALYSIS OF AN EMBANKMENT DAM

EQ2 earthquake considering only horizontal component

HORIZZONTAL DISPLACEMENTS VS TIME

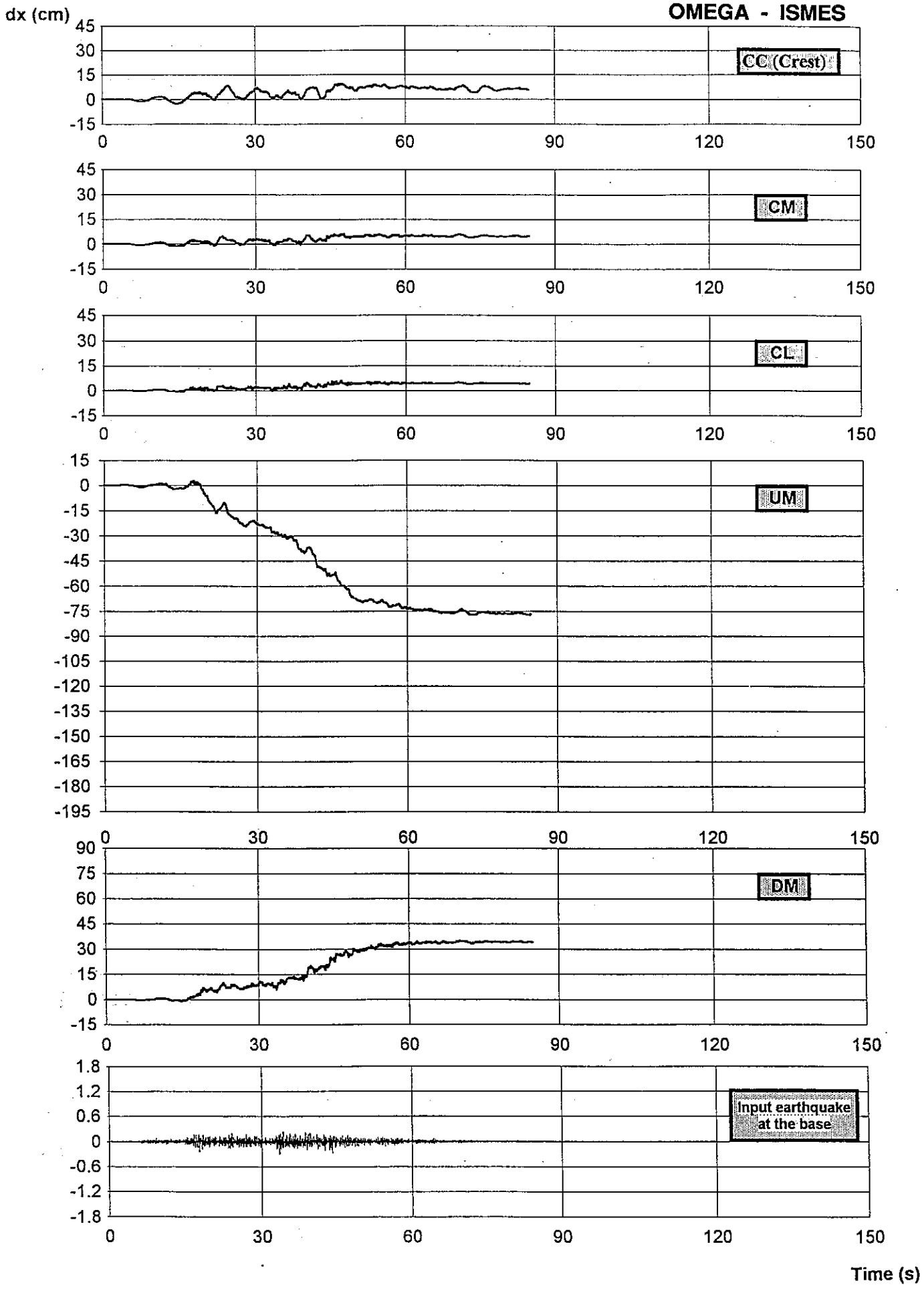

Fig. 2a

3rd. ICOLD 1994 - DYNAMIC ANALYSIS OF AN EMBANKMENT DAM

EQ2 earthquake considering only horizontal component

VERTICAL DISPLACEMENTS VS TIME

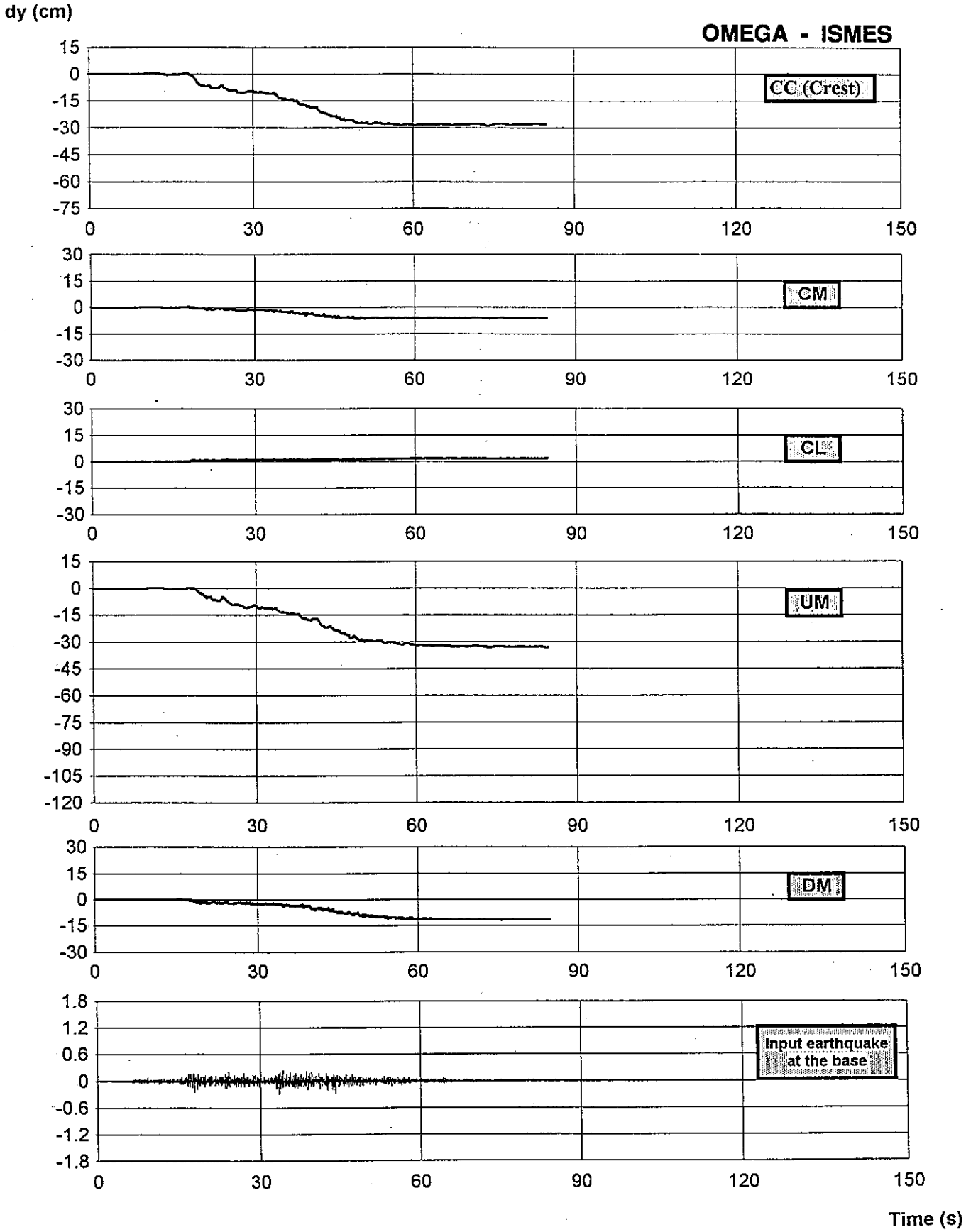

Fig. 2b

EQ2 earthquake considering horizontal and vertical components

HORIZZONTAL DISPLACEMENTS VS TIME

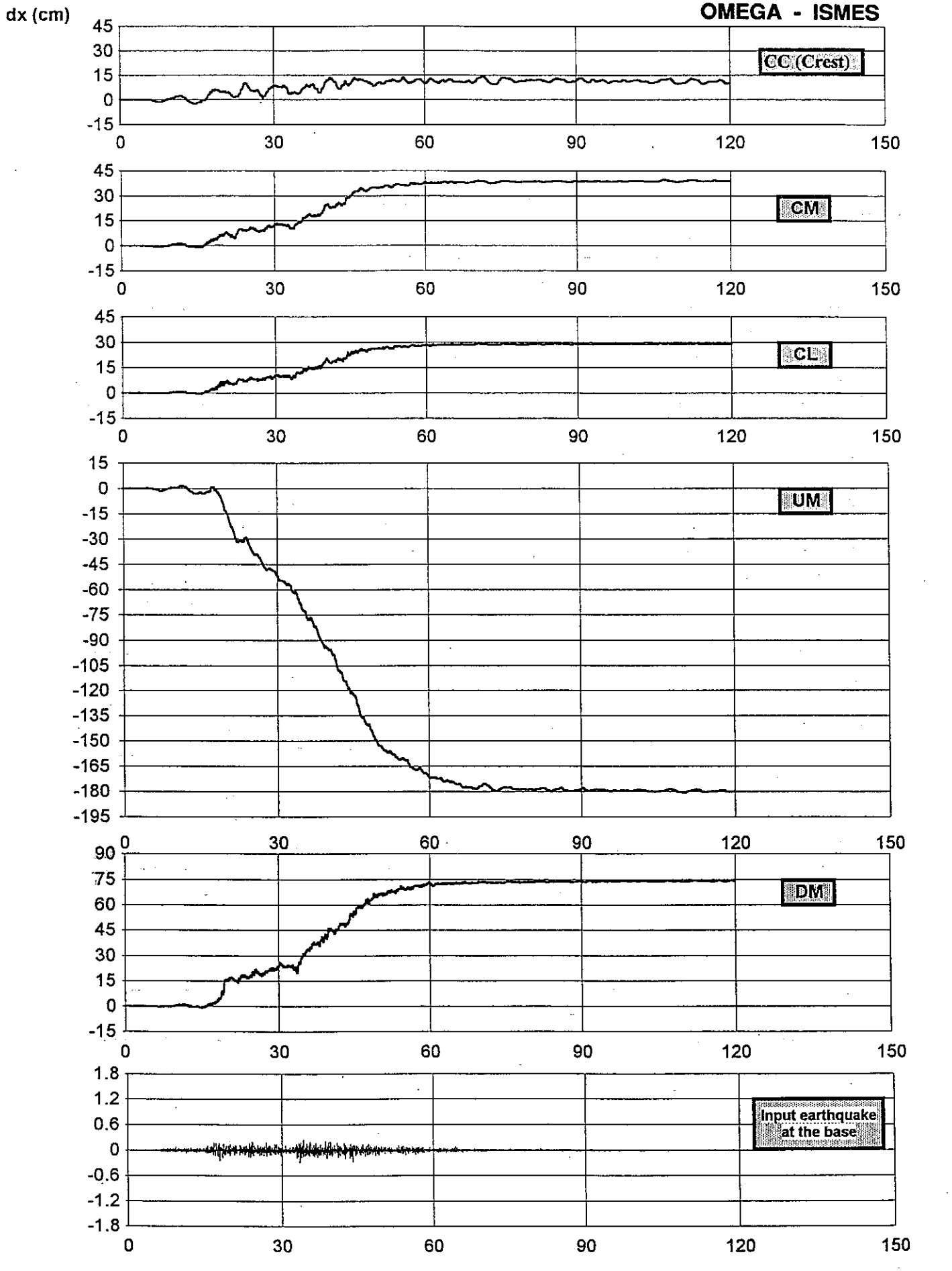

Fig. 3a

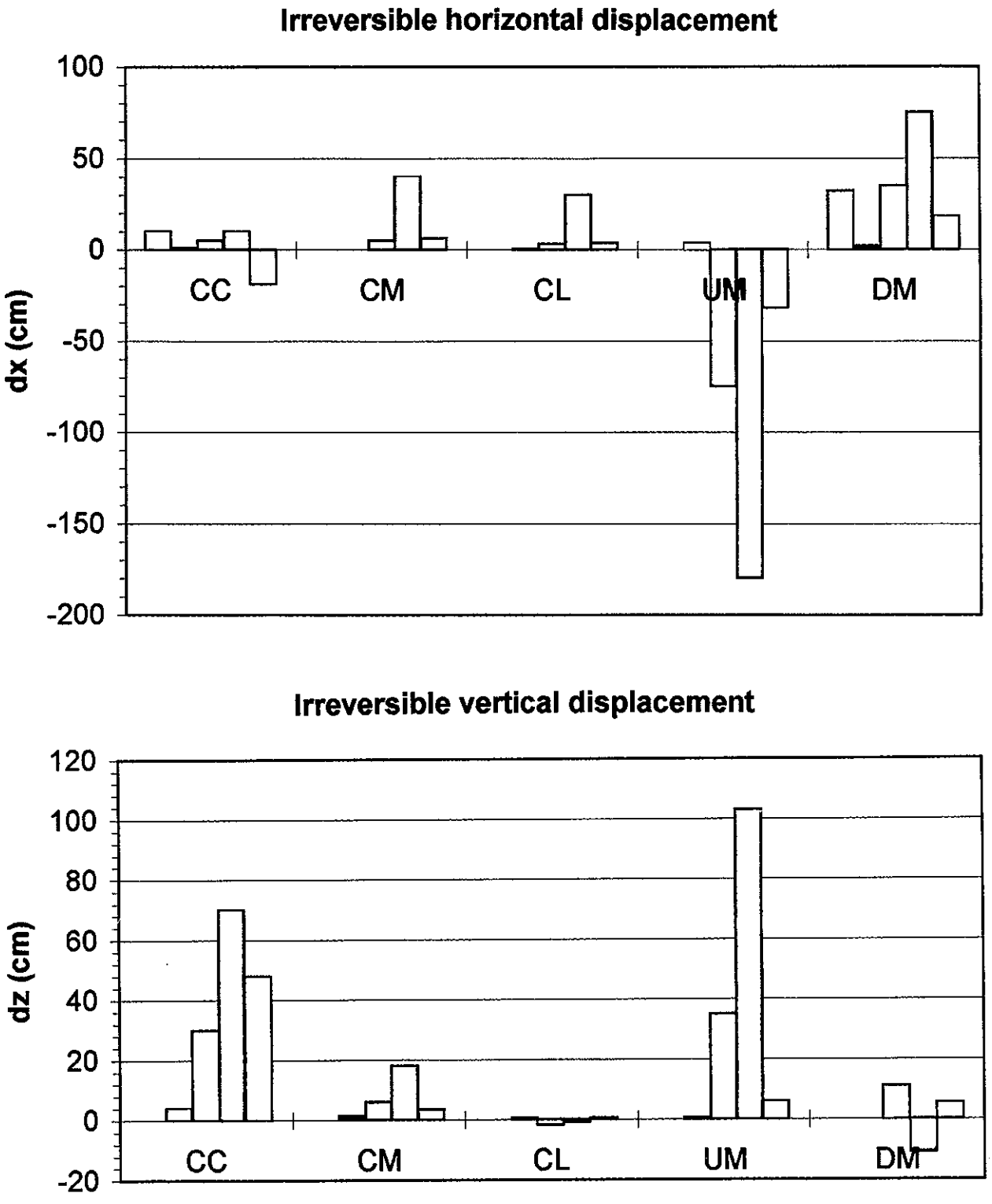
Irreversible horizontal displacement
dx (cm)
100
50
0
-50
-100
-150
-200
CC
CM
CL
UM
DM
Irreversible vertical displacement
dz (cm)
120
100
80
60
40
20
0
-20
CC
CM
CL
UM
DM
FLUSH - CVG EDELCA
FLUSH - DEFORM - Univ. Bucharest
OMEGA - ISMES - INPUT X only
OMEGA - ISMES - INPUT X and Y
GEFDYN - COYNE ET BELLIER

Fig. 6a

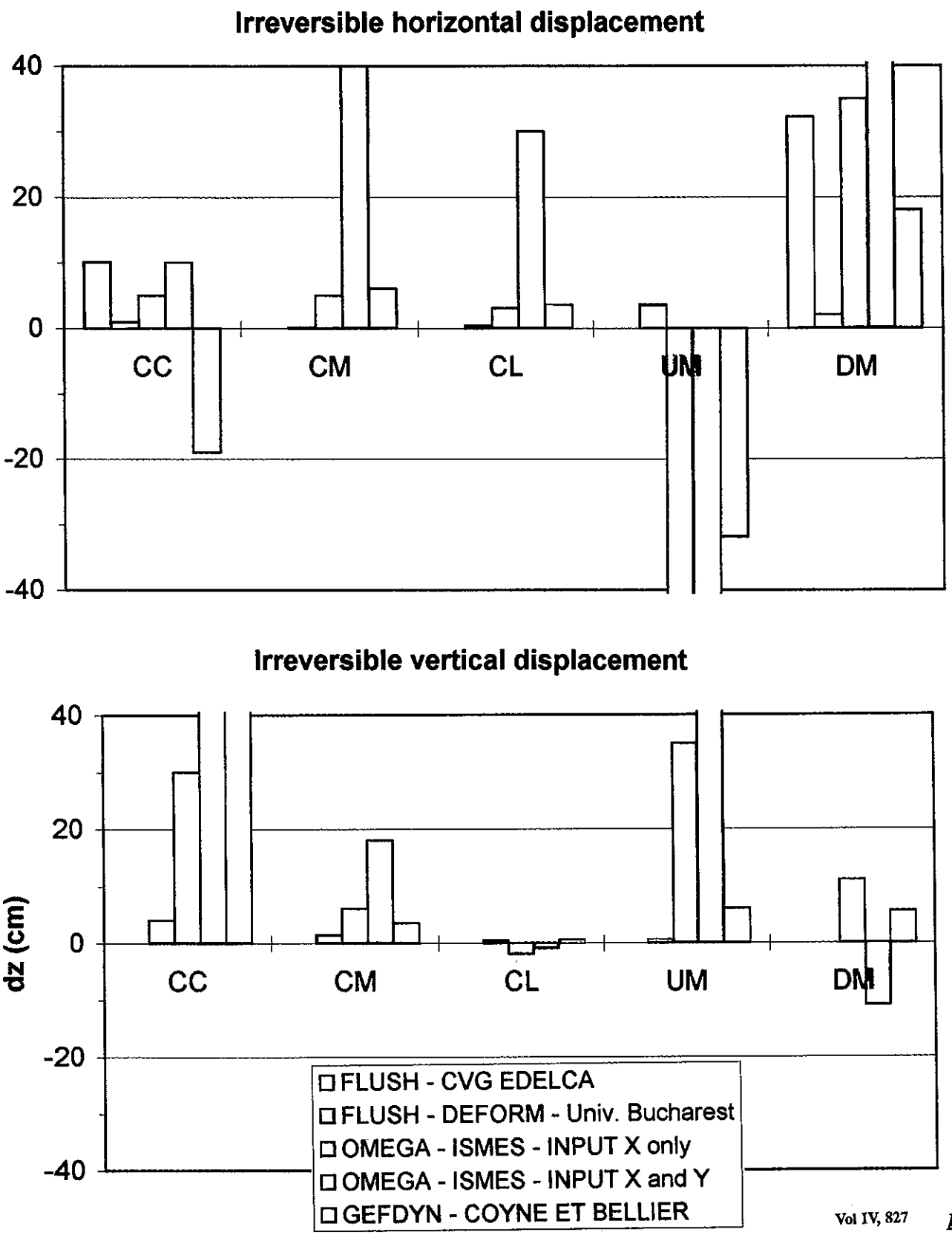
Irreversible horizontal displacement
40
20
0
-20
-40
CC
CM
CL
UM
DM
Irreversible vertical displacement
dz (cm)
40
20
0
-20
-40
CC
CM
CL
UM
DM
FLUSH - CVG EDELCA
FLUSH - DEFORM - Univ. Bucharest
OMEGA - ISMES - INPUT X only
OMEGA - ISMES - INPUT X and Y
GEFDYN - COYNE ET BELLIER

Fig. 6b

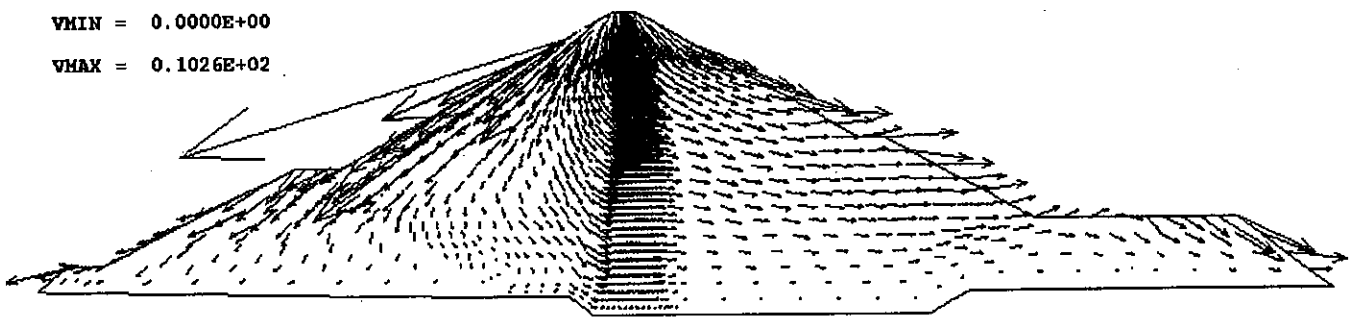

TOTAL DISPLACEMENT VECTORS (m)

Fig. 7a

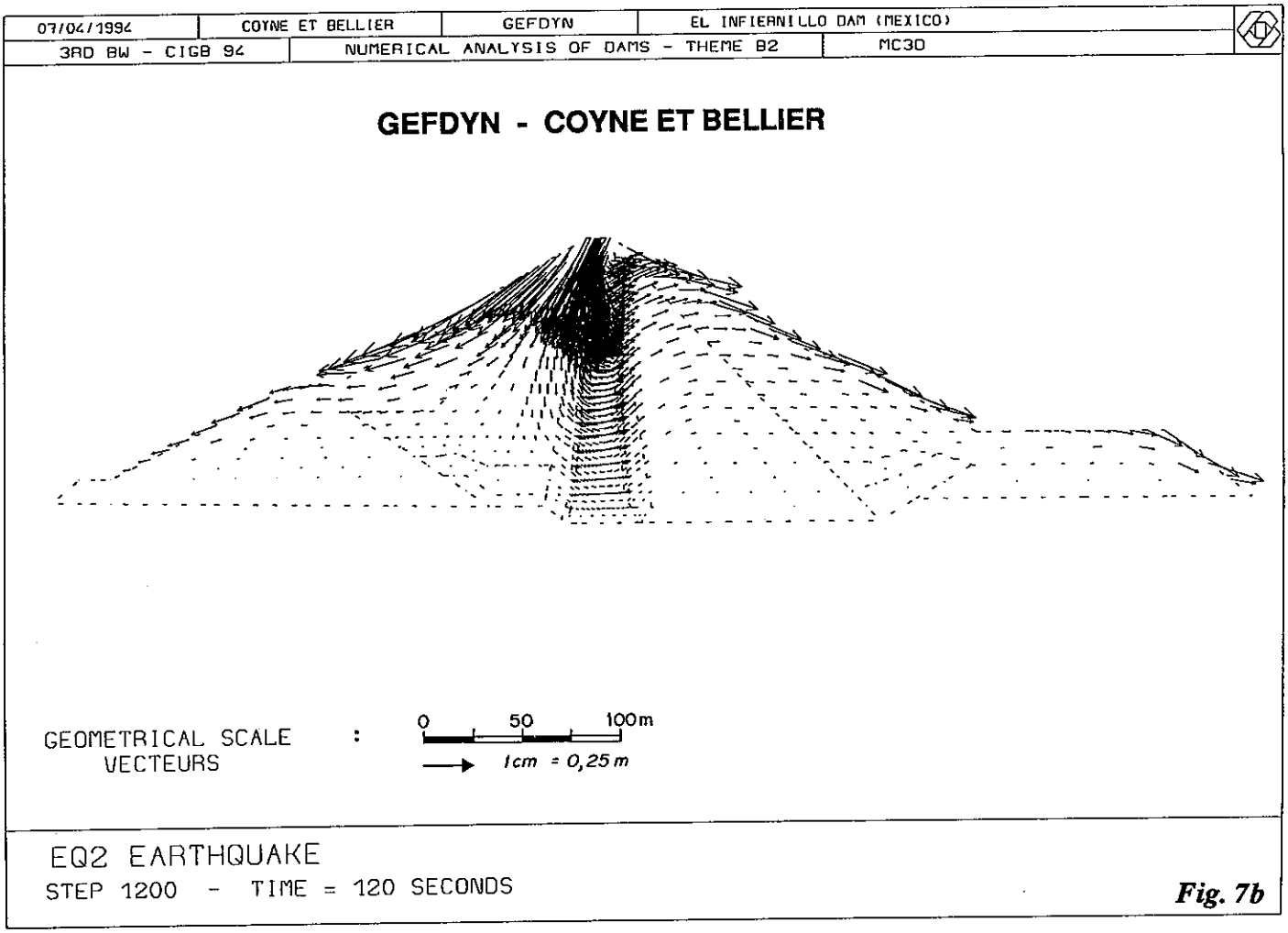

Fig. 7b

Irrecoverable displacement field at the end of earthquake EQ2

Fig. 7

Excess Pore Pressure

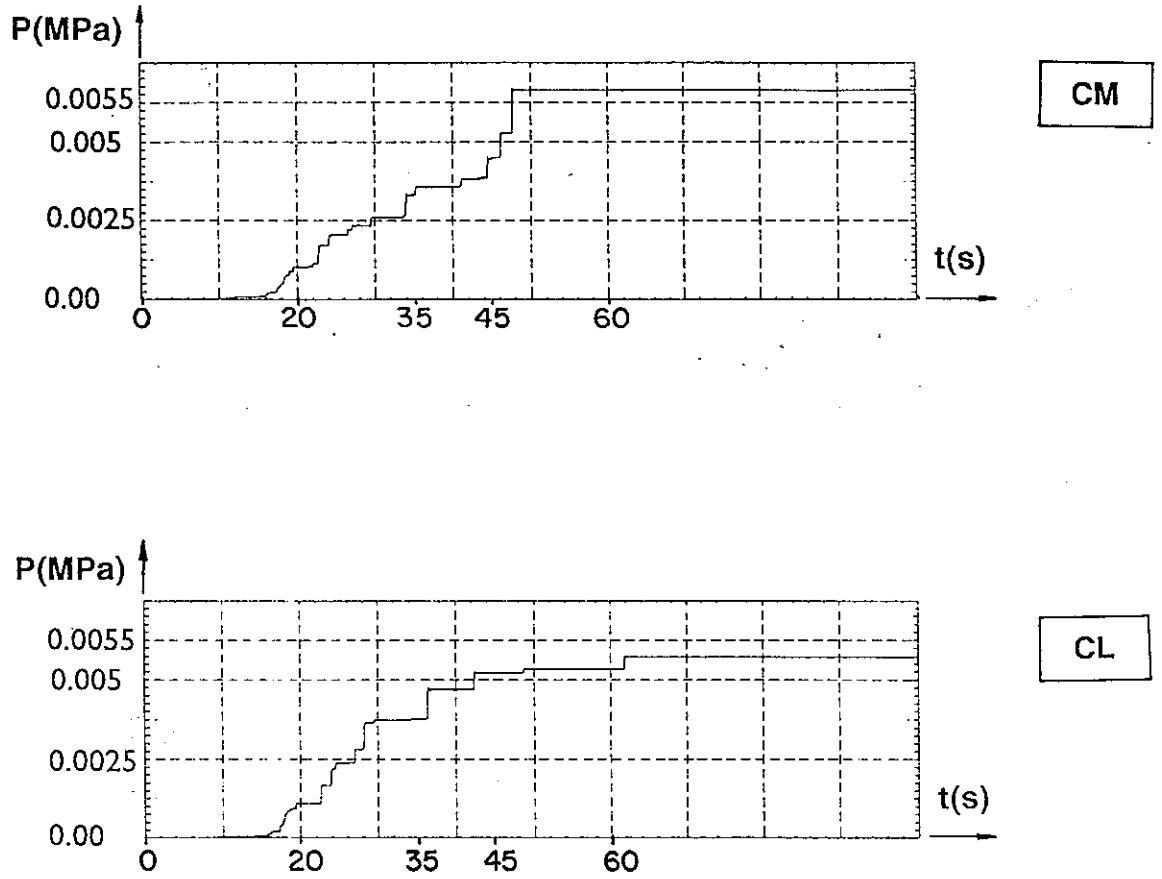

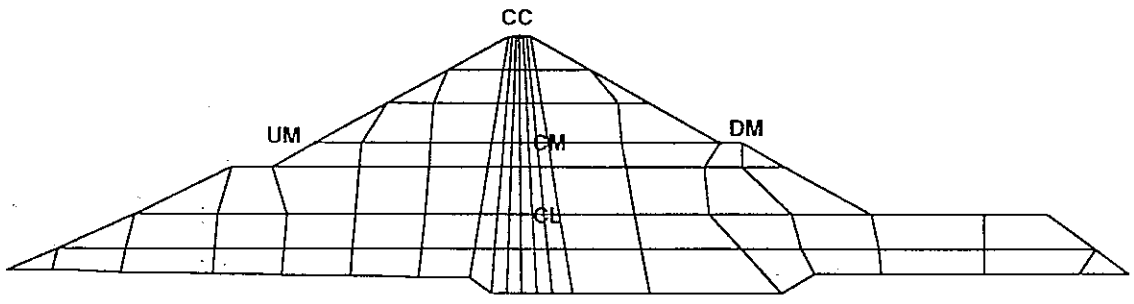

El Infiernillo dam clay core - Excess pore pressure time history during EQ2 accelerogram applied horizontally.

3rd. ICOLD 1994 - DYNAMIC ANALYSIS OF AN EMBANKMENT DAM

EQ2 earthquake considering only horizontal component

EXCESS PORE WATER PRESSURE VS TIME

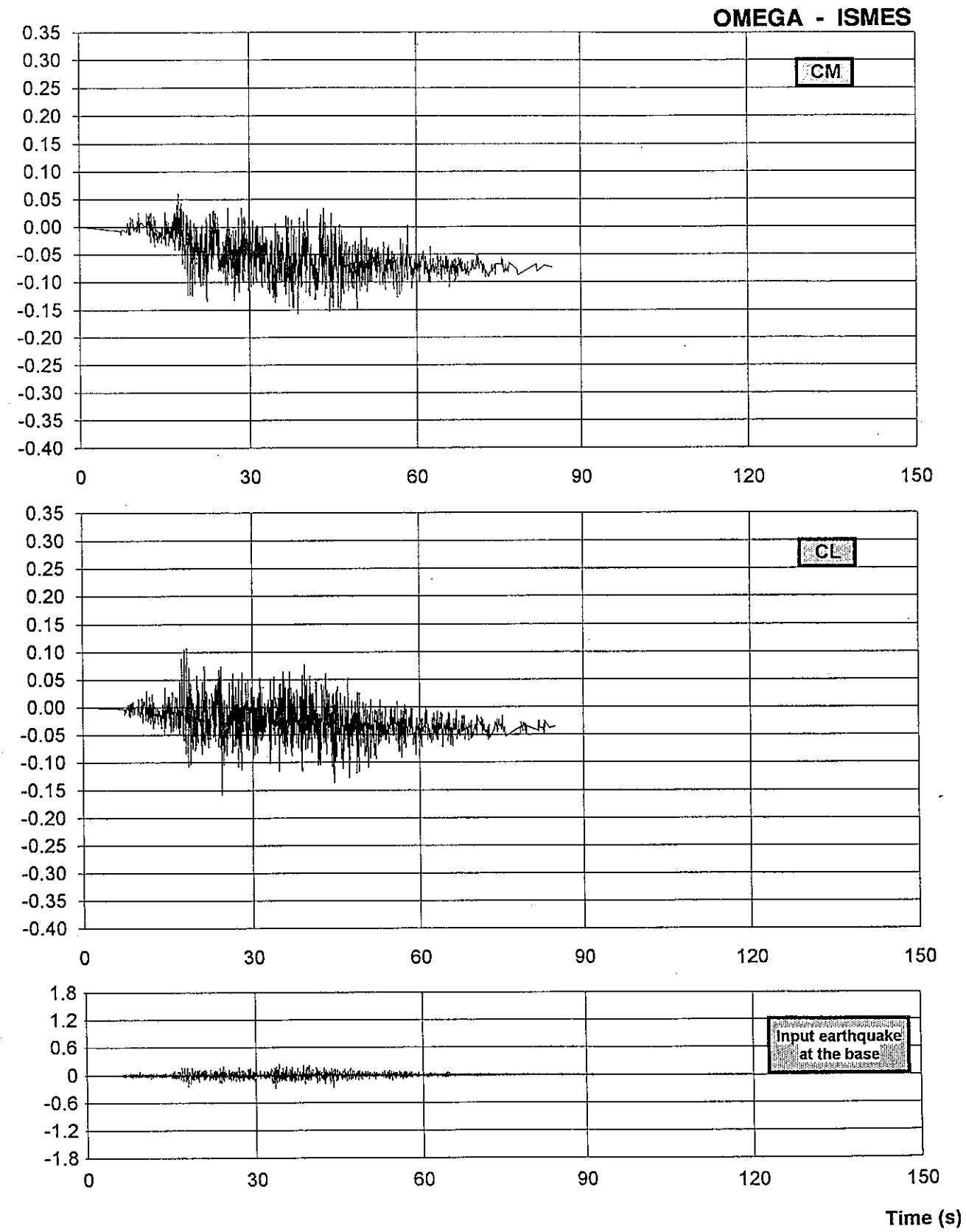

Fig. 9a

3rd. ICOLD 1994 - DYNAMIC ANALYSIS OF AN EMBANKMENT DAM

EQ2 earthquake considering horizontal and vertical components

EXCESS PORE WATER PRESSURE VS TIME

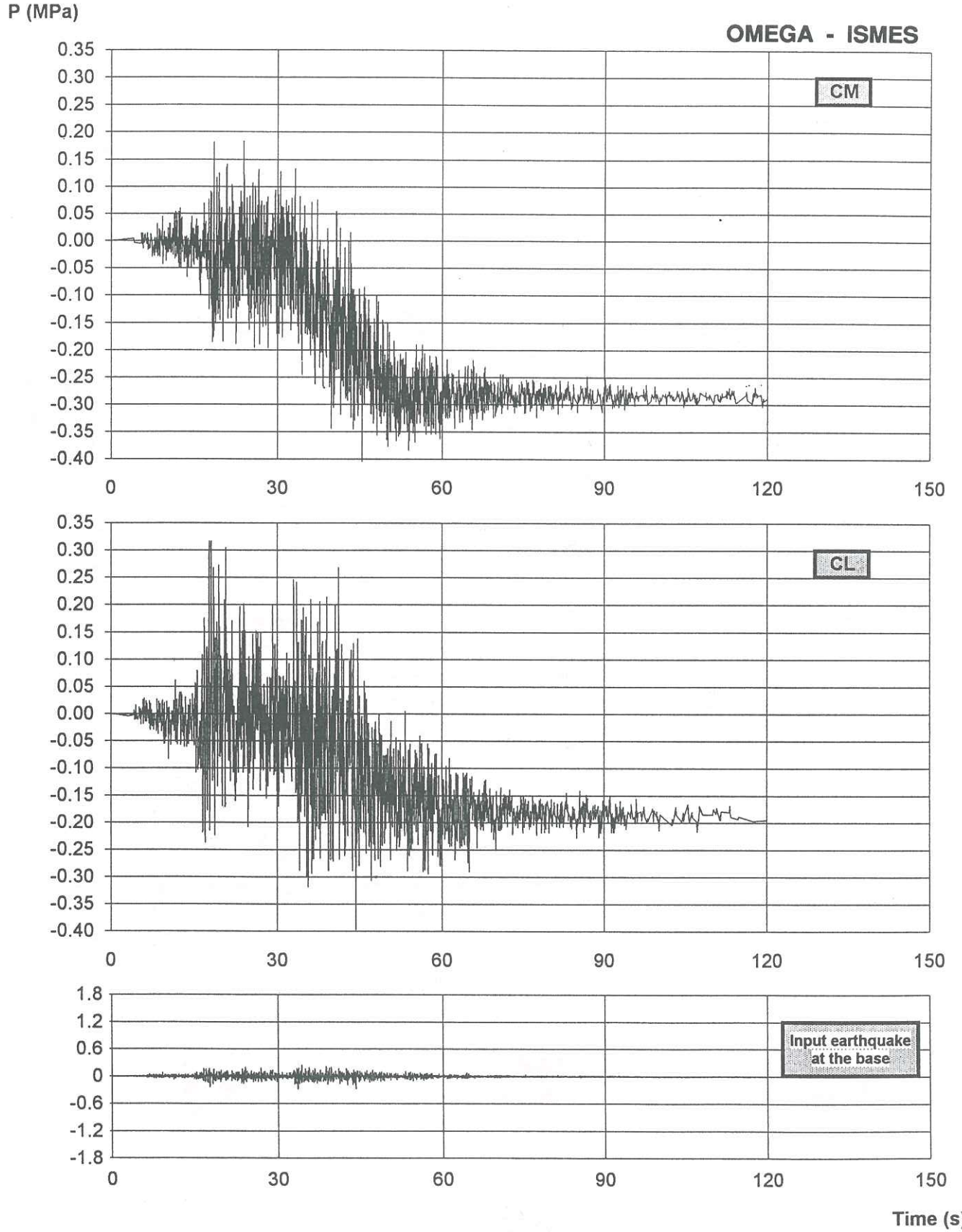

3rd. ICOLD 1994 - DINAMIC ANALYSIS OF AN EMBANKMENT DAM

EXCESS PORE WATER PRESSURE

OMEGA - ISMES

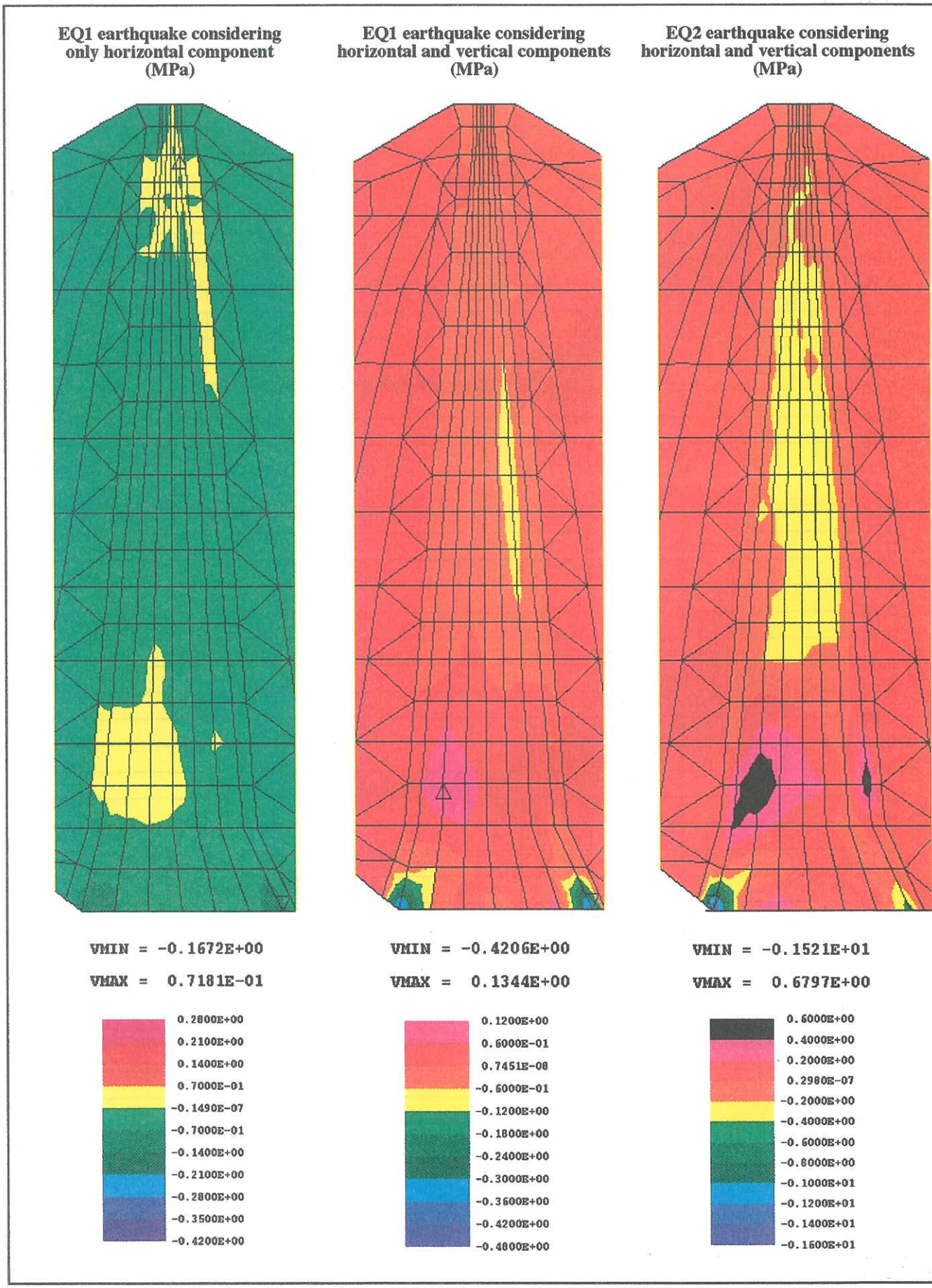

Fig. 11a

Third Benchmark Workshop on
NUMERICAL ANALYSIS OF DAMS
Gennevilliers, France, September 29-30, 1994

THEME B2

Dynamic analysis of an embankment dam under a strong earthquake

PAPERS

- FLUSH : P.H. Perazzo, CVG-EDELCA, Venezuela
- FLUSH & DEFORM & LASS III : A. Popovici, I. Toma, R. Sarghiuta, Civil Engineering Institute of Bucharest and Institute for Hydraulic Studies and Design, Romania
- GEFDYN : O. Ozanam, F. Lacroix, B. Tardieu, Coyne et Bellier, France
- OMEGA : G. La Barbera, A. Bani, G. Mazza', ISMES SpA and ENEL-CRIS, Italy

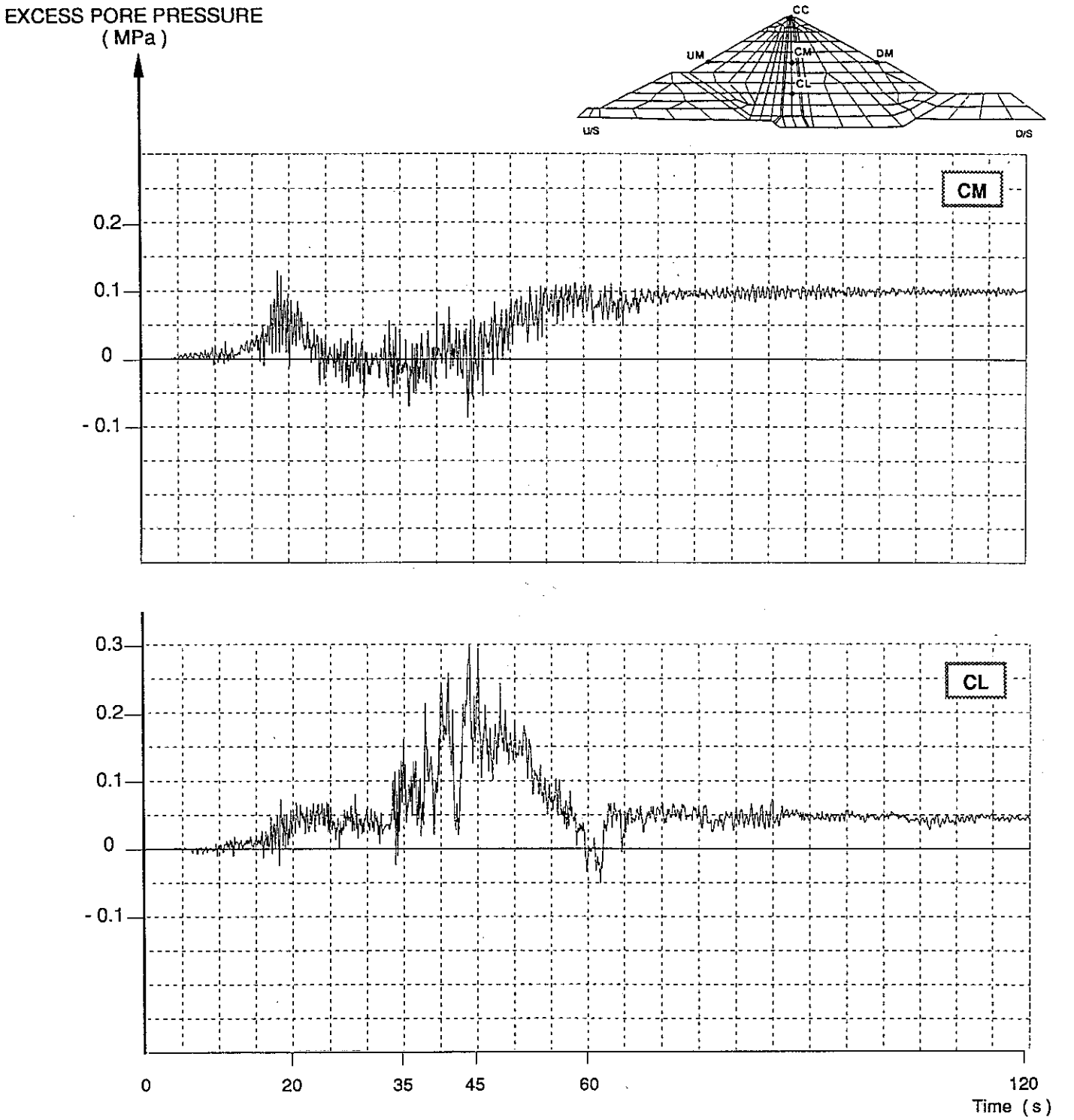

EQ2.DAT
Record at base rock, 1985

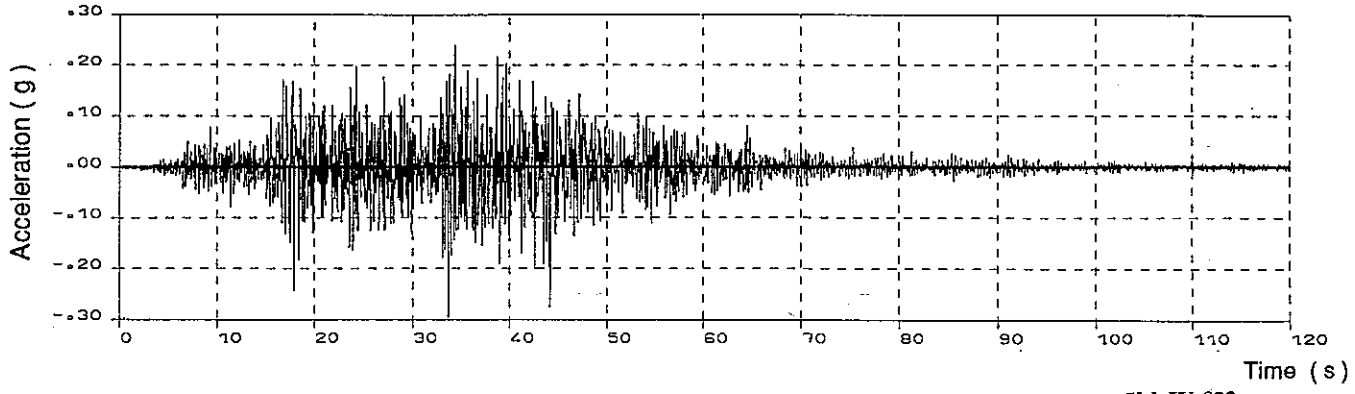

Excess pore pressure time history - Earthquake EQ2 ***Fig. 10***

07/04/1994	COYNE ET BELLIER	GEFDYN	EL IN
3RD BW - CIGB 94	NUMERICAL ANALYSIS OF DAMS - THEME B2		

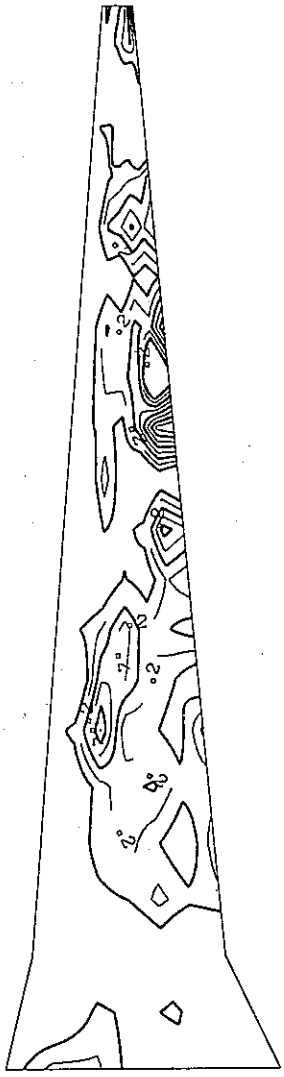

GEOMETRICAL SCALE : .00100

EQ2 EARTHQUAKE

EXCESS PORE PRESSURE - TIME = 120 SECONDS

Fig. 11b

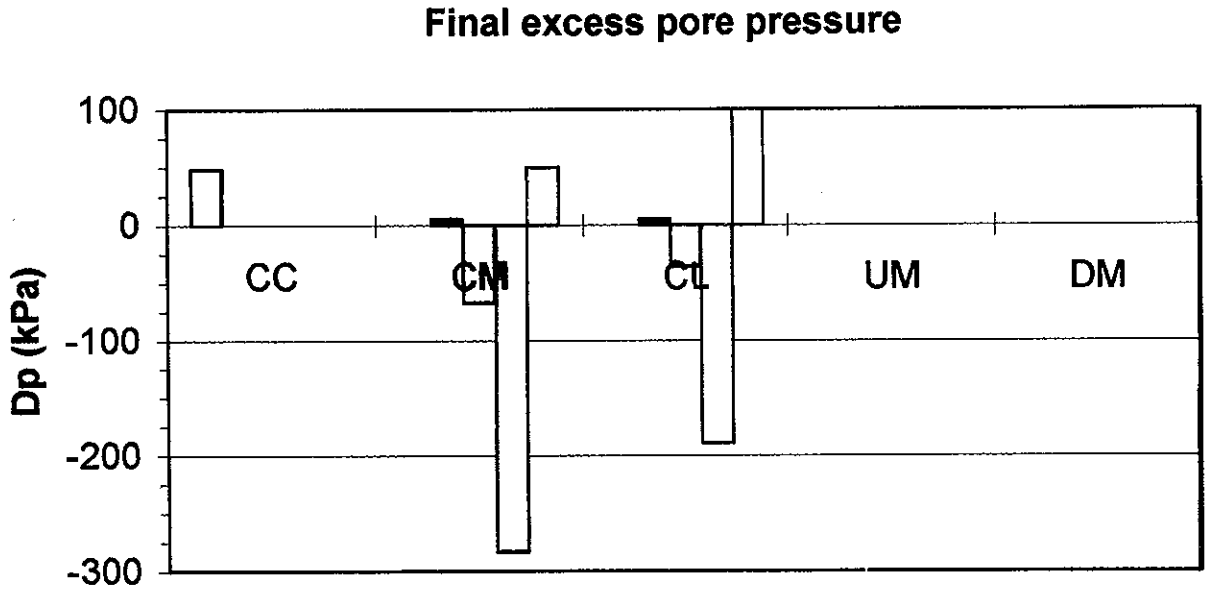
Final excess pore pressure
100
0
-100
-200
-300
Dp (kPa)
CC
CM
CL
UM
DM

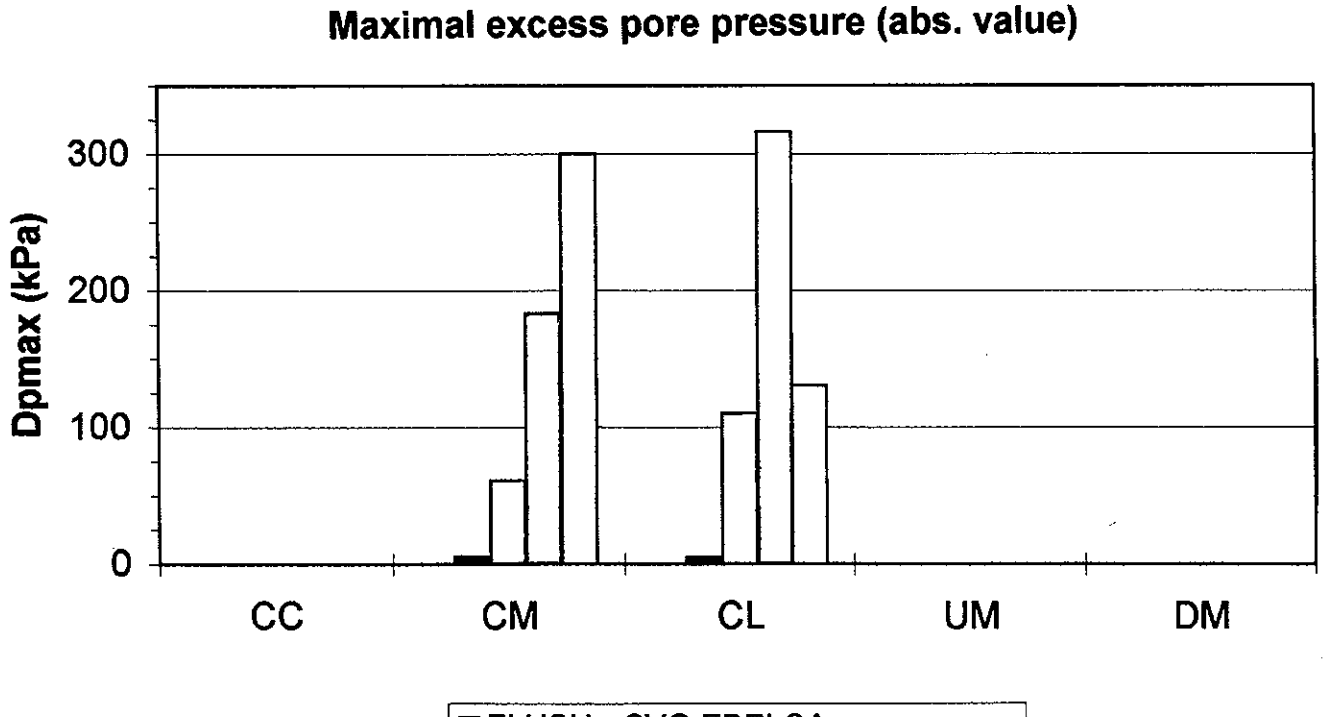
Maximal excess pore pressure (abs. value)
300
200
100
0
Dpmax (kPa)
CC
CM
CL
UM
DM
FLUSH - CVG EDELCA
FLUSH - DEFORM - Univ. Bucharest
OMEGA - ISMES - INPUT X only
OMEGA - ISMES - INPUT X and Y
GEFDYN - COYNE ET BELLIER

Fig. 12

NOTES

NOTES

NOTES

Analyses of the Infiernillo Dam

Based on The Methodology Adopted in Recent Dynamic Analyses of Embakment Dams in Venezuela

by

Pascual H. Perazzo Ch.
Section Head, Geotechnical Department
C.V.G - EDELCA
(Venezuela)

ABSTRACT.

This paper presents the results of dynamic analyses performed on the Infiernillo Dam based on the Methodology adopted in recent dynamic analyses on Earth and Concrete Faced Rockfill Dams located in moderate and high seismicity areas of Venezuela.

Six different dams have been recently evaluated in Venezuela (1987 - 1994). The first in 1987, corresponded to the re-evaluation of Guri Right Embankment Dam, followed by the evaluation for design purposes of Caruachi left Embankment and right Concrete Face Rockfill dam (1992), all of them part of the hydroelectric developments on the Caroni River, located in the Southeastern part of Venezuela, which corresponds to an area of moderate seismicity. Seismic evaluations show the possibility of a probable maximum earthquake occur in this area of magnitude 6.5 on the Richter Scale, with a peak acceleration of 0.24g.

Other dynamic analyses have been performed on dams located in different areas of Northern Venezuela, where an earthquake of magnitude 7.8 with a peak acceleration of 0.59g could be expected. These analyses correspond to the dynamic evaluation of the existing Petaquire hydraulic fill embankment dam (1993), and the Mamo Concrete Face Rockfill Dam (1993) currently under design. The Yacambu Concrete Face Rockfill Dam (1994), currently under construction, is located in the Northwestern Venezuela, where an earthquake of magnitude 7.9 can be expected.

The technique used for the dynamic evaluation consisted generally in determining an appropriate input ground motion based either on probabilistic or deterministic basic to estimate the maximum level of shaking. Develop an understanding and idealized model of the site stratigraphy and material properties derived from local geology; in situ investigations using SPT, undisturbed sampling, geophysical measurements, construction records for existing embankments and laboratory testing including index tests, static strength tests, cyclic triaxial test and resonant column test. The next step is to estimate in situ effective stresses in the foundation and the dam prior to the earthquake, using a nonlinear finite element static stress analysis. Dynamic response is estimated with total stress equivalent linear two - dimensional finite element model.

For the Earth Embankment Dams, zones of liquefied materials, residual strength, and excess pore pressure build up are estimated using Seed's procedures by comparing the stress level which could be developed during the earthquake with the cyclic strength of the foundation and embankment materials. Afterwards a post earthquake stability analysis is performed combining the liquefied (residual strength) and excess pore pressure zones using a limited equilibrium method.

For a Rockfill Dams there can be no build up of pore pressures due to an earthquake. Consequently, there is no tendency for strength reductions. Newmark's sliding block analyses was used to estimate deformations during shaking. The purpose is to establish whether the estimated deformations exceeded an acceptable level.

The same technique have been adopted for the evaluation of the Infiernillo dam regarding the exercise proposed to the Third ICOLD Benchmark Workshop on Numerical Analysis of Dams, Theme B2, Dynamic analysis of an embankment dam under a strong earthquake.

The results for the Infiernillo dam togheter with the methodology of the analysis, the selected computation method, the main assumptions of the numerical model adopted, the software used and the computation time and hardware used are reported in this paper.

INTRODUCTION.

The dynamic analysis of embankment dams in Venezuela has advanced significantly during the past 7 years, beginning with the evaluation of Guri left earth embankment dam (Ref. 1), followed by the dynamic analyses of Caruachi left Embankment and right Concrete Face Rockfill dams (Ref. 2 and

3), and continue with Petaquire hydraulic fill embankment dam (Ref. 4), the Mamo Concrete Face Rockfill Dam (Ref.5) and the Yacambu Concrete Face Rockfill Dam (Ref. 6). ***Much of this achievement can be attributed to the successful application of computer software technology such as the computer program FEADAM " Finite Element Analyses of Dams" (Ref. 7), SHAKE " A Computer Program For Earthquake Response Analyses of Horizontal Layered Sites" (Ref. 8) and FLUSH " A Computer Program Approximate 3 - D Analysis of Soil Structure Interaction Problems". (Ref.9).***

The approach used for the dynamic analysis of the embankment dams places the emphasis on the determination of permanent deformations for rockfill dams and quantification of excess pore pressure due to the shaking to asses post earthquake stability by limit equilibrium analyses of the slope for earth dams. The general procedure used to analyze the dams for earthquake response may be devided into three parts: Determination of design seismic events, Determination of embankment response to site ground motion, and the Evaluation of embankment capability.

The purpose of this paper is to present the results of the dynamic analyses of the Infiernillo dam and synthesized the technology used in a detailed and unified manner so that its capabilities as well as its limitations may be understood.

GROUND MOTION RECORDS

Two Earthquake record were submitted by the Technical Committee for the evaluation of the Infiernillo Dam both of them horizontal accelerations recorded at the base rock.

The firsts record designated as EQ1 with peak acceleration of 0.10g, was used togheter with the measurements of maximum accelerations and irreversible displacements made on site, during and after the earthquake, for fitting the dynamic properties required for the analyses.

The second record designated as EQ2 , with a peak acceleration of 0.29g represents the horizontal upstream-downstream acceleration at the base of the dam and was used for the dynamic analysis as it was requested by the Technical Committee.

METHODOLOGY OF THE ANALYSIS.

The steps used to evaluated all of this dams and the Infiernillo dam (with the available data) were as follow:

Interpret subsoil conditions to identify transverse cross - sections utilizing engineering classification, penetration resistance and natural moisture contents obtained from field and laboratory testing programs.

Use SPT (standard penetration test) to characterize in - situ strength.

Define the Maximum Credible Earthquake (MCE) and recommend a design earthquake applicable to the dam site. Evaluate seismic hazard at the site and determine acceptable level of risk for the project and select real ground motions based on seismic hazard and associated level of risk.

Develop model for use in dynamic response analysis. Stiffness of soil layers and type of materials were determined on the basis of both shear wave velocity, crosshole data and SPT data.

Perform preliminary and final dynamic response analysis utilizing the computer program SHAKE and FLUSH. Dynamic stresses and accelerations profile throughout the foundation and the dam were developed.

Perform static stress analysis of the embankment and its foundation using finite element program FEADAM. Results were used to develop correction factors for non - standard confinement and sloping ground conditions. Hyperbolic stress - strain parameters used by FEADAM were obtained by consolidated drained triaxial test.

Perform cyclic tests on selected undisturbed samples recovered from the dam site. Develop design liquefaction curve.

Compute blow count value required to prevent liquefaction and loss of strength. The values of dynamic stress ratios obtained from FLUSH results were appropriately corrected from the effects of confinement and non level ground conditions.

Compare blow count values required to blow count value measured. Potentially unstable areas in the foundation were identified.

Perform post - earthquake stability analyses at critical sections. Excess pore pressure were determined using the design liquefaction curve. The pore pressure plus hydrostatic pressure were input into stability - analysis.

The earthquake induced maximum deformation corresponding to the maximum section of the dam, was evaluated using a combination of Seed and Makdisi - Seed (Ref. 10) procedure. Those method are based on the assumption that the permanent deformations take place whenever the rigid body acceleration of a potential sliding mass exceeds the yield acceleration of that mass.

Yield acceleration is determined by performing a series of pseudo - static stability analyses. The yield acceleration of a potential sliding mass is the coefficient of the lateral force, expressed in the units of gravity, that confers a factor of safety of 1.0, against sliding of that mass. The critical yield acceleration (Ky) were determine for the downstream slope.

The acceleration distributions in the dams (Kmax) corresponds to the accelerations recorded of the design earthquake on each particular location and were computed with the dynamic response analysis program FLUSH. The non - linear stress - strain characteristic of the dams are taken into account by using an equivalent - linear representation of the rockfill characteristics that involve the use of the strain - dependent modules and damping properties.

The dynamic properties for pressure - dependent , strain - dependent and the shear modules were conveniently represented by the formula:

$$G = 1000 * K2 * (Sig\ m)^{0.5}$$

Where G is the effective shear modules at any given strain level, (Sig m) is the effective mean principal stress at any point and K2 is the soil modules coefficient that depends on the stiffness of the fill, general in the range of 120 to 150 for compacted rockfill.

Once the yield and maximum acceleration were determined for the sliding mass the maximum deformations were calculated by using the chart provided by Seed and Makdisi (Ref.10). Permanent deformations corresponding to each critical failure surface were calculated by using the relation between the horizontal displacement; U of the sliding mass to the ratio KY/Kmax for the maximum magnitude of the design earthquake for each particular dam site.

SELECTED COMPUTATION METHOD AND SOFTWARE USED.

The selected computation method is presented for the calculation of the Initial Conditions, Dynamic Response (accelerations, dynamic stresses and excess pore pressures) and Displacement Estimations.

Initial Conditions.

The determination of the in situ effective stress for the static load case corresponding to the whole history of the dam before the earthquake, was modeled using ***the FEADAM system*** and incremental finite element program for two - dimensional, plane strain analysis of earth and rockfill dams and slopes. It calculates the stresses, strains, and displacements due to incremental embankment construction and or load application. The non - linear and stress history dependent stress - strain and volumetric strain properties of soils are approximated using a hyperbolic model develop by Duncan, Byrne, Wong and Mabry (Ref.11).

Dynamic Response.

Dynamic response was estimated with total stress, equivalent linear two - dimensional finite element method ***FLUSH*** . Zones of liquefied materials, residual strengths, and excess pore pressures buildup are then estimated using Seed´s procedures (Seed and Harder Ref.12, Marcuson et al. Ref 13). The excess pore pressures determine based on the triaxial test compiled by De Alba et al. (Ref 14) as show in figure N°1 indicating that there is a somewhat unique relationships between the excess pore pressure ratio **ru** and the cycle ratio **Neqk/Nl.** the excess pore pressure ratio is equal to the ratio of the excess pore pressure **ug,** generated by the cyclic loading, to the initial vertical effective stress. The value of **Neqk** is the number of cycles in a earthquake motion of any given magnitude that can be considered to consist of a succession of uniform cycles delivering the amount of energy equivalent to the amount contained in the actual motion. Seed and Idriss (Ref. 15) have proposed the relation between number of uniform cycles and magnitude shown in figure N° 2

Limit equilibrium analyses of the slope with these residual strength and excess pore pressure zones are used to assess stability.

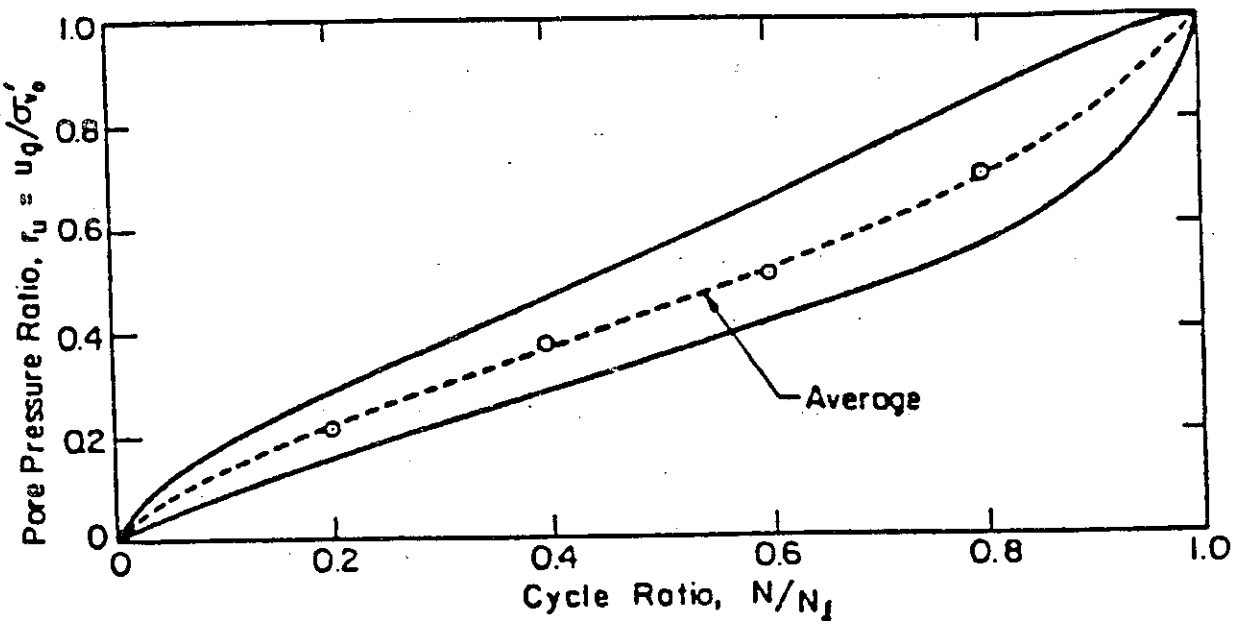

Figure N° 1. Rate of Pore Water Pressure Build Up in Cyclic Triaxial Tests.

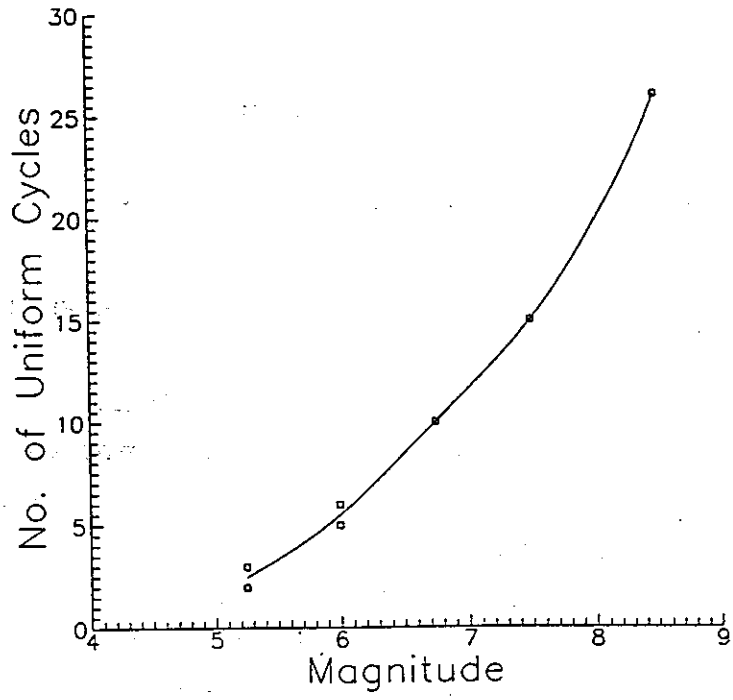

Figure N° 2. No. of Uniform Cycles vs. Magnitude.

Irreversible Displacement.

The irreversible displacement are computed using the concept of yield acceleration (Makdisi, Seed 1978, Ref. 10) but is based on the evaluation of the dynamic response of the embankment rather than a rigid body behavior. The permanent deformations are estimated by numerical double integration of the time history of induced accelerations for various depth of the potential sliding mass. Curve develop by Makdisi, Seed subject to base accelerations representing earthquake of magnitude between 6.5 and 8.25 are presented in figure N° 3.

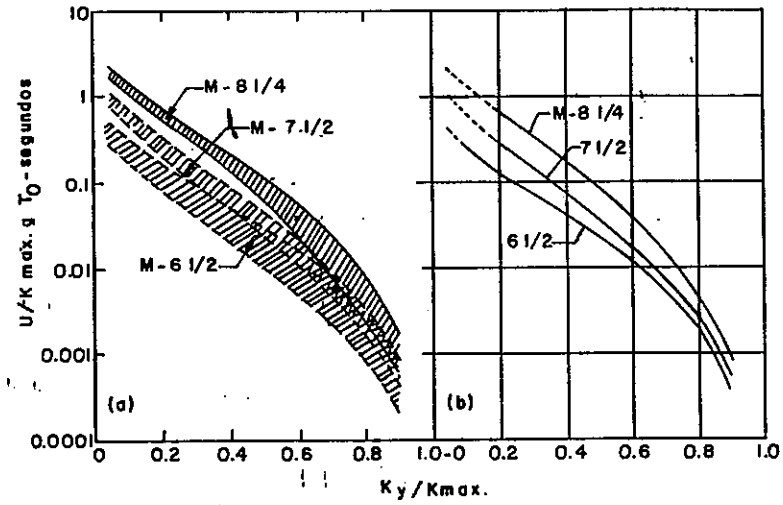

Figure N°3. Relation Acceleration vs. Displacement.

MAIN ASSUMPTIONS OF THE NUMERICAL MODEL ADOPTED.

The following main assumptions were assumed on each of the numerical model adopted:

In calculating the initial conditions effective stress using the ***FEADAM system,*** the main assumption is based on a successive - increment procedure for approximating non - linear stress and stress history dependent behavior of soil, in which progressive loading is divided into a number of small increments, and the soil behavior obeys the hyperbolic stress - strain and volumetric relationships which are consider to be linear within each increment of load. The load increments are simulated by applying forces to represent the weight of the added layer of fill. The post - construction load increments are represented by applied nodal points forces which are desirable to be applied in several increments in order to improve the accuracy with which the non - linear soil behavior is simulated.

Dynamic response analysis using the ***FLUSH program***, can be performed with different degrees of approximation or sophistication. The main assumptions for a good analytical procedure may be summarized as follows:

1.- ***P and S waves*** are assumed to have the same attenuation factor. This assumption may not be physically correct but is the best can be made with the present knowledge of wave propagation in soils.

2.- ***The free field motions*** are computed on the assumption that the free field consists of horizontal soil layers and that the seismic excitation consists of vertically propagation P or S waves.

3.- ***The equivalent linear method.*** This method take into the large shear deformations which occur in soils during strong earthquakes that introduce significant non linear effects. The approximate non linear solution can be obtained by linear analysis compatible with the effective shear strain amplitudes at all points of the system. It should be mentioned here that reliable total displacements cannot be expected from FLUSH or any other equivalent linear method. FLUSH is essentially designed to compute acceleration time histories and spectra, and time histories of stress, strain or relative displacement between nodal points.

COMPUTATION TIME AND HARDWARE USED.

The FEADAM System runs on an IBM XT, AT or any other compatible microcomputer capable of running MS-DOS version 2.0 or higher. The FEADAM system requires the following minimum hardware: 80287 math coprocessor, 512 K memory, 2 floppy disk drives. The computation time for the example of the Infiernillo dam in a 386 IBM compatible computer was 37 minutes.

FLUSH requires 4 Mbytes of memory and one disc drive and a hard drive of approximately 100 Mega bytes. An 80387 math co - processing chip is required to run the program. The computation time using the earthquake record EQ2 for the Infiernillo dam was 3 Hr and 23 minutes.

PRESENTATION OF RESULTS.

Finite Element Mesh.

The basic mesh proposed and already used for the two previous Benchmark Workshops have been adopted for the analyses. Neither the filters nor the transition zones were considered into the analyses.

Dynamic Properties of the Materials.

The importance of using soil properties which accurately represent the material cannot be overemphasized (Ref 16). The following properties were established for each material modeled by the finite element analysis: Total unit weight, Maximum Shear Modulus, Variation of maximum shear modulus with the mean effective principal stress, Variation of shear modulus with shear strain, Variation of damping ratio with shear strain and the Poisson´s ratio.

For the core material the variation of shear modulus with shear strain was determine fitting the parameters from a back analyses using by an iterative process with the earthquake input of March 14, 1979 (EQ1.DAT). The procedure were based on the trial and error for adjusting the following equation:

$$Gc = Kc * Fc$$

Where, Gc is the shear modulus of the core material for any given strain level, Kc is and average strain function for low plasticity clays and F is a factor which generally is the undrained shear strength of the clay. The factor F was then calculated by a back analyses adopting a maximum acceleration at the crest of 0.362 g, resulting a value of 1.70 Kg/cm2 which is very close to the average qu value of 1.84 Kg/cm2.

For the rockfill materials the dynamic properties for pressure - dependent , strain - dependent and the shear modules were conveniently represented by the formula:

$$G = 1000 * K2 * (Sig\ m)^{0.5}$$

Where G is the effective shear modules at any given strain level, (Sig m) is the effective mean principal stress at any point and K2 is the soil modules coefficient that depends on the stiffens of the fill, general

in the range of 120 to 150 for compacted rockfill. A value of 140 and 80 where adopted for the Compacted and Dumped Rockfills.

For the estimation of excess pore pressures a typical liquefaction curve for a compacted low plasticity clay of Guri Dam Clay Core was adopted into the analyses and is shown on figure N° 4.

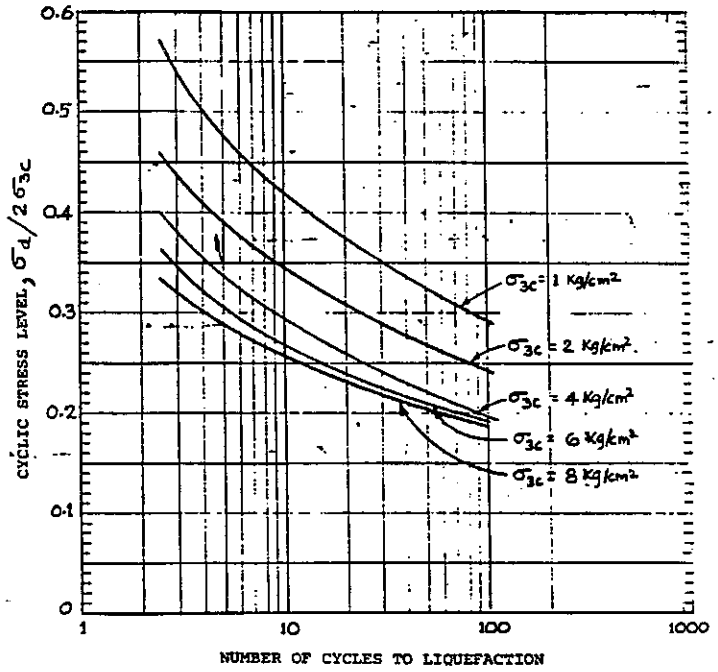

Figure N° 4. Liquefaction Curve for Clay Core.

Acceleration, Displacement and Excess pore pressures.

Only absolute values of acceleration, displacement of a specified potential slide and absolute values of excess pore pressures could be determine using the methodology adopted for the analysis.

The results are summarized in the following table for the points required by the Technical Committee (see figure N° 5).

Points of the dam section					
	CC	**CM**	**CL**	**UM**	**DM**
Maximum horizontal acceleration (in g) (1)	0.75	0.49	0.41	0.65	0.57
Maximum vertical acceleration (in g) (1)	-	-	-	-	-
Irreversible slide displacemt. (in cm) (3)	10.08	0.00	0.00	0.00	32.24
Final excess pore pressure (in Mpa) (4)	0.048	0.00	0.00	-	-

(1) The required accelerations are ***absolute accelerations***
(2) Sign + : from U/S to D/S
(3) Sign + : from top to bottom
(4) Only the excess pore pressure will be given. The pore pressures obtained at the end of the static analysis must not be cumulated.

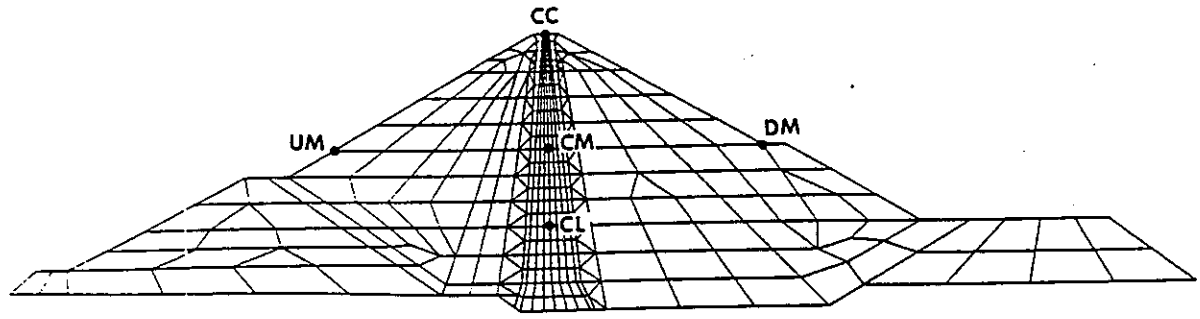

Table 1
3rd Benchmark Workshop - Theme B2
Results of the dynamic study - EQ2 earthquake

REFERENCE

1.- HARZA Engineering Company, "Guri Final Stage, Static and Dynamic Analyses of the Right Embankment Dam" July, 1987.

2.- Perazzo Pascual, C.V.G - EDELCA, Caruachi, Static and Dynamic Analyses of the Left Embankment Dam. ,September,1992.

3.- Pascual Perazzo and Bernard S. Liu, "The Design of the Concrete Face Rockfill Dam of the Caruachi Project". , Proceeding of the International Symposium on High Rockfill Dams, Beijing, China, October, 1993.

4.- De Fries K., "Seismic Evaluation of Petaquire Dam". Report prepared for Consortium Hidrocalec, Caracas, July, 1992.

5.- Pascual Perazzo,"Seismic Analyses of Mamo2, Concrete Face Rockfill Dam. Report for Consortium Hidrocalec. C. A., Febrero 1994.

6.- Pascual Perazzo, "Preliminary Dynamic Analyses of Yacambu Concret Face Rockfill Dam". Report for SIstema Hidráulico Yacambu - Quibor. , Marzo, 1994.

7.- Duncan, J.M., Wong, K.S., and Ozawa, Y., "FEADAM: A Computer Program for Finite Element Analysis of Dams," Department of Civil Engineering, University of California, Berkeley, December 1980.

8.- Schanabel, P.B., Lysmer, J. and Seed, H.B. (1972) "SHAKE- A Computer Program for Earthquake Response Analysis of Horizontally Layared Sites," Report No EERC 72-12, Earthquake Engineering Research Center, University of California, Berkeley, California.

9.- J. Lysmer, T. Udaka, C.F. Tsai and H.B. Seed, (1975). "FLUSH: A Computer Program for approximate 3-D analysis of soil-structure iteration problems." Earthquake Engineering Research Center, Report No. EERC 75-30.

10.- Makdisi F.I, Seed H. B. " Simplified Procedure for Estimating Dam and Embankment Earthquake - Induced Deformation". Journal of the Geotechnical Engineering Division. Vol. 104 NO. GT7. July 1978.

11.- Duncan, J. M., Byrne,P., Wong,K.S., and Mabry,P.,"Strenght, Stress-Strain and Bulk Modules Parameters for Finite Element Analyses of Stresses and Movements in Soil Masses,"

12.- Seed, R. B., and Harder, L. F. (1990). "SPT - Based Analysis of Cyclic Pore Pressure Generation and Undrained Residual Strenght", Proceeding of the H. Bolton Seed, Memorial Symposium, University of California, Berkeley.

13.- Vil Marcussen (1992) " State of the Art Paper: Dynamic Analyses of Embankment Dams." Proceeding of the symposium on Stability and Performance of Embankment and Slope II., University of California, Berkeley, California.

14.- De Alba P.,Chan, C.K., and Seed H.B., (1975). "Determination of Soil Liquefaction Characteristics by Large-Scale Laboratory Tests," Report No EERC 75-14, Earthquake Engineering Research Center, University of California Berkeley, Berkeley, California.

15.- H. B. Seed and I.M. Idriss. (1970) "Soil Moduli and Damping Factors for Dynamic Response Analyses" Earthquake Engineering Research Center, Report No . EERC 70-10, Berkeley, California.

16.- Bureau of Reclamation, (1976) "Dynamic Analysis of Embankment Dams", United States Department of the Interior, Bureau of Reclamation, Engineering and Research Center, Denver, Colorado.

Third ICOLD Benchmark Workshop
on Numerical Analysis of Dams
Paris (France) September 29 - 30, 1994

Theme B2

NONLINEAR SEISMIC ANALYSIS OF AN EMBANKMENT DAM

A. POPOVICI*, I. TOMA**, R. SARGHIUTA*

* Civil Engineering Institute of Bucharest
124, Lacul Tei Bd., 72302-Bucharest Romania
** Institute for Hydroelectric Studies and Design
5-7, Galati St., 79669-Bucharest Romania

1. Introduction

The paper refers to the results of seismic analysis in the cross section of maximum height (H= 132 m) of El Infiernillo embankment dam with clay core. The seismic responses of the dam in terms of accelerations, displacements and pore pressures were computed successively for a low earthquake (EQ1, $a_{max.}$ = 0.1 g).and for a medium / strong earthquake (EQ2, $a_{max.}$ = 0.29 g). The both earthquake accelerograms were applied on horizontal direction.

In order to evaluate the dam material properties before earthquakes, the hyperbolic Duncan-Chang model was used to represent the behaviour of the embankment materials during dam erection, first consolidation phase, reservoir impounding and second consolidation phase. The clay core consolidation process was analysed according to Terzaghi theory.

The dam nonlinear seismic response was computed step by step in time by linear equivalent method developed by Seed and Idriss (1970) [1]. A strain compatible material properties $\gamma\% = f (G / G_{in})$, $\gamma\% = f (D\%)$ (where $\gamma\%$ is shear strain, G_{in} - initial shear modulus, G - running shear modulus, D percent fraction of critical damping) were assimilated in agreement with the literature published data. The permanent seismic deformations were determined by equivalent nodal point force approach method developed by Seed et al (1976) [2]. In this method the dam body material behaviour is modelled by hyperbolic stress-strain relationship after Duncan-Chang.

The computed results concerning seismic response of the dam due to EQ1 earthquake accelerogram were compared with in site measurements performed during and after earthquake (maximum accelerations, irreversible displacements) in order to check up the performance of the applied mathematical models. The concordance between equivalent computed and recorded values was satisfactory.

The excess pore pressure generated in the dam clay core due to EQ2 accelerograme was predicted for a vertical column in the clay core axis according to Ghaboussi et al model (1979) [3].

The software used consists of a computer codes package developed within Department of Hydraulic Structures from Civil Engineering Institute of Bucharest based mainly on adaptation of some well-known international computer codes ISBILD, FLUSH, FEAP, DEFORM, (developed through University of California - Berkeley), LAS-III (developed through University of Illinois).

2. Finite element mesh and input data for seismic analysis

The finite element mesh used for all static and dynamic analysis performed for El Infiernillo dam is presented in Figure 1. The mesh consists of 96 isoparametric incompatible quadrilateral (triangular) elements with 4(3) nodes. The rock foundation considered as rigid and impermeable was not included in the finite element mesh.

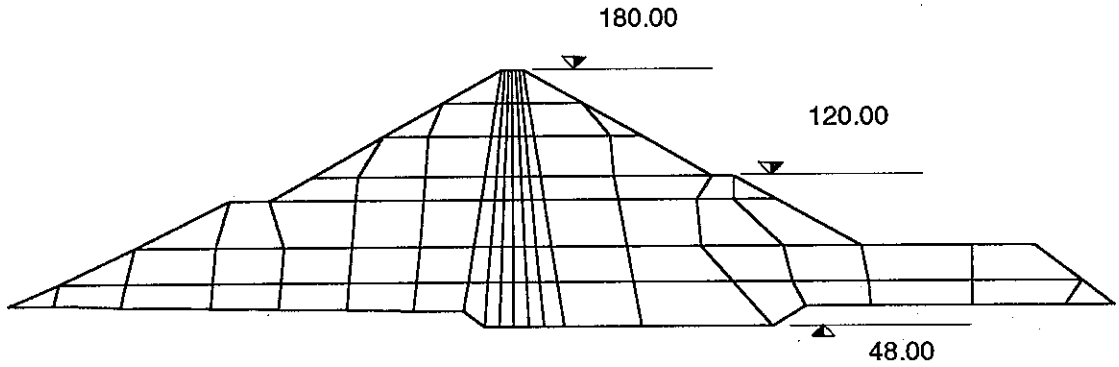

Fig. 1 El Infiernillo Dam - Finite Element mesh

The mesh dimensions were limited by performances of the hardware and software used, but satisfactory for proposed problem. According to relation [1]:

$$h_{\max} = \frac{1}{5}\frac{v_s}{f_{\max}}$$

where v_s is the lowest shear wave velocity reached during dynamic analysis and $f_{\max}$ the highest interesting frequency, may be concluded that for 18 m layer height accepted in the dam finite element mesh, the maximum filtered frequency is about 4 Hz.

The dam body material properties corresponding to start of the earthquakes were computed simulating dam construction and operation history. Dam erection (from October 1962 to December 1963) was simulated by seven steps of two month each, a new layer of 18.85 m height being carried-out at each step. The first consolidation period of five months before starting of the reservoir impounding was modelled in one step. The reservoir impounding was modelled in two steps of 3.5 months each of them. The second consolidation with constant level full reservoir period was modelled in two steps of 12 months each of them. At the end of this period the steady

Material properties

Table I

Code Nr.	Material	γ (t/cm)	K	Kd	n	c	φ	R_f	μ	F	D	kv (m/s)	Poroz.	kv/kh
1	U/S Rockfill	2.2	550.	650.	0.45	0.	40.	0.75	0.35	0.15	4.			
2	Clay Core	1.95	550.	650.	0.40	0.	35.	0.70	0.32	0.10	4.			
3	Filter	2.0	300.	400.	0.55	20.	22.	0.76	0.38	0.10	3.5	8.10^{-10}	0.3	0.25
4	D/S Rockfill	1.90	550.	650.	0.45	0.	40.	0.75	0.35	0.15	4.			
5	Dumped U/S Rockfill	2.1	550.	650.	0.40	0.	37.	0.75	0.30	0.15	4.			
6	Dumped D/S Rockfill	1.8	550.	650.	0.40	0.	37.	0.75	0.30	0.15	4.			

Vertical Settlements (cm)

Table 2

	Points of the dam section				
	CC (El.180)	CM (El.120)	CL (El.80)	UM (El.120)	DM (El.120)
1.End of Construction					
Observed	0	165(1) 209(2)	105(1) 184(2)		
Hyperbolic model	0	164	96	25	32
2.End of Impounding					
Observed	34(4)	180(4) 224(3)	108(4) 200(3)		38
Hyperbolic model	9	153	108	26	41
3.End of 2nd Consolidation					
Observed	106(4)	203(4) 227(3)	117(4) 209(3)		82
Hyperbolic model	6	159	135	26	87

Sign + : from top to bottom
(1) : Observed in section 0+135 E (maximum height = 135 m) from inclinometer I_1
(2) : Extrapolated from observed value
(3) : Obtained by adding the observed settlement after the end of construction and the extrapolated settlement at the end of construction
(4) : Observed in section 0+135 E (maximum height = 125 m)

Horizontal Displacements (cm)

Table 3

	Points of the dam section				
	CC (El.180)	CM (El.120)	CL (El.80)	UM (El.120)	DM (El.120)
1.End of Construction					
Observed	0				
Hyperbolic model	0	0	-0.7	-39	34
2.End of Impounding					
Observed	-5	14	9		45
Hyperbolic model	92	120	51	31	91
3.End of 2nd Consolidation					
Observed	32	47	21		74
Hyperbolic model	90	116	45	31	87

Sign + : from U/S to D/S

state of the clay core pore pressures and dam body material properties was reached, according to the results of the analysis.

The initial parameters in compliance with hyperbolic Duncan-Chang model [4] of the dam body materials are presented in Table 1. The clay core consolidation process was modelled by pseudotridimensional consolidation theory. As is known, this theory is based on tridimensional extension of the unidimensional consolidation model developed by Terzaghi. The only parameter describing clay solid particles is compressibility and the water flow through porous media is governed by Darcy law.

The analysis was performed with MATLOC computer code developed within Civil Engineering Institute of Bucharest (1984) [5]. Some results on vertical settlements and horizontal displacements at different stages of dam erection or operation are illustrated in Tables 2 and 3. The observed values were collected from Second Benchmark Workshop on Numerical Analysis of Dams (1992) [6].

Material properties for seismic analysis

Table 4

Code Number	Material type	G_0 (MPa)	Poisson ratio
1	U/S Rockfill	10 ... 120	0.38 ... 0.42
2	Filter	20 ... 80	0.41 ... 0.42
3	Clay core	20 ... 100	0.38 ... 0.42
4	D/S Rockfill	40 ... 120	0.38 ... 0.42
5	Dumped U/S Rockfill	10 ... 80	0.38 ... 0.42
6	Dumped D/S Rockfill	10 ... 80	0.38 ... 0.42

The material properties resulted at the end of second consolidation period were used for estimating the material data for dynamic analysis. In this view the material static characteristics were corrected for dynamic analysis case (1984) [7], [8]. The main material characteristics used for dynamic analysis are presented in Table 4.

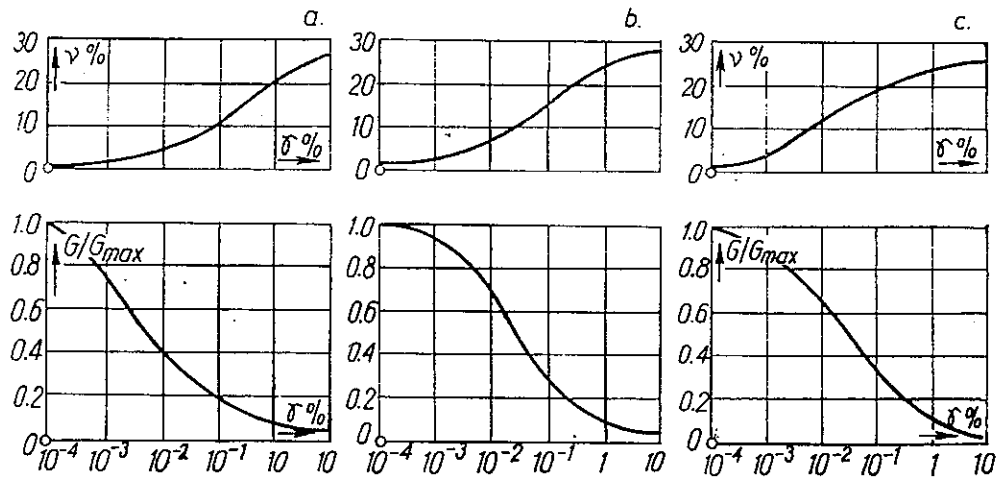

Fig. 2 Strain compatible dynamic properties considered for El Infiernillo dam materials: a - clay, b - filters, c - shells.

The nonlinear seismic analysis was based on shear strain compatible relations versus shear modulus degradation and fraction of critical damping. The diagrams of compatibility for different material types existent in the dam body used for seismic analysis are presented in Figure 2. They were assimilated in compliance with literature data (1988).[9], [10].

3. The checking up on performance of the model for seismic analysis

The EQ1 accelerogram applied on horizontal direction was considered in order to compare the results in seismic analysis with the actual measurements carried out on El Infiernillo dam site two days after this earthquake. In the Table 5 are presented comparatively some results. Taking into account the complexity of the problem, the correspondence between computed and measured equivalent values (accelerations, displacements) may be considered satisfactory.

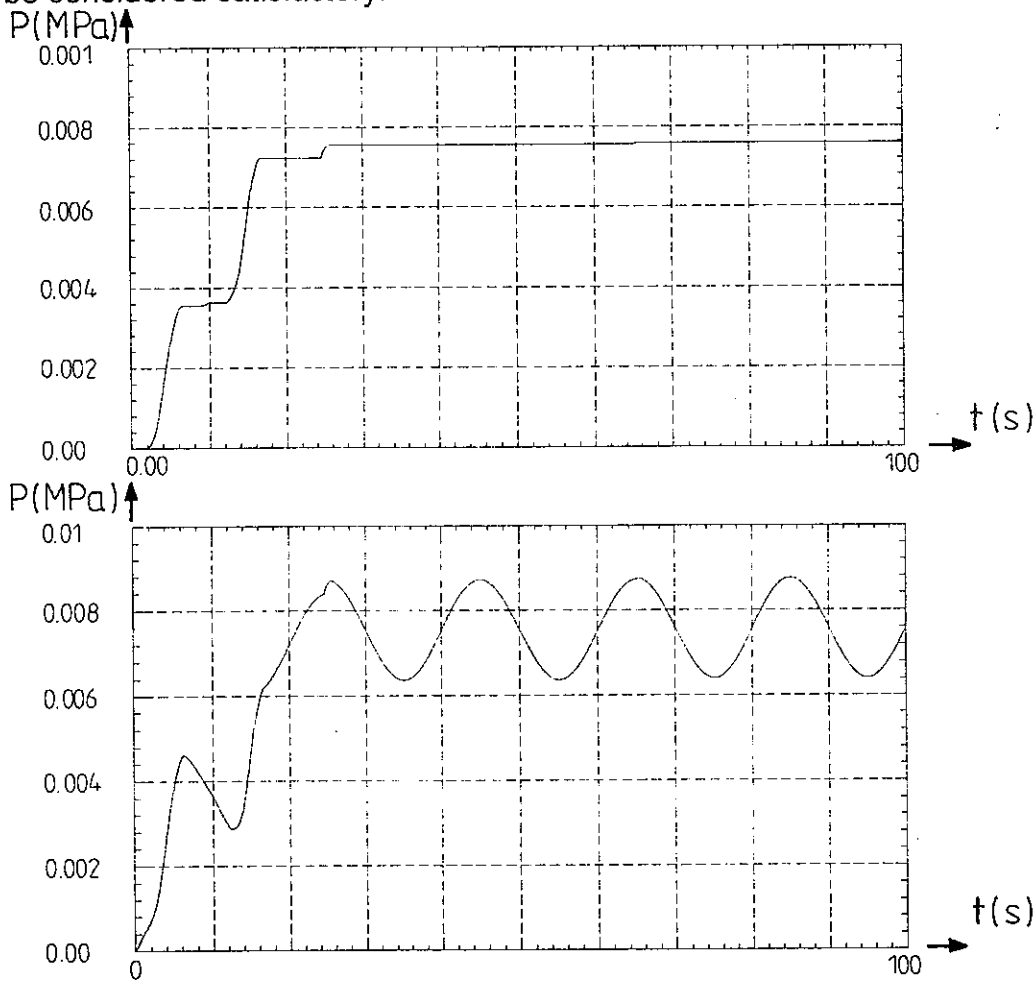

Fig. 3 El Infiernillo dam clay core. Excess pore pressures time history due to harmonic sinusoidal accelerogram (0.1g maximum acceleration, 10 seconds/cycle) applied horizontally (a) and both horizontally and vertically (b).

Computed and recorded seismic response of El Infiernillo dam under EQ1 March, 14, 1979 earthquake

Table 5

Point	Maximum absolute acceleration response (g)		Irreversible displacements (cm)			
	Horizontal direction		Horizontal displacements		Settlements	
	Measured	Computed	Measured	Computed	Measured	Computed
CC (crest)	0.362	0.266	3.8	1.0	11.0	3.5
CM (El 120)	-	0.280	-	0.7	1.0	0.9
CL (El 80)	-	0.290	-	0.5	0.0	0.3
DM (El 120)	-	0.439	1.5	0.9	1.5	0.1

Results of the dynamic study - EQ2 earthquake

Table 6

	Points of the dam section				
	CC	CM	CL	UM	DM
Maximum horizontal absolute acceleration (in g) (1)	0.266	0.262	0.292	0.317	0.440
Maximum vertical absolute acceleration (in g) (1)	0.227	0.188	0.167	0.208	0.193
Irreversible horizontal displacement (in cm) (2)	0.9	0.1	0.3	3.5	2.0
Irreversible vertical displacement (in cm) (3)	4.0	1.4	0.5	0.5	0.0
Maximum excess pore pressure (in MPa) (4)	-	53.10^{-4}	46.10^{-4}	-	-
Final excess pore pressure (in MPa) (4)	-	53.10^{-4}	46.10^{-4}	-	-

(1) Absolute accelerations
(2) Sign + : from U/S to D/S
(3) Sign + : From top to bottom
(4) Only the excess pore pressure is given. The pore pressures obtained at the end of the static analysis are not cumulated

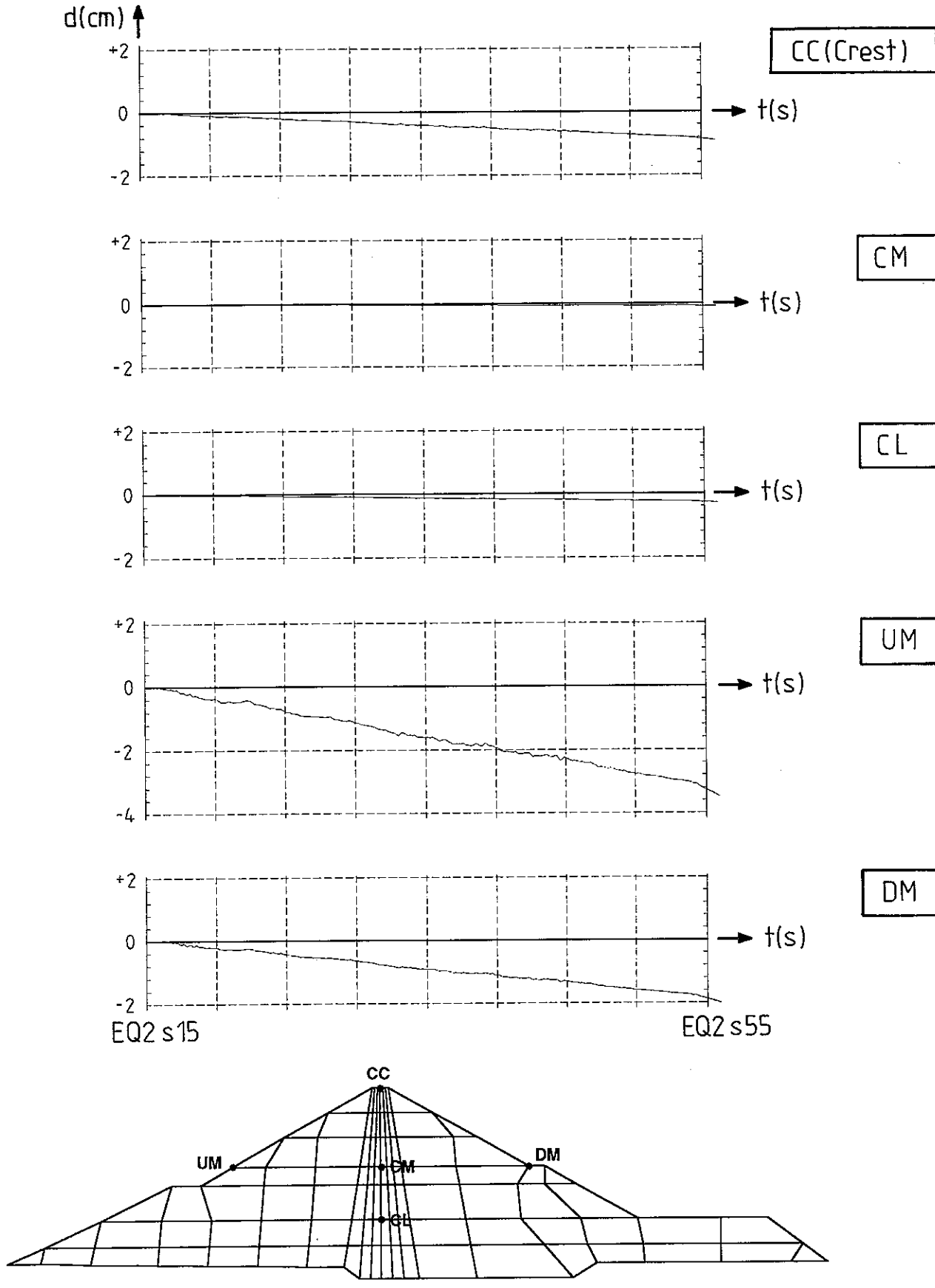

Fig. 4 El Infiernillo dam - Horizontal displacement time history during EQ2 accelerogram applied horizontally.

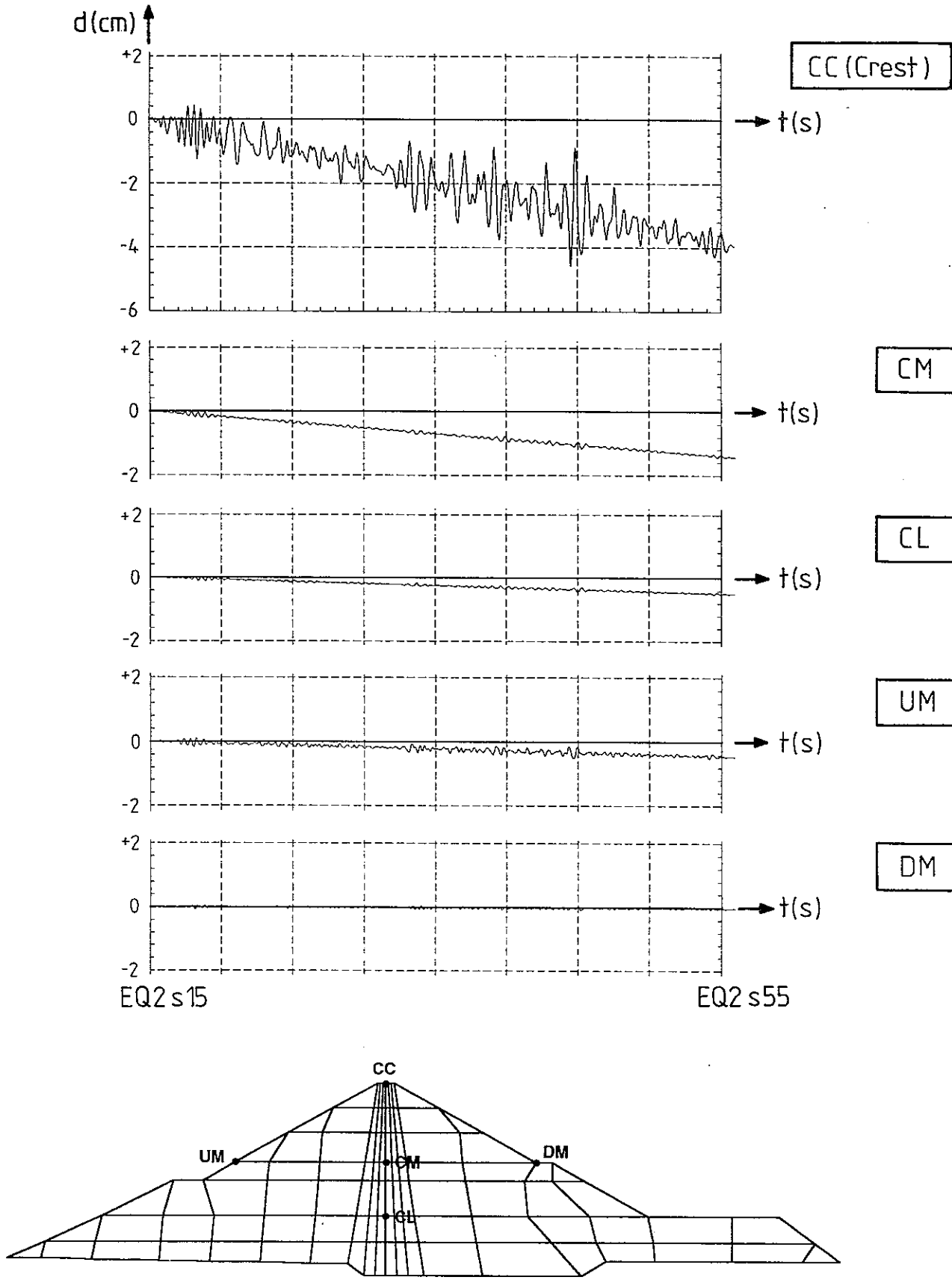

Fig. 5 El Infiernillo dam - Vertical displacement time history during EQ2 accelerogram applied horizontally.

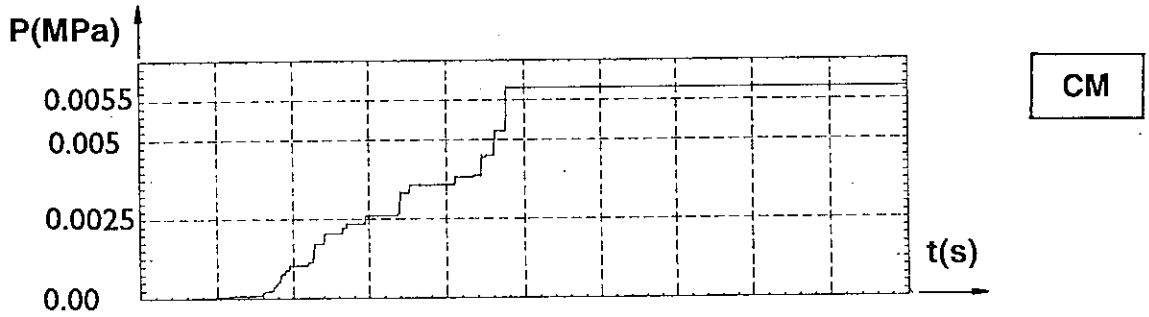

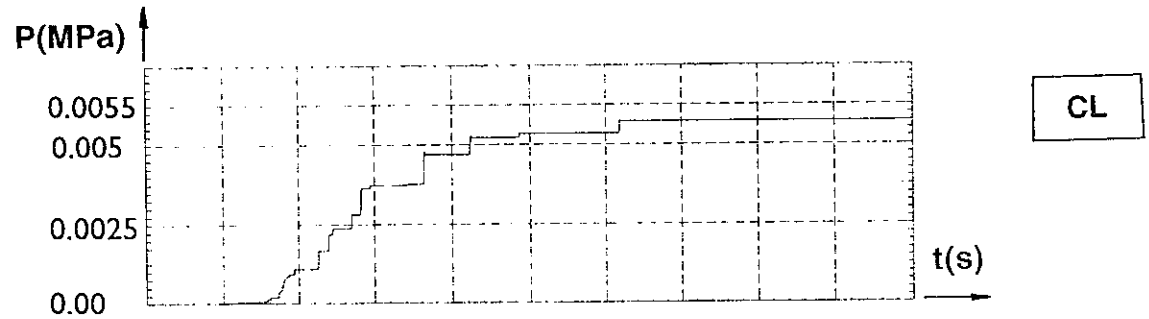

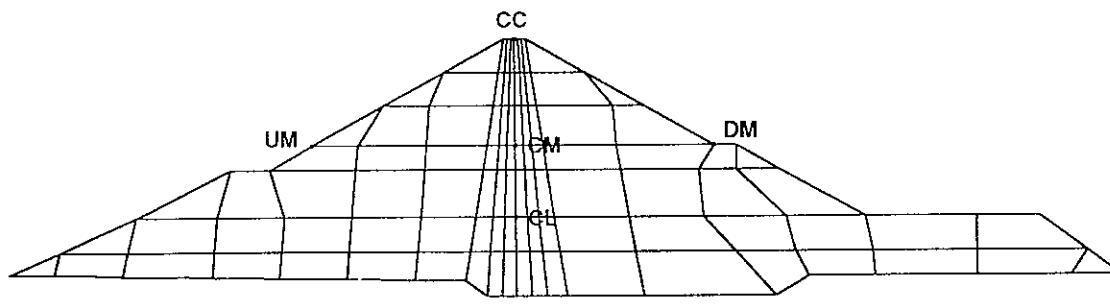

Fig. 6 El Infiernillo dam clay core - Excess pore pressure time history during EQ2 accelerogram applied horizontally.

The software used has not capacity to perform the simulation of triaxial cyclic tests requested at step 2 of the Benchmark Workshop theme B2. In these circumstances, the clay core discretized column considered for computing excess pore pressures under EQ2 accelerogram, was shaken initially by five cycles of sinusoidal accelerogram with 0,1g maximum acceleration and 10 seconds per cycle period. Some results in terms of excess pore pressure versus time and shear stresses versus shear strains for two cases: accelerogram applied on both horizontal and vertical directions are illustrated in Figure 3. The ratio between maximum vertical acceleration (a_v) and horizontal one (a_h) was 0.5.

4. Results in seismic analysis for EQ2 earthquake

The EQ2 accelerogram applied only on horizontal direction was considered in seismic analysis of El Infiernillo dam under medium/strong earthquake. The software and hardware existent capacity for seismic analysis by FLUSH [2] constrained to select a maximum number of 2048 discrete values from a total of 6000 discrete points of EQ2 recommended accelerogram. Consequently, the most important zone from second 15 to second 55 of the EQ2 recommended accelerogram of 120s total recording was selected.

In order to compute the irreversible seismic displacements the equivalent seismic nodal static forces according to DEFORM computer code were evaluated from the seismic maximum shear strains resulted in seismic analysis by FLUSH. A linear rate of irreversible seismic displacement development during EQ2 40 seconds accelerogram was accepted.

The excess pore pressure time history was computed for a vertical column in the clay core central part according to LAS III computer program [3]. The pressures correspond to first 100s from $EQ2_2$ accelerogram, applied horizontally at the column base. The saturated material below the water table is modelled as a coupled two phase medium coupled through volumetric strains: porous deformable granular solid and pore water. The pore water flow is governed by Darcy flow law. The coefficient of permeability is considered constant and a nonlinear elasto-plastic model is used to model the granular solid behaviour.

The results of the analysis in terms of absolute accelerations, relative displacements and excess pore pressures are presented in the typical table or template formats recommended for Benchmark Workshop. (Table 6 and Figures 4, 5, 6)

5. Information on computation time and hardware used

The analyses presented above have been performed on hardware equipment existent at Civil Engineering Institute of Bucharest - Department of Hydraulic Structures and Institute for Hydroelectric Studies and Design Bucharest - Computation office. Some information on this subject including computation time are presented in Table 7.

Table 7

Type of computer	Type of analysis	Computation time (minutes)
AT 486 DX 33MHz CPU	Static analysis (MATLOC computer code)	4
CORAL 8730	Seismic analysis under EQ2 (FLUSH computer code)	15
CORAL 8730	Irreversible seismic displacements due to EQ2 (DEFORM computer code)	2
AT 486 DX 33MHz CPU	Excess pore pressures due to EQ2 (LASS III computer code)	3

6. Concluding remarks

The authors agree that theme proposed for debating under section B2 of this Third Benchmark Workshop is a research one with high degree of difficulty. The results presented in this paper offer an alternative to solve this problem, with inherent approximations and uncertainties. However, the values of El Infiernillo dam seismic response to medium/strong earthquake resulted by numerical analysis can be considered as realistic and possible for an engineering judgement. A more refined finite element mesh of the dam cross section would been desired but it was limited by hardware disponibility.

In our opinion, the existent unsatisfactory volume of the recording data concerning embankment dams seismic behaviour under medium/strong earthquakes shaking and the complexity of the phenomenon make impossible, in this stage, to choose an unique reference mathematical solution of this problem.

The basic criteria for selecting a reference mathematical solution must be the model capacity to simulate with sufficient accuracy on site seismic response recordings.

In order to enrich the knowledge in this field we think that would be very useful to propose again this theme for next Fourth Benchmark Workshop. Also, the theme might be completed with analysis on new aspects concerning seismic response modelling of embankment dams, as follows: spectral analysis, slope stability, seismic crack analysis, three-dimensional effects on response, seismic safety analysis.

References

1. *Lysmer, J., Udaka, T., Tsai, C.F., Seed,* H.B. FLUSH - A Computer Program for Approximate 3-D Analysis of Soil-Structure Interaction Problems. Report EERC No.75-30, University of California, Berkeley, 1975.
2. *Serif, N., Seed, H.B., Makdisi, F.I., Chang, C.Y.*, Earthquake Induced Deformations of Earth Dams. Report EERC No.76-4, University of California, Berkeley, 1976.
3. *Ghaboussi, J., Dikmen, S.U.*, LASS III, Computer Program for Seismic Response and Liquefaction of Layered Ground under Multi-directional Shaking, University of Illinois, Urbana-Illinois, 1979.
4. *Popovici, A., Popescu, C.*, Dams for Water Storage (in Romanian), Ed. Tehnica, Bucharest, 1992.
5. *Stematiu, D., Popescu, R.*, Solution Technique for Dam Clay Core Consolidation. International Conference on Numerical Method for Transient and Coupled Problems, Venice, 1984.
6. *Ozanam, O., Lacroix, F., Bonnechose, E.*, Static and Dynamic Coupled Analysis of El Infiernillo Dam. Second Benchmark Workshop on Numerical Analysis of Dams, Bergamo, 1992.
7. *Popovici, A., Tabatabai, J.*, Seismic Behaviour Prediction of a Large Dam at the Maximum Expected Earthquake. Scientific Bulletin, I.C.B., Nr.2, 1984
8. *Popovici, A., Corda, I., Cristidis, V.*, Soil-Structure Interaction Effects on Seismic Response of Earth Dams. Proceedings 8-th European Conference on Earthquake Engineering, Lisbon, September, 1986.
9. *Popovici, A., Toma, I., Nafessi, F., Gudarzi, F. A.* Comprehensive Seismic Analysis of a Large Iranian Dam. Scientific Bulletin, I.C.B., Nr.1, 1988.
10. *Popovici, A.*, New Concepts Concerning Embankment Dams Earthquake Analysis. Proceedings of First International Conference on Seismology and Earthquake Engineering, Tehran, May, 1991.

NOTES

Third Benchmark Workshop on Numerical Analysis of Dams
Gennevilliers (France) - September 29-30, 1994

Theme B2 :

DYNAMIC ANALYSIS OF AN EMBANKMENT DAM UNDER A STRONG EARTHQUAKE

GEFDYN ANALYSIS

O.OZANAM, F. LACROIX, B. TARDIEU

Coyne et Bellier, Bureau d'Ingénieurs Conseils
9, Allée des Barbanniers - 92632 Gennevilliers CEDEX

This contribution to theme B2 of the third Benchmark Workshop on Numerical Analysis of Dams by Coyne et Bellier presents a coupled solid/fluid analysis of the dynamic response of the selected El Infiernillo embankment dam using the finite element software GEFDYN [1]. Both 1979 and 1985 earthquakes were applied to the numerical model and the effect of two successive earthquakes was analyzed in order to highlight the influence of material hardening.

1. METHODOLOGY

1.1 Selection of constitutive models

For this theme (B2) the benchmark data provided is sufficiently general to allow each participant to choose the constitutive model he wants to use for each material. In the present study the Hujeux/Aubry constitutive model [2,3] has been adopted for the core material. Indeed this model is able to simulate the hysteretic behaviour of soils during cyclic loadings because of hardening parameters. The other materials of the dam are modelized with the Mohr Coulomb model. Because, quite exceptionally, results of triaxial tests on rockfills were available, the Hujeux constitutive model could have been used for the shoulders. In fact, this option was not selected because of :

- the large uncertainty concerning the volumetric strain curves,
- the current inability of any available models to simulate the swelling of rockfill during moistening, which is the main constitutive behaviour of these materials,
- the more complex computation, which induces a longer computation time,
- the relatively good adaptation of the Mohr Coulomb model for this type of materials.

Only the hardening of the materials during the cyclic loadings is not well simulated. But, as the results show, the Mohr Coulomb model is able to create sliding surfaces in the shoulders.

1.2 Fitting of clay properties

The provided curves for the CU triaxial tests on the core material - deviator stress vs. axial strain - were not sufficient to determine the whole set of parameters of the Hujeux model. Especially the mean effective stress at the end of the triaxial test (at the critical state) was not available. Therefore the friction angle could not be determined. On the basis of correlations made by J. Florentin [4], its value was set to 25°, which corresponds to intact samples of clay with a plasticity index of 26. The other parameters were determined by fitting with the available curves of the triaxial tests (see Table 1 and Fig. 1). The same parameter set was used in the core material for the static and dynamic computations.

Table 1 : Parameter sets used for each material of the dam

Parameter	Core Hujeux-Aubry	Filter Mohr Coulomb	Transition - dense rockfill loose rockfill Mohr Coulomb	
E_i (MPa)	60	58	58	
E_d (MPa)	-	400	400	
P_i (MPa)	1.0	1.0	1.0	
ν	0.3	0.3	0.3	
nel	0	0.4	0.4	
C (MPA)	0	0.01	0.01	R_T
(MPA)	0	0	0	
φ	25	35	42	
ψ	25	5	5	
β	50			
P_{c0} (MPa)	0.35			
e_0	0.5			
a	0.001			
b	1.0			
a_{cyc}	0.0005			
α	1			
r_{ela}	0.001			
r_{hys}	0.002			
r_{mbl}	0.05			
c	0.0002			
d	2.0			
c_{cyc}	0.0001			
r_{4ela}	0.001			
m	2.4			
k_v (m/s)	2.10^{-10}			
k_h (m/s)	8.10^{-10}			

The given core permeability (2.10^{-10} m/s) is supposed to be the vertical one and a ratio between horizontal and vertical permeabilities is set at 4, in accordance with the granulometry and low permeability of the material.

1.3 Fitting of rockfill and filter properties

CD triaxial tests on rockfill samples indicate a variation of the friction angle between 37° at a confining pressure of 2.5 MPa and 46° at 0.7 MPa. A mean value of 42° for dumped rockfill, compacted rockfill and transitions was used in the model. A usual value for the friction angle for sands (35°) was set for the filter material.

Fitting of the Young's modulus on triaxial tests for such an elastic perfectly plastic model is too inaccurate because this elasticity modulus is a secant modulus. A better way is to fit this modulus with the measured settlements during dam construction. To improve the standard Mohr Coulomb model, three developpements of the model (available in GEFDYN software) are used :

- non-linear elasticity - the tangent Young's modulus E varies with the mean effective stress p:
$$E = E_i \, (p/p_i)^{nel}$$
in which E_i is the Young's modulus for a reference mean stress p_i;
- non associated flow rule - the friction angle is set to a small value (5°) in order not to have large dilatancy (as in associated formulation) and to have some small volumetric strain;
- no tension behaviour - the tension strength is set to zero in order to avoid any tension in the filters and rockfill.

For the dynamic computation, the elasticity modulus E_d used in the Mohr Coulomb model was increased because it is thus the « real » modulus at very small cyclic strains. Its value was chosen equal to 10 times the secant modulus for strain of 5%. In addition, the elastic behaviour is assumed to be linear.

1.4 Simulation of undrained cyclic triaxial tests

To verify the ability of the parameter set used in the core to induce pore pressure increase under cyclic loading, the two undrained triaxial tests proposed in the Benchmark specifications were modelized with GEFDYN.
The results of the CU test with a confining pressure of 0.1 MPa and a deviator stress variation of ±0.02 MPa are presented in Figs. 2a and 2b. After five cycles the sample reaches a state close to liquefaction. For the second CU test with a confining pressure of 0.3 MPa and a deviator stress variation of ±0.05 MPa, the mean effective stress decreases to 0.17 MPa after five cycles (i.e. 43% decrease), as shown in Figs. 3a and 3b.

1.5 Simulation of the whole dam history

The constitutive model used for the core takes account of the previous stress states of the materials by using hardening parameters. In order to have a nearly realistic initial state of the dam for the dynamic analysis, the whole history of El Infiernillo dam was modelized from construction in 1962 to the steady state before the 1985 earthquake. More precisely, the following stages were computed successively:

- construction (October 1962-December 1963) in 10 regular steps with an average rate of 15 metres per month,
- consolidation period of 5 months in 2 steps of 2.5 months,
- impounding (June 1964 - December 1964) in 5 variable steps, with a maximum rate of 70 metres in 2 weeks,
- consolidation period (January 1965 - March 1979), in 2 steps of 6 months and 13.75 years, which provides the steady state of the dam before the first main earthquake,

- March 14, 1979 earthquake (EQ1), with a duration of 10 seconds and a maximum acceleration of 0.1 g,
- consolidation period after the 1979 earthquake (March 1979 - September 1985), which provides the steady state of the dam before the second main earthquake.

The stress and hardening parameters fields obtained at the end of these computations were used as the initial state for the computation of the 1985 earthquake (EQ2). The 120 seconds of the recorded base acceleration and the postseismic consolidation were simulated. Of this large number of computations only two are dynamic studies.

2. MAIN ASSUMPTIONS

The following assumptions proposed in the benchmark data were taken into account:

- the mesh used was not modified,
- the bedrock is assumed to be rigid and impervious.

Because of the high contrast between permeabilities in the core and the filter, only the behaviour of the core was simulated with the coupled solid/fluid model under static [5,6] and dynamic conditions [7], according to Biot Theory.

The other parts of the dam are presumed to be perfectly drained and in these zones the computation is performed in terms of effective stresses. During impounding and the following phases,

- the buoyancy volumetric forces are applied inside the upstream rockfill and filters,
- pore pressure is set at hydrostatic pore pressure on the upstream face of the core,
- and a hydrostatic mechanical pressure is applied on the wetted upstream face of the core, in order to equilibrate the total stresses computed in the core zone and the effective stresses computed in the shoulder zones.

This method avoids having to compute the known pore pressure in the rockfill and saves computation time. However the transient flow of water in the core is fully computed.

For the static computations (and especially during impounding and consolidation periods) the following assumptions were added :

- the initial degree of saturation in the core was set to the given value (0.96); according to non-saturated triaxial tests performed in France [8], the corresponding water suction (i.e. negative pore pressure) has been chosen equal to -0.3 MPa;
- seepage boundary conditions were assumed on the upstream and downstream faces of the core [9].

For the two dynamic computations (EQ1 and EQ2),

- the core faces are assumed to be impervious, i.e. no flow can occur through the core boundaries;
- the base acceleration is introduced in the numerical model as an inertial force, because of the rigid base boundary condition; therefore the results are provided in terms of relative displacements, velocities and accelerations.

3. NUMERICAL FEATURES

For the space discretization, the implemented shape functions are the same for the displacement and pore pressure unknowns.

The time discretization is performed using the Newmark implicit time integration scheme. The time step of the computations and the Newmark coefficients are given in Table 2. No damping factor is explicitly used in the numerical formulation. For earthquake EQ1 damping is induced by plasticity hysteresis only, according to the β and γ Newmark coefficients used in this case. But for earthquake EQ2 these Newmark coefficients should be slightly increased in order to ensure numerical convergence of the numerical scheme. In this last case some numerical damping appears in addition to the damping induced by plasticity hysteresis. An estimation of this numerical damping is proposed in Table 2 [10].

Table 2 : Integration scheme of Newmark : time steps, coefficients

earthquake	EQ1	EQ2
damping ξ (%)	no	0.8 N*
β	0.5	0.55
γ	0.25	0.28
time step Δt (s)	0.04	0.05

* N is one of the eigenfrequencies of the structure (around 1Hz for the dam)

The time step of the computation is relatively large, but it is sufficient to provide a good reproduction of the input accelerogram, and it reduces computation time. Due to this large time step, the acceleration time histories obtained with the Newmark scheme are not acceptable; therefore they were derived from the displacement time histories by a Fourier transform method. In addition frequencies higher than 5 Hz (approx. maximum frequency for the filter effect of the mesh) were filtered in the computation of the accelerations.

After space and time discretization, the obtained non-linear system of algebraic equations must be solved at each time-step by using an iterative scheme, decomposed into a predictor stage and corrector stage; this scheme is based on a modified Newton method (elasticity auxiliary matrix). Convergence criteria should lead to the mechanical equilibrium requirement and to the conservation of fluid mass.

4. RESULTS OF EQ1 DYNAMIC ANALYSIS

4.1 Summary table

As shown in the summary table, the maximum horizontal and vertical absolute accelerations computed at the crest are very close to observed values. A relatively large amplification of horizontal acceleration (ratio of 3) is also noticeable at the base of the core and on the downstream slope. The vertical acceleration is amplified at the selected points with approximately the same ratio of 4.5.

The irrecoverable displacements after the earthquake are given just at the end of the earthquake, i.e. after a short stabilization period (some seconds), and after the postseismic consolidation: postseismic settlement represents 25% of the total settlement at the crest and 50% at the point CM in the centre of the core.

Concerning the pore pressure, it is difficult to analyze values at 2 points only, because of its large variation in space. Examination of the pore pressure distribution at the end of the earthquake and during consolidation (Fig. 4) shows that :

- the maximum excess pore pressure is reached after the earthquake;
- there are zones of positive excess pore pressure (sometimes highly positive) corresponding to contraction strains and zones of negative excess pore pressure corresponding to dilatant strains.

Table 3 : General Summary : results for the dynamic study earthquake EQ1 (1979 - γ_{max} = 0.1 g)

	Points of the dam section				
	CC (El. 180)	CM (El. 120)	CL (El. 80)	UM (El. 120)	DM (El. 120)
Max. horizontal acceleration (g)					
observed	0.36(1,2)				
computed	0.32	0.15	0.32	0.25	0.43
Max. vertical acceleration (g)					
observed	0.34(2)				
computed	0.38	0.31	0.29	0.30	0.31
Irrecoverable horiz. displ. (cm)*					
observed	+ 2 (2)				
	+ 3.8 (4)			+ 1.1(2)	
computed end of earthquake	-2.5	+5.1	+ 3.1	- 6.5	+ 2.9
computed after consolidation	-2.5	+5.4	+ 3.5	-6.0	+2.2
Irrecoverable vertical displ. (cm)**					
observed	+ 10.6 (2)				
	+ 9.1 (3)	+0.8 (3)	0 (3)		+1.4 (2)
computed end of earthquake	+12.2	+3.7	+2.2	+1.1	0.2
computed after consolidation	+16.4	+7.0	+3.8	+1.3	+1.1
Max. excess pore pressure (MPa)					
computed	-	0.12	0.09	-	-
Final excess pore pressure (MPa)					
computed	-	0.11	-0.04	-	-

(1) corrected because of bad record of accelerogram
(2) from ref. [11] in section 0 + 170
(3) from ref. [11] in section 0 + 135
(4) from ref. [12]
* sign + : from U/S to D/S
** sign + : from top to bottom

4.2 Displacements

Displacement time histories for each selected point during the earthquake are drawn in Fig. 5. The displacement is composed in an irrecoverable part which increases regularly in time and in a reversible elastic component, which has a period of around one second. Fig. 6 represents the irrecoverable displacement at the end of the earthquake on the whole mesh. This graphic output shows clearly some skin sliding and particularly a sliding surface on the upstream shell.

The comparison of the computed values with the available measured data (maximum acceleration and irrecoverable displacements) shows that the chosen parameter set and the overall assumptions adopted for earthquake EQ1 are sufficiently well determined and can be used for earthquake EQ2.

5. RESULTS OF EQ2 DYNAMIC ANALYSIS

5.1 Summary table

The amplification factor of horizontal acceleration does not vary significantly along the centre core line and it is less than 2. On the downstream slope this factor could reach 2.5. The vertical acceleration is amplified with approximately the same ratio of 2.

Table 4 : General Summary : results for the dynamic study earthquake EQ2 (1985 - γ_{max} = 0.29 g) initial state : after EQ1 postseismic consolidation

	Points of the dam section				
	CC (El. 180)	CM (El. 120)	CL (El. 80)	UM (El. 120)	DM (El. 120)
Max. horizontal acceleration (g) computed	0.55	0.37	0.40	0.45	0.70
Max. vertical acceleration (g) computed	0.52	0.54	0.58	0.57	0.62
Irrecoverable horiz. displ. (cm)* computed end of earthquake	-19	+6.0	+ 3.5	-32.0	+18
computed after consolidation	-19	+6.7	+ 3.7	-31.0	+17
Irrecoverable vertical displ. (cm)** computed end of earthquake	+48	+3.5	+0.5	+6.0	+5.5
computed after consolidation	+54	+7.0	+2.0	+6.1	+5.8
Max. excess pore pressure(MPa) computed	-	0.3	0.13	-	-
Final excess pore pressure(MPa) computed	-	0.05	0.1	-	-

* sign + : from U/S to D/S
** sign + : from top to bottom

As for earthquake EQ1 the irrecoverable displacements after the earthquake are given just at the end of the earthquake, i.e. after a short stabilization period (some seconds), and after postseismic consolidation (6 months). The additionnal irrecoverable settlement due to consolidation is around 10% of the total settlement at crest and still 50% at point CM in the centre of the core.

The pore pressure distribution at the end of the earthquake and during consolidation is represented in Fig. 7. The same remarks as for earthquake EQ1 are also applicable.

5.2 Displacements

Displacement time histories for each selected point during the earthquake are drawn in Fig. 8. The displacement curves clearly show the main events of the input accelerogram (at 20s, 35s and 45s). At each of these events an irrecoverable displacement occurs. As for earthquake EQ1 Fig. 9 represents the irrecoverable displacements in the dam at the end of the earthquake. It shows similarly sliding surfaces, but they are mainly located on the downstream face of the shoulders.

5.3 Hardening effect

In order to quantify the influence of the initial stress state and especially of the hardening parameters state, the same computation was performed with the initial stress state used for earthquake EQ1, i.e. after impounding and steady state in March 1979. Table 5 and Figure 10 clearly show that the settlements in the core are smaller if earthquake EQ2 is modelled after EQ1 than with the same initial state. The effect of successive earthquakes, which induce a hardening of the dam materials, is well reproduced with the Hujeux/Aubry constitutive model used in the core.

Table 5 : effect of the initial state - values computed at the end of the earthquake earthquake EQ2 (1985 - γ_{max} = 0.29 g)

(a) initial state after EQ1 postseismic consolidation
(b) initial state identical to EQ1 initial state

	Points of the dam section					
	CC (El. 180)	CM (El. 120)	CL (El. 80)	UM (El. 120)	DM (El. 120)	
Irreversible horiz. displ. (cm)						(a)
after EQ1	-19	+6.0	+ 3.5	-32.0	+18	
(b) instead of EQ1	-13	+12.5	+ 7.0	-32.	+18	
Irreversible vertical displ. (cm)						(a)
after EQ1	+48	+3.5	+0.5	+6.0	+5.5	
(b) instead of EQ1	+65	+7.0	+2.3	+6.0	+4	
Max. excess pore pressure(MPa)						(a)
after EQ1	-	0.3	0.13	-	-	
(b) instead of EQ1	-	0.25	0.1	-	-	
Final excess pore pressure(MPa)						(a)
after EQ1	-	0.05	0.1	-	-	
(b) instead of EQ1	-	0.16	-0.1	-	-	

6. CONCLUSION

First the influence of hardening parameters, analyzed in section 5.3, points out that :

- for dynamic non-linear analyses, it is important to compute an initial state which is as close as possible to the real state of the materials before the dynamic event;
- and it is necessary to use an elastoplastic constitutive model with hardening in order to take account of the previous history of the materials and therefore of the effect of successive earthquakes.

The second main conclusion of this study concerns the displacement field observed at the end of the earthquake. The localization of the displacement along sliding lines, as observed in Figs 6 and 9, should allow an easier comparison with the classical stability analyses, which assume the form of the sliding lines and determine the stability of the structure in terms of safety factors. Therefore it seems that these two methods, which have completely different approaches, could be used to complement each other and may provide similar results.

7. COMPUTATION TIME

The computations were performed with an optimized GEFDYN executable file on an HP9000/715 workstation (48 Mb RAM, frequency 50 Mhz, 62 Mips, 13 Mflop). The CPU times for each computation stage are given in table 6.

Table 6
Computation time

Construction and consolidation (10+2 steps)	5850 s = 1h37mn
Impounding and consolidation (5+2 steps)	2890 s = 48mn
EQ1 (250 steps)	13661 s = 3h48mn
Consolidation after EQ1	10706 s = 2h58mn
EQ2 (2400 steps)	82895 s ≅ 23h
TOTAL CPU TIME	32h11mn

References

[1] GEFDYN rev. 6.1 - *Users Manual and Scientific Manual*, March 1994 - Coyne et Bellier, EDF/CNEH, ECP/LMSS.

[2] D. AUBRY, J.C. HUJEUX, F. LASSOUDIERE, Y. MEIMON (1982) : *A double memory model with multiple mechanisms for cyclic soil behaviour* - Int. Symp. Num. Models Geomechanics, Zurich, Balkema, 3-13.

[3] J.C. HUJEUX (1985) : *Une loi de comportement pour le chargement cyclique des sols* - Génie Parasismique (Ed. Davidovici), Presses ENPC, 287-302.

[4] J. FLORENTIN - Document MECASOL (1972).

[5] D. AUBRY, D. CHOUVET, O.OZANAM, J.-P. PERSON (1986) : *Coupled mechanical-hydraulic behaviour of earth dams with partial saturation* - Eur. Conf. Num. Methods in Geomechanics, Stuttgart, Germany, Vol.2.

[6] D. AUBRY, O.OZANAM, J.-P. PERSON (1987) : *Ecoulements non saturés en milieux poreux déformables* - 9th Eur. Conf. on Soil Mechanics and Foundation Eng., Dublin, Ireland, August 31-Sept.1st 1987, pp.537-540.

[7] D. AUBRY, H. MODARESSI (1988) : *Numerical modelling of the dynamics of saturated and elastoplastic soils in seismic hazard in Mediterranean regions,* J. Bonin et al (Eds), pp. 151-171.

[8] GRECO GEOMATERIAUX - *Rapport scientifique 1990* - pp.409-412.

[9] D. AUBRY, O.OZANAM (1988) : *Free surface tracking through non-saturated models* - 6th Int. Conf. Num. Methods in Geomechanics, April 11-15, 1988, Innsbruck, Austria, Vol.3, pp. 757-763.

[10] T.J.R. HUGHES : *The Finite Element Method - Linear Static and Dynamic Finite Element Analysis* - Prentice-Hall, Inc., New Jersey - chap. 9.

[11] F.G. VALENCIA : *Efectos en la presa El Infiernillo, Michoagan.* Chapter 4 - CFE Document.

[12] E. MORENOS, J.M. CAMPOS (1980) : *Behaviour records of El Infiernillo and La Villita dams from construction to March 1979.* Chapter 5 in "Performance of El Infiernillo and La Villita dams in Mexico including the earthquake of March 14, 1979". CFE - Mexico.

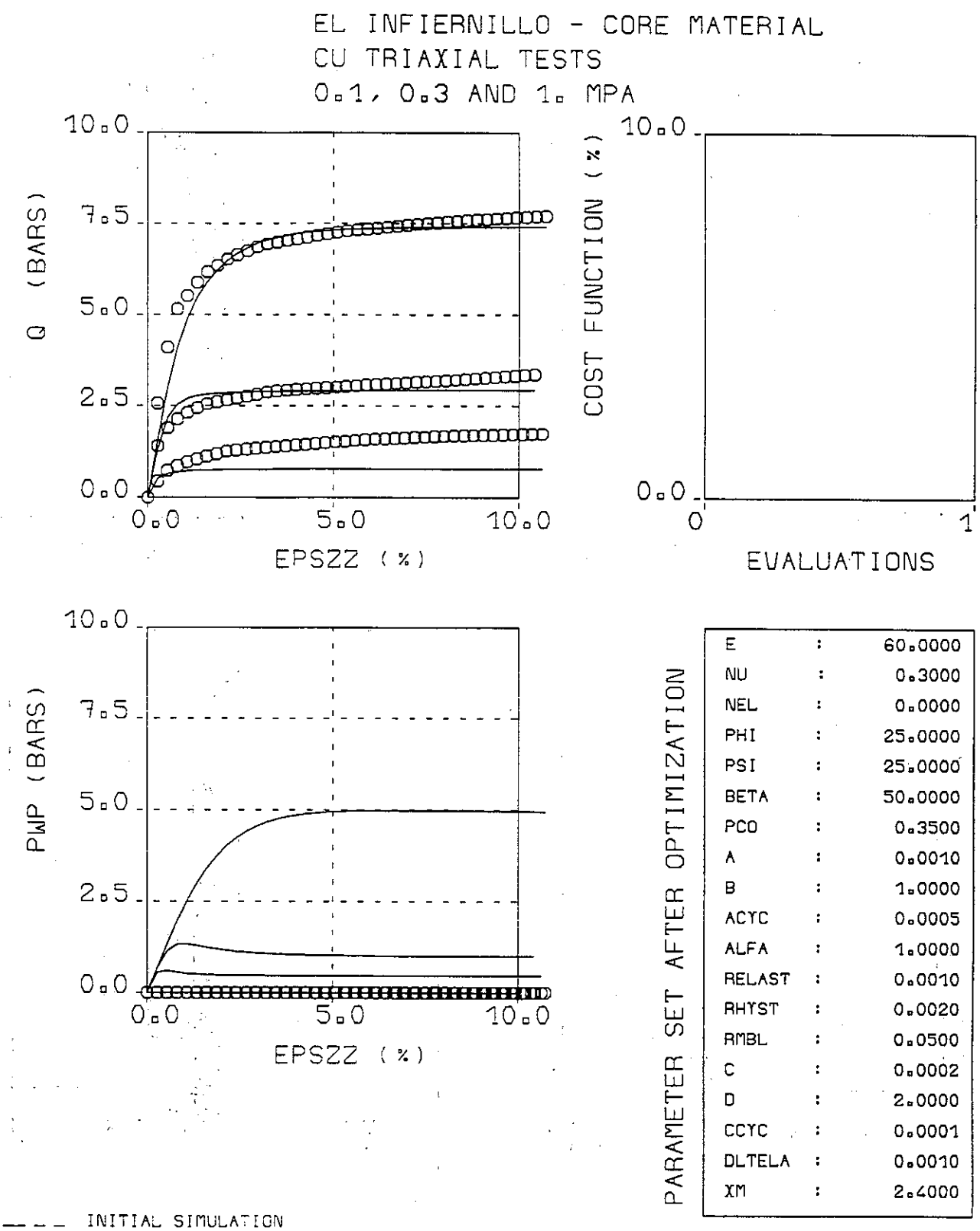

Fitting of core parameters on undrained triaxial test : (q,ε_1) and (u,ε_1) curves

Fig. 1

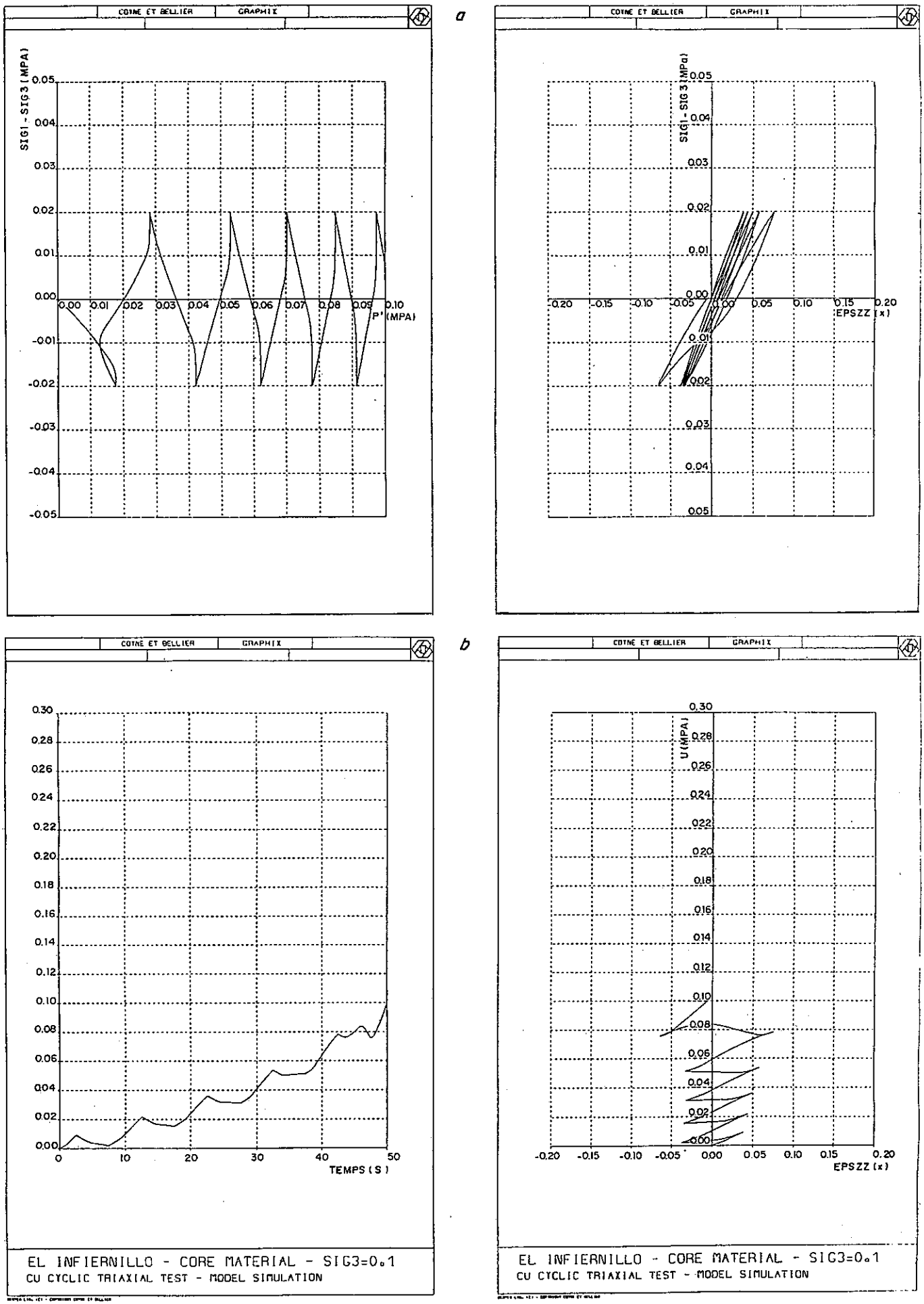

Undrained cyclic triaxial test on core material - σ_3 = 0.1 MPa - Δq = +/- 0.02 MPa

(a) - (p', q) and (q,ε_1) curves

(b) - (u, time) and (u,ε_1) curves

Fig. 2

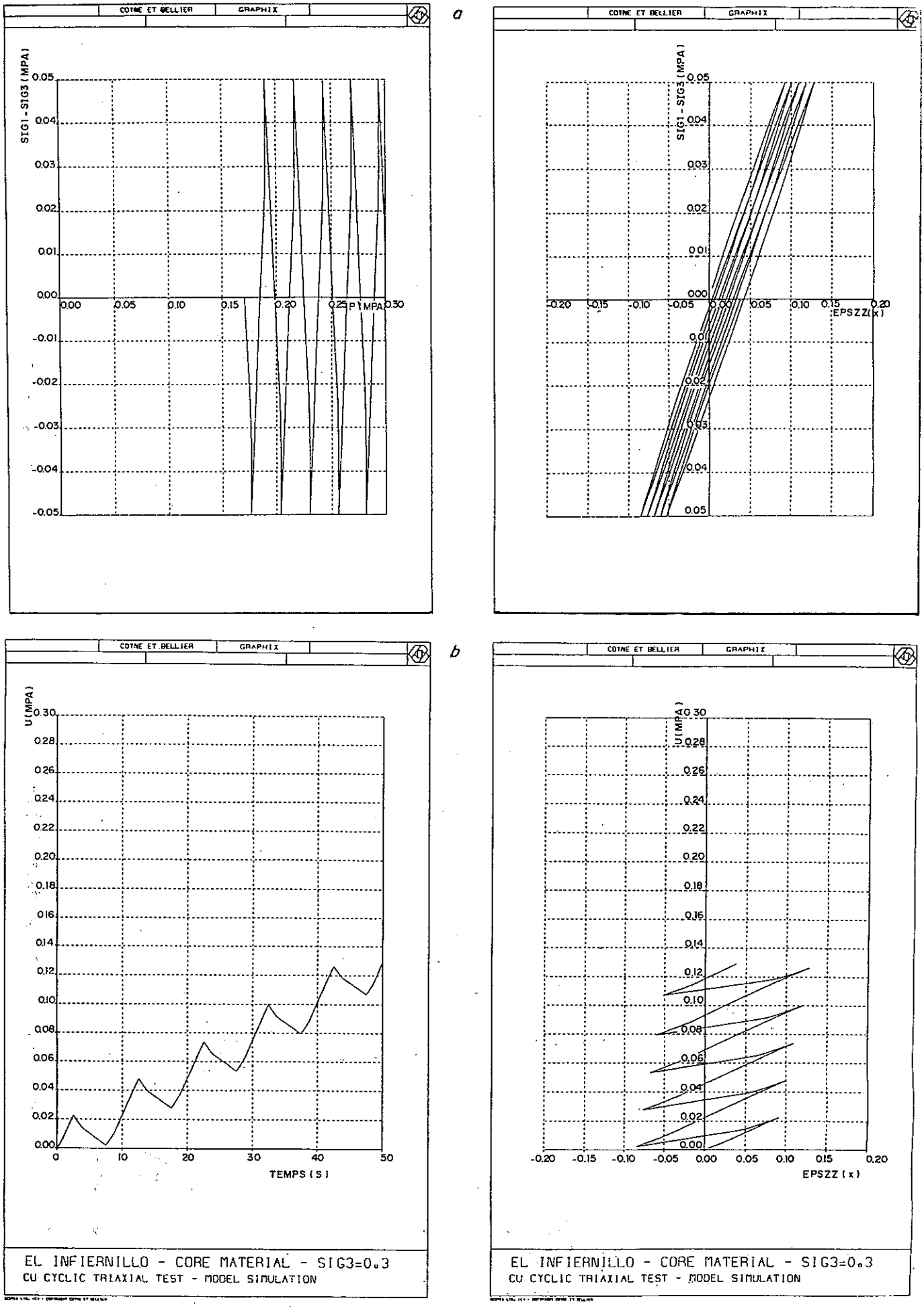

Undrained cyclic triaxial test on core material - σ_3 = 0.3 MPa - Δq = +/- 0.05 MPa

(a) - (p', q) and (q,ε_1) curves

(b) - (u, time) and (u,ε_1) curves

Fig. 3

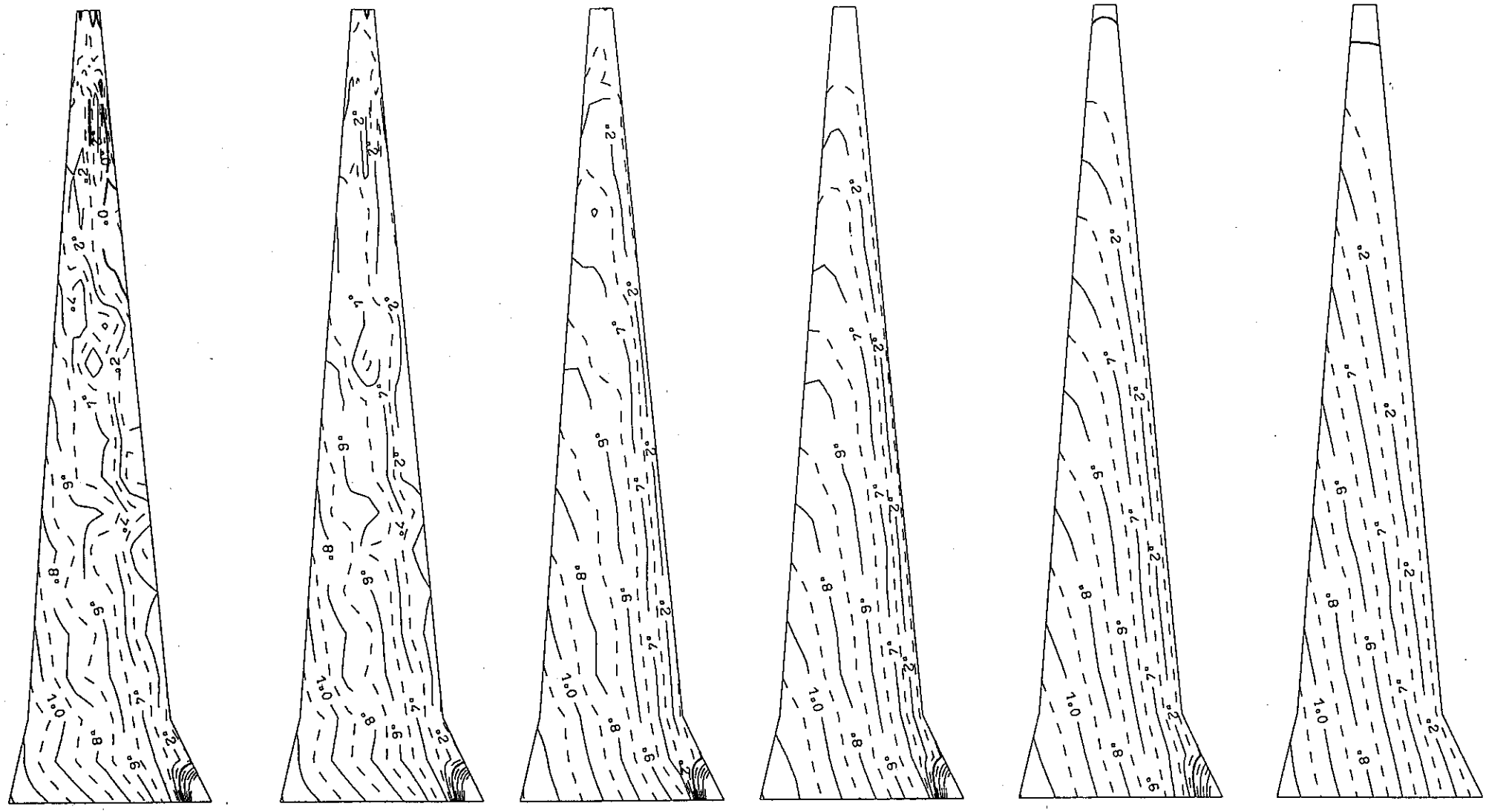

Pore pressure contour lines (in MPa) - evolution in time during EQ1 postseismic consolidation

Fig. 4

COYNE ET BELLIER - 11/94

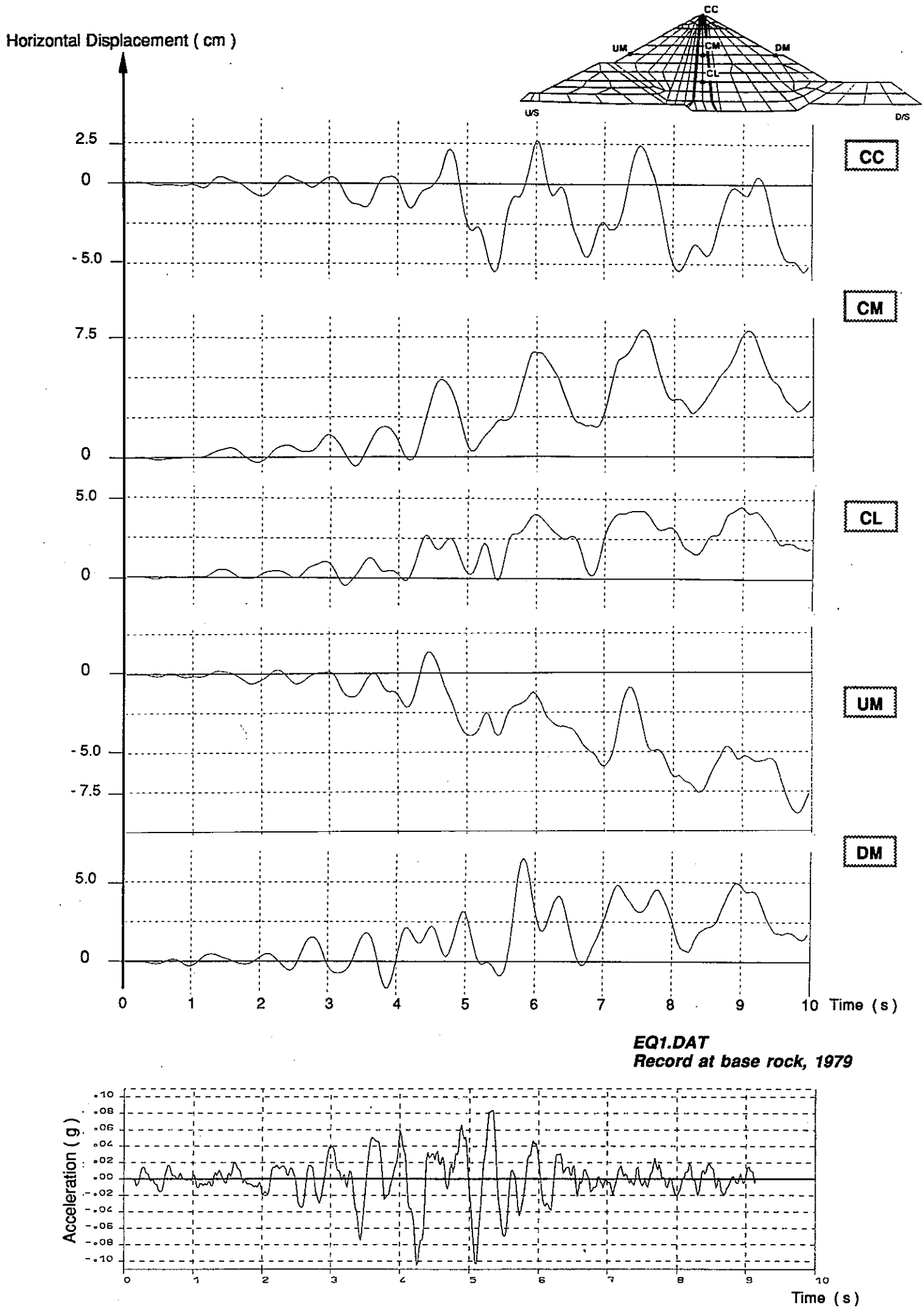

COYNE ET BELLIER - 11/94

Horizontal displacement time history - Earthquake EQ1

Fig. 5a

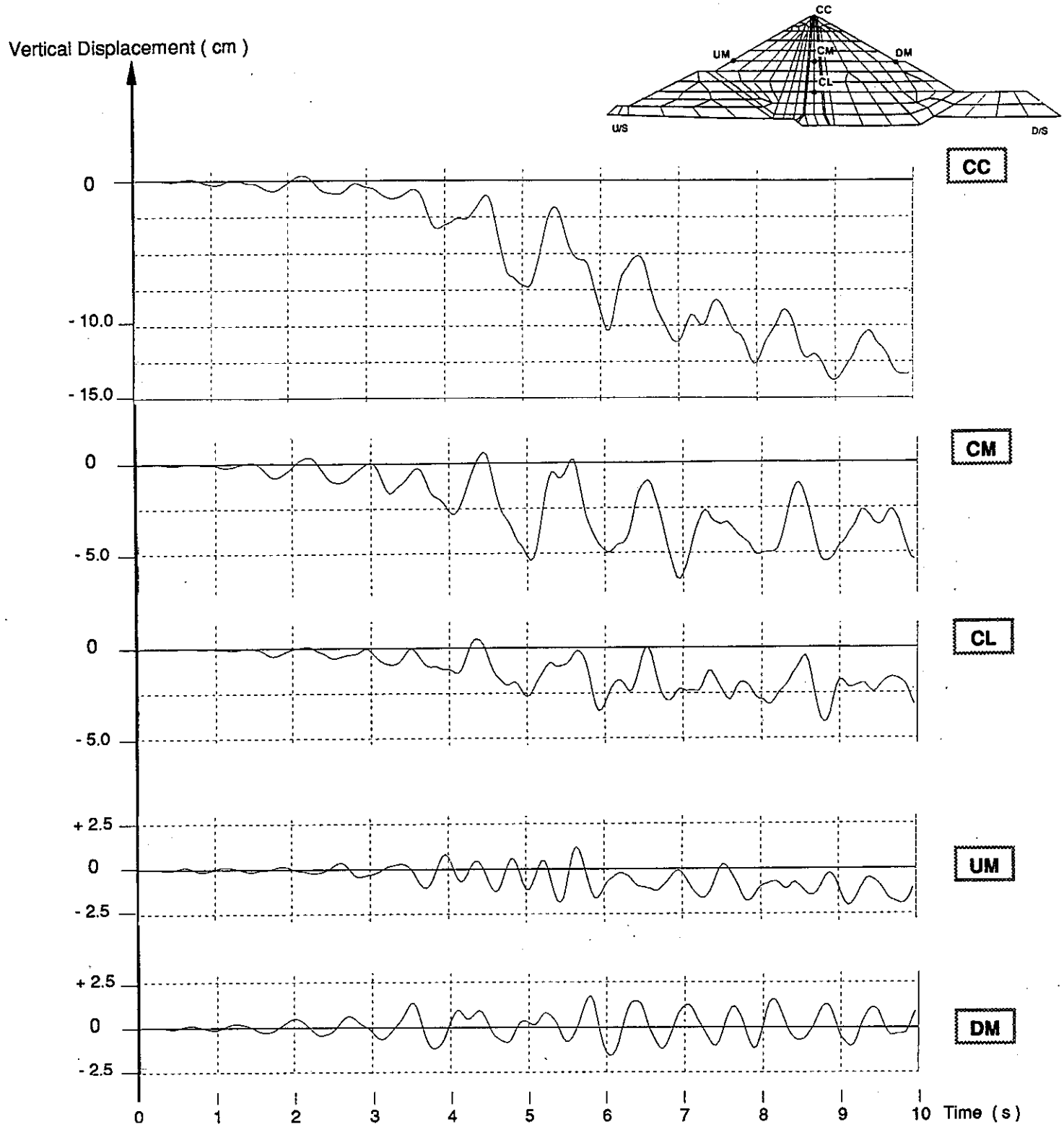

EQ1.DAT
Record at base rock, 1979

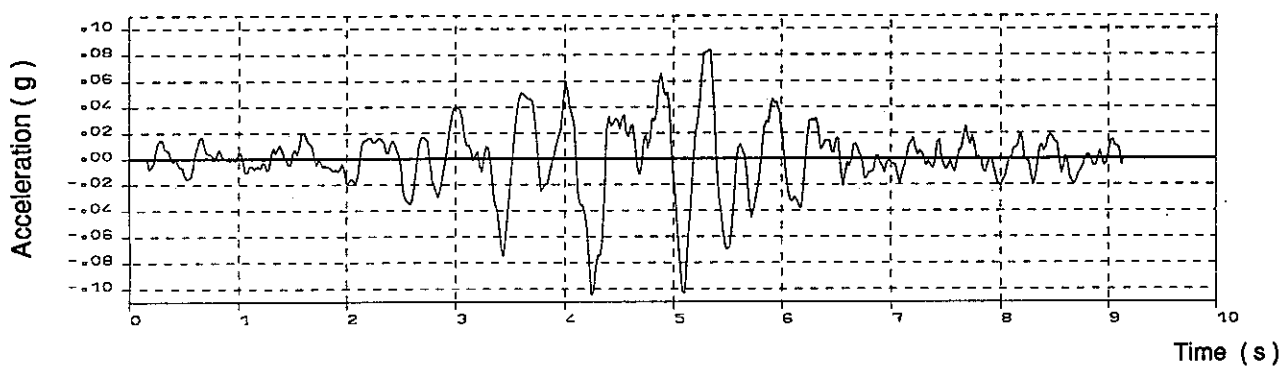

Vertical displacement time history - Earthquake EQ1 ***Fig. 5b***

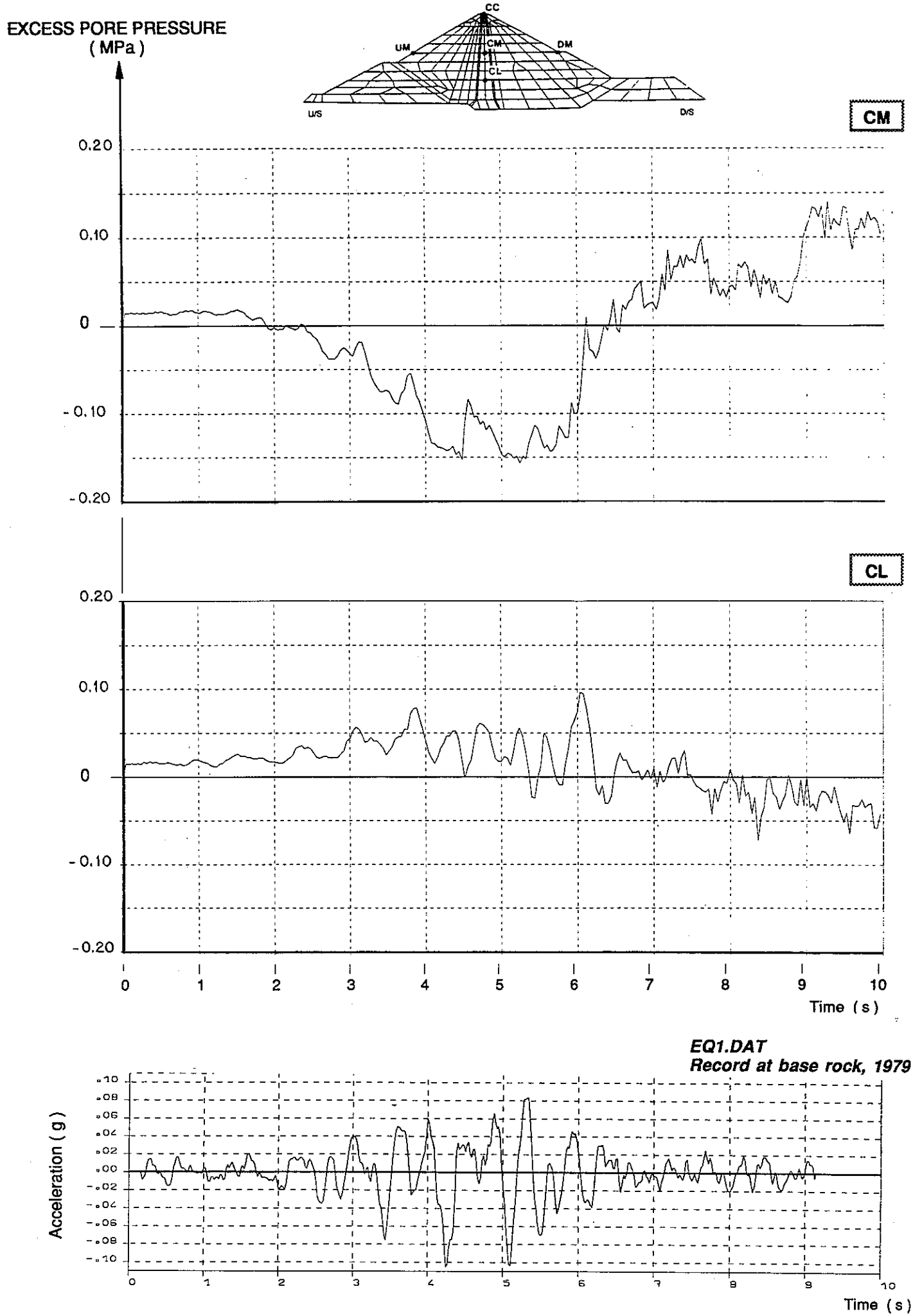

COYNE ET BELLIER - 11/94

Excess pore pressure time history - Earthquake EQ1

Fig. 5c

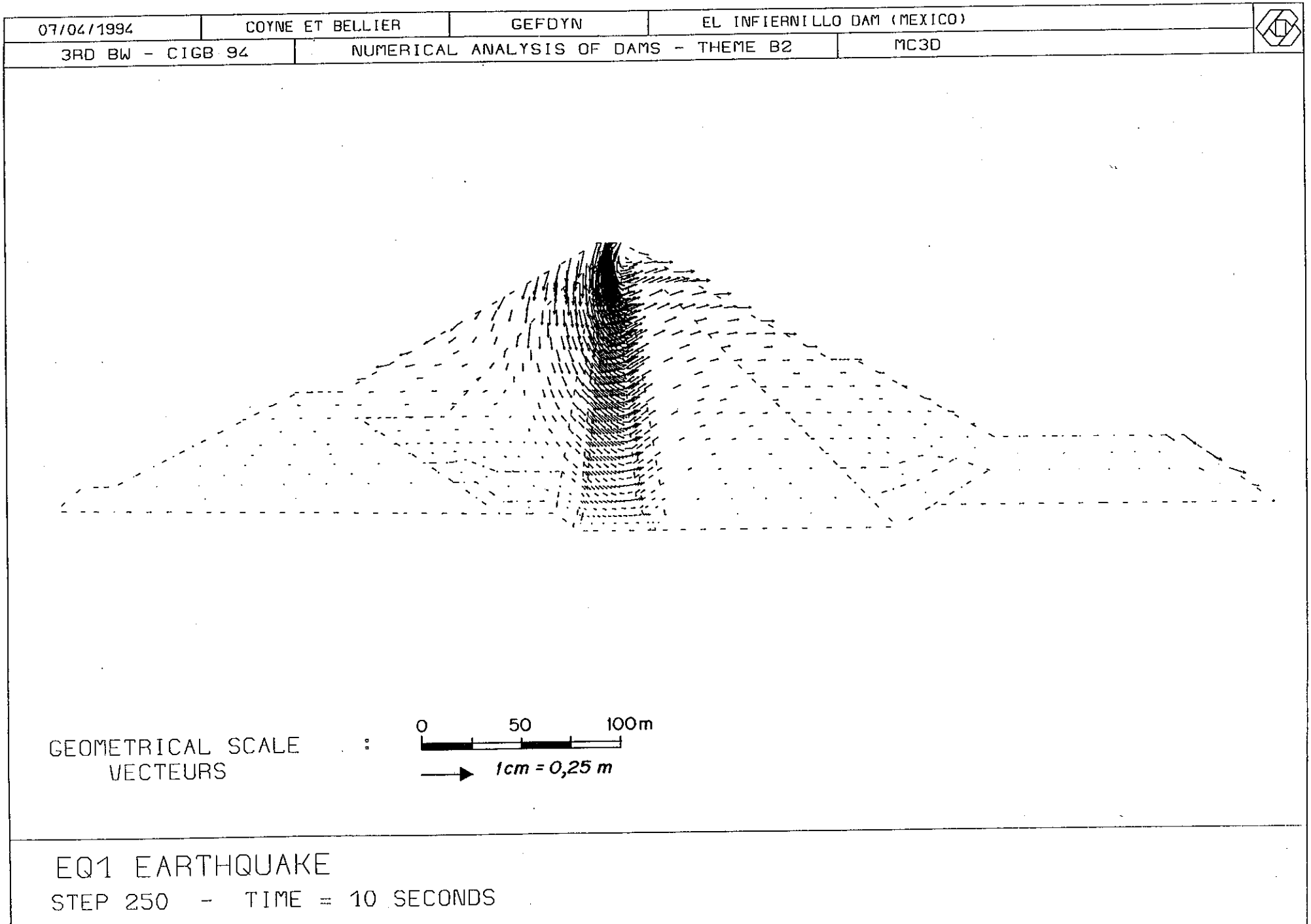

Irrecoverable displacement field at the end of earthquake EQ1

Fig. 6

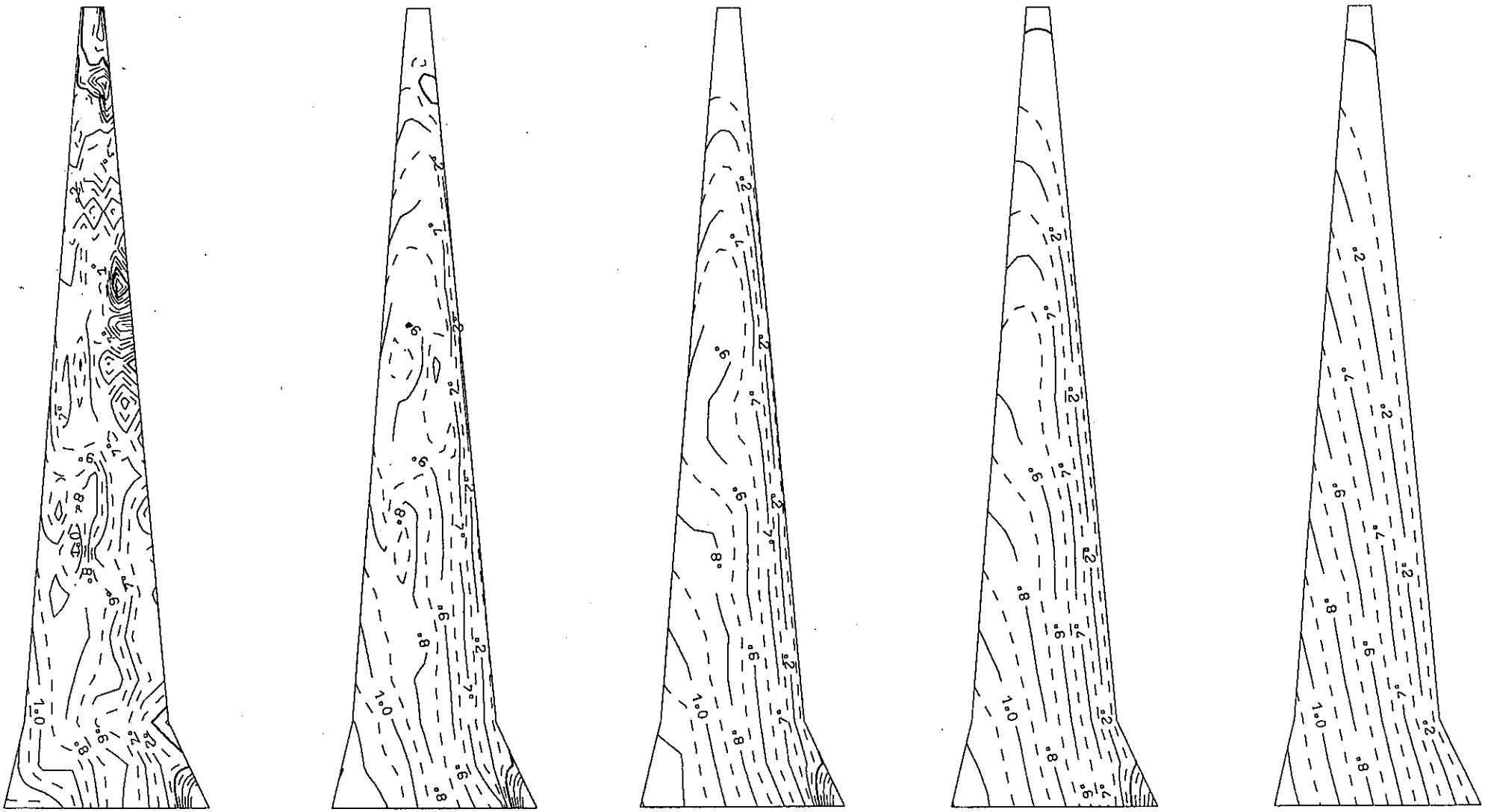

Pore pressure contour lines (in MPa) - evolution in time during EQ2 postseismic consolidation

Fig. 7

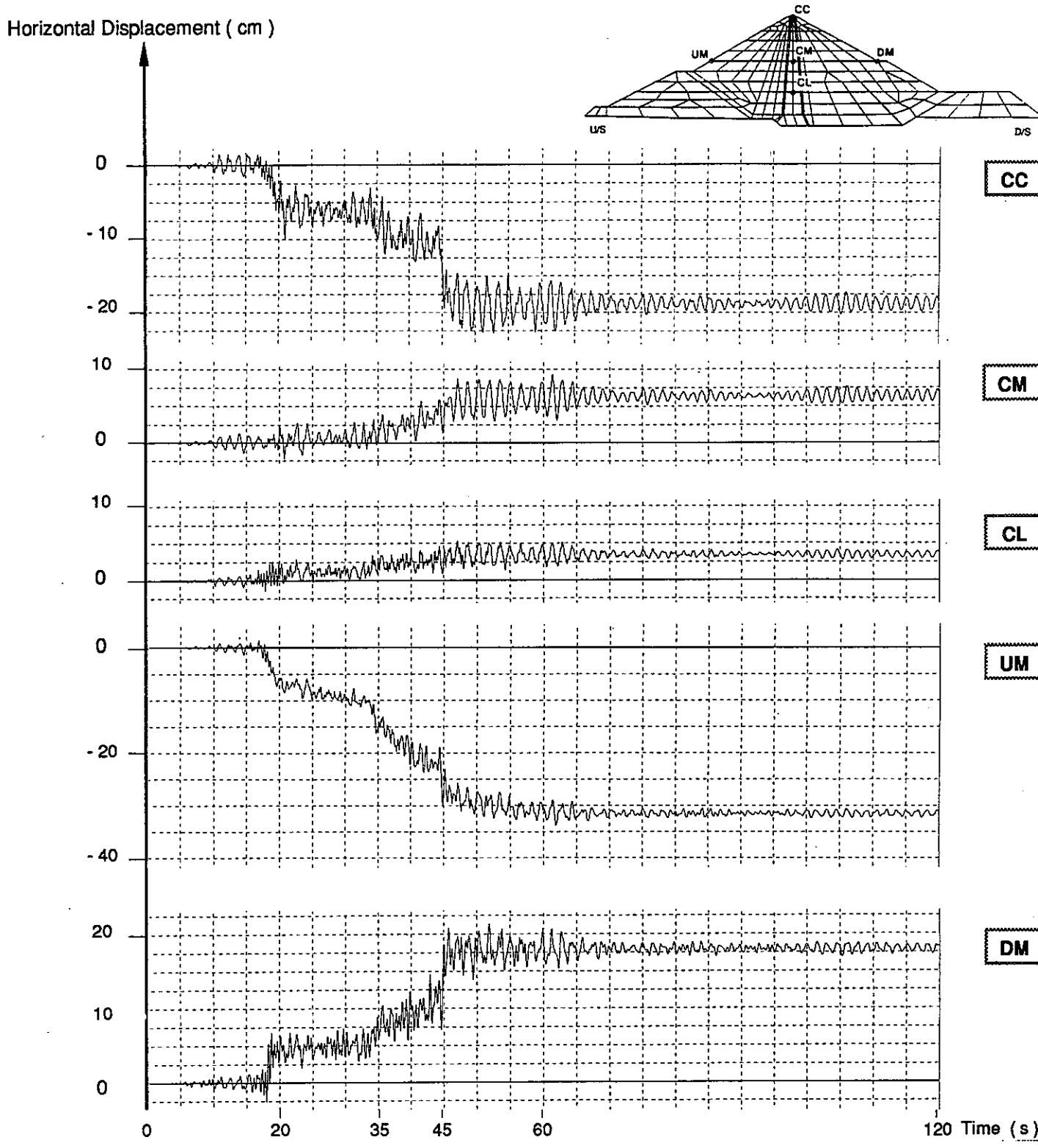

EQ2.DAT
Record at base rock, 1985

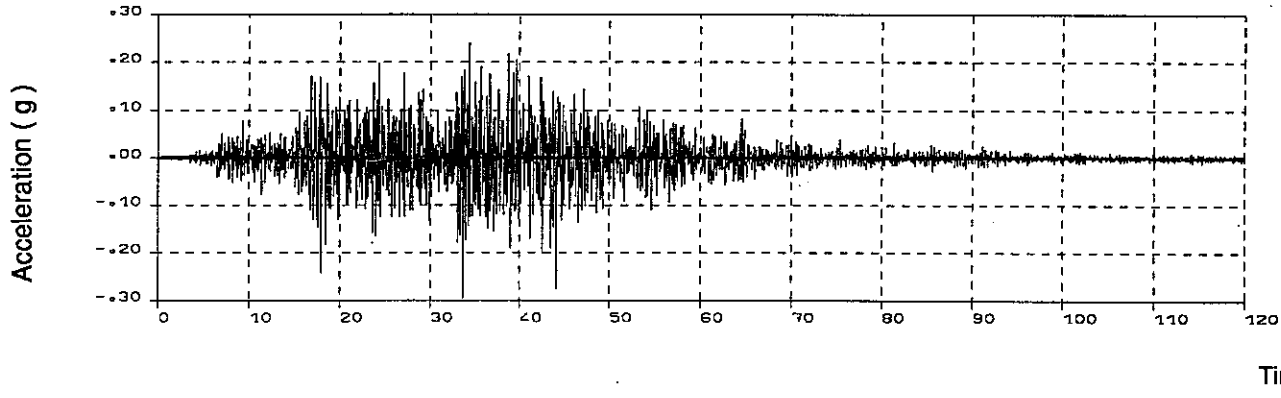

Horizontal displacement time history - Earthquake EQ2

Fig. 8a

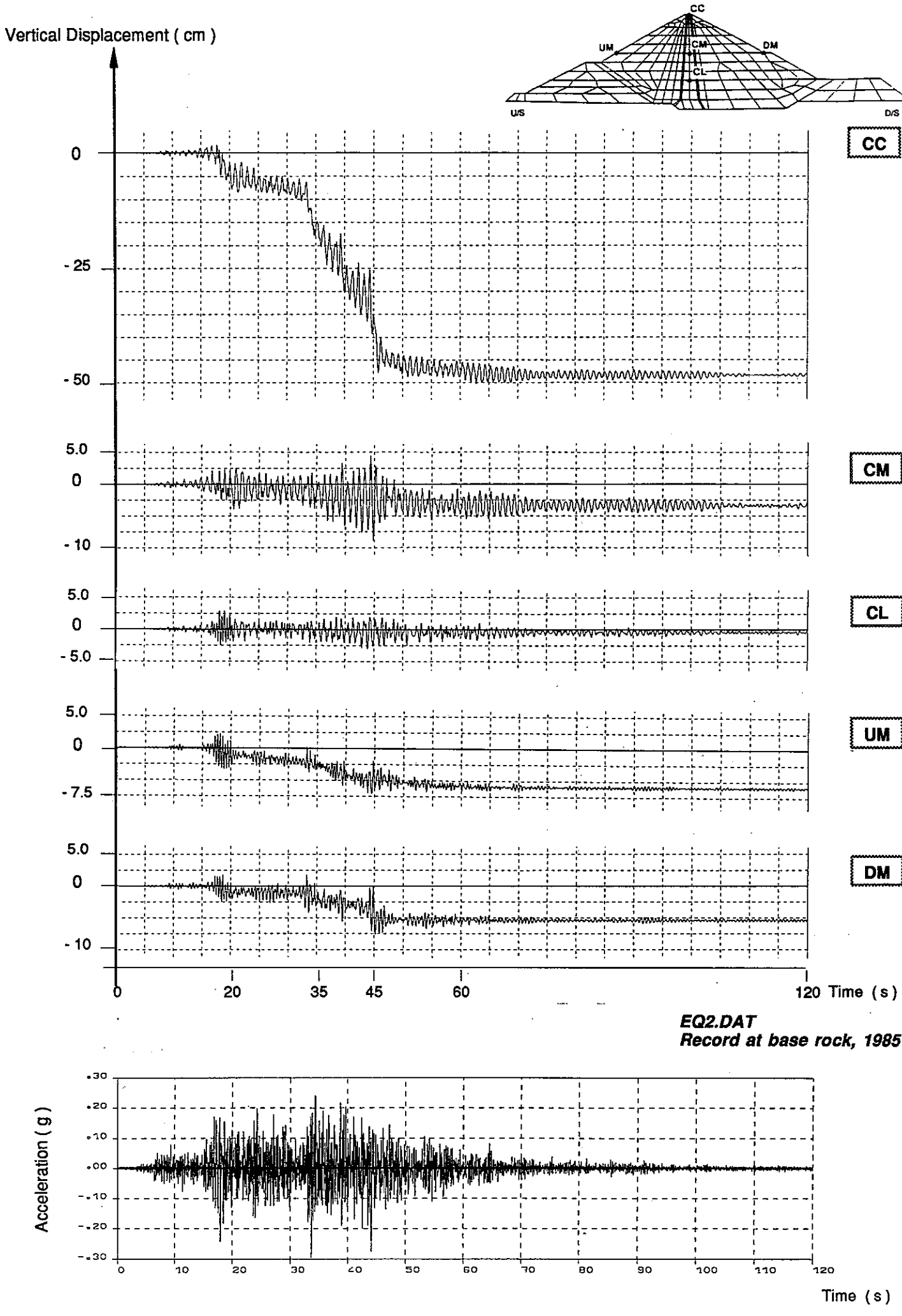

EQ2.DAT
Record at base rock, 1985

COYNE ET BELLIER - 11/94

Vertical displacement time history - Earthquake EQ2

Fig. 8b

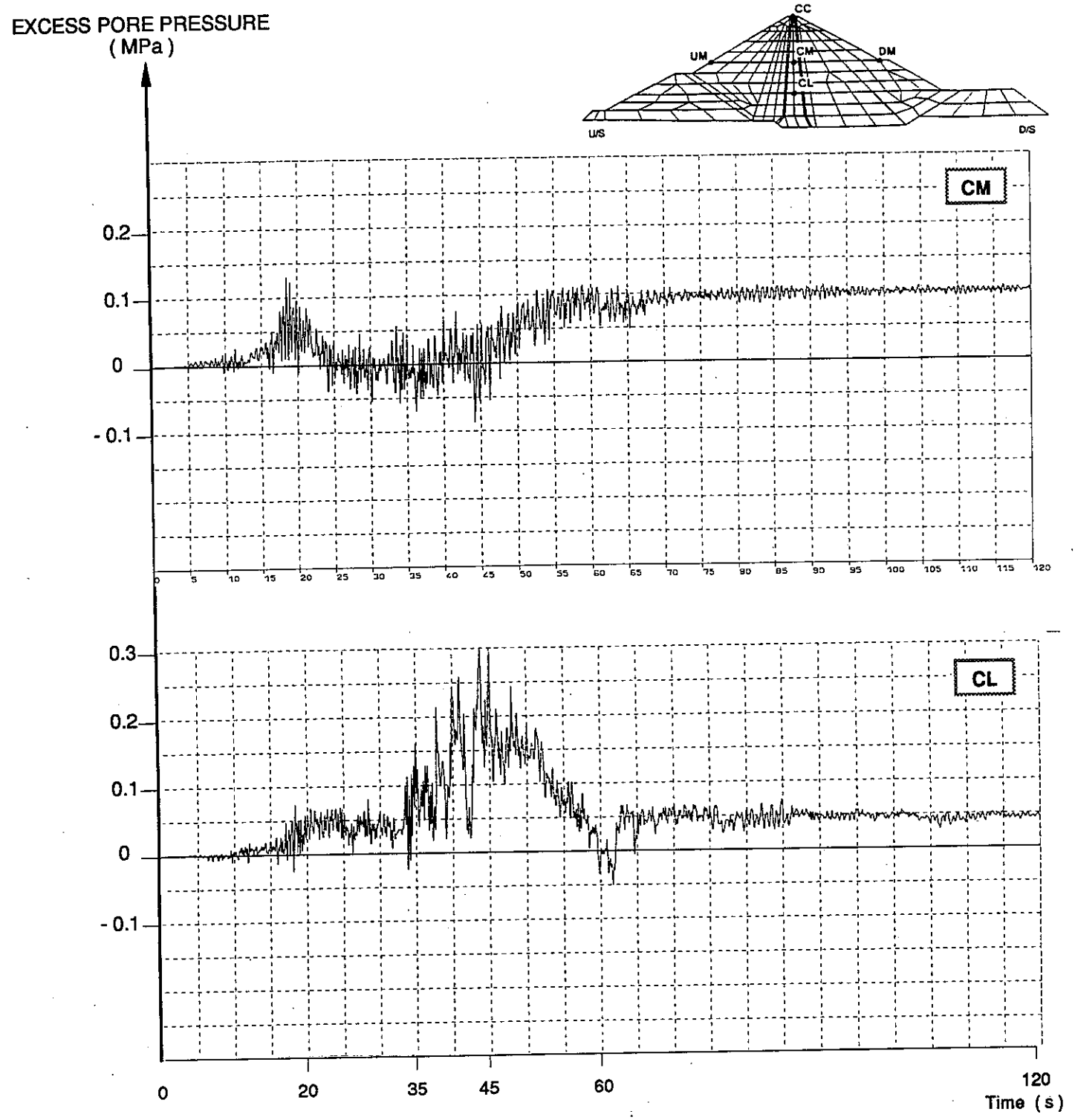

EQ2.DAT
Record at base rock, 1985

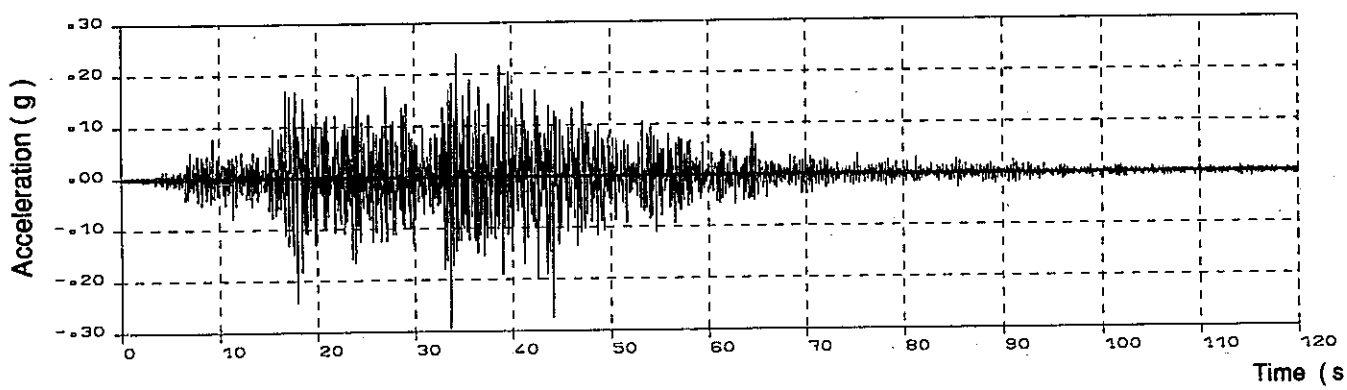

Excess pore pressure time history - Earthquake EQ2

Fig. 8c

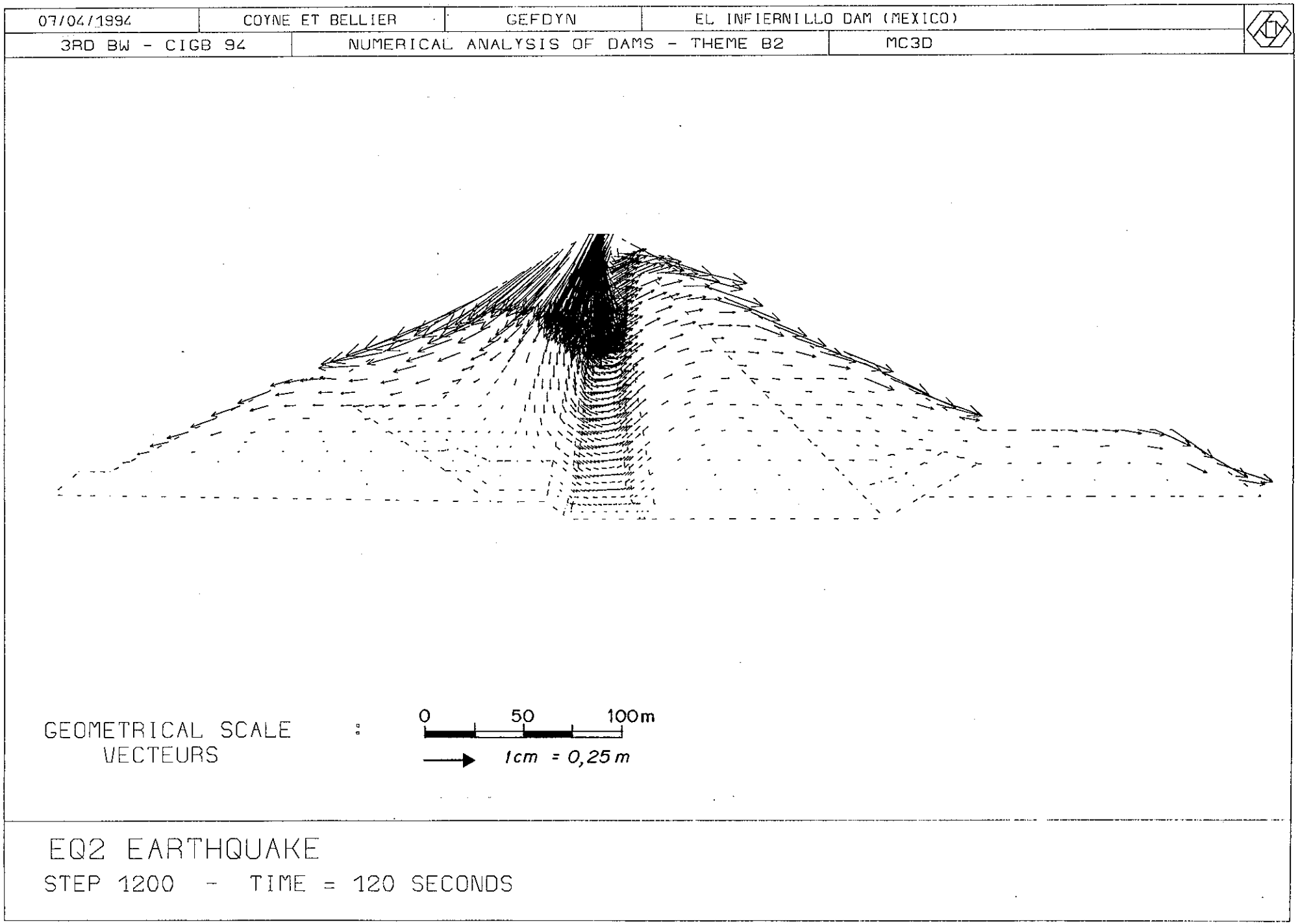

Irrecoverable displacement field at the end of earthquake EQ2

Fig. 9

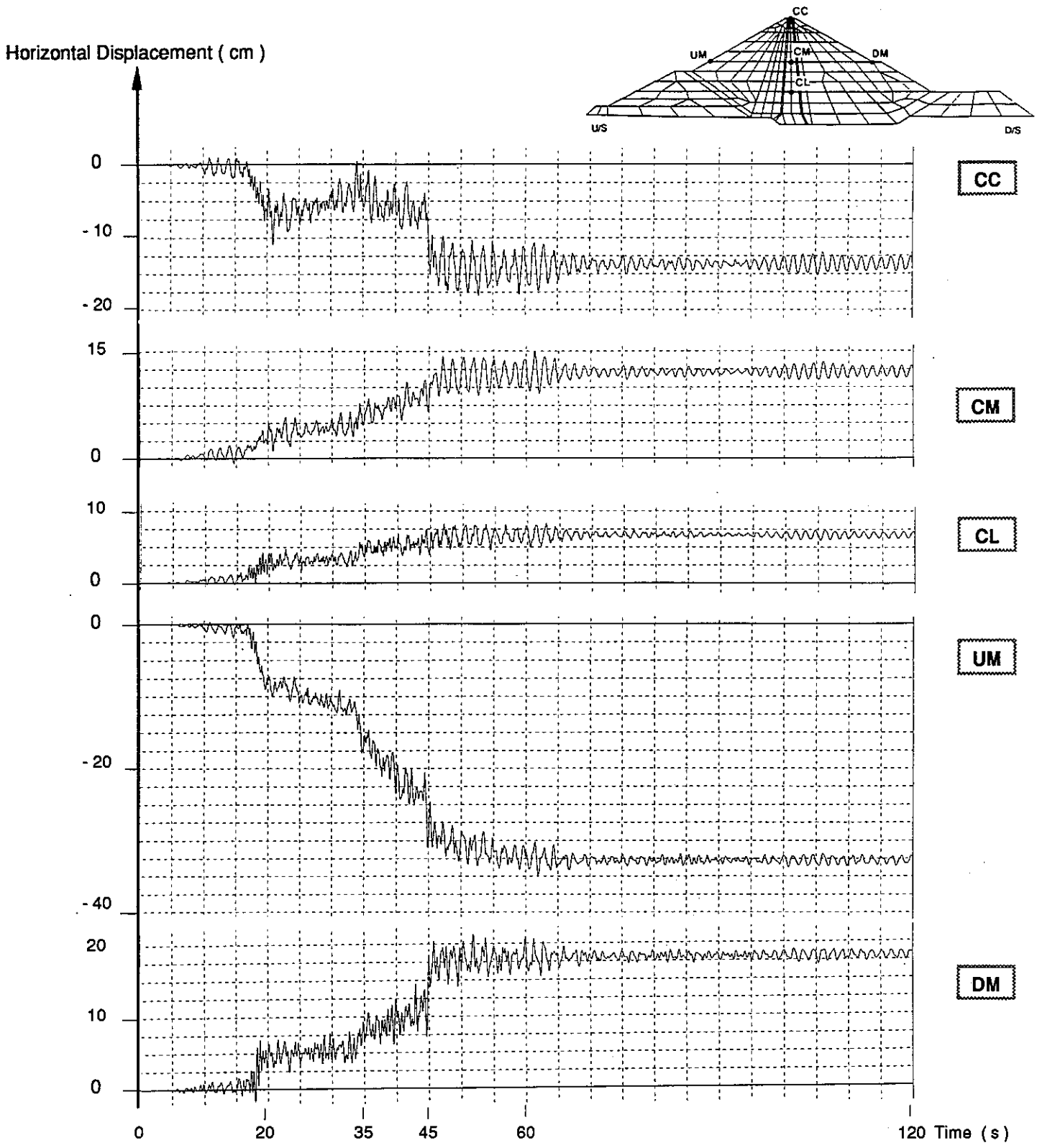

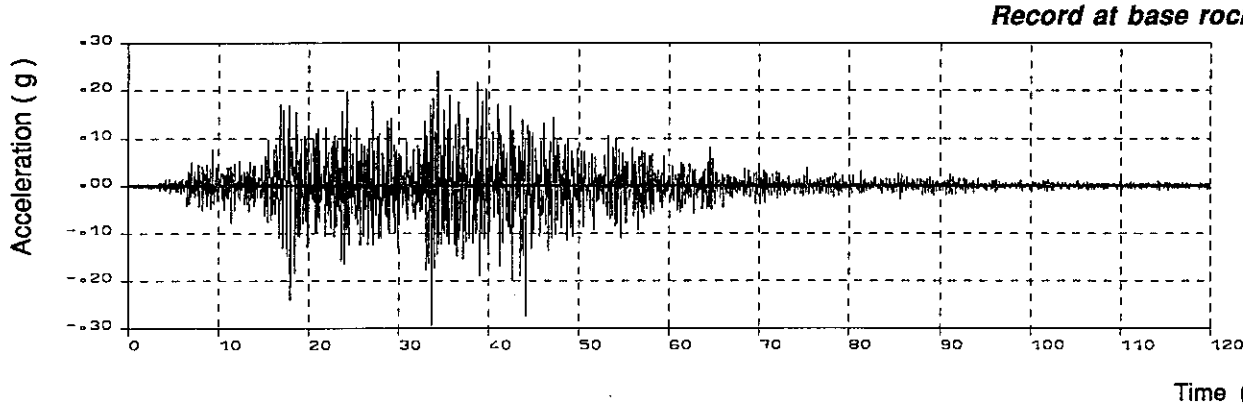

Horizontal displacement time history - Earthquake EQ2 initial state identical to EQ1 initial state

Fig. 10a

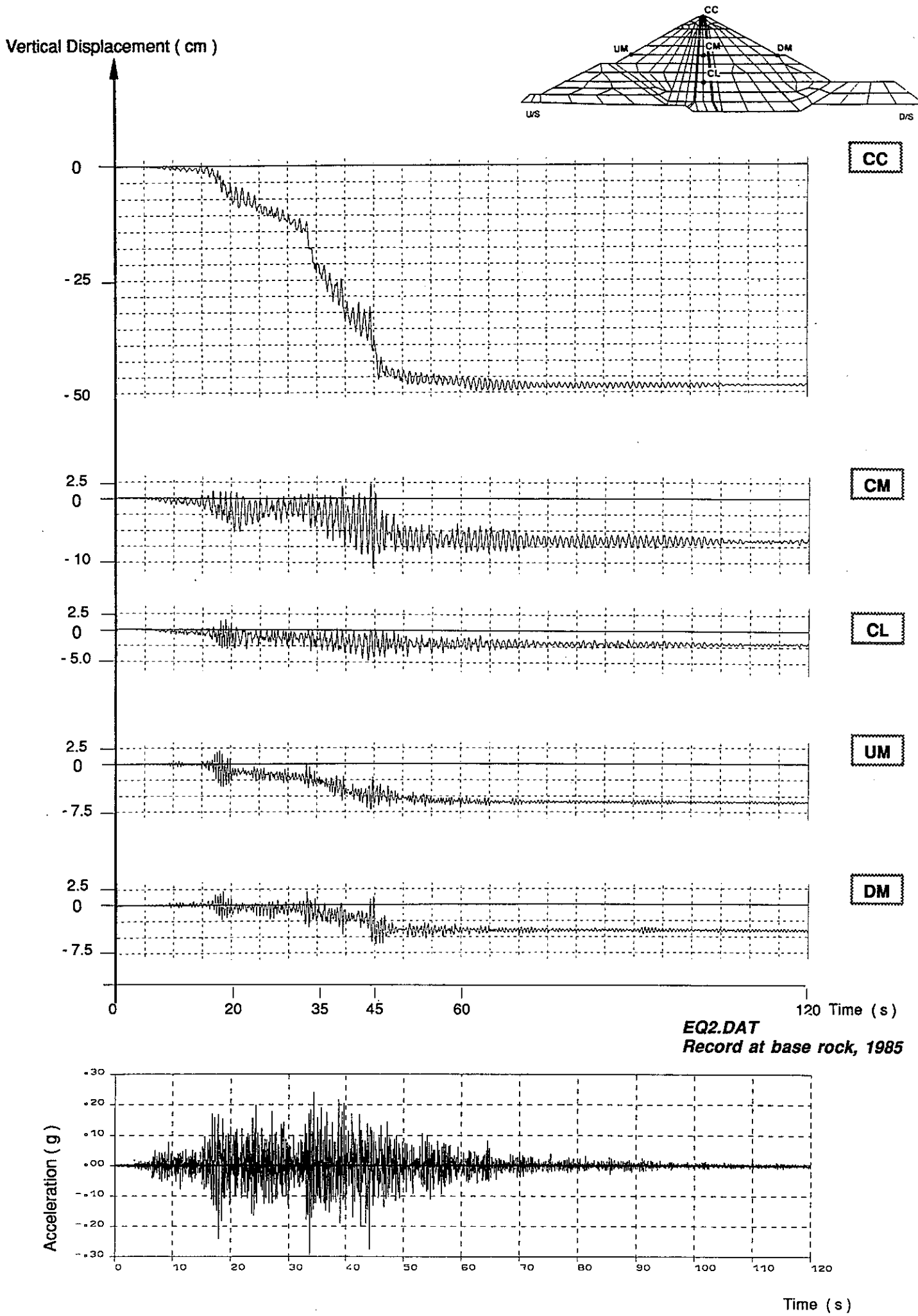

Vertical displacement time history - Earthquake EQ2
initial state identical to EQ1 initial state

Fig. 10b

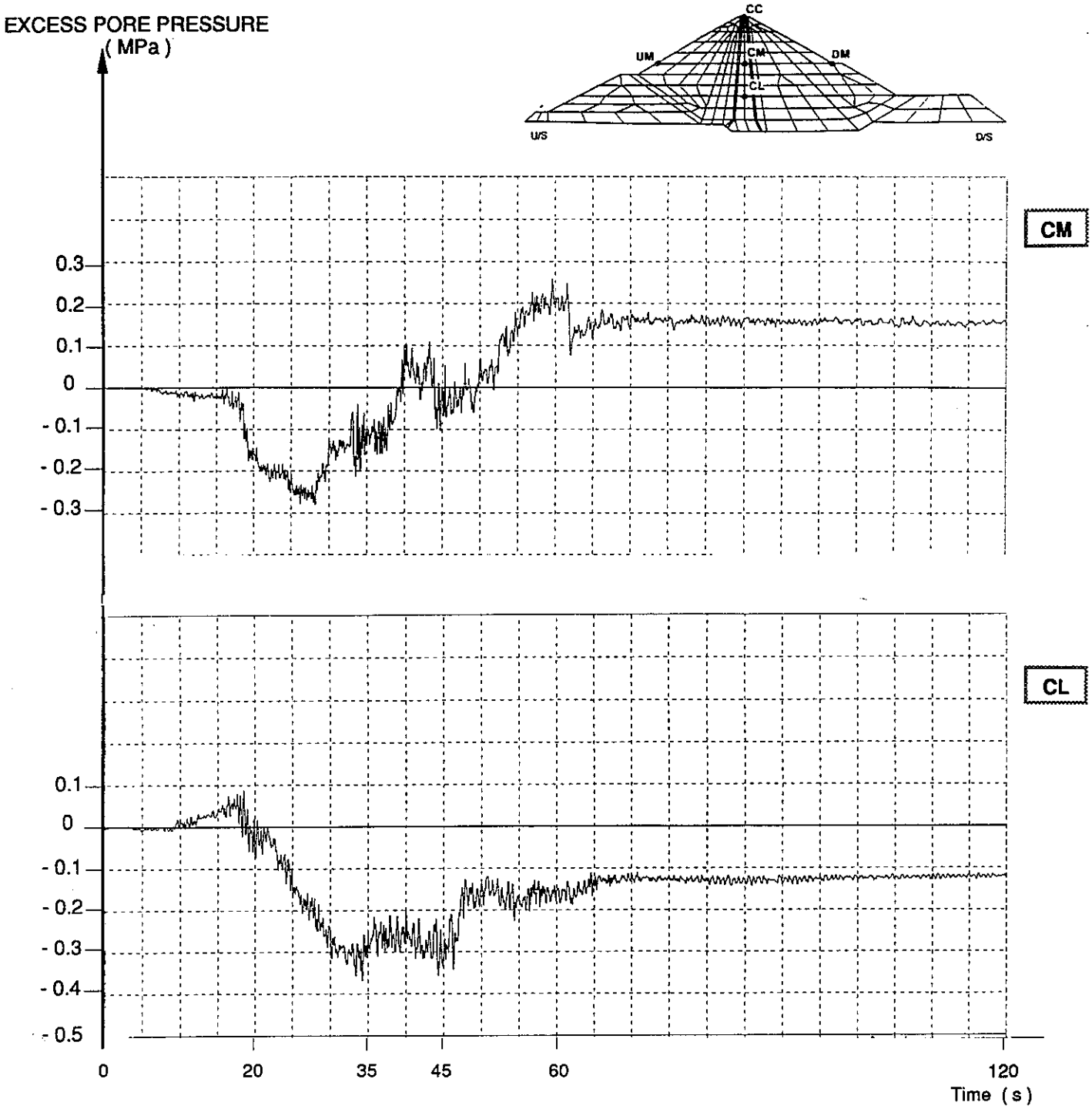

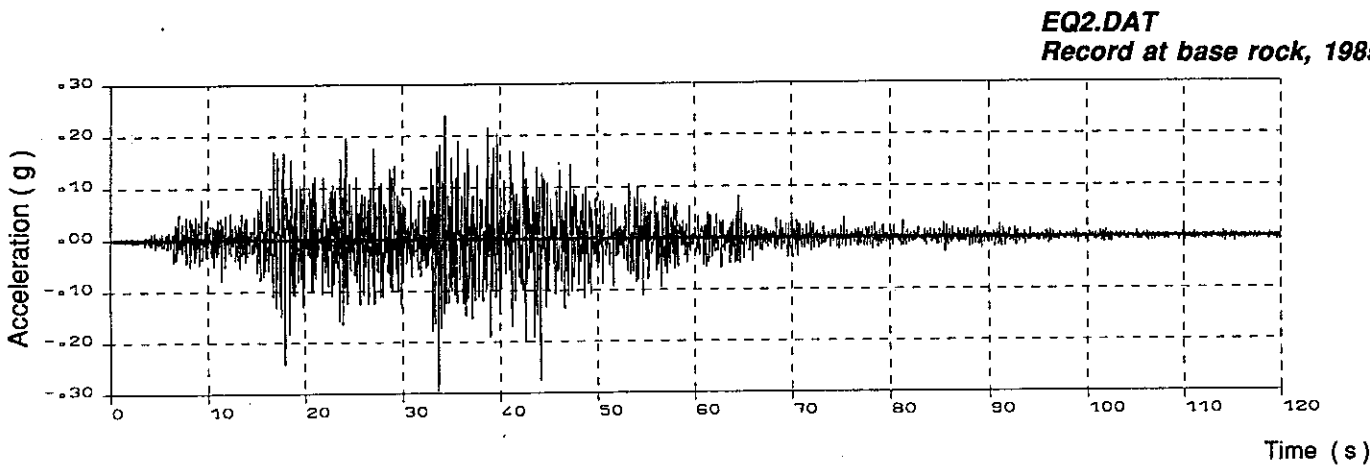

Excess pore pressure time history - Earthquake EQ2 initial state identical to EQ1 initial state

Fig. 10c

Third ICOLD Benchmark Workshop on Numerical Analysis of Dams
PARIS (FRANCE), SEPTEMBER 29-30, 1994

THEME B2

DYNAMIC ANALYSIS OF AN EMBANKMENT DAM UNDER A STRONG EARTHQUAKE

G. La Barbera, A. Bani - ISMES S.p.A. Bergamo
G. Mazzà - ENEL/CRIS Milano

1. INTRODUCTION

The paper presents the results of the analysis carried out for the "El Infiernillo" dam, built in Mexico in 1962-63. It is a 145 m high rockfill dam with a central impermeable clay core (Fig. 1). The foundation is composed of sound rock consisting of silicified conglomerate with basaltic dikes and can therefore be considered rigid and impermeable.
The analysis has been performed adopting an undrained coupled formulation for the elements in the clay core material and fully drained uncoupled formulation for the remaining elements of the dam.
As proposed in the technical specification of the Benchmark Workshop, the dynamic analysis has been carried out in three steps as described in the next chapter 3.
The computer program used for the analysis is OMEGA, a 2-D 3-D f.e.m. code for the numerical solution of non-linear analysis of both one-phase solid and two-phases solid-fluid medium subjected to static and dynamic load conditions. The code has been jointly developed by ISMES S.p.A. (Bergamo, Italy) and CIMNE (Barcelona, Spain), on the basis of the theoretical formulation presented in [4], [5], [6], [7].
The numerical computations have been carried out on the CONVEX C3220 parallel/vectorial super computer at the ISMES computer facilities in Bergamo.

2. ADOPTED FORMULATION

The dynamic coupled problem has been solved adopting an explicit time integration scheme recently implemented in OMEGA [9]. Such implementation has proved to be as accurate as the implicit algorithm already available in the code provided that an adequate time increment is selected. However, the explicit algorithm allows a considerable save in computational time, for example, the explicit solution of the EQ1 earthquake Benchmark dynamic problem has required 1/5 of the CPU of that required by the explicit solution. Moreover, although the results in terms of displacement coincide in both solution procedures, the accelerations calculated by the explicit scheme appear much more realistic.
Two types of constitutive equation have been adopted:

- A non-linear elastic-plastic strain hardening material, called SUOLO, for the clay core material;
- A linear elastic perfectly plastic Drucker-Prager model for all the remaining material dam.

The SUOLO model [3], allows to simulate plastic deformation, and then accumulation of excess pressure, under cyclic loads

3. PROBLEM DEFINITION

The finite element mesh (Fig. 2) is the one proposed by the Organising Committee, optimised with an algorithm for profile and wave front reduction of sparse matrices. There are two different types of elements: the isoparametric 8-node quadrilateral and 6-node triangle. Numerical integration for the two types of

elements has been performed using respectively the Gauss and the Radau rule, both with 4 integration points for each element.
Preliminary checks has shown that because of the permeability values involved in this problem the results are practically identical by using the following alternative problem definition:

1) Fully drained coupled formulation for the whole elements in the dam;
2) Undrained coupled formulation for the elements in the core and fully drained uncoupled formulation for the remaining elements of the dam.

Since the solution using the latter formulation is by far less expensive, all the analyses have been performed under this conditions.
Three sets of analyses have been performed:

- The first one has been performed to identify the dynamic material parameters by the best fit among the calculated and the observed behaviour of the dam under the EQ1 earthquake seismic excitation;
- The second one consisted in the simulation of undrained triaxial cyclic tests with the determined parameter set of the core material in the previous steps;
- The third one consisted in the direct dynamic analysis with the EQ2 earthquake input.

The initial stress field used to start the analysis is that presented in the first contribution [11] describing the numerical simulation of the static construction procedure of the dam.

4. MATERIAL PARAMETERS

Both constitutive models employed in the analysis adopt the same limit state surface, namely The Drucker and Prager. The values of material parameters c and ϕ controlling the shape of this surface have been determined as described in [11].
The additional parameter values required by SUOLO are reported in the following table 1. They have been estimated in order to obtain the best fit of the soil behaviour resulting from the oedometer tests reported in the Technical specifications of the 2nd Benchmark Workshop of 1992.

Table 1: Additional material properties assumed for the SUOLO model

Mat. No.	λ	x	$\frac{\overline{P_y}}{\hat{P}_y}$	$\frac{\overline{P_y}}{\overline{P_c}}$	Over-consolidation ratio O.C.R.
Clay Core Material n. 1	0.0977	0.0147	1.10	2.0	1.1

Figures 3 and 4 report the simulation of a soil sample under undrained cyclic triaxial test.
Finally, the first set of tests performed using the EQ1 seismic input has entirely devoted to identify the viscous damping factor of the dam. It resulted that the best value for the damping factor α is 0.5.

4.1. Damping factor definition

According to Rayleigh the damping matrix can be defined as:

$$\mathbf{D} = \gamma \mathbf{K} + \alpha \mathbf{M}$$

where: $\mathbf{D}$ = damping matrix;
$\mathbf{K}$ = stiffness matrix;
$\mathbf{M}$ = mass matrix.

Assuming the hypothesis of linear elastic behaviour of the structure the eigenvalues and the eigenvectors of the equation system can be determined. Due to the orthogonality property of the eigenvectors the **D** matrix can be decoupled as:

$$\Phi^T \mathbf{D}\, \Phi = \Phi^T (\gamma \mathbf{K} + \alpha \mathbf{M})\, \Phi$$

where: Φ are the eigenvectors.
Normalising the eigenvectors as:

$$\Phi^T \mathbf{M}\, \Phi = \mathbf{I} \qquad \text{then}$$

$$\Phi^T \mathbf{D}\, \Phi = \gamma \begin{vmatrix} - & - & - \\ - & \omega_i^2 & - \\ - & - & - \end{vmatrix} + \alpha \mathbf{I}$$

$$2\, \beta_i\, \omega_i = \gamma\, \omega_i^2 + \alpha$$

where β_i is the damping ratio defined as: $\beta_i = \dfrac{d}{d_{crit}}$

and $d_{crit} = 2\sqrt{\mathbf{KM}}$ is the critical damping,

then: $\beta_i = \dfrac{1}{2}\left(\gamma\, \omega_i + \dfrac{\alpha}{\omega i}\right)$

assuming that the damping matrix is only proportional to the mass matrix, we obtain:

$$\beta_i = \frac{1}{2}\,\frac{\alpha}{\omega i}$$

Assuming:

- a damping ratio $\beta_i = 5\%$

- $T_1 = 2.61 \dfrac{h}{V_s}$

- $\omega_1 = \dfrac{2\pi}{T_1} = \dfrac{2\pi\, V_s}{2.61\, h}$ then

$$0.05 = \frac{1}{2}\,\frac{\alpha\, 2.61\, h}{2\pi\, V_s}$$

in our case h = 145 (dam height); assuming V_s (shear wave velocity) = 300 m/sec:

$\alpha = 0.5$; $T_1 = 1.26$ sec; $\omega_1 = 4.99$ rad/sec; $f_1 = 0.79$ Hz

A parametric sensitivity study has been carried out varying the value of the damping coefficient α.
In Fig.5 the time histories of the total acceleration calculated at the dam crest (point CC) are reported.
Three different curves are reported corresponding to different analyses which have been carried out giving as input the values of damping coefficient $\alpha = 0.3;\ 0.5;\ 1.0$.

5. ADOPTED SOLUTION STRATEGY

For al the conducted dynamic analyses a time step increment of 0.0005 sec has been adopted.
The analyses conducted for the EQ1 earthquake required 30.000 steps; those conducted for the EQ2 earthquake required 240.000 steps.
The integration scheme of the non-linear constitutive law was the modified Newton-Raphson with no updating of the initial stiffness matrix. A tolerance of 1% have been imposed for all the analyses. The convergence is checked comparing the norm of the residual force with the norm of the total external forces.
The time integration scheme is the central difference.

6. RESULTS OF DYNAMIC ANALYSES

6.1. EQ1 earthquake analysis

The first analysis required by the technical committee is supposed to analyse the behaviour of the dam subjected to both horizontal and vertical accelerations. The time history of such components are supposed to be the same while the amplitude is assumed to respect the following ratio:

$$\frac{a_y}{a_x} = 0.65$$

Such assumption implies that the shear and compression waves act at the same time. Since this situation is, fortunately, a very rare event a first preliminary analysis with non vertical component has been performed.
In figures 6-10 the time histories of accelerations, displacements and excess pore water pressures are reported, while table 2a summarises them as required in the ICOLD technical specifications.
Then a second analysis has been performed imposing also the vertical component of the acceleration as required by the technical specifications. In figures 11-15 the time histories of total accelerations, displacements and excess pore water pressures are reported, while table 2b summarises them as required by the technical specifications.
As expected, the contemporaneously application of both vertical and horizontal accelerations at the same time as required by the technical specifications causes a significant increase of all the calculated quantities.

6.2. EQ2 earthquake analysis

The third set of analysis required by the technical committee is the direct dynamic analysis with the EQ2 earthquake as input, considering both horizontal and vertical accelerations. The time history of such component are supposed to be the same while the amplitude is assumed to respect the following ratio:

$$\frac{a_y}{a_x} = 1.0$$

For the same reasons espoused in the previous paragraph a first preliminary analysis with no vertical component has been performed.
In figures 16-20 the time histories of total accelerations, displacements and excess pore water pressures are reported, while table 3a summarises them as required in the ICOLD technical specifications.
A second analysis has been performed imponing also vertical component of the accelerations as required by the technical specifications.
In figures 21-25 the time histories of total accelerations, displacements and excess pore water pressures are reported, while table 3b summarises them as required in the ICOLD technical specifications.

Table 2a

EQ1 earthquake considering only horizontal component					
	Points of the dam section				
	CC	CM	CL	UM	DM
Maximum horizontal acceleration (g) (1)	0.27	0.12	0.13	0.14	0.25
Maximum vertical acceleration (g) (1)	0.21	0.12	0.10	0.80	0.16
Irreversible horizontal displacement (cm) (2)	1.60	0.70	0.80	20.00	4.90
Irreversible vertical displacement (cm) (2)	7.20	0.60	-0.30	7.00	1.50
Maximum excess pore pressure (MPa) (4) (1)	0.00	0.04	0.10	0.00	0.00
Final excess pore pressure (MPa) (4)	0.00	-0.02	0.00	0.00	0.00

Table 2b

EQ1 earthquake considering horizontal and vertical components					
	Points of the dam section				
	CC	CM	CL	UM	DM
Maximum horizontal acceleration (g) (1)	0.42	0.13	0.15	0.23	0.21
Maximum vertical acceleration (g) (1)	0.61	0.20	0.17	0.19	0.28
Irreversible horizontal displacement (cm) (2)	-0.10	3.20	2.60	-33.30	6.30
Irreversible vertical displacement (cm) (2)	9.60	0.90	-0.90	12.00	0.10
Maximum excess pore pressure (MPa) (4) (1)	0.00	0.06	0.28	0.00	0.00

(1) The reported values are **absolute values.**
(2) Sign. +: from U/S to D/S.
(3) Sign. +: from top to bottom.
(4) Only the excess pore pressure will be given.
The pore pressure obtained at the end of the static analysis must not be cumulated.

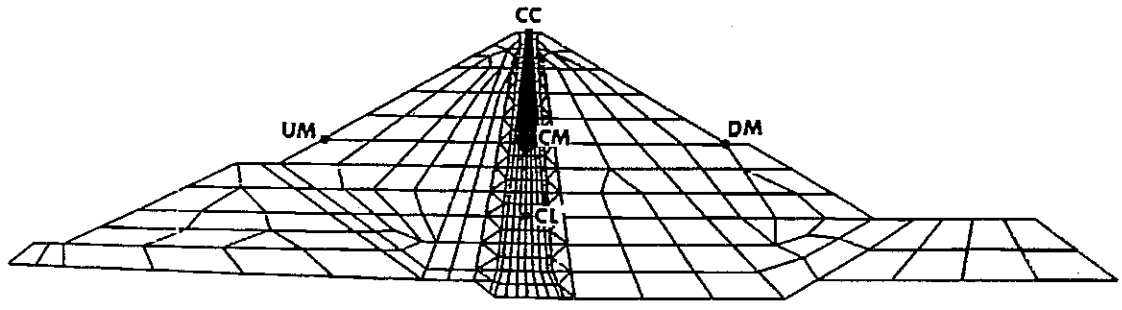

Table 3a

EQ2 earthquake considering only horizontal component					
	Points of the dam section				
	CC	CM	CL	UM	DM
Maximum horizontal acceleration (g) (1)	0.82	0.31	0.29	0.25	0.45
Maximum vertical acceleration (g) (1)	0.67	0.18	0.30	0.12	0.33
Irreversible horizontal displacement (cm) (2)	5.60	4.80	4.30	-76.50	34.20
Irreversible vertical displacement (cm) (2)	28.30	6.20	-1.70	33.10	11.70
Maximum excess pore pressure (MPa) (4) (1)	0.00	0.06	0.11	0.00	0.00
Final excess pore pressure (MPa) (4)	0.00	-0.07	-0.04	0.00	0.00

Table 3b

EQ2 earthquake considering horizontal and vertical components					
	Points of the dam section				
	CC	CM	CL	UM	DM
Maximum horizontal acceleration (g) (1)	1.87	0.47	0.44	0.25	0.70
Maximum vertical acceleration (g) (1)	1.04	0.38	0.68	0.40	1.12
Irreversible horizontal displacement (cm) (2)	10.40	38.90	29.00	-179.00	74.00
Irreversible vertical displacement (cm) (2)	70.00	18.90	-2.00	102.10	-12.40
Maximum excess pore pressure (MPa) (4) (1)	0.00	0.18	0.32	0.00	0.00

(1) The reported values are **absolute values.**
(2) Sign. +: from U/S to D/S.
(3) Sign. +: from top to bottom.
(4) Only the excess pore pressure will be given.
The pore pressure obtained at the end of the static analysis must not be cumulated.

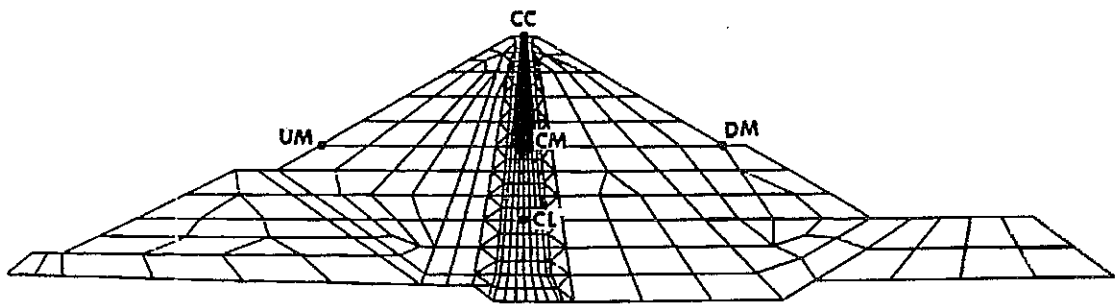

7. REQUIRED COMPUTATION TIMES

In Table 4 the required CPU times are summarised for each earthquake.

Table 4.

Dynamic Analysis	**CPU time** (hh:mm)
EQ1 earthquake	09 : 13
EQ2 earthquake	66 : 12

8. CONCLUDING REMARKS

In the present paper all the results concerning the dynamic analyses carried out for the Infiernillo Dam are presented or discussed. The following remarks can be made on the basis of the obtained results:

- It is very difficult to calibrate the value of the damping coefficient α because of it's dependence on the frequency content of the input accelerogram;

- It must be emphasised that the seismic input, as required by the technical specifications, consider both horizontal and vertical component of the acceleration. The time histories of such components are supposed to be the same, acting at the same time. Such assumption implies that the shear and compression waves act at the same time, however this situation is a very rare event. As showed by the results this assumption causes significant increase of all the calculated quantities.

- It is necessary to remember also that we didn't consider the possibility of losses of energy due to radiation of the seismic waves through the base of the dam. The influence of such parameter should be considered with an appropriate modelling through adsorbing or transmitting boundaries.

9. REFERENCES

[1] Biot M.A. (1941). General theory of free dimensional consolidation J Appl. Phys.

[2] Biot M.A. (1956). The theory of propagation of elastic waves in a fluid saturated porous solid. J. Acou.Soc.Am., 168 191.

[3] De Crescenzo A., Fusco A., La Barbera G. (1994). A constitutive equation for soils. I quaderni dell'ISMES n. 326.

[4] Fusco A. (1985). Continuum mechanics and finite element numerical solutions in geomechanics. Ph. D. Thesis, University of Ottawa.

[5] Fusco A. (1993). Numerical Analysis for engineers. Monograph CIMNE, N.19

[6] Fusco A. (1993). The continuum Mechanics Theory for engineers. Monograph CIMNE, N.20

[7] Fusco A. (1993). The Finite Element Method for engineers. Monograph CIMNE, N.21.

[8] Fusco A. and Cervera M. (1993). Coupled solid-pore fluid problems solved by Finite Elements, Monograph CIMNE, N.22.

[9] Fusco A. (1994). Procedura di soluzione esplicita per problemi dinamici in OMEGA. Rapporto per conto ISMES.

[10] La Barbera G. et al. (1992). Static analysis and seismic response of the El Infiernillo Embankment dam: Coupled effective stress analysis. Second ICOLD Benchmark Workshop, Bergamo (Italy), July 16 17.

[11] La Barbera G., Bani A., Mazza' G. (1994). Evaluation of pore pressure and settlements of an embankment dam under static loading. Third ICOLD Benchmark Workshop on Numerical Analysis of Dams. Paris (France) September 29-30 1994.

[12] Fusco A. et al. (1991). The seismic Response of the El Infiernillo Embankment dam: coupled effective stress elasto-plastic analysis. First Benchmark Workshop Bergamo (Italy), May 28 29.

[13] Sandhu R.S. (1968). Fluid flow in saturated porous elastic media. PhD Thesis, Univers. of California at Berkeley.

[14] Sandhu R.S. and Wilson E.L. (1969). Finite element analysis of seepage in elastic media Proceeding ASCE, Mechanics Division, Vol. 95, No. EM3.

[15] Seed H.B. (1979). Considerations in the earthquake resistant design of earth and rockfill dams. Geotechnique 29, No. 3.

[16] Zienkiewicz O.C., Bettess P. (1982). Soil and saturated media under transited dynamic conditions; general formulation and the validity of various simplifying assumption In Soil Mechanics Transient & Cyclic Loads (Eds. G.N. Pande & O.C. Zienkiewicz)

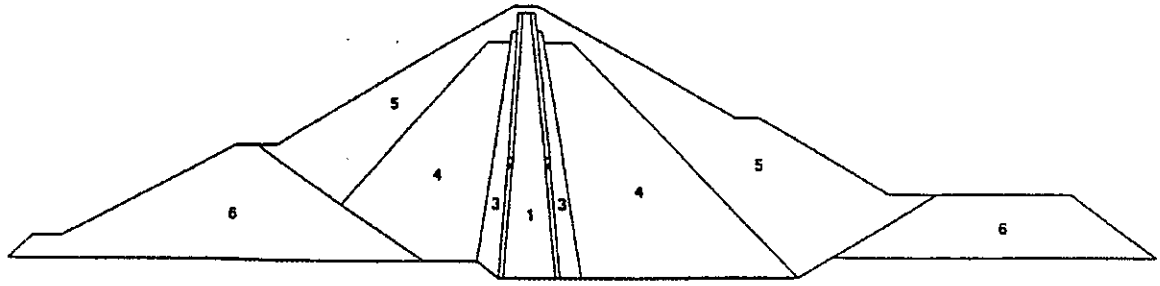

1. Impervious clay core
2. Filters (sand)
3. Transition Zone
4. Inner Shoulder compacted rockfill
5. Outer Shoulder dumped rockfill
6. Cofferdams (integrated) dumped rockfill

Fig. 1: 3rd Benchmark Workshop - Theme B2
Material property zones

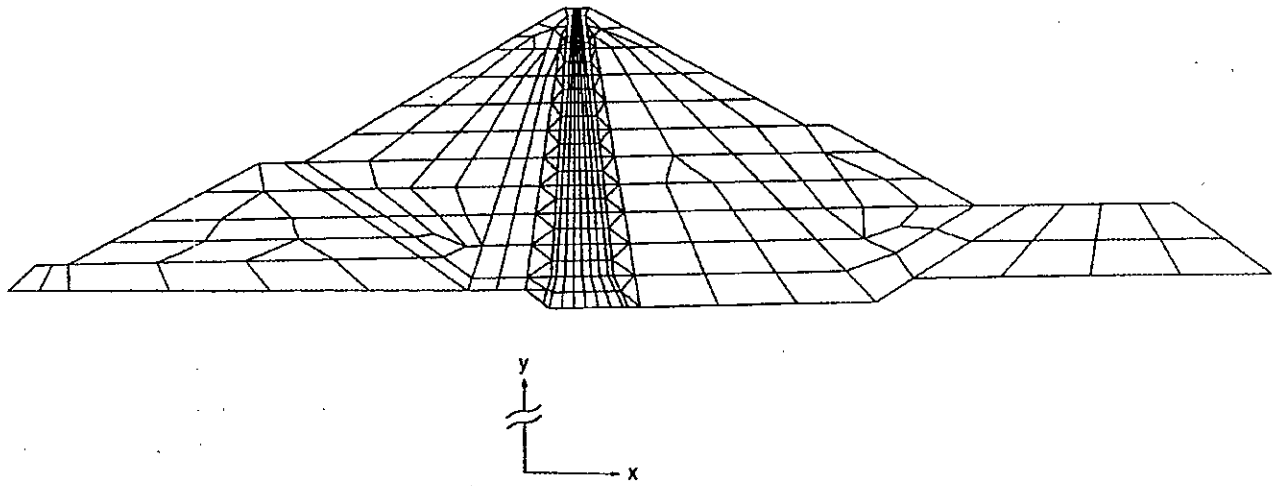

Fig. 2: 3rd Benchmark Workshop - Theme B2
Finite element mesh

Simulation of cyclic undrained triaxial test

$\sigma 3$=0.1 (MPa)

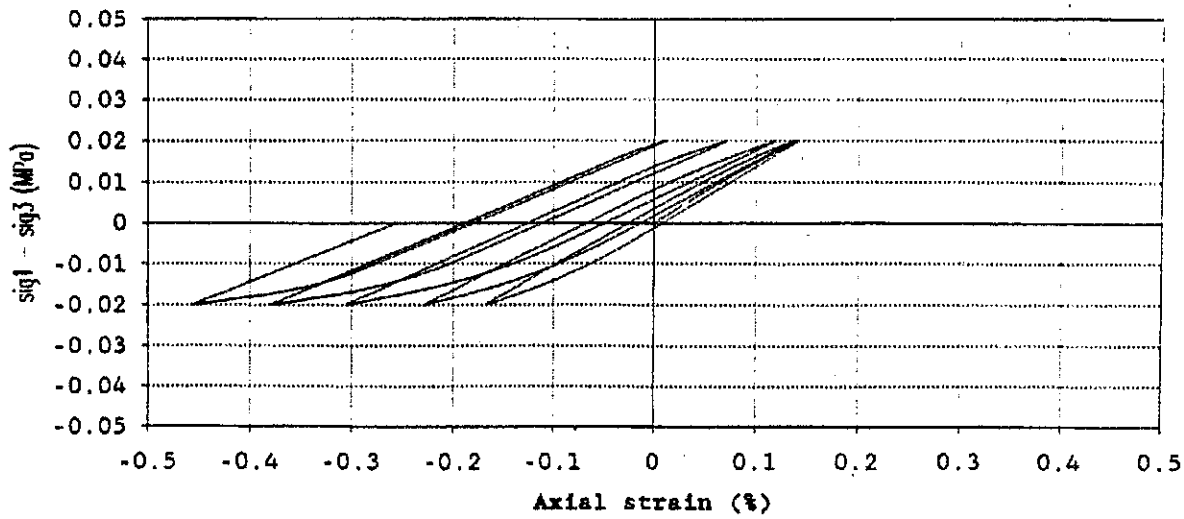

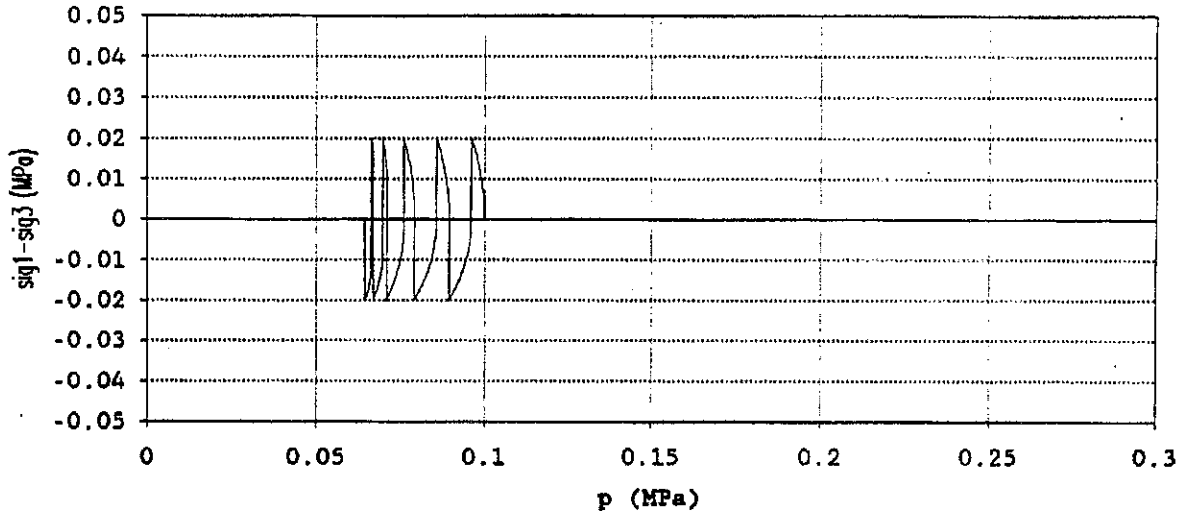

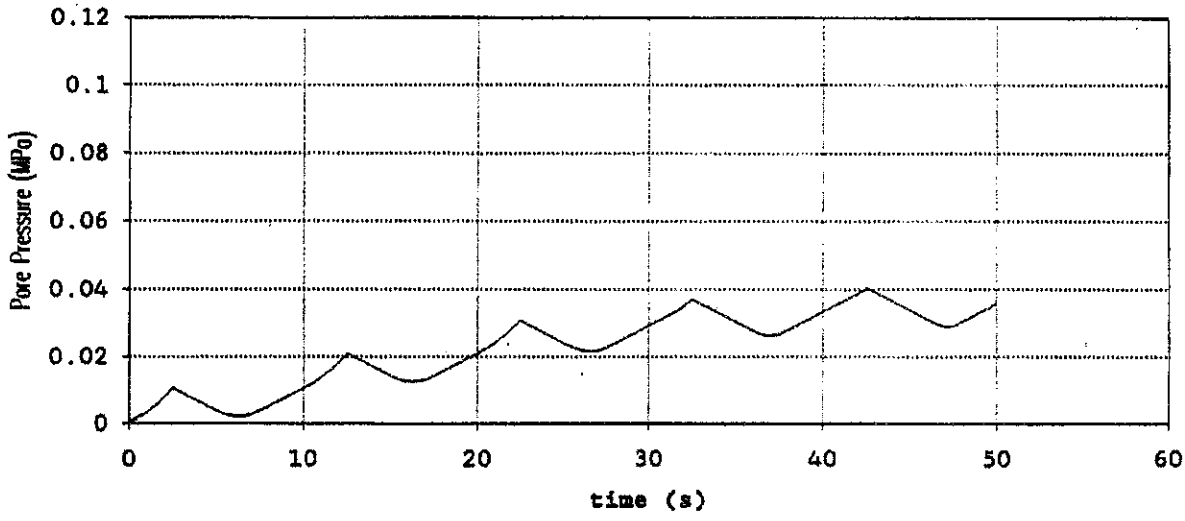

Fig. 3

Simulation of cyclic undrained triaxial test

$\sigma 3 = 0.3$(MPa)

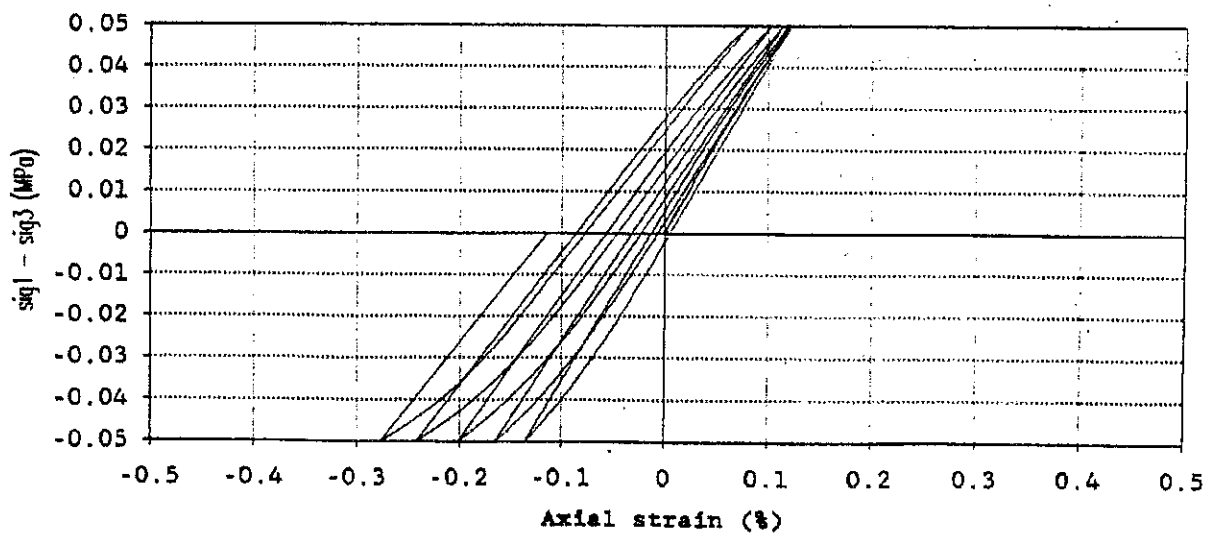

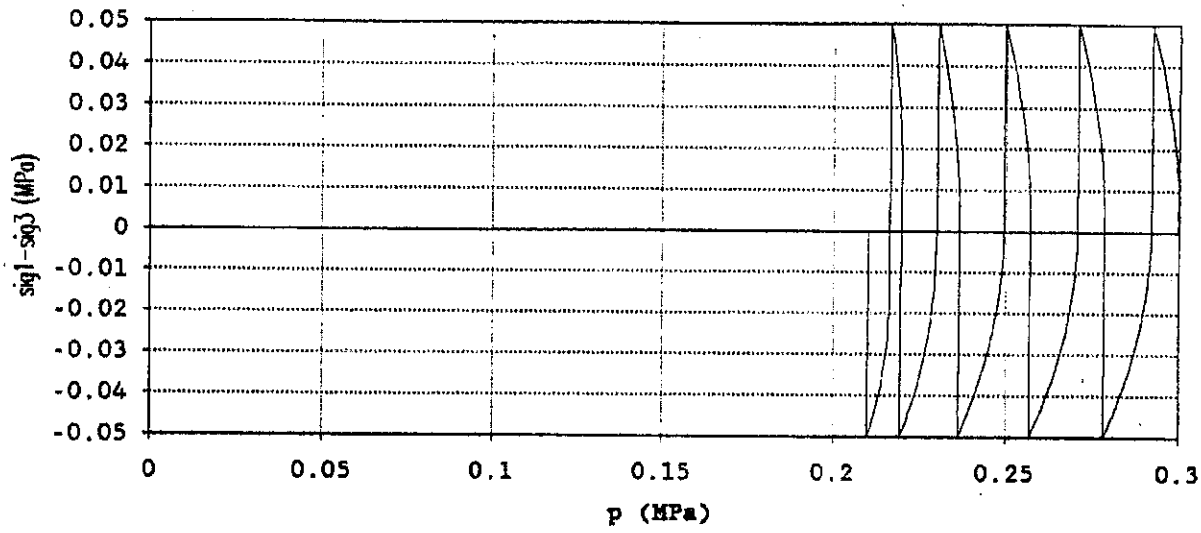

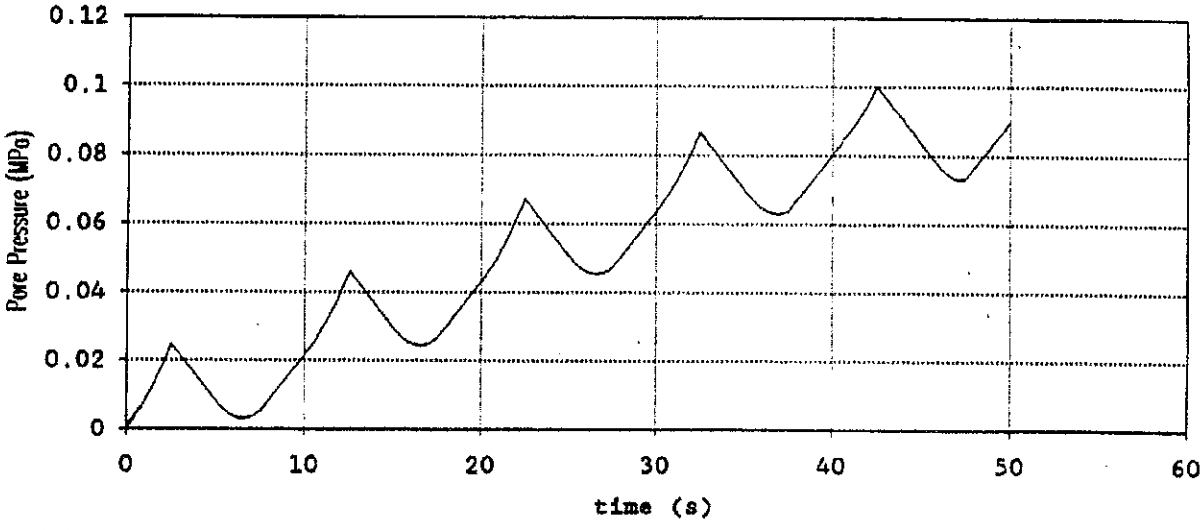

Fig. 4

3rd. ICOLD 1994 - DYNAMIC ANALYSIS OF AN EMBANKMENT DAM

EQ1 earthquake considering only horizontal component - Sensibility analysis

ACCELERATION IN X DIRECTION VS TIME

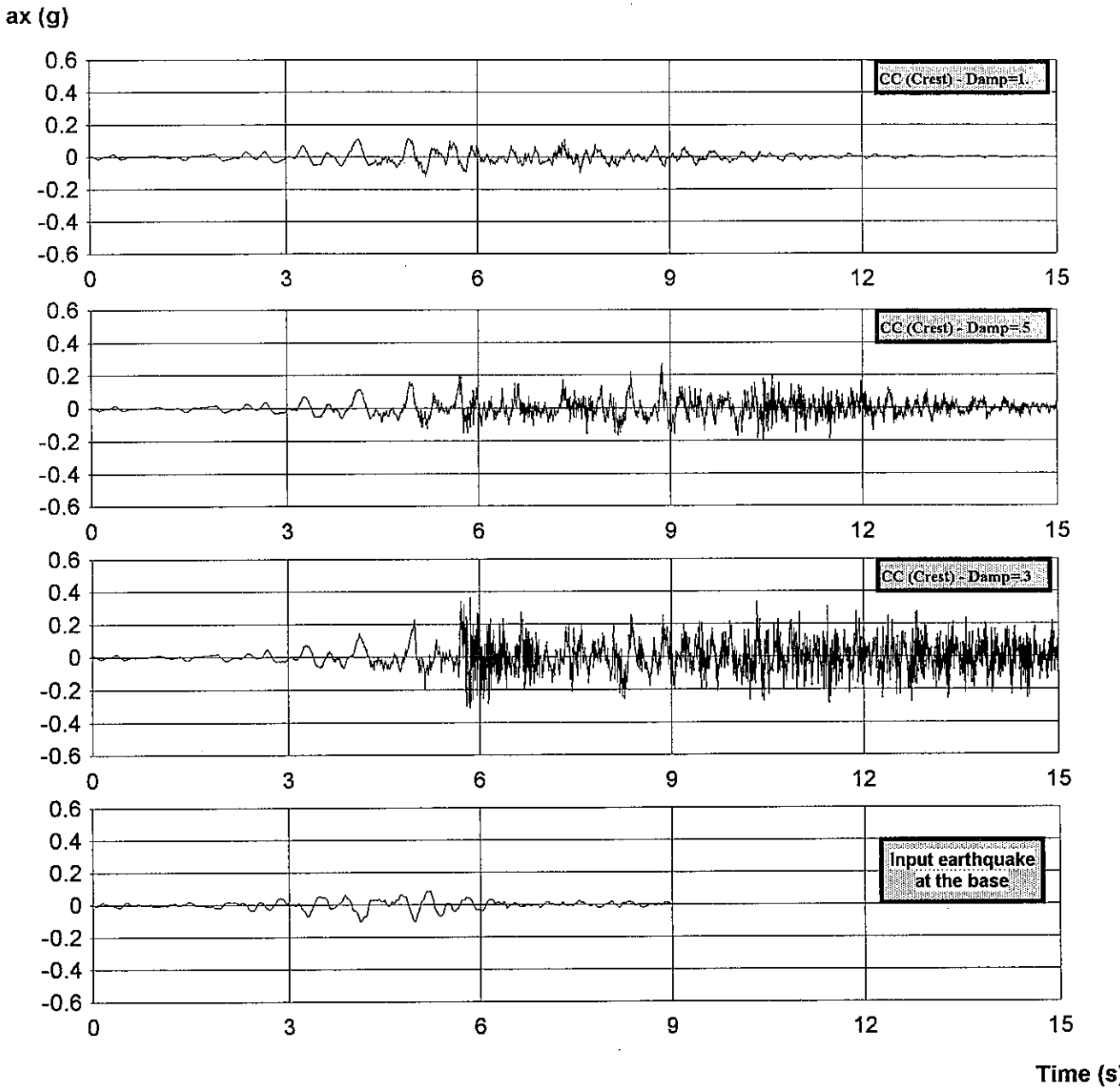

Fig. 5

EQ1 earthquake considering only horizontal component

ACCELERATION IN X DIRECTION VS TIME

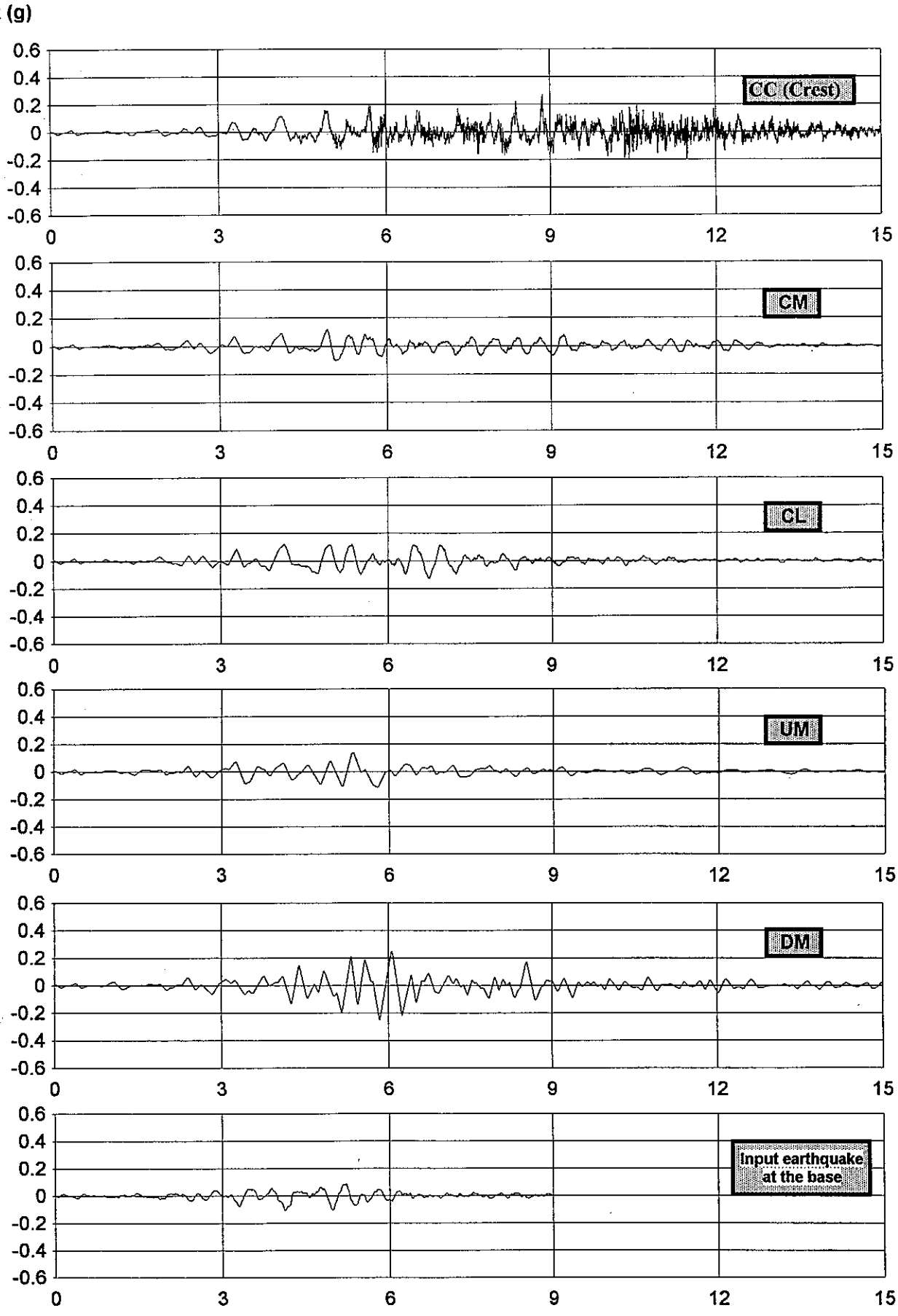

Fig. 6

EQ1 earthquake considering only horizontal component

ACCELERATION IN Y DIRECTION VS TIME

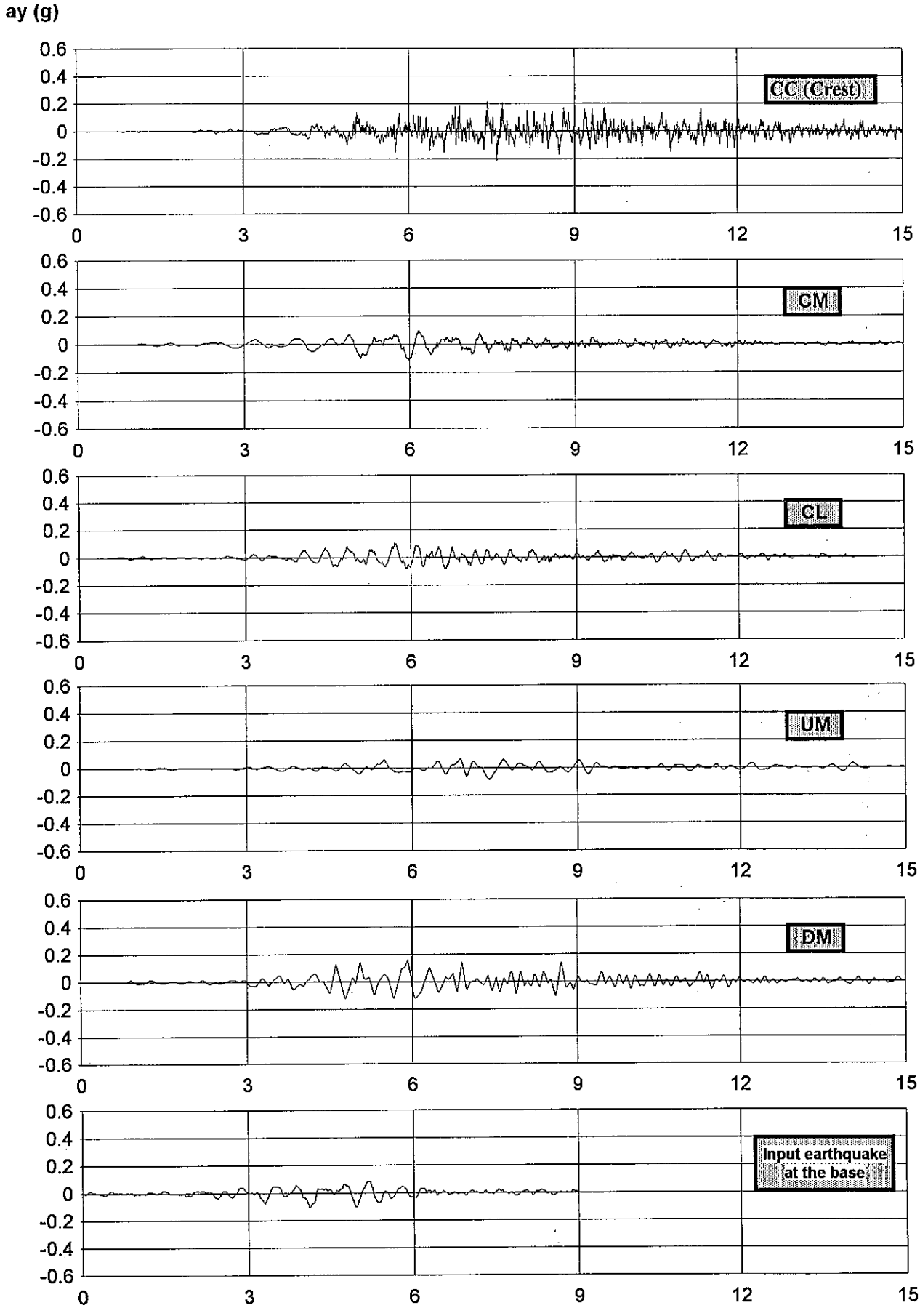

Fig. 7

3rd. ICOLD 1994 - DYNAMIC ANALYSIS OF AN EMBANKMENT DAM

EQ1 earthquake considering only horizontal component

HORIZZONTAL DISPLACEMENTS VS TIME

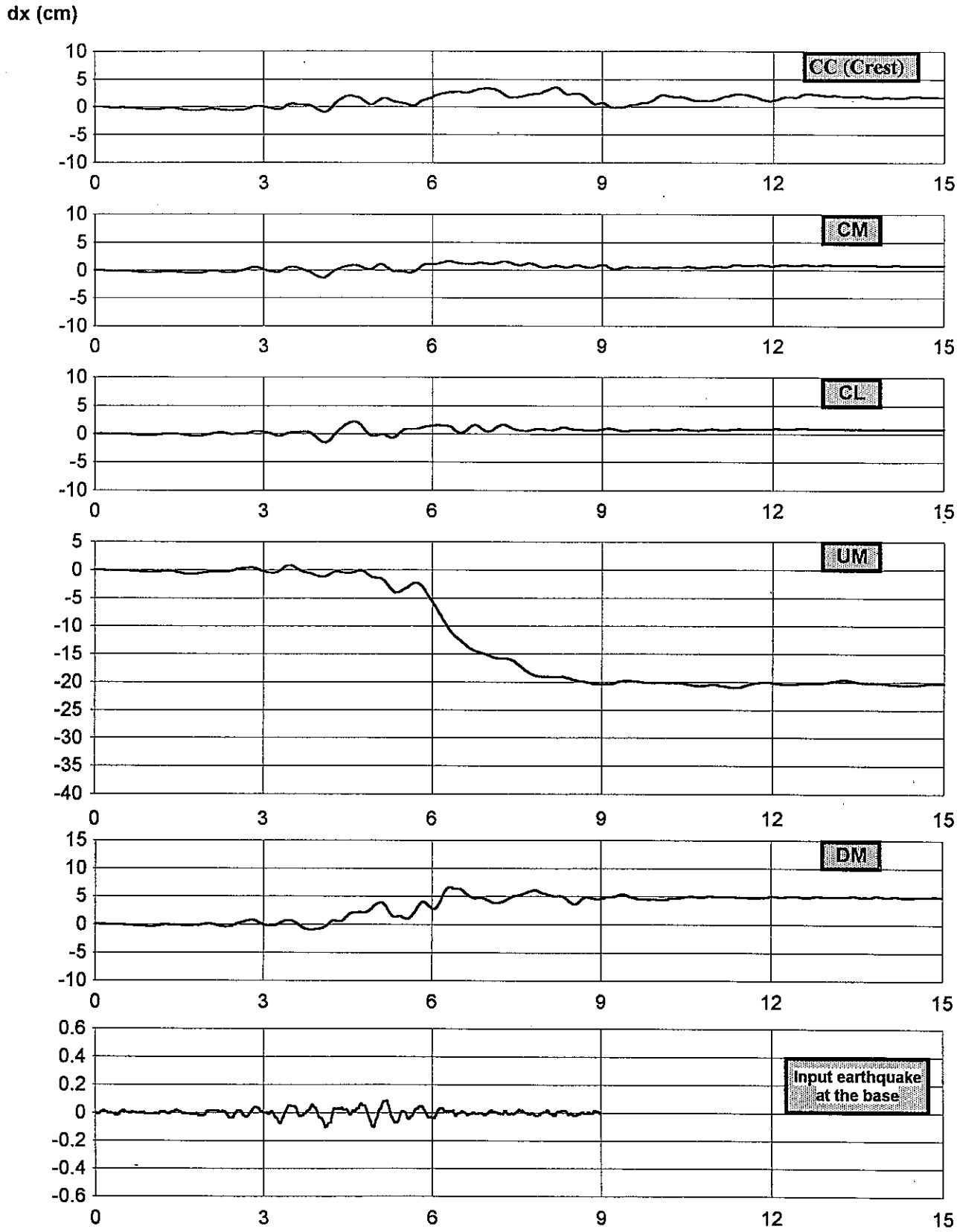

Fig. 8

3rd. ICOLD 1994 - DYNAMIC ANALYSIS OF AN EMBANKMENT DAM

EQ1 earthquake considering only horizontal component

VERTICAL DISPLACEMENTS VS TIME

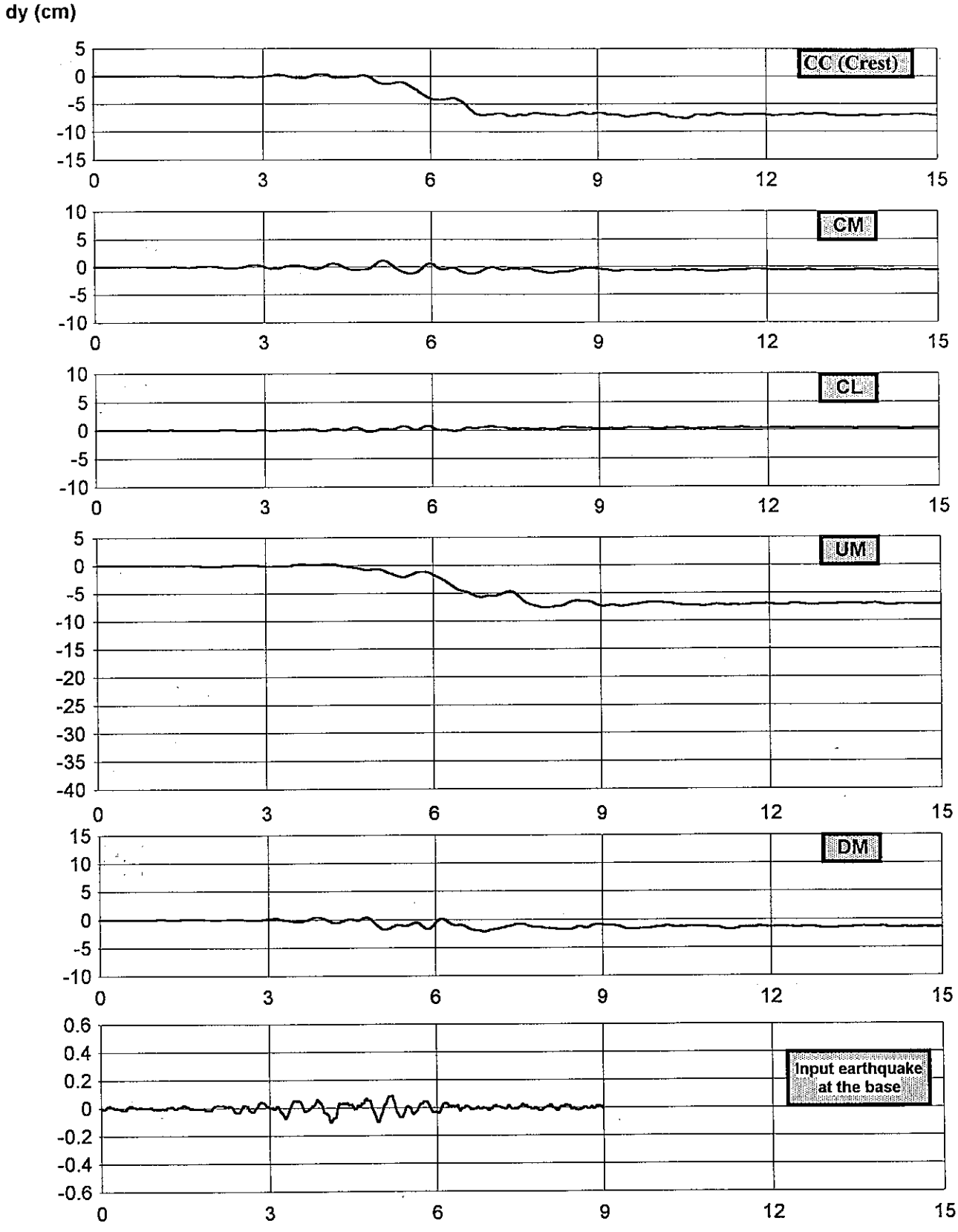

Fig. 9

3rd. ICOLD 1994 - DYNAMIC ANALYSIS OF AN EMBANKMENT DAM

EQ1 earthquake considering only horizontal component

EXCESS PORE WATER PRESSURE VS TIME

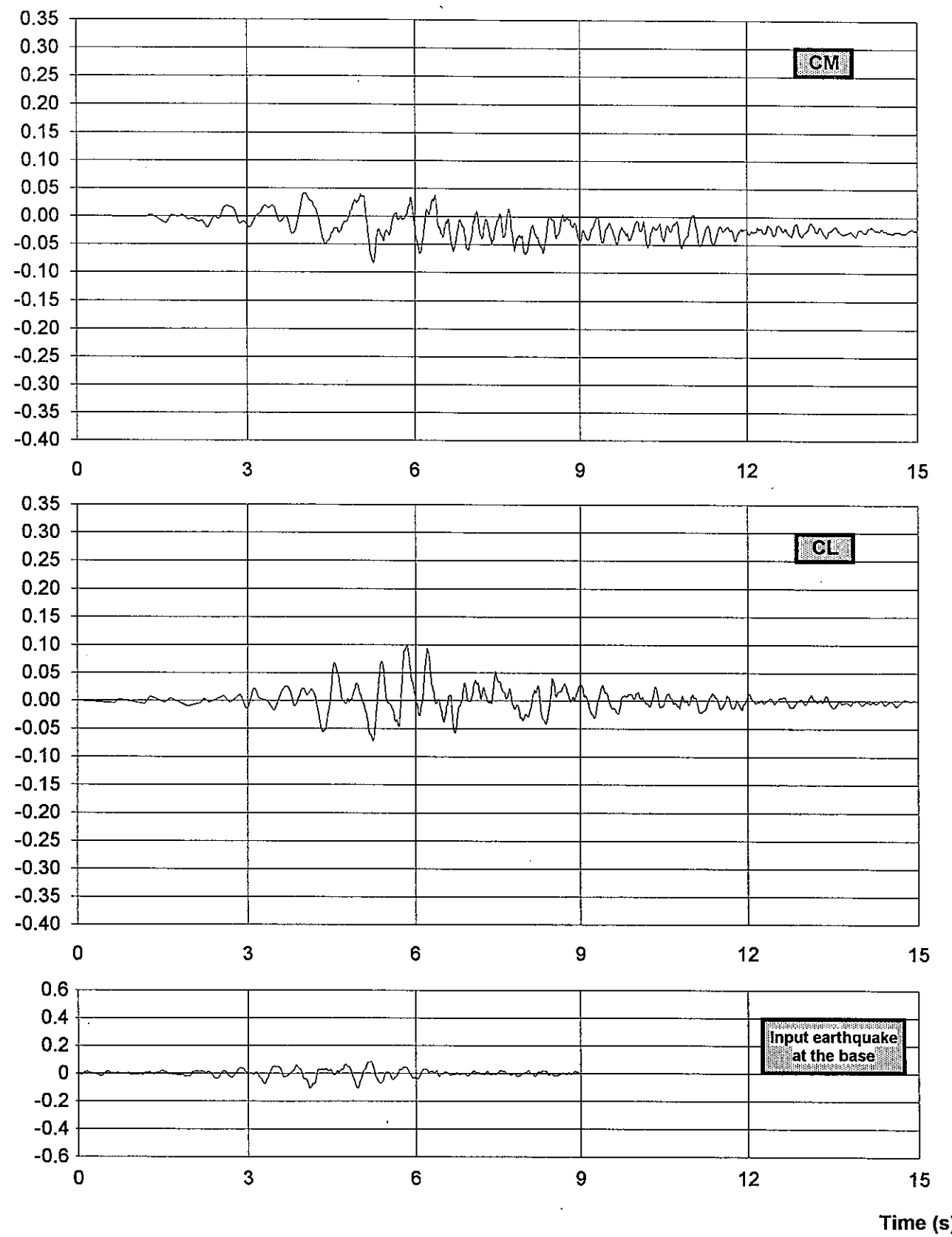

Fig. 10

3rd. ICOLD 1994 - DYNAMIC ANALYSIS OF AN EMBANKMENT DAM

EQ1 earthquake considering horizontal and vertical components

ACCELERATION IN X DIRECTION VS TIME

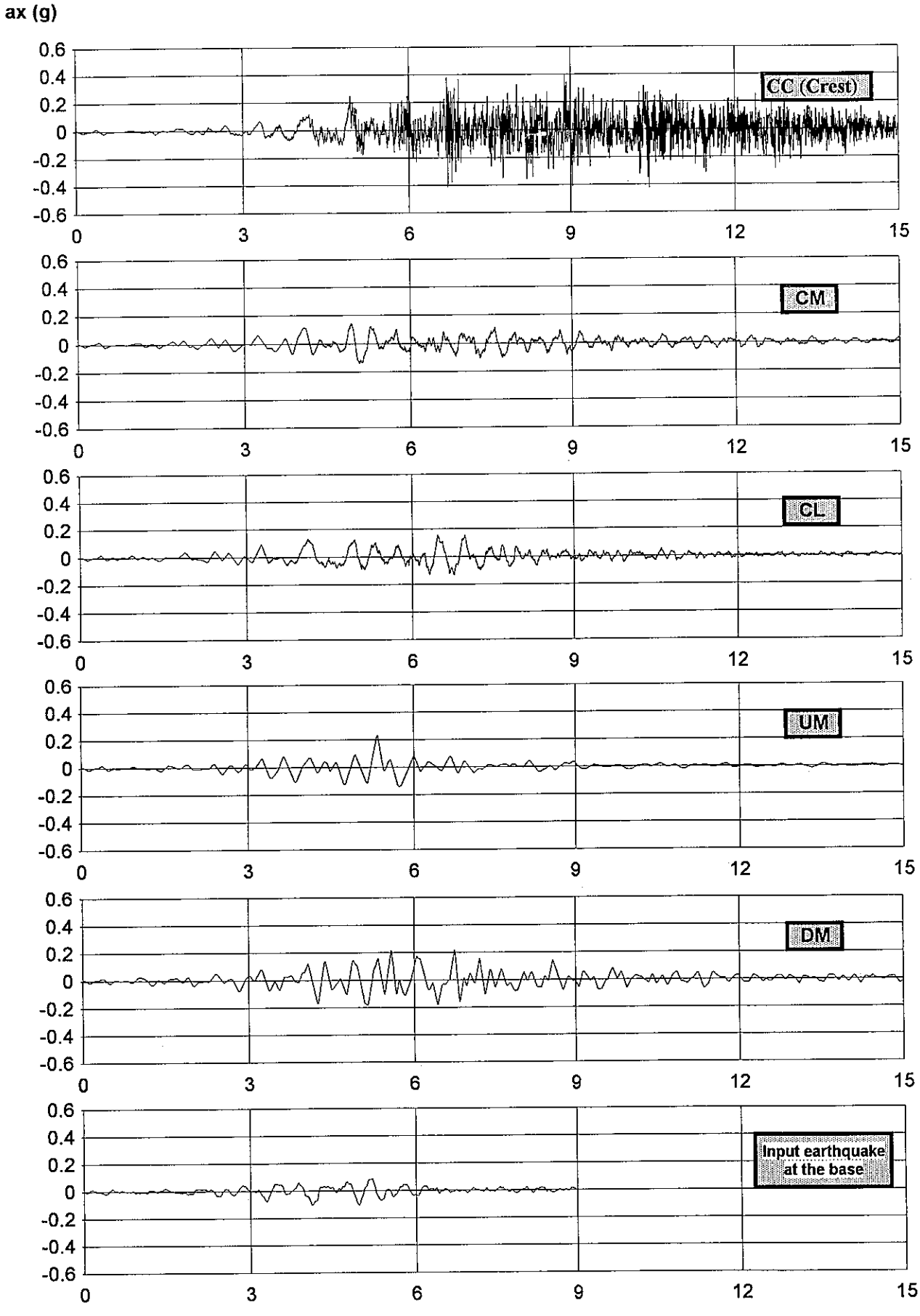

Fig. 11

3rd. ICOLD 1994 - DYNAMIC ANALYSIS OF AN EMBANKMENT DAM

EQ1 earthquake considering horizontal and vertical components

ACCELERATION IN Y DIRECTION VS TIME

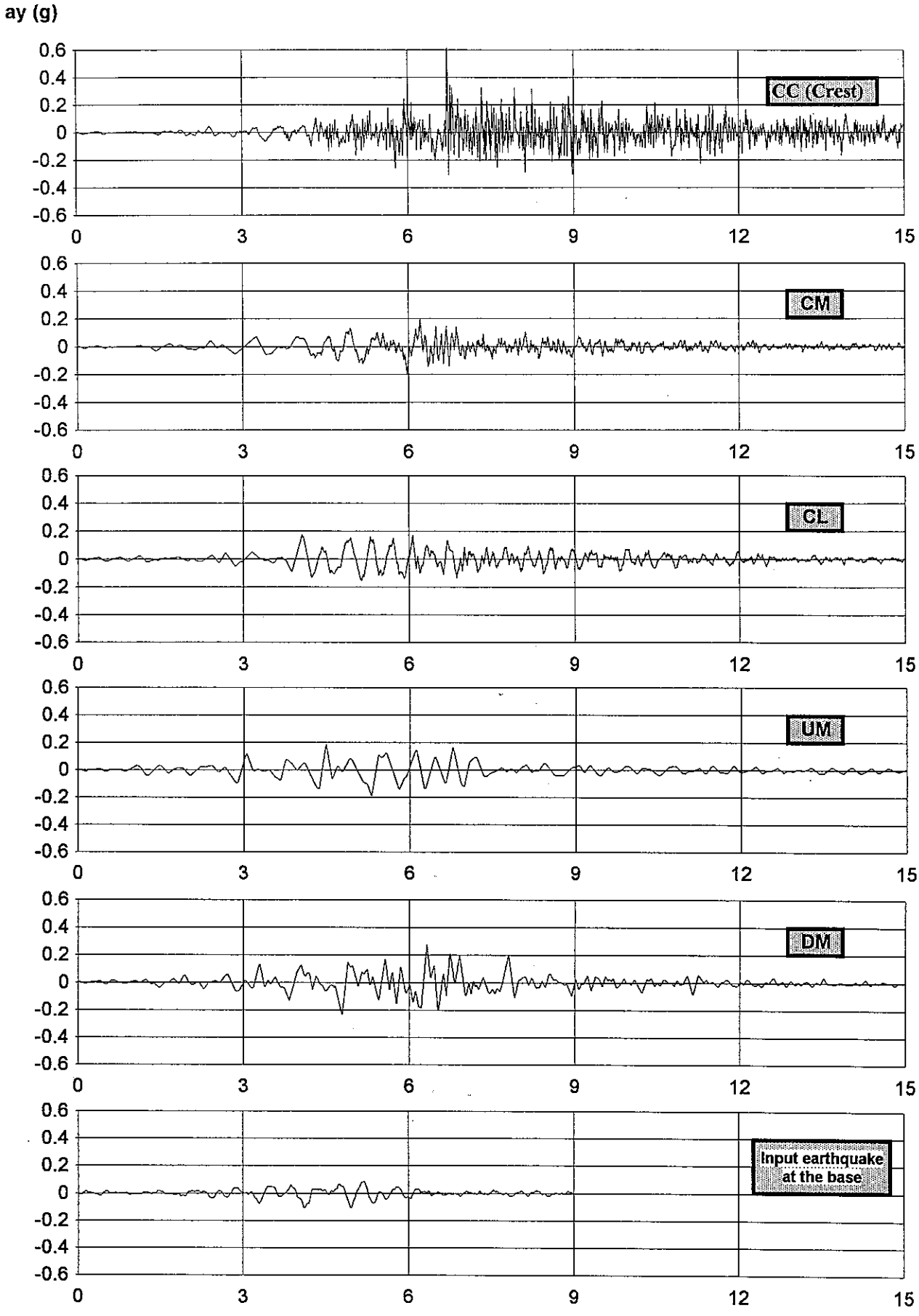

Fig. 12

3rd. ICOLD 1994 - DYNAMIC ANALYSIS OF AN EMBANKMENT DAM

EQ1 earthquake considering horizontal and vertical components

HORIZZONTAL DISPLACEMENTS VS TIME

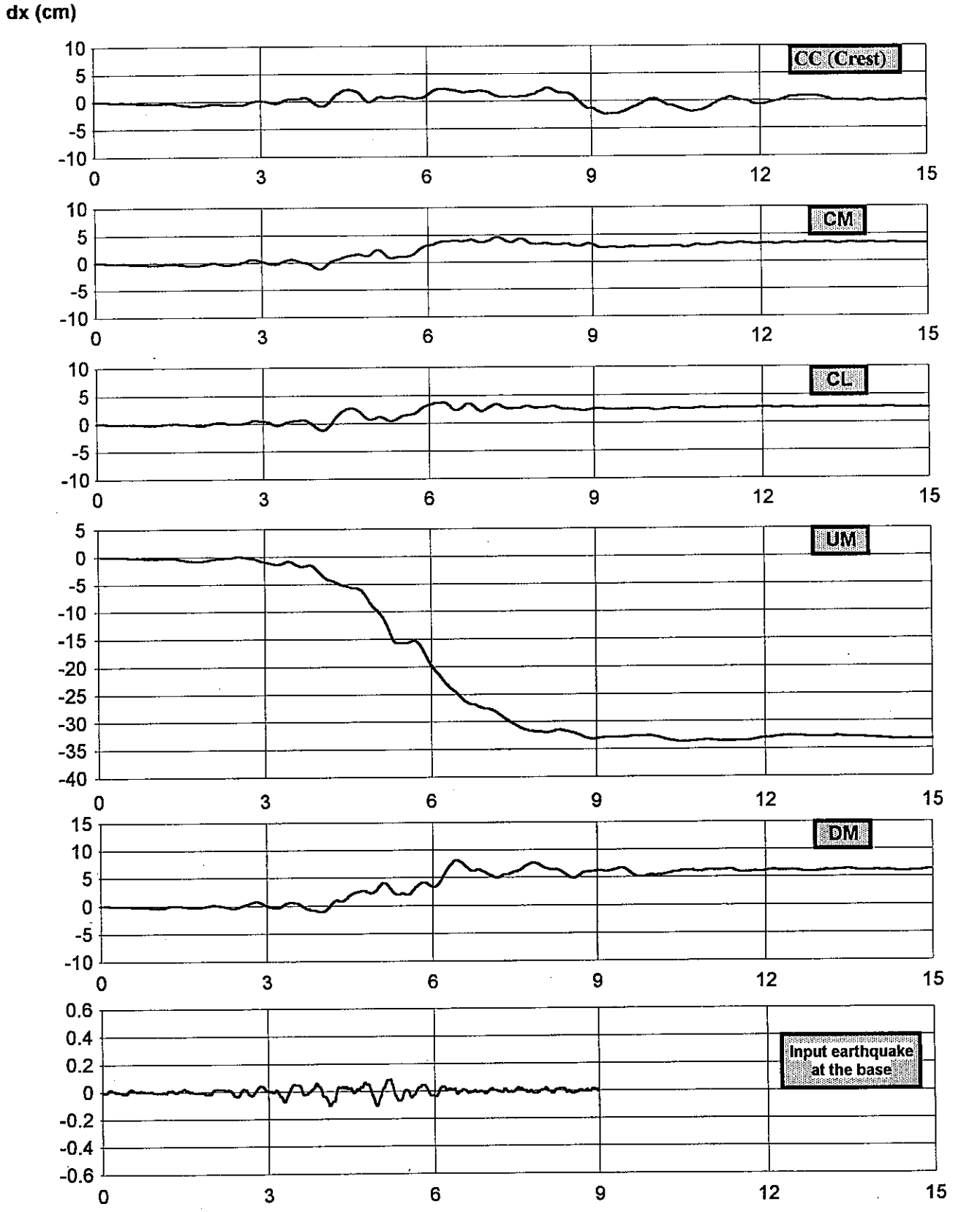

Fig. 13

3rd. ICOLD 1994 - DYNAMIC ANALYSIS OF AN EMBANKMENT DAM

EQ1 earthquake considering horizontal and vertical components

VERTICAL DISPLACEMENTS VS TIME

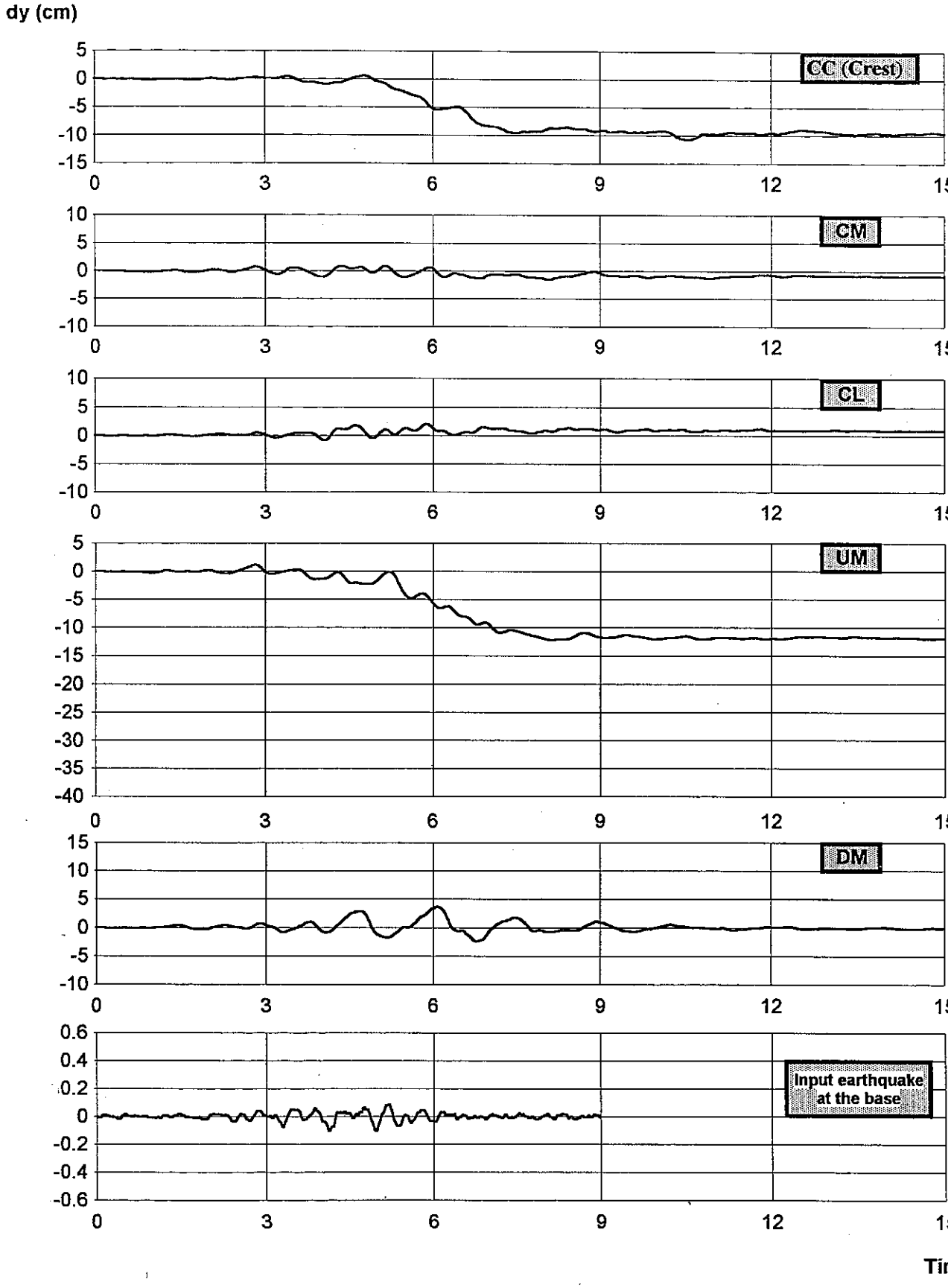

Fig. 14

3rd. ICOLD 1994 - DYNAMIC ANALYSIS OF AN EMBANKMENT DAM

EQ1 earthquake considering horizontal and vertical components

EXCESS PORE WATER PRESSURE VS TIME

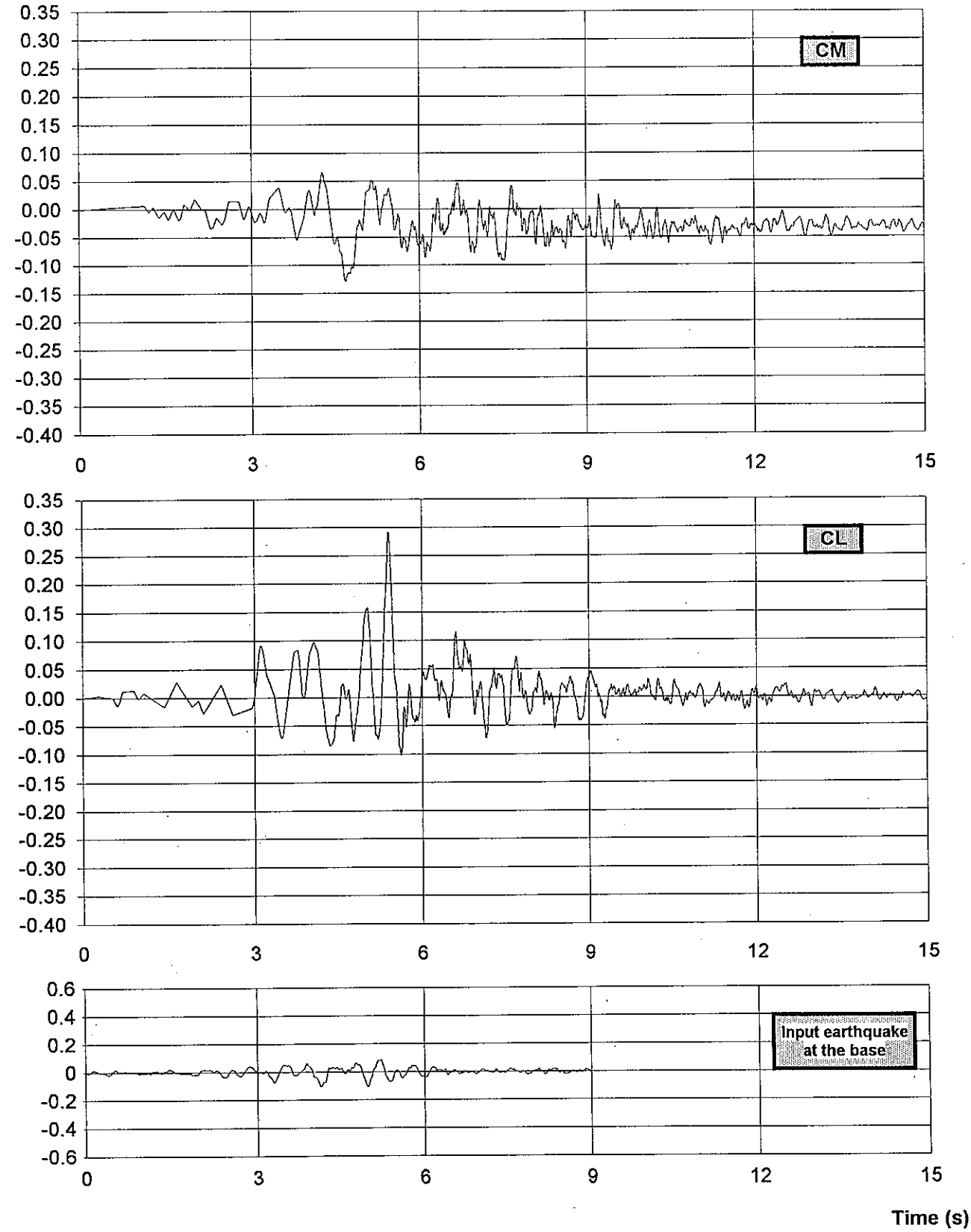

Fig. 15

3rd. ICOLD 1994 - DYNAMIC ANALYSIS OF AN EMBANKMENT DAM

EQ2 earthquake considering only horizontal component

ACCELERATION IN X DIRECTION VS TIME

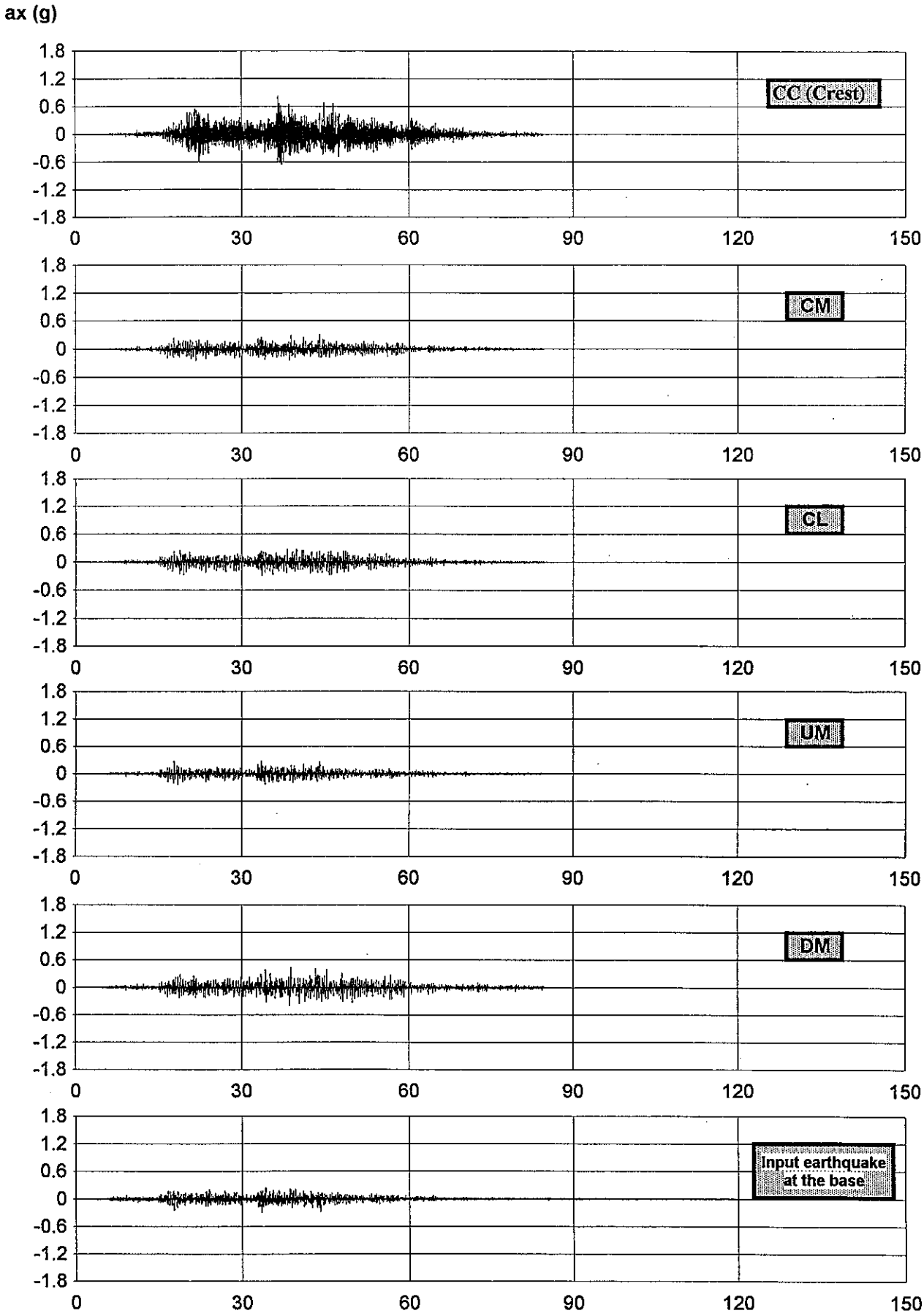

Fig. 16

3rd. ICOLD 1994 - DYNAMIC ANALYSIS OF AN EMBANKMENT DAM

EQ2 earthquake considering only horizontal component

ACCELERATION IN Y DIRECTION VS TIME

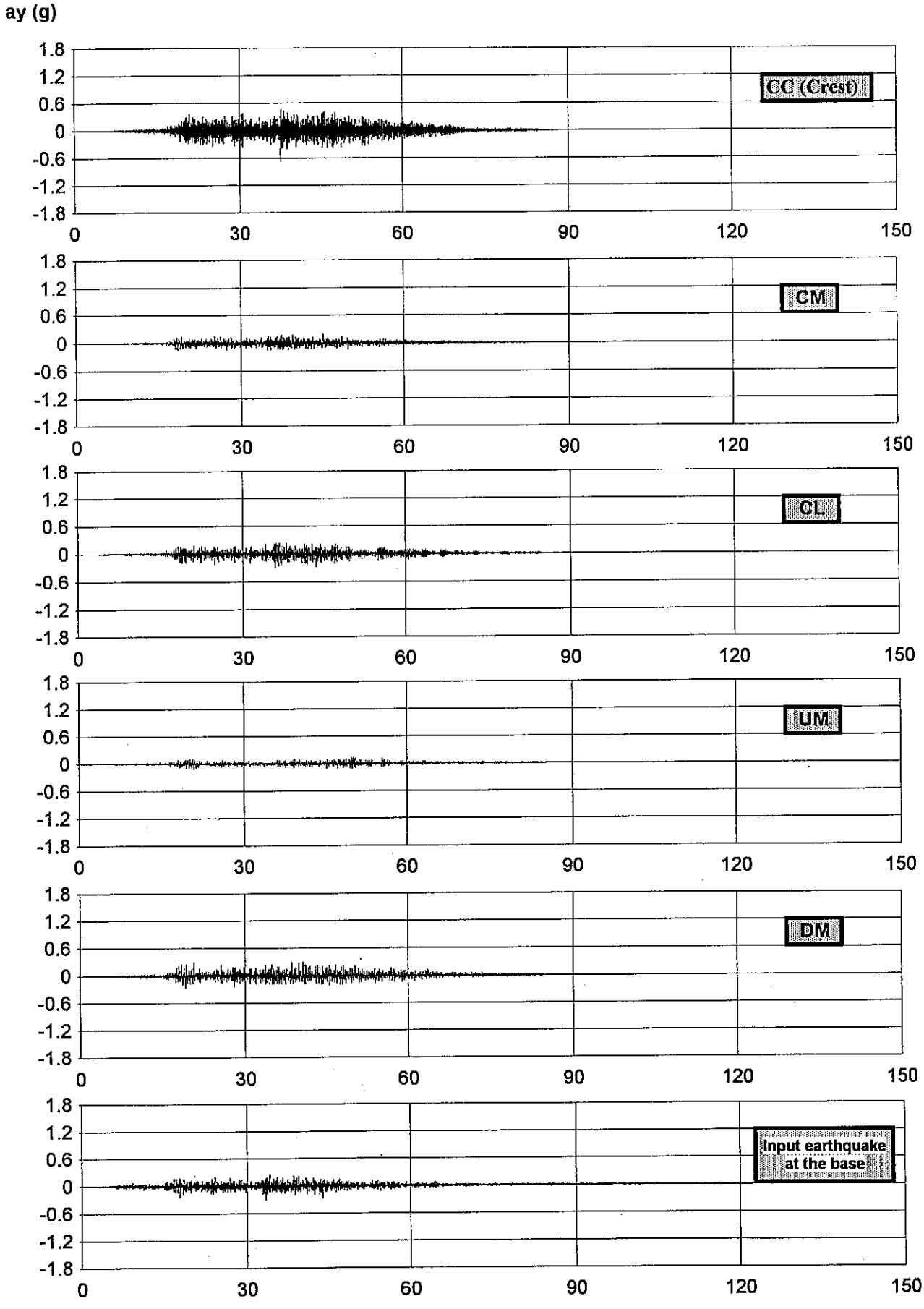

Fig. 17

3rd. ICOLD 1994 - DYNAMIC ANALYSIS OF AN EMBANKMENT DAM

EQ2 earthquake considering only horizontal component

HORIZZONTAL DISPLACEMENTS VS TIME

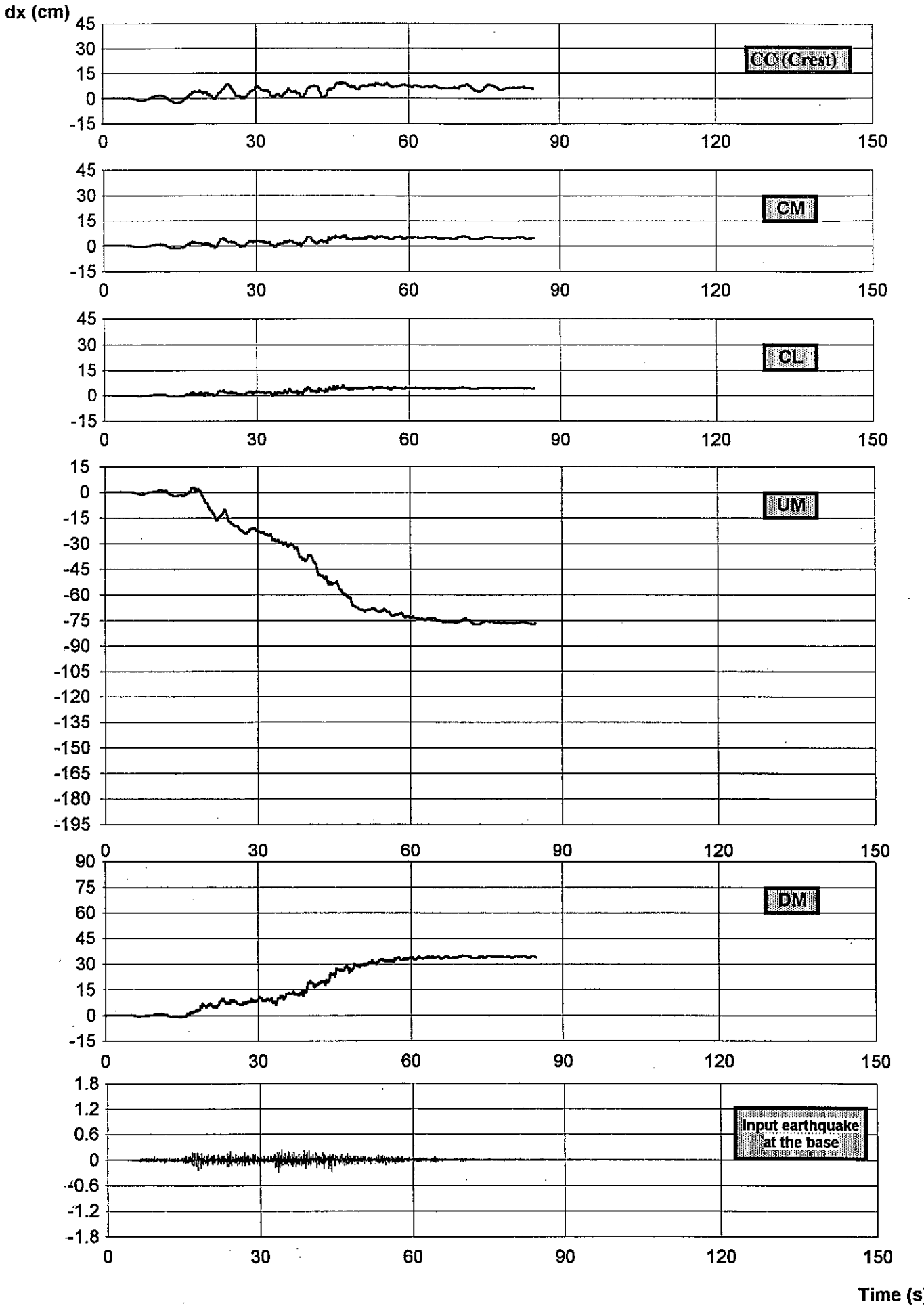

Fig. 18

3rd. ICOLD 1994 - DYNAMIC ANALYSIS OF AN EMBANKMENT DAM

EQ2 earthquake considering horizontal and vertical components

ACCELERATION IN X DIRECTION VS TIME

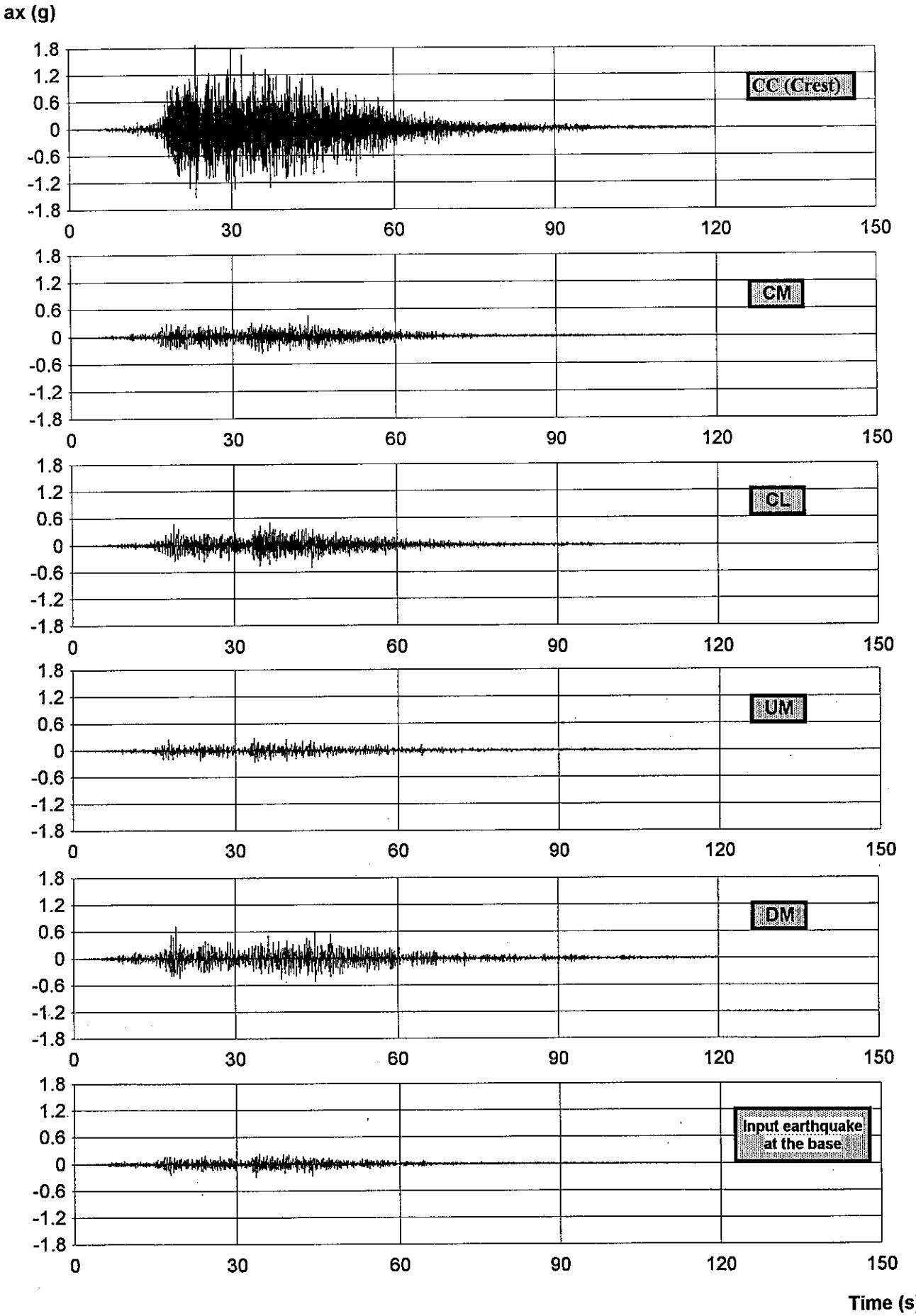

Fig. 21

3rd. ICOLD 1994 - DYNAMIC ANALYSIS OF AN EMBANKMENT DAM

EQ2 earthquake considering horizontal and vertical components

ACCELERATION IN Y DIRECTION VS TIME

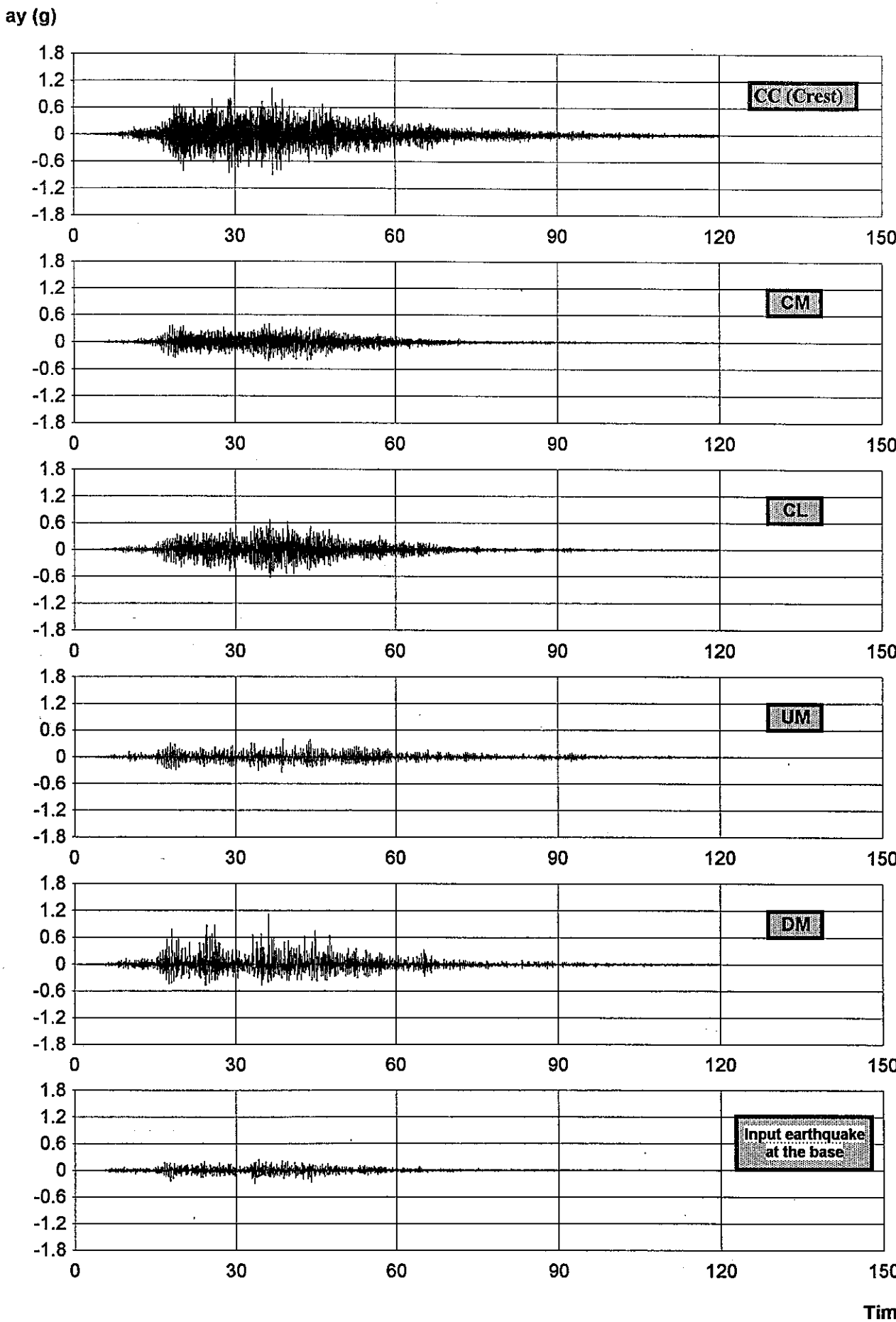

Fig. 22

3rd. ICOLD 1994 - DYNAMIC ANALYSIS OF AN EMBANKMENT DAM

EQ2 earthquake considering horizontal and vertical components

HORIZZONTAL DISPLACEMENTS VS TIME

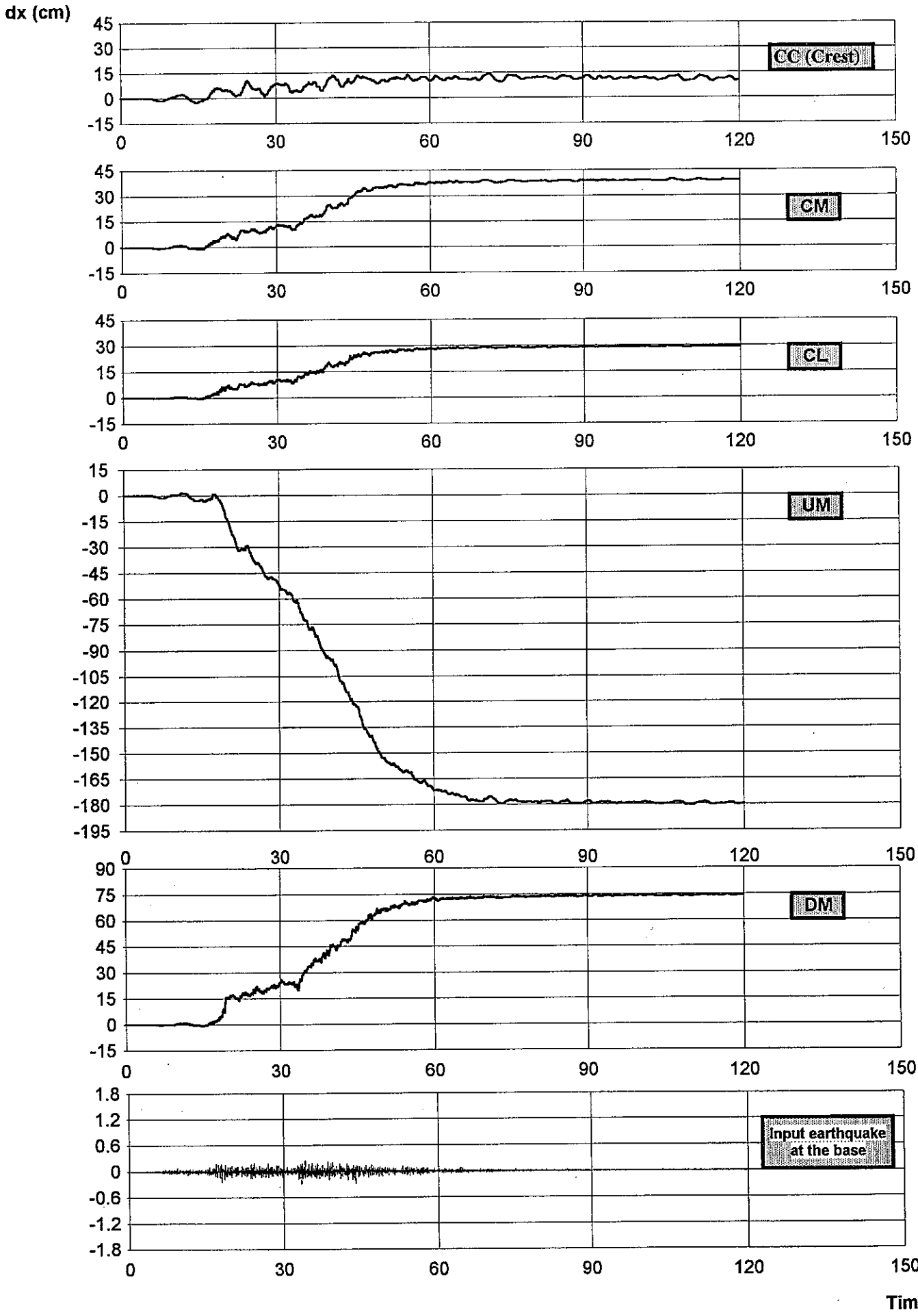

Fig. 23

3rd. ICOLD 1994 - DYNAMIC ANALYSIS OF AN EMBANKMENT DAM

EQ2 earthquake considering horizontal and vertical components

VERTICAL DISPLACEMENTS VS TIME

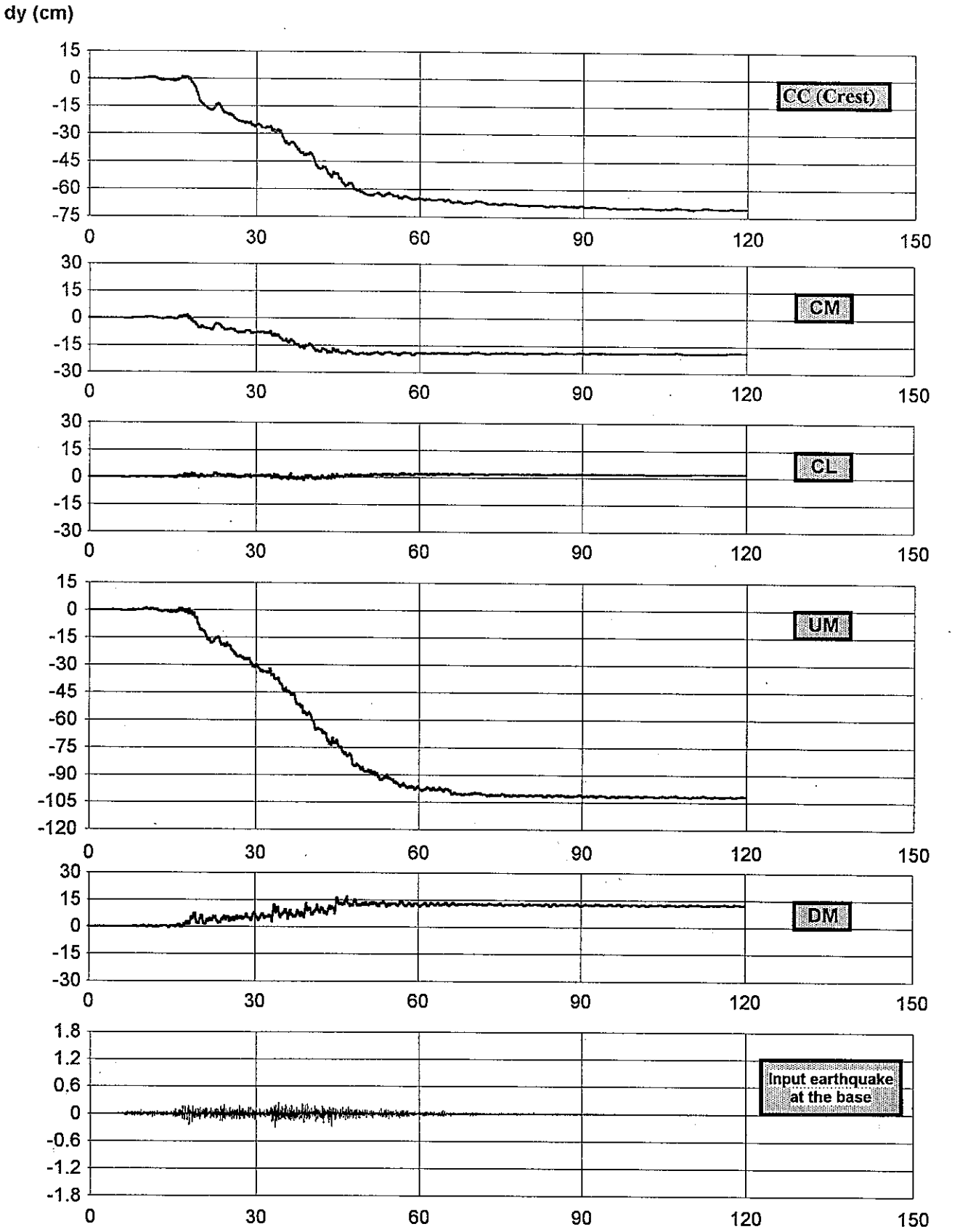

3rd. ICOLD 1994 - DYNAMIC ANALYSIS OF AN EMBANKMENT DAM

EQ2 earthquake considering horizontal and vertical components

EXCESS PORE WATER PRESSURE VS TIME

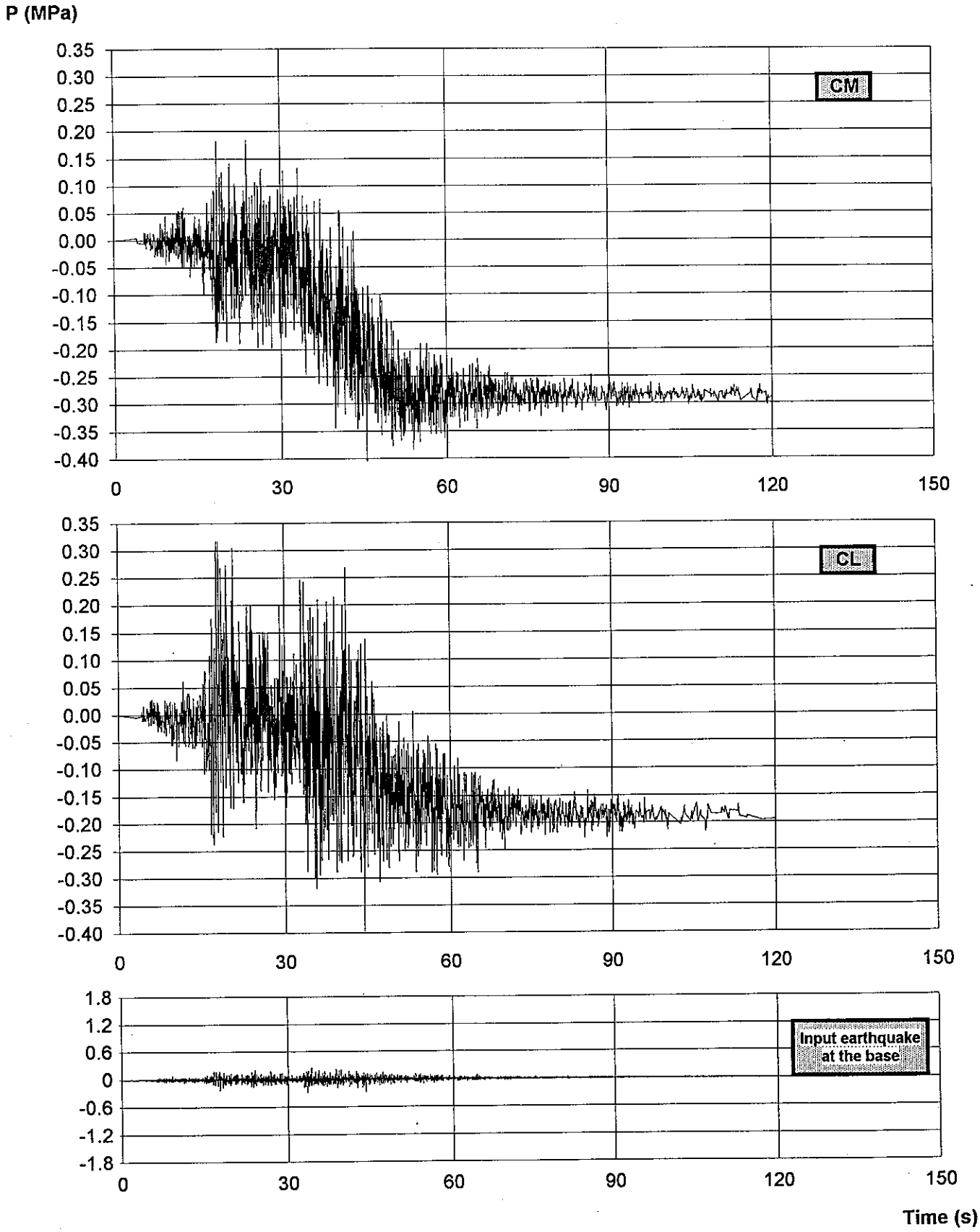

Fig. 25

FOURIER SPECTRUM

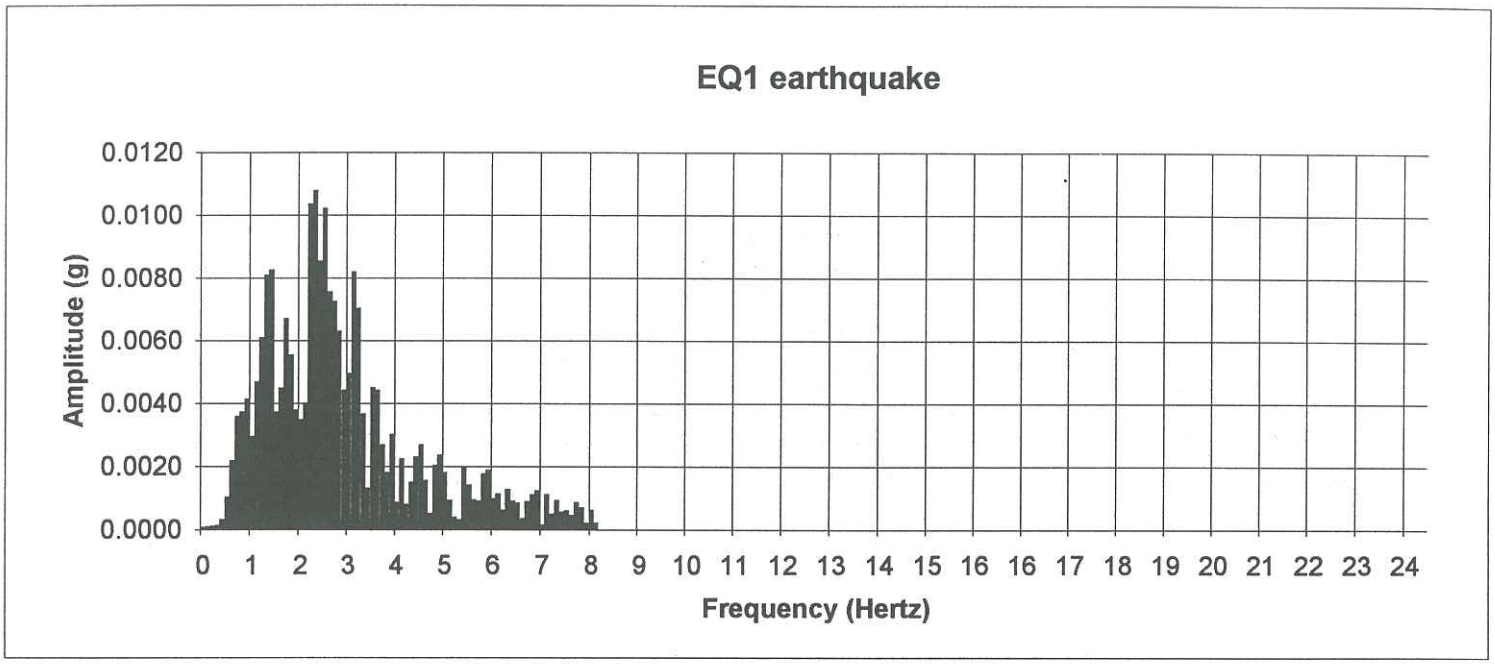

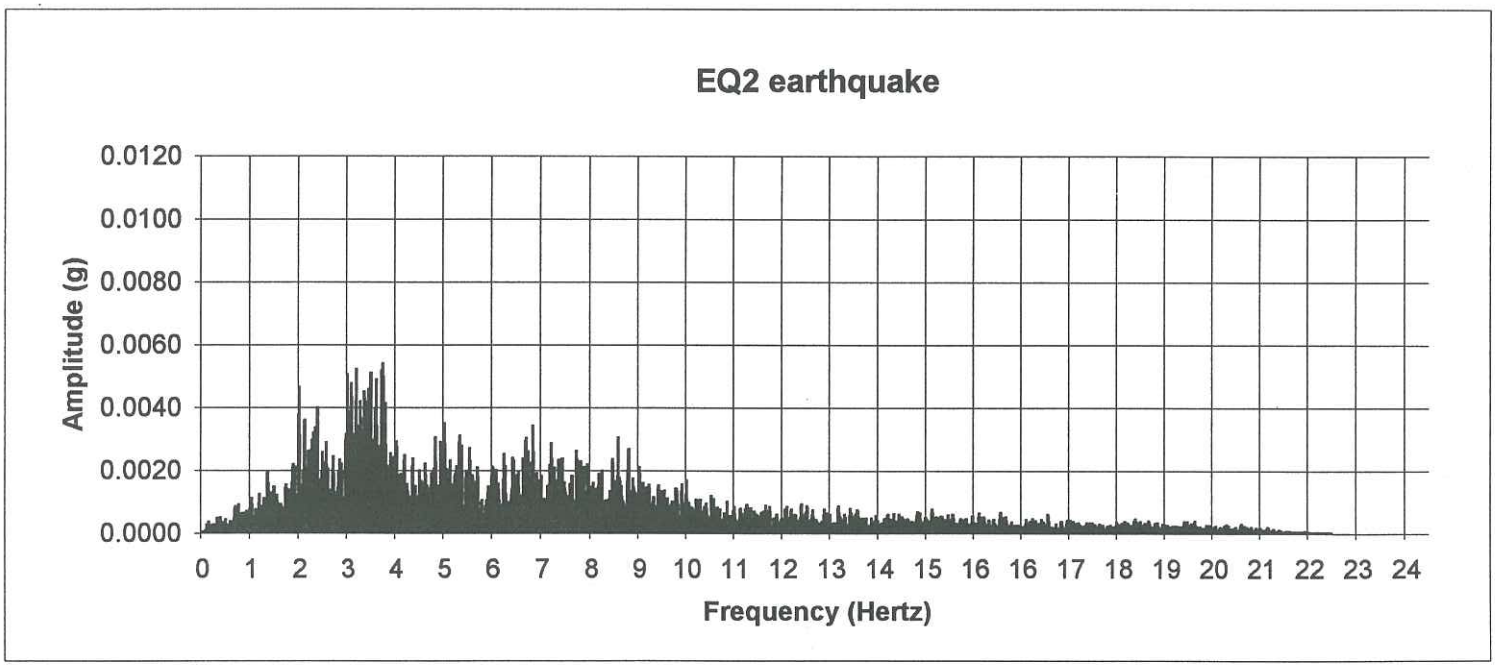

Fig. 26

EQ1 earthquake considering only horizontal component

DEFORMED MESH

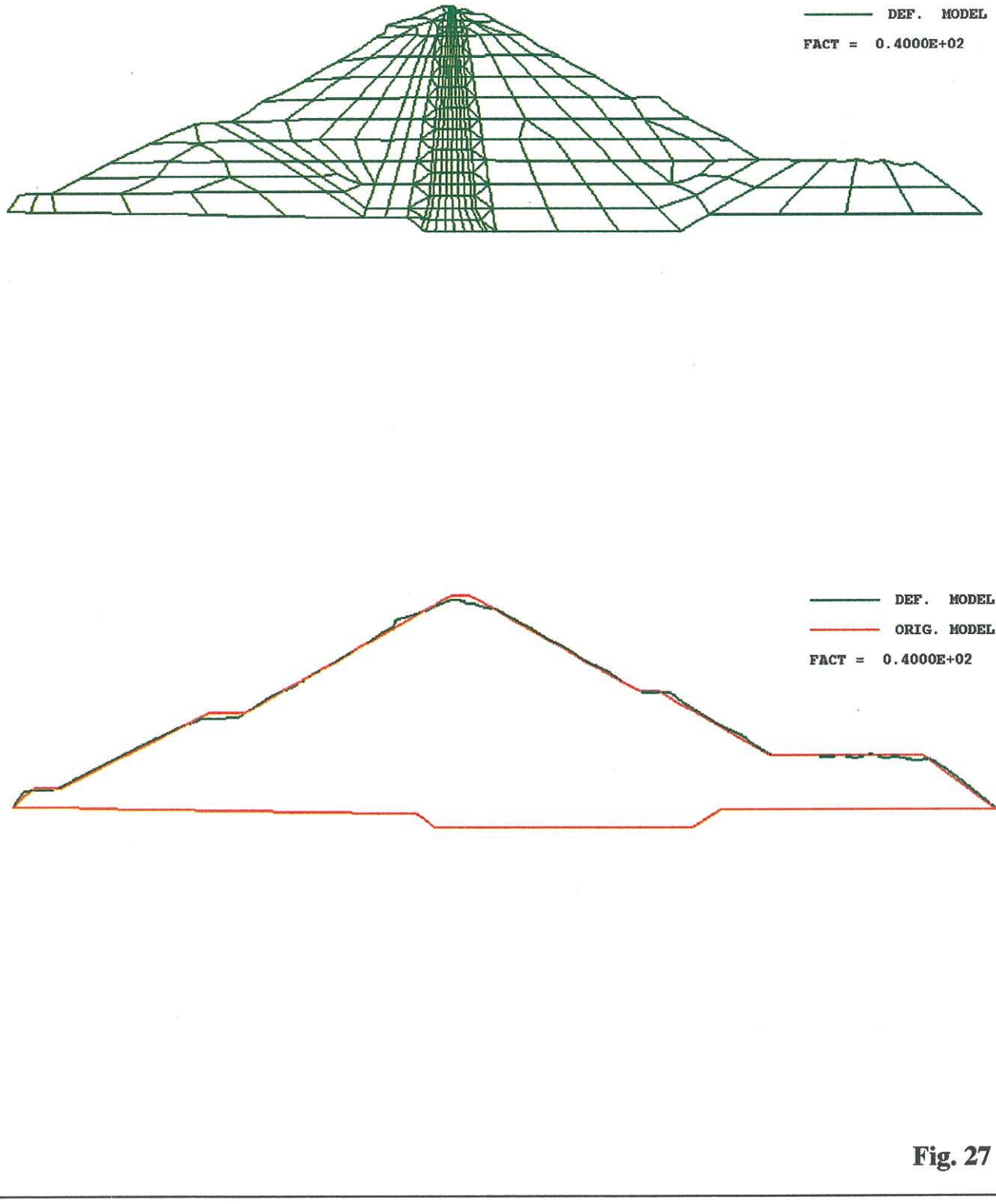

Fig. 27

EQ1 earthquake considering only horizontal component

DISPLACEMENTS

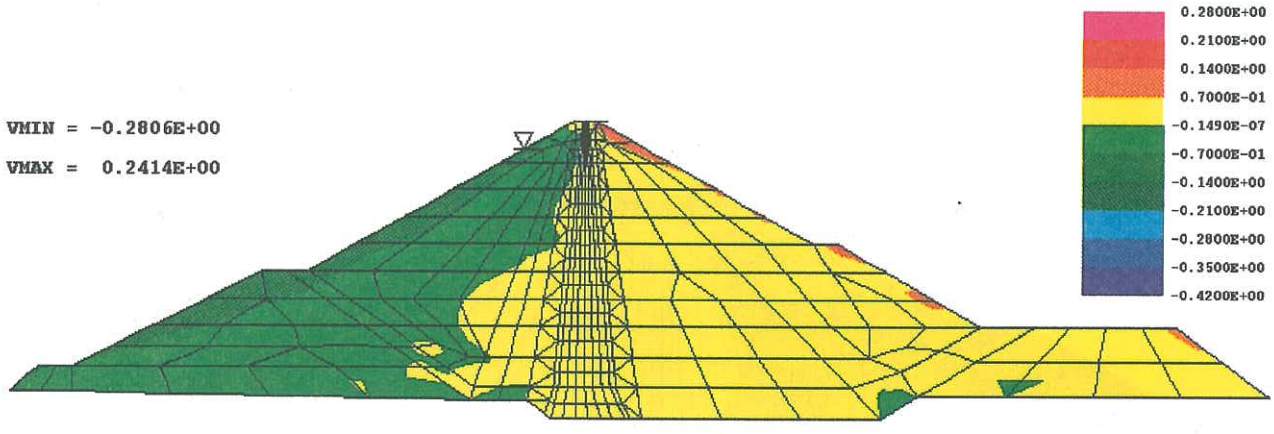

HORIZONTAL DISPLACEMENTS (m)

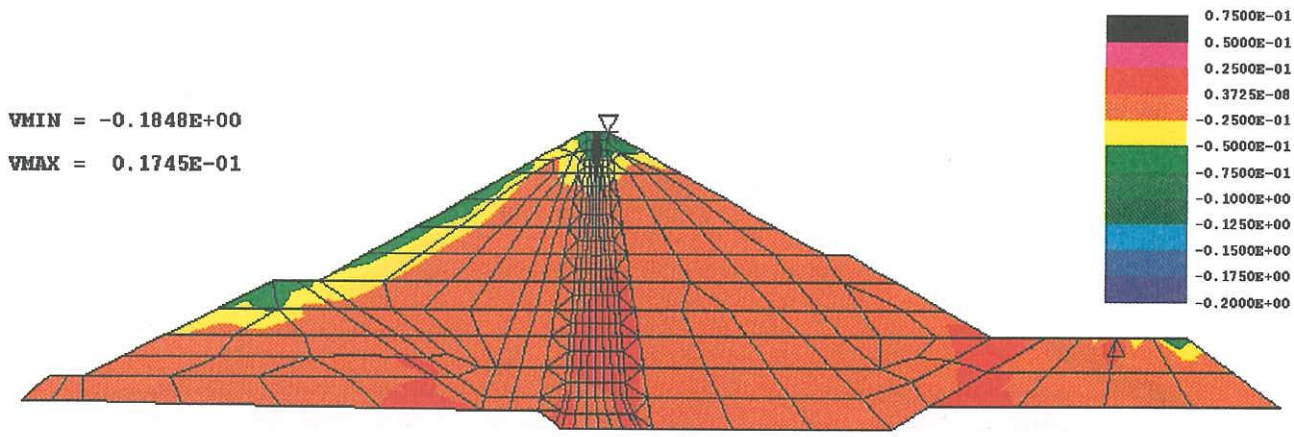

VERTICAL DISPLACEMENTS (m)

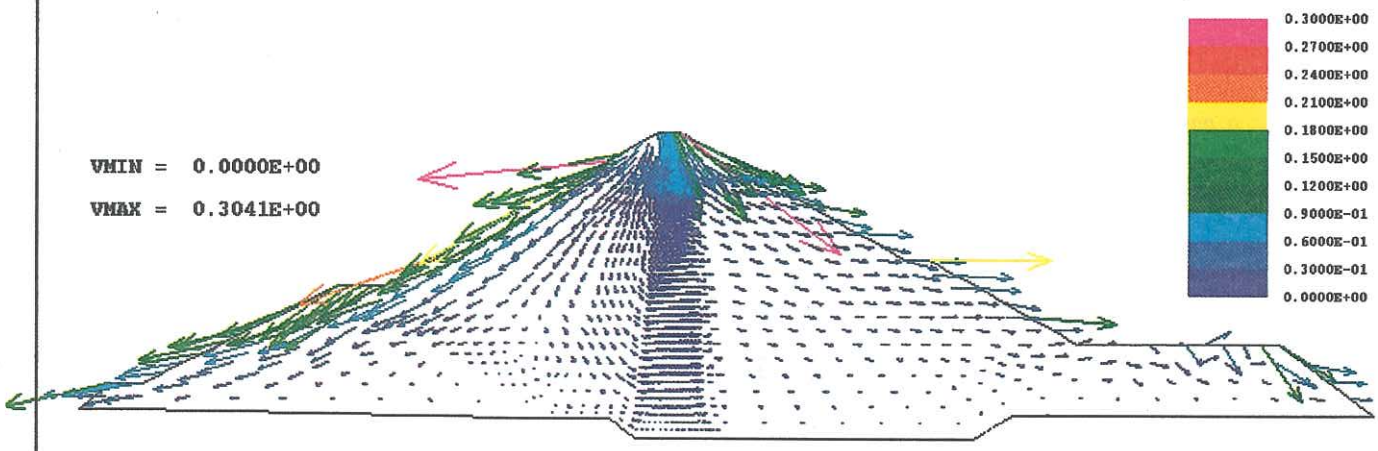

TOTAL DISPLACEMENT VECTORS (m)

Fig. 28

3rd. ICOLD 1994 - DYNAMIC ANALYSIS OF AN EMBANKMENT DAM

EQ1 earthquake considering only horizontal component

DISPLACEMENTS: ZOOM IN THE UPPER PART

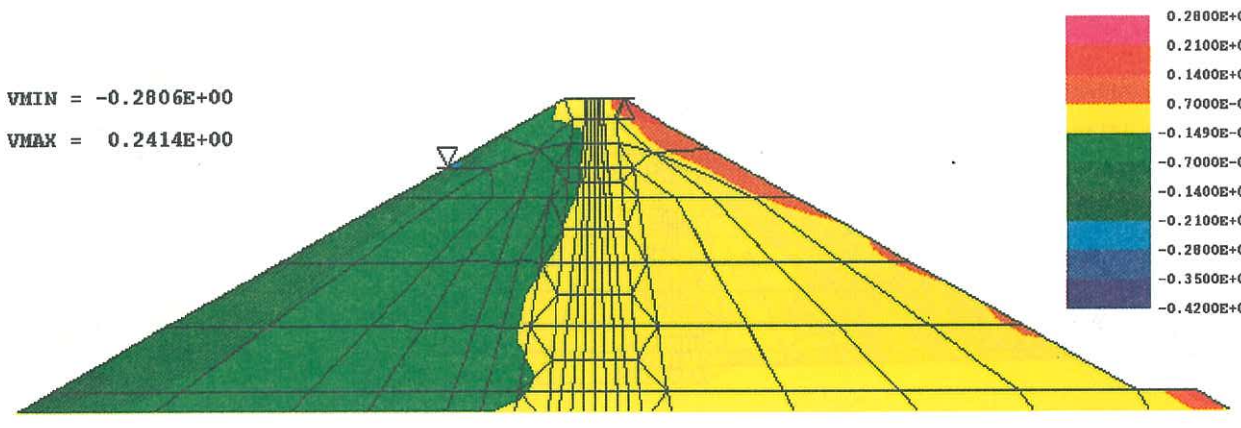

HORIZONTAL DISPLACEMENTS (m)

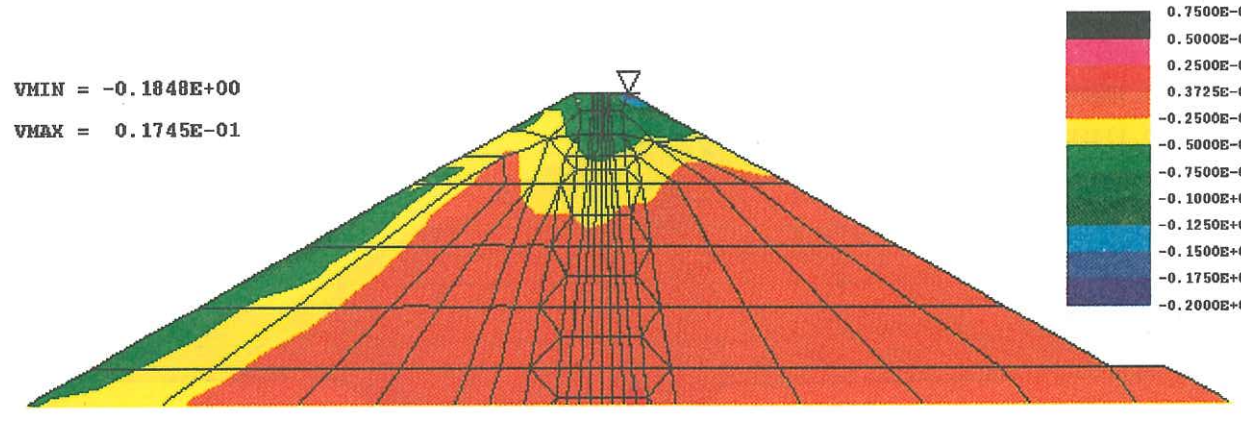

VERTICAL DISPLACEMENTS (m)

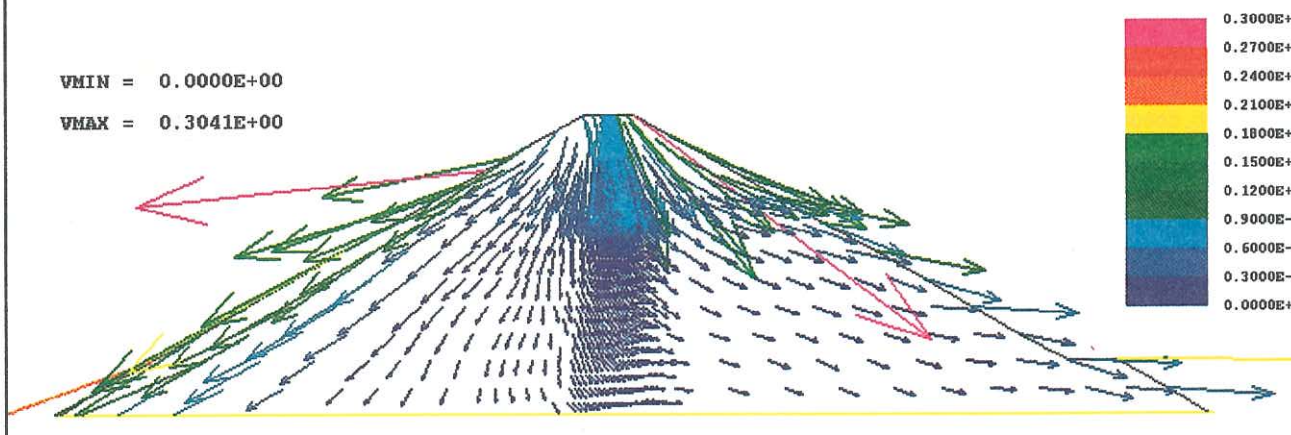

TOTAL DISPLACEMENT VECTORS (m)

Fig. 29

EQ1 earthquake considering horizontal and vertical components

DEFORMED MESH

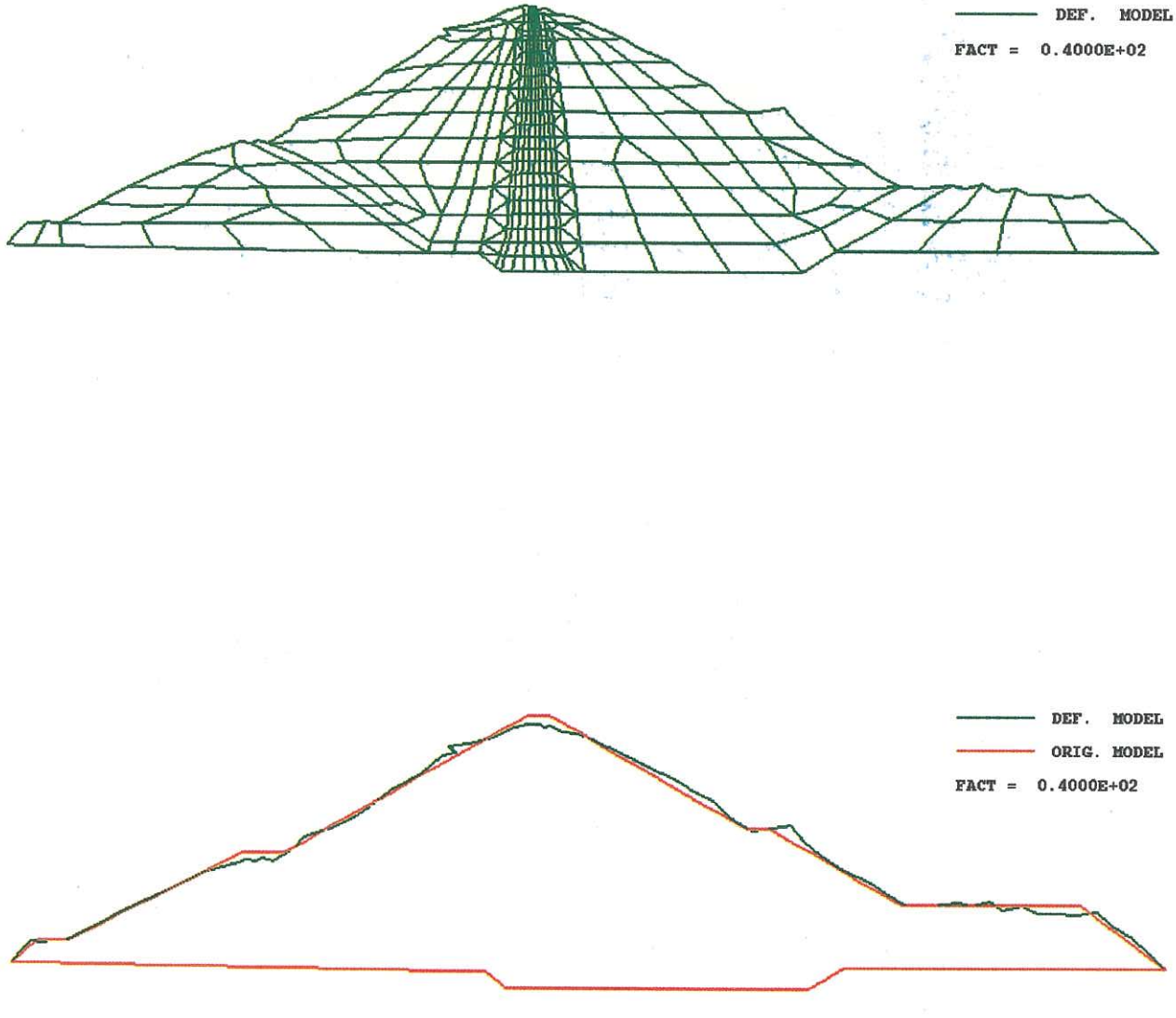

Fig. 30

EQ1 earthquake considering horizontal and vertical components

DISPLACEMENTS

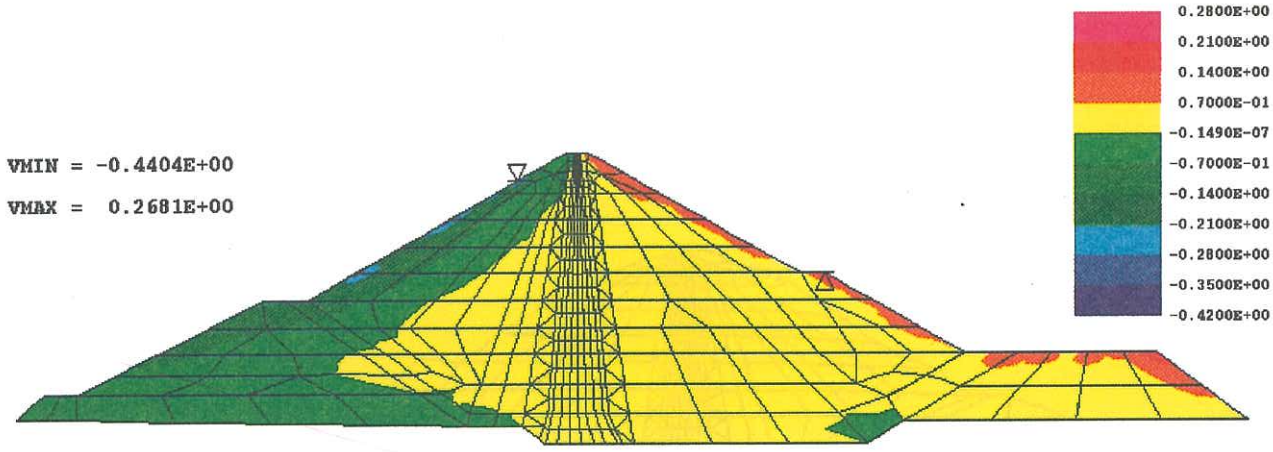

HORIZONTAL DISPLACEMENTS (m)

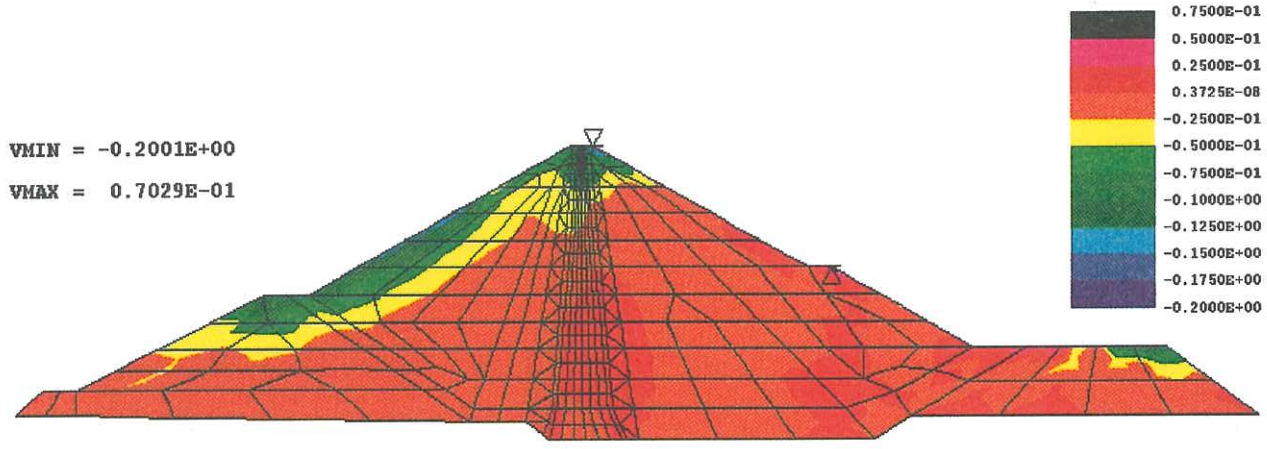

VERTICAL DISPLACEMENTS (m)

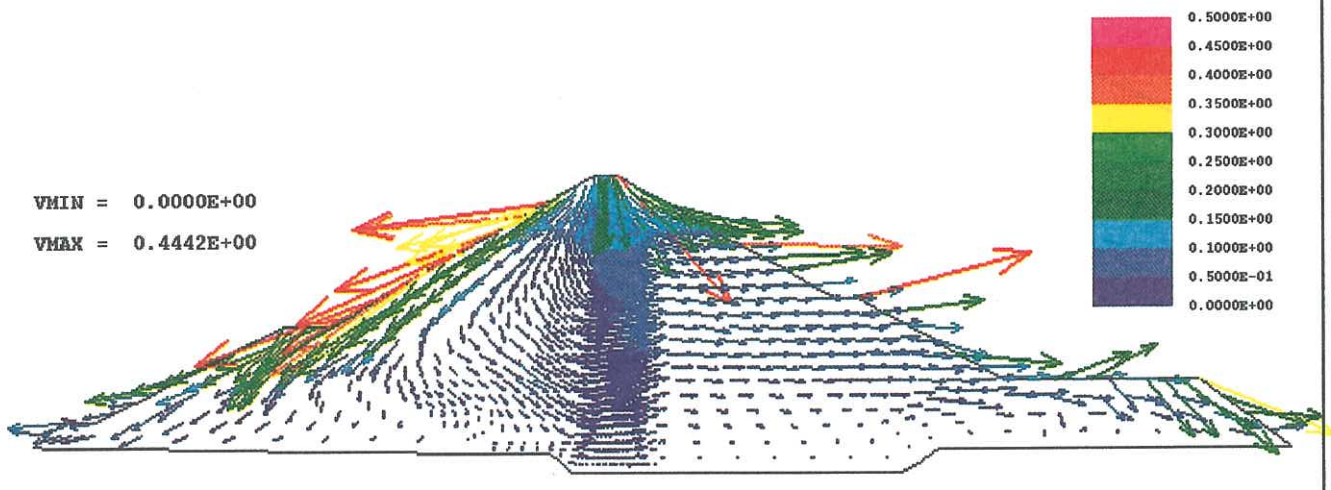

TOTAL DISPLACEMENT VECTORS (m)

Fig. 31

3rd. ICOLD 1994 - DYNAMIC ANALYSIS OF AN EMBANKMENT DAM

EQ1 earthquake considering horizontal and vertical components

DISPLACEMENTS: ZOOM IN THE UPPER PART

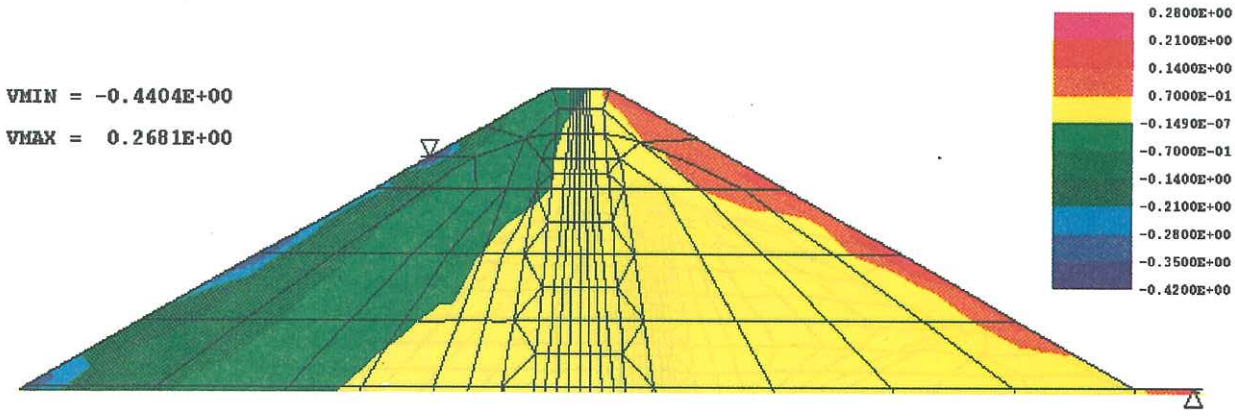

HORIZONTAL DISPLACEMENTS (m)

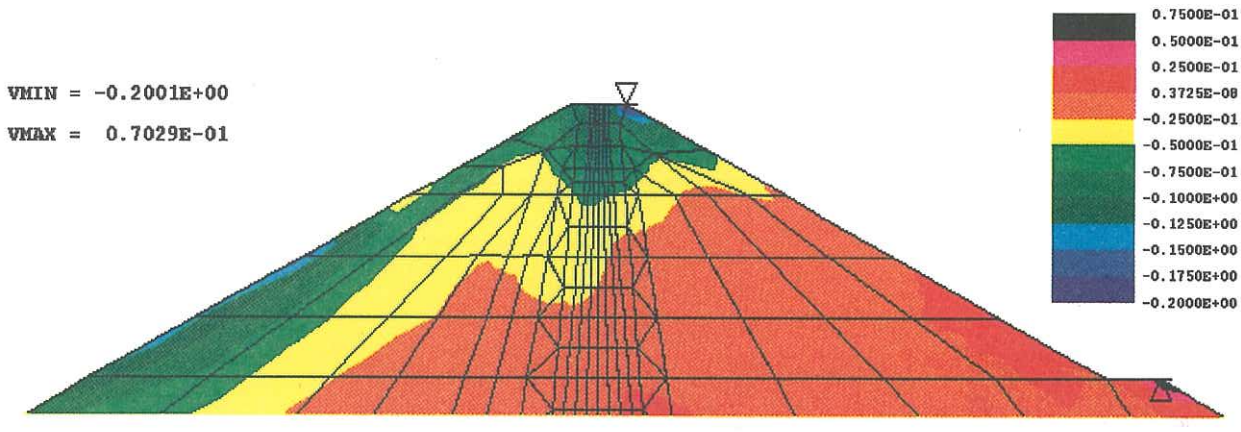

VERTICAL DISPLACEMENTS (m)

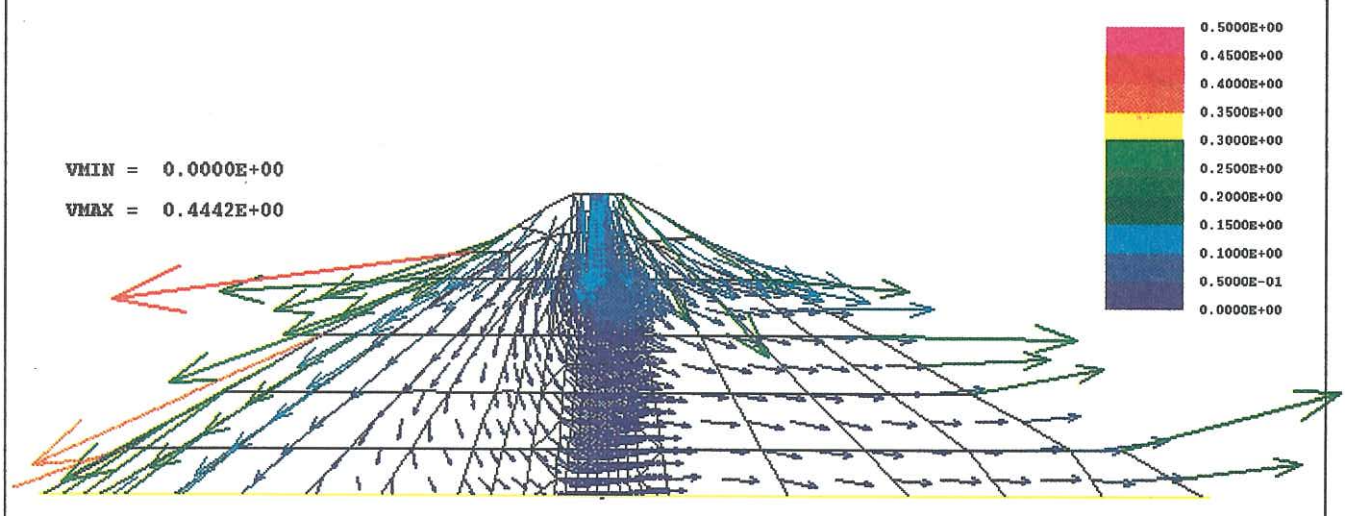

TOTAL DISPLACEMENT VECTORS (m)

Fig. 32

EQ2 earthquake considering horizontal and vertical components

DEFORMED MESH

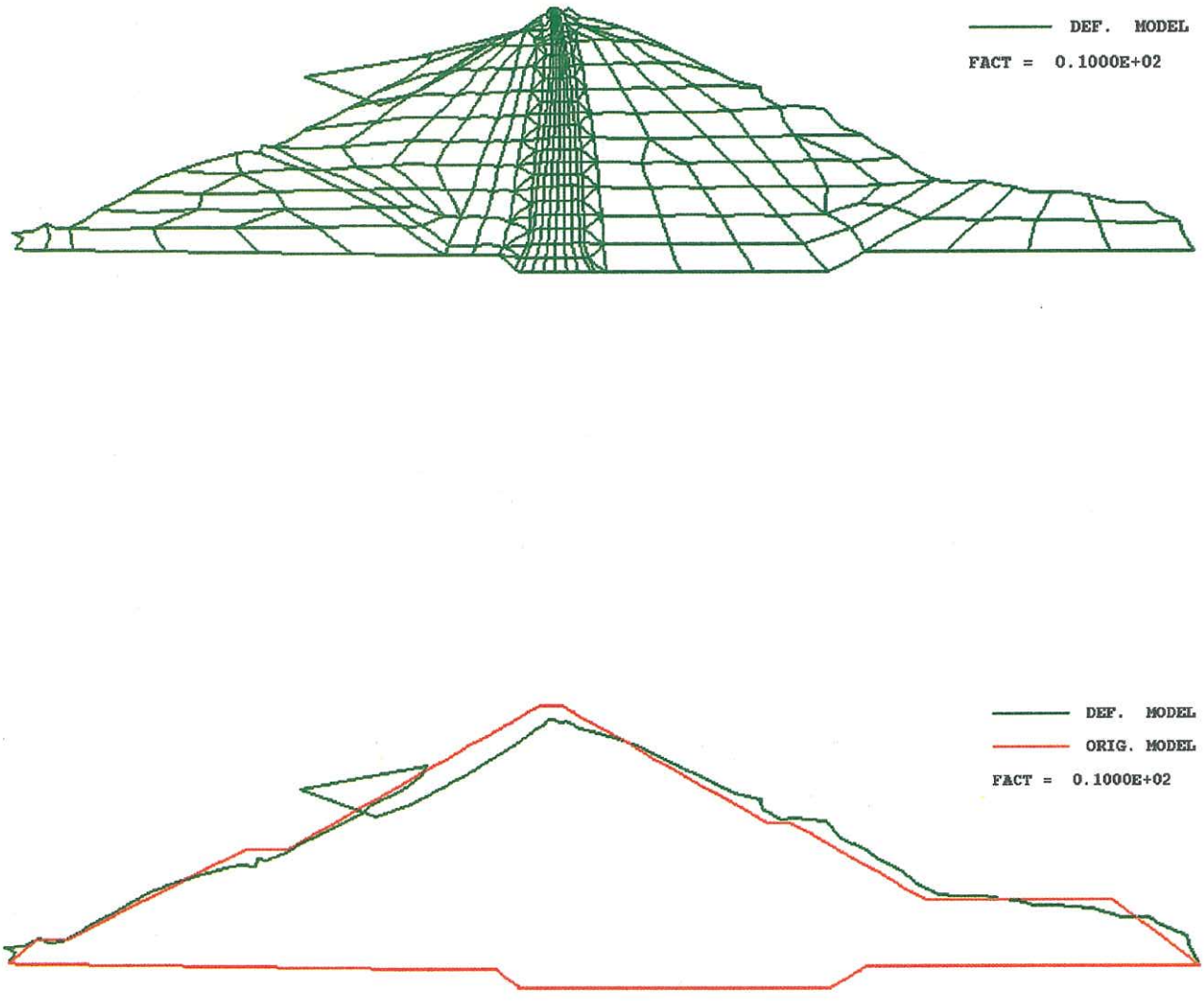

Fig. 33

EQ2 earthquake considering horizontal and vertical components

DISPLACEMENTS

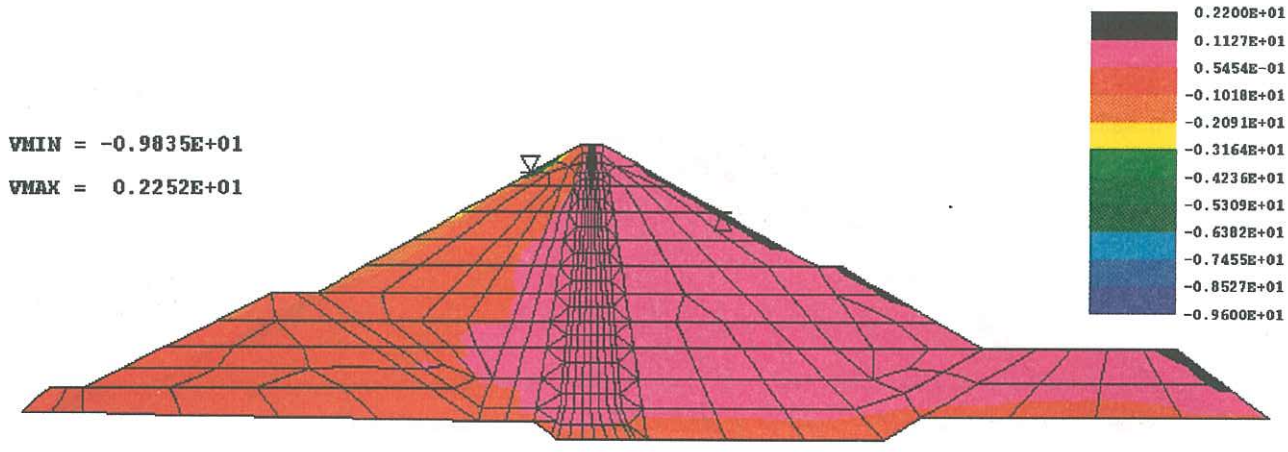

HORIZONTAL DISPLACEMENTS (m)

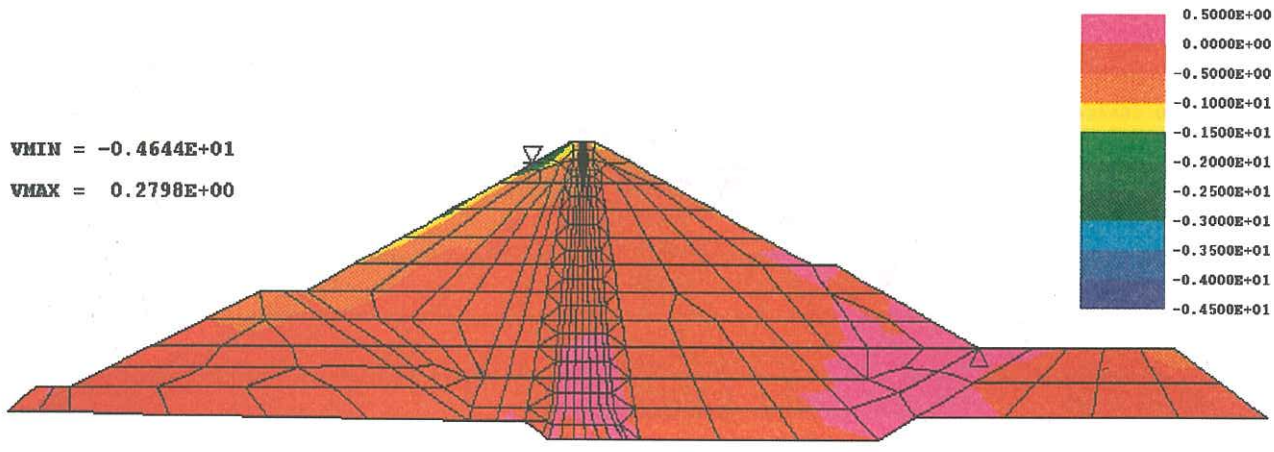

VERTICAL DISPLACEMENTS (m)

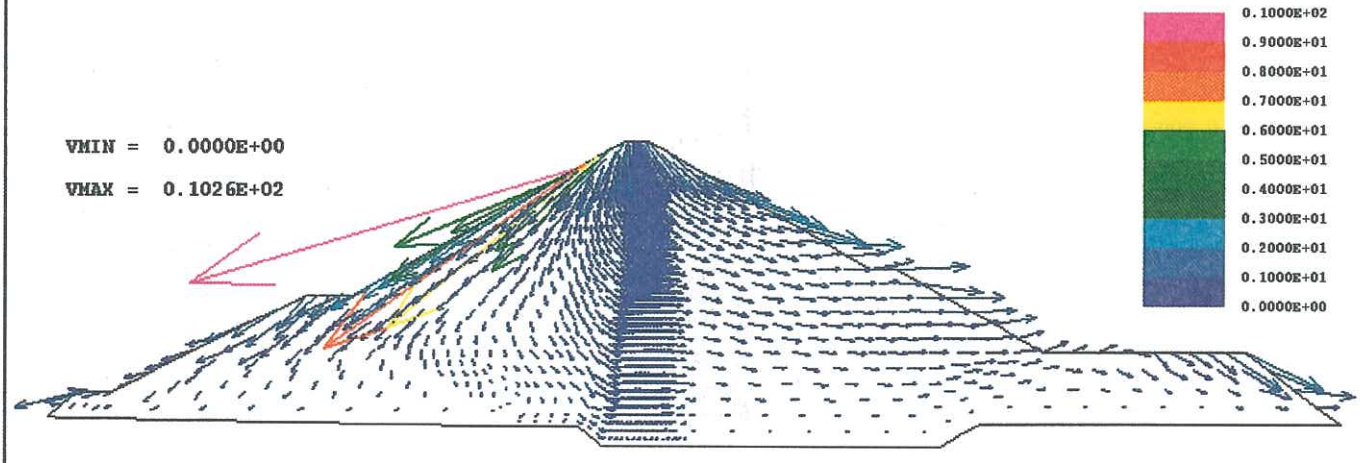

TOTAL DISPLACEMENT VECTORS (m)

Fig. 34

3rd. ICOLD 1994 - DYNAMIC ANALYSIS OF AN EMBANKMENT DAM

EQ2 earthquake considering horizontal and vertical components

DISPLACEMENTS: ZOOM IN THE UPPER PART

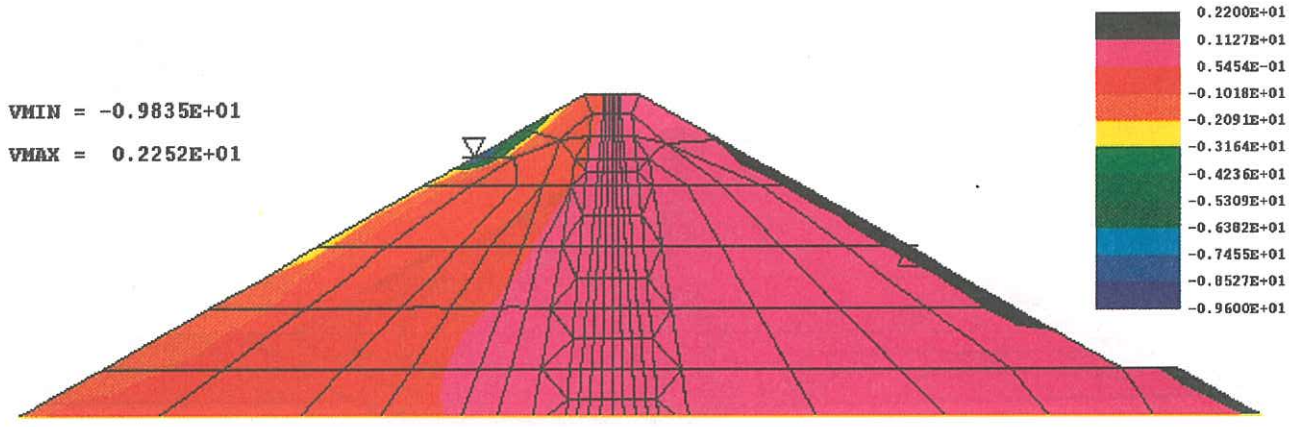

HORIZONTAL DISPLACEMENTS (m)

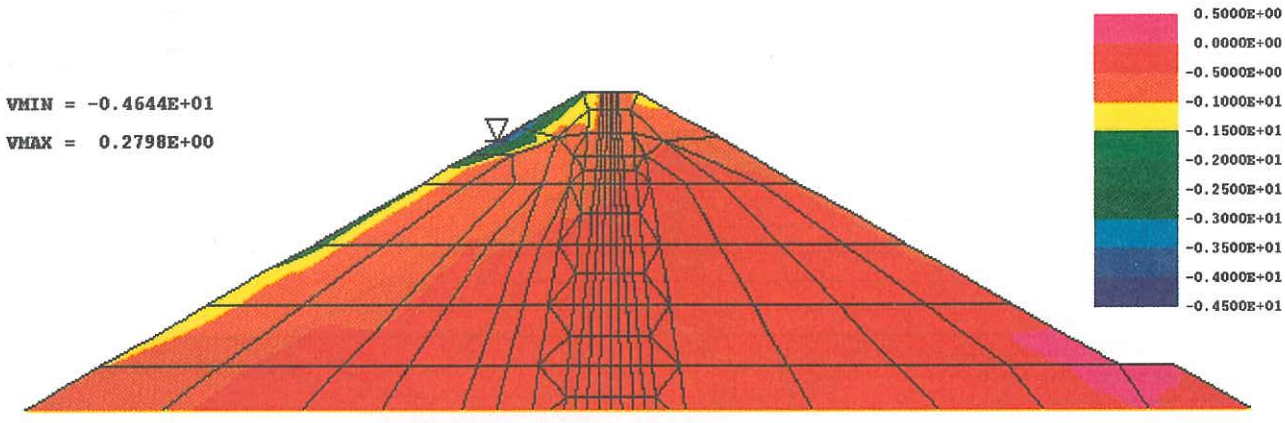

VERTICAL DISPLACEMENTS (m)

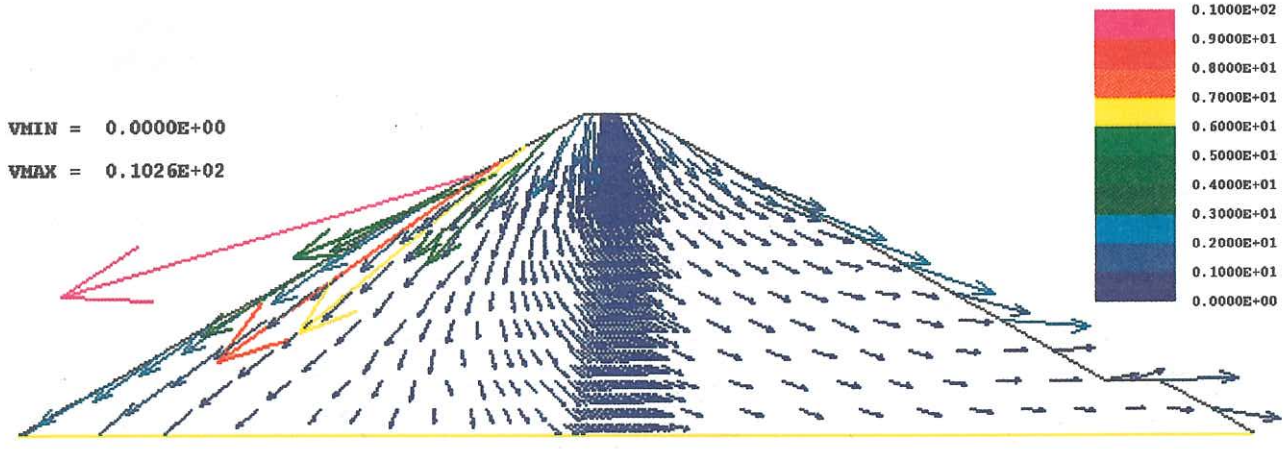

TOTAL DISPLACEMENT VECTORS (m)

Fig. 35

EXCESS PORE WATER PRESSURE

EQ1 earthquake considering only horizontal component (MPa)

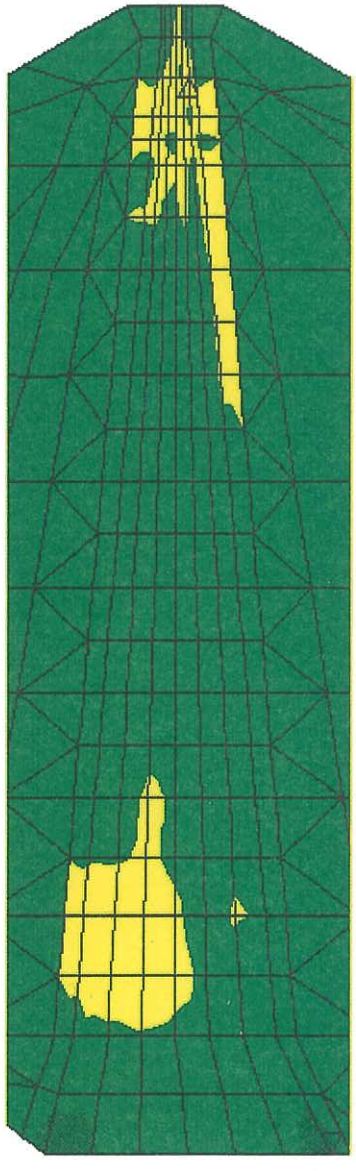

VMIN = -0.1672E+00

VMAX = 0.7181E-01

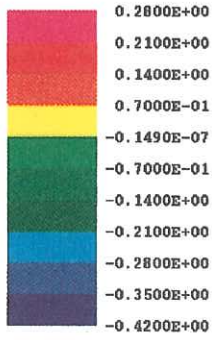

EQ1 earthquake considering horizontal and vertical components (MPa)

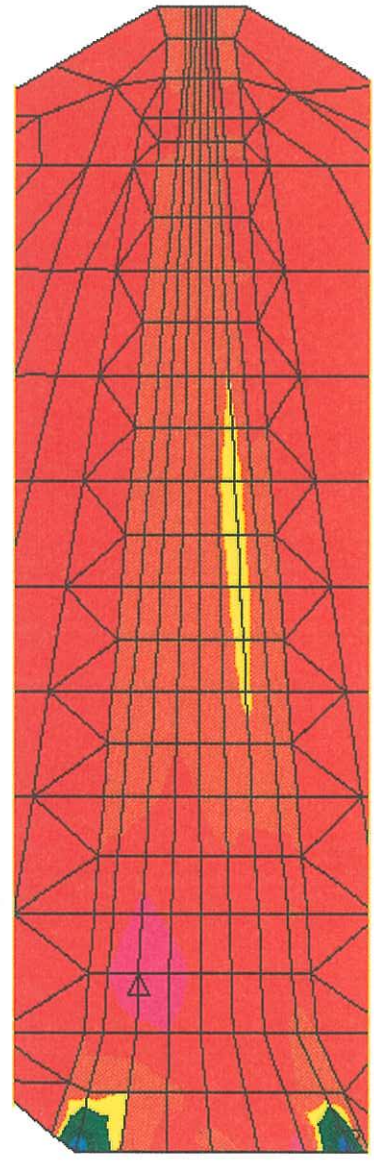

VMIN = -0.4206E+00

VMAX = 0.1344E+00

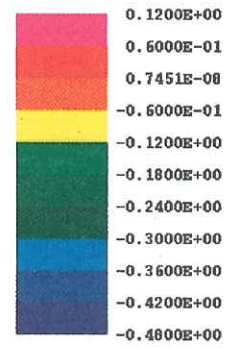

EQ2 earthquake considering horizontal and vertical components (MPa)

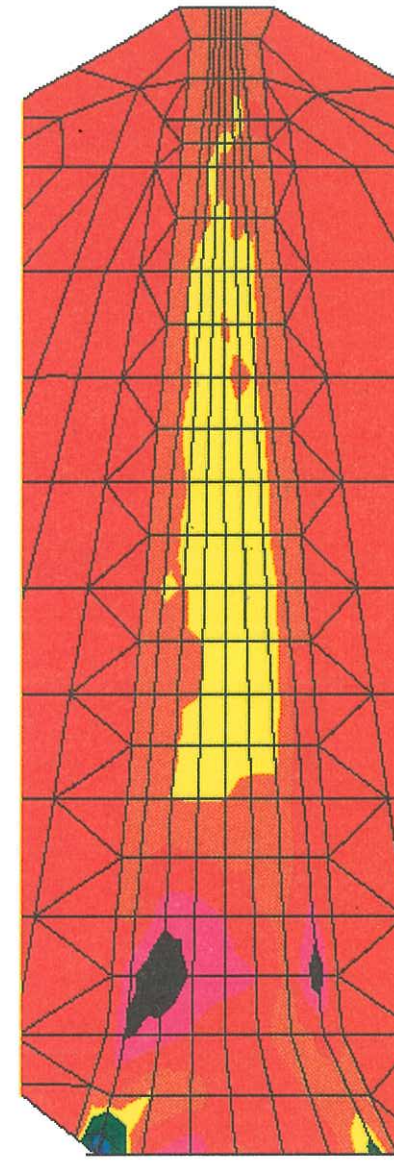

VMIN = -0.1521E+01

VMAX = 0.6797E+00

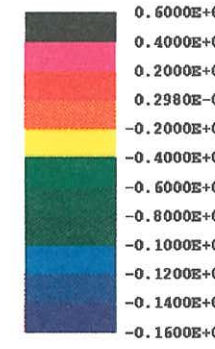

Fig. 36